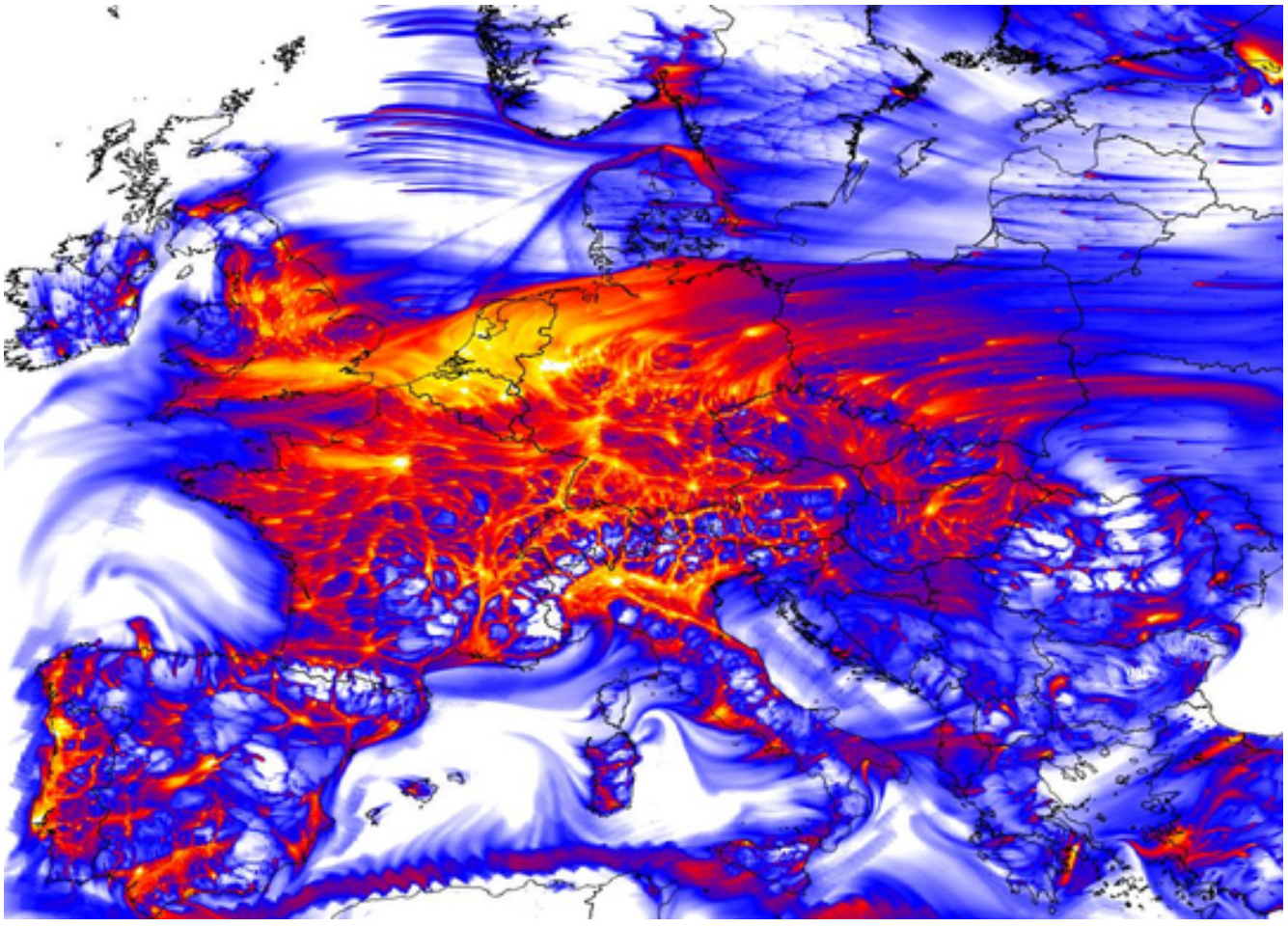
Documentation of the chemistry-transport model

Chimere

[version *chimere 2014b*]



NO_2 surface concentrations with a 1.5km model resolution

- This documentation and the model are freely available at the following internet adresse:

  http://www.lmd.polytechnique.fr/chimere/

- CHIMERE is distributed under the GNU General Public License
- Copyright (C) 2007 LMD (C.N.R.S.), INERIS, LISA (C.N.R.S.)
- For questions, send an e-mail to chimere@lmd.polytechnique.fr
- *Last update of this documentation: September 11, 2014*

Contents

1 Model overview and last changes **11**
- 1.1 Short Description of the model . . . 11
- 1.2 Main characteristics . . . 11
- 1.3 The CHIMERE software . . . 13
- 1.4 Last changes in this version *chimere 2014b* . . . 14
- 1.5 About this documentation . . . 14

2 First CHIMERE simulation **17**
- 2.1 Main sources installation . . . 17
- 2.2 The first run tutorial . . . 17
  - 2.2.1 Download required data and programs . . . 18
  - 2.2.2 Simulation configuration . . . 19
- 2.3 Main options of *chimere.par* . . . 20
- 2.4 Direct run outputs . . . 25
  - 2.4.1 The output on screen . . . 25
  - 2.4.2 The output files . . . 26
- 2.5 Post-processing the results . . . 27
- 2.6 Some figures to validate your first CHIMERE simulation for the 2009 Test Case . . . 28

3 CHIMERE model source code **31**
- 3.1 CHIMERE general code structure . . . 31
- 3.2 CHIMERE time integration . . . 33
- 3.3 Directories . . . 34
- 3.4 Model Files . . . 35
  - 3.4.1 Scripts . . . 35
  - 3.4.2 Makefiles . . . 35
  - 3.4.3 Meteo interface - 1st stage . . . 36
  - 3.4.4 Source directories . . . 37
  - 3.4.5 Dynamic files generated at runtime . . . 38
- 3.5 Routine calls sequence . . . 38
- 3.6 Parallelism . . . 39
  - 3.6.1 Domains division . . . 39
  - 3.6.2 Recommendations . . . 41
- 3.7 The 'chimere.nml' model namelist . . . 42
- 3.8 How to add a variable in the code? . . . 44
  - 3.8.1 From the master to workers . . . 44
  - 3.8.2 From workers to the master . . . 44
  - 3.8.3 Write variable into outfile . . . 45

4 [domains]: Domains and landuse **47**
4.1 The *domains/domainlist.nml* file . . . 47
4.2 Land Use Types, Data, and Interface . . . 48
4.2.1 Land use interface . . . 50
4.3 Details on output files . . . 51
4.3.1 Horizontal domain COORD . . . 51
4.3.2 Vertical grid VCOORD . . . 51

5 [chemprep]: The chemical preprocessor **53**
5.1 Options available in *chimere.par* . . . 53
5.2 The first-level script *make-chemistry.sh* . . . 54
5.3 The second-level scripts . . . 54
5.4 Manual changes of the mechanism . . . 54
5.5 Syntax of the REACTIONS file . . . 56
5.6 Syntax of the PHOTORATES file . . . 57

6 Emissions **59**
6.1 Anthropogenic surface emissions . . . 59
6.1.1 User's precompiled emissions . . . 59
6.1.2 The emiSURF interface . . . 59
6.2 Biogenic emissions . . . 62
6.2.1 The biogenic emitted species . . . 62
6.2.2 Biogenic emission interface . . . 63
6.3 Mineral dust emissions . . . 63
6.3.1 Dust emissions over Africa . . . 64
6.3.2 Dust emissions over Europe . . . 67
6.3.3 Data used for the mineral dust emissions calculations . . . 69
6.4 Fire emissions . . . 71

7 Depositions and resuspension **73**
7.1 Dry deposition . . . 73
7.1.1 For gases : . . . 73
7.1.2 For aerosols: . . . 74
7.2 Wet scavenging . . . 75
7.3 Resuspension of particulate matter . . . 75

8 Initial and boundary conditions **77**
8.1 Chemical boundary conditions . . . 77
8.1.1 Boundary conditions from global models . . . 77
8.1.2 Structure of the boundary conditions from global models . . . 79
8.1.3 Adding new sources of input data . . . 81
8.1.4 Boundary conditions interface . . . 81
8.1.5 Internal boundary conditions . . . 82
8.2 Initial concentrations . . . 82
8.2.1 Initial concentrations species . . . 82
8.2.2 Initial concentrations interface . . . 82

9 Meteorology **83**
9.1 Meteorological input data . . . 83
9.2 Diagnostics of parameters: . . . 85
9.2.1 Management of additional parameters . . . 85
9.2.2 Estimation of the vertical velocity . . . 86
9.2.3 Deep convection fluxes . . . 86
9.3 Transport and mixing . . . 89
9.3.1 Horizontal transport . . . 89
9.3.2 Vertical transport . . . 90
9.3.3 Turbulent mixing . . . 91

10 Chemistry **93**
10.1 The TWO-STEP time numerical solver . . . 93
10.2 Gas-phase chemistry . . . 94
10.2.1 Chemical mechanisms (gas phase) . . . 94
10.2.2 Species list of the reduced MELCHIOR1 gas-phase chemical mechanism . . . 95
10.2.3 Species list of the reduced MELCHIOR2 gas-phase chemical mechanism . . . 104
10.2.4 Species list of the SAPRC-07-A gas-phase chemical mechanism . . . 109
10.3 Aerosol processes . . . 117
10.3.1 Overview . . . 117
10.3.2 Composition and mathematical representation of aerosols . . . 118
10.3.3 Coagulation . . . 119
10.3.4 Absorption . . . 119
10.3.5 Nucleation . . . 120
10.3.6 ISORROPIA . . . 120
10.3.7 Multiphase chemistry . . . 121
10.3.8 Secondary organic aerosol chemistry . . . 122
10.4 Impact of clouds . . . 124
10.4.1 Impact on photolysis . . . 124
10.4.2 Wet scavenging . . . 125
10.5 Radiative transfers and photochemical reaction rates . . . 125
10.5.1 Processes taken into account . . . 125
10.5.2 Optical preprocessing using prep_mie . . . 126
10.5.3 Fast-JX initialisation . . . 127
10.5.4 Online calculation of photochemical reaction rates . . . 127
10.5.5 Using the old photorates ? . . . 127

Bibliography **127**

A References using CHIMERE **137**
A.1 Reference papers . . . 137
A.2 List of papers . . . 137

B History **149**
B.1 chimere2008 . . . 149
B.2 V200606 . . . 150
B.2.1 Parallelization . . . 150
B.2.2 Toolbox . . . 150
B.2.3 Scripts . . . 150
B.2.4 makefiles changes . . . 151

C Some scripts used in the CHIMERE suite **153**
C.1 The *domains/makeCOORDdomains* script for horizontal grid definition . . . 153
C.2 The *util/define_geom* script for vertical grid definition . . . 154

D How To install NetCDF under GNU/Linux **155**
D.1 Background . . . 155
D.2 Download . . . 155
D.3 Configure NetCDF . . . 155
D.3.1 ifort . . . 156
D.3.2 g95 . . . 156
D.3.3 pgf90 . . . 157
D.3.4 ifort 64 bit on Intel EMT64 or AMD Opteron . . . 157
D.3.5 g95 64 bit on Intel EMT64 or AMD Opteron . . . 157
D.3.6 pgf90 64 bit on Intel EMT64 or AMD Opteron . . . 158
D.4 Manually Configure CHIMERE . . . 158

E How To install MPI under GNU/Linux **161**
E.1 Background . . . 161
E.2 LAM/MPI Installation . . . 161
E.3 Testing . . . 162
E.4 Uniprocessor users . . . 162
E.5 Installation from source . . . 163
E.6 Open MPI installation . . . 163

F Notes on using CHIMERE with LAM MPI **165**
F.1 Specific case of single node envrionment . . . 165

G Structure of the CHIMERE netCDF files **167**
G.1 EMIS.[domain].[MM].[SPEC].s.nc and EMIS.[domain].[MM].[SPEC].p.nc . . . 167
G.2 exdomout.nc . . . 168
G.3 meteo.nc . . . 170
G.4 AEMISSIONS.nc . . . 172
G.5 BEMISSIONS.nc . . . 174
G.6 BOUN_CONCS.nc . . . 175
G.7 end.nc . . . 175
G.8 Fire emissions EMIS.[domain].[MM].[SPEC].f.nc . . . 180

List of Figures

1.1 *General principle of a chemistry-transport model such as CHIMERE. In the box 'Meteorology', u_* stands for the friction velocity, Q_0 the surface sensible heat flux, L the Monin-Obukhov length and BLH the boundary layer height. c_{mod} and c_{obs} are for the chemical concentrations fields for the model and the observations, respectively.* . . . 13

2.1 Figures to validate the March 2009 Test Case simulation . . . 29

3.1 *General structure of CHIMERE model* . . . 32
3.2 *General CHIMERE structure for time integration of all processes* . . . 33
3.3 *Calculation of the number of integration steps per hour to respect the CFL over a complete 120 hours simulation.* . . . 34
3.4 *Detailed list of CHIMERE routines and time loops* . . . 39
3.5 *Time processing in CHIMERE* . . . 40

4.1 *Examples of horizontal domains. The dots represent the MM5 EUR1 grid cells centers and the rectangle represents the boundaries of the CHIMERE CONT3 domain.* . . . 48

6.1 *Top-down processing of EMEP anthropogenic emissions with the emiSURF interface* . . . 61
6.2 *Domains of mineral dust emissions estimations.* . . . 64
6.3 *Estimation of weights as a function of the prescribed binding energies e_1, e_2 and e_3.* . . . 67
6.4 *Relative part of the most important soil class for each model cell. A value of 0.5 means that the most present soil represents 50% of the model cell.* . . . 69

8.1 *Surface ozone concentrations modelled with LMDz-INCA and MACC for july.* . . . 79
8.2 *Surface mineral dust concentrations modelled with GOCART and LMDzINCA for july.* . . . 80

9.1 *Flow chart of the meteorological CHIMERE pre-processor. WRF model is shown as an example of a weather forecast model driving CHIMERE. Programs are shown in yellow and NetCDF files in blue.* . . . 83
9.2 *[left] Temperatures changes due to shallow and deep convection and [right] Schematic view of a convective cloud* . . . 87
9.3 *Entrainment and detrainment fluxes in the updrafts and downdrafts.* . . . 88
9.4 *Convective atmopsheric column and its environment* . . . 89

10.1 *Principle of 'operator-splitting' versus Chimere integration* . . . 93
10.2 *Routines, files and scripts involved in the calculation of radiative transfers* . . . 126

List of Tables

1.1 *Main properties of the CHIMERE model* 12

2.1 *Useful URL adresses for the development and the use of the CHIMERE model and its modules* . . 18
2.2 *Variables in the METEO output file.* 27

4.1 *Landuse categories used in CHIMERE* 49
4.2 *GLCF land cover types used in CHIMERE* 49
4.3 *GlobCover land cover types used in CHIMERE* 50

6.1 *Gas and particle emissions required for MELCHIOR and SAPRC* 60
6.2 *Notations used to describe the saltation and sandblasting processes. * i=3 in this case.* 65
6.3 *Fractions (p_i) of the kinetic energy for the three binding energies e_i, after [Alfaro et al., 1997]* . . 66
6.4 *Needed parameters for the mineral dust emissions fluxes calculations* 69
6.5 *Description of soil types. CS= Coarse sand; FMS=Fine medium sand.* 70

9.1 *Mandatory and optional variables in* **exdomout.nc** *meteo file. Note that all meteorological 3D variables must be provided at half-layers levels.* 84
9.2 *Constant values used for the calculation of additionnal parameters in the routine calc_turb.* 86

10.4 *List of aerosol species. (*): ions, molecules, crystals* 118
10.5 *Characteristics of the look-up table used for the calculation of the thermodynamic equilibrium with ISORROPIA.* 121
10.6 *Relative humidity at deliquescent points for the species used by ISORROPIA in the system sulfate-nitrate-ammonium-water.* 121
10.7 *Gas phase chemical scheme for SOA formation in CHIMERE. The surrogate SOA compounds consist of six hydrophilic species that include an anthropogenic nondissociative species (AnA0D), an anthropogenic once-dissociative species (AnA1D), an anthropogenic twice-dissociative species (AnA2D), a biogenic non dissociative species (BiA0D), a biogenic once-dissociative species (BiA1D) and a biogenic twice-dissociative species (BiA2D), three hydrophobic species that include an anthropogenic species with moderate saturation vapor pressure (AnBmP), an anthropogenic species with low saturation vapor pressure (AnBlP) and a biogenic species with moderate saturation vapor pressure (BiBmP), and two surrogate compounds for the isoprene oxidation products.* 123

Acknowledgments

The model is developed at IPSL/LMD (Palaiseau), INERIS (Verneuil en Halatte) and IPSL/LISA (Creteil) in France.
For questions about the model development, parameterizations or variables choices, you can send an e-mail to the developers: **chimere@lmd.polytechnique.fr**.
This will send an e-mail to: Laurent Menut, Dmitry Khvorostiyanov, Myrto Valari, Solene Turquety, Sylvain Mailler (LMD), Bertrand Bessagnet, Augustin Colette (INERIS) and Guilaume Siour (LISA).
For questions about the model use, to share pre- or post-processing tools with the other users, or just present your result, you can register to the chimere users mailing list here: http://www.lmd.polytechnique.fr/chimere/subscribe.php

In case of use of the MACC global dataset as boundary conditions, please add in your publications the following acknowledgment: *"This data set was provided by the MACC-II project, which is funded through the European Union Framework 7 programme. It is based on the MACC-II reanalysis for atmospheric composition; full access to and more information about this data can be obtained through the MACC-II web site (http://www.copernicus-atmosphere.eu)."*

The CHIMERE developers acknowledge:

- Gabriele Curci for the biogenic emissions interface
- Richard Engelen for the global concentrations dataset in the framework of the MACC project.
- Eric Chaxel for the WRF model meteorological interface
- Christian Seigneur and Betty Pun (AER) for the reduced SOA scheme,
- Mian Chin and Paul Ginoux (NASA) for the GOCART aerosols concentrations fields used as boundary conditions,
- Sophie Szopa and Didier Hauglustaine (IPSL/LSCE) for the LMDz-INCA gas concentrations fields used as boundary conditions,
- Athanasios Nenes and the ISORROPIA team for the free use of ISORROPIA model,
- the EMEP-MSCWEST team (`http://www.emep.int`) for anthropogenic emissions database,
- the EMEP-MSCEAST team for benzo(a)pyrene, benzo(k)fluoranthene and benzo(b)fluoranthene data (`http://www.msceast.org`).
- José Antonio Souto for section 3.8.2 on how to add a new variable in the code.

Chapter 1

Model overview and last changes

1.1 Short Description of the model

The CHIMERE multi-scale model is primarily designed to produce daily forecasts of ozone, aerosols and other pollutants and make long-term simulations for emission control scenarios. CHIMERE runs over a range of spatial scales from the regional scale (several thousand kilometers) to the urban scale (100-200 Km) with resolutions from 1-2 Km to 100 Km. On CHIMERE server, documentation and source codes are proposed for the complete multi-scale model. However most data are valid only for Europe and should be revisited for applications on other continents.
CHIMERE proposes many different options for simulations which make it also a powerful research tool for testing parameterizations, hypotheses. Its use is relatively simple so long as input data is correctly provided. It can run with several vertical resolutions, and with a wide range of complexity. It can run with several chemical mechanisms, simplified or more complete, with or without aerosols.
Currently, the model may be used for:

- Physical and chemical processes research
  - Transport and mixing, turbulence
  - Aerosols chemistry
  - Dust and fire emissions and transport
  - Particles deposition
  - Clouds, radiation and chemistry
  - Vegetation and chemistry interactions
- Scenarios and climatologies
  - Past and future emissions impacts
  - Ensemble analysis
- Forecast
  - Experimental forecast at LMD
  - Operational forecasts (PREVAIR, AQ networks, GEMS, MACC, etc.)

The main properties of the CHIMERE processes calculations are described in Table 1.1 .

1.2 Main characteristics

CHIMERE is an Eulerian off-line chemistry-transport model (CTM). External forcings are required to run a simulation: meteorological fields, primary pollutant emissions, chemical boundary conditions. Using these input data, CHIMERE calculates and provides the atmospheric concentrations of tens of gas-phase and aerosol species over

Process	Methodology
Meteorological forcing	ECMWF, GFS, MM5, WRF
Landuse	GLCF or GlobCover global datasets
Horizontal resolution	from 1km to few degrees
Horizontal advection	upwind, Van Leer or PPM
Vertical advection	upwind or Van Leer
Deep convection	the Tiedke scheme
Boundary-layer turbulence	the Troen and Mahrt scheme
Anthropogenic emissions	EMEP, HTAP or local inventories
Biogenic emissions	online MEGAN model
Sea salt emissions	Monahan scheme
Mineral dust emissions	Alfaro and Gomes scheme
Chemical mechanism	SAPRC or MELCHIOR
Aerosols representations	bins
Secondary Organic Aerosols	Pun scheme
Photolytic rates	online FastJX radiative transfer model
Numerical solver	the TwoStep solver
Aerosol thermodynamic equilibrium	online ISOROPIA
Dry deposition	Wesely parametetrization

Table 1.1: *Main properties of the CHIMERE model*

local to continental domains (from 1 km to 1 degree resolution). The key processes affecting the chemical concentrations represented in CHIMERE are: emissions, transport (advection and mixing), chemistry and deposition, as presented in Figure 1.1. Note that forcings have to be on the same grid and time step as the CTM simulation. In this sense, CHIMERE is not only a chemical model but a suite of numerous pre-processing programs able to prepare the simulation. The model is now used for pollution event analysis, scenario studies, operational forecast and more recently for impact studies of pollution on health ([Valari and Menut, 2010]) and vegetation ([Anav et al., 2011]).

The first model version was released in 1997 and was a box model covering the Paris area including only gas-phase chemistry ([Honoré and Vautard, 2000], [Vautard et al., 2001]). In 1998, the model is implemented for its first forecast version (Pollux) during the ESQUIF experiment ([Menut et al., 2000b]) still over the Paris area ([Vautard et al., 2000]). At the same time, the adjoint model was developed to estimate the sensitivity of concentrations to all parameters ([Menut et al., 2000a]). In 2001, the geographical domain was extended over Europe with a cartesian mesh ([Schmidt et al., 2001]) and the new experimental forecast platform (PIONEER) is set up. In 2003, the experimental forecast became operational with the PREVAIR system operated at INERIS ([Honoré et al., 2008], [Rouïl et al., 2009]). The aerosol module is implemented in 2004 ([Bessagnet et al., 2004]) with further improvements concerning the dust natural emissions and resuspension over Europe ([Vautard et al., 2005a], [Hodzic et al., 2006a] [Bessagnet et al., 2008]) and evaluated against long-term and field measurements ([Hodzic et al., 2005], [Hodzic et al., 2006b]). The development of the mineral dust version started in 2005 ([Menut et al., 2005]). Chemistry was not included in that version and a new horizontal domain had been designed to cover the whole northern Atlantic and Europe, including the Saharan desert and downwind regions. In 2006, an important step is achieved with the development of the parallel version of the model and its first implementation on a massively parallel computer (the ECMWF computer in the framework of the FP6/GEMS project).

The CHIMERE model is now considered as a state-of-the-art model. It has been involved in numerous intercomparison studies mainly focusing on ozone and PM_{10} from the urban scale ([Vautard et al., 2007, Van Loon et al., 2007, Schaap et al., 2007]) to continental scale ([Solazzo et al., 2012], [Zyryanov et al., 2012]). Moreover, the model has been mainly applied over Europe, but also more recently over Africa and the North Atlantic for dust sim-

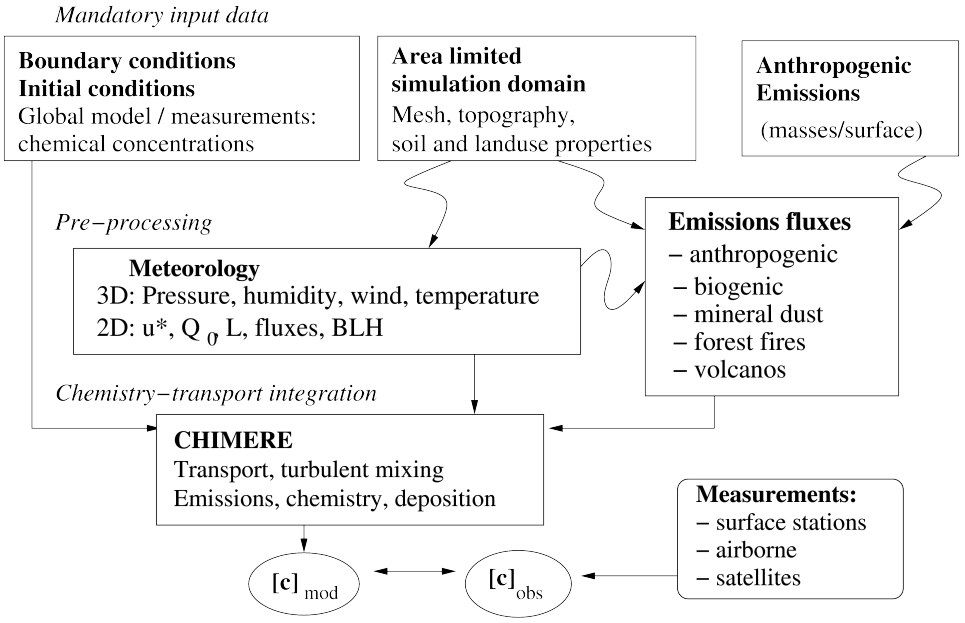


Figure 1.1: *General principle of a chemistry-transport model such as CHIMERE. In the box 'Meteorology', u_* stands for the friction velocity, Q_0 the surface sensible heat flux, L the Monin-Obukhov length and BLH the boundary layer height. c_{mod} and c_{obs} are for the chemical concentrations fields for the model and the observations, respectively.*

ulations, over Central America during the MILAGRO project to study organic aerosols ([Hodzic et al., 2009], [Hodzic et al., 2010b], [Hodzic et al., 2010a]) and over the US within the AQMEII project ([Solazzo et al., 2012]). Finally, the development of CHIMERE follows three main rules. First, concentrations of main pollutants are calculated with the best possible accuracy using well evaluated and state-of-the-art parameterisations. Second, a modular framework is maintained to allow updates to the code by developers but also all interested users. Third, the code is kept computationally efficient to allow long-term simulations, climatological studies and operational forecast.

1.3 The CHIMERE software

In order to facilitate software distribution, CHIMERE is protected under the General Public License. The source code and the associated documentation is available on a web site www.lmd.polytechnique.fr/chimere. The documentation is both technical and scientific. It includes a chapter dedicated to the set-up of a test case simulation that allows new users to easily carry out a CHIMERE simulation: model configuration and data (meteorology and emissions files) are provided to simulate the 2003 heat wave in western Europe.
CHIMERE is a National Tool of the French Institut des Sciences de l'Univers, meaning that support has to be provided to the users of model. Two mailing lists exist for this support: chimere@lmd.polytechnique.fr to send questions to the model developers and chimere-users@lmd.polytechnique.fr to initiate discussions, exchange programs or data between users. In addition, two-day training courses are organised twice a year. Each training course is free of charge for participants and offers a complete training to be able to install the code, launch a simulation and change surface emissions or other parameters in the code.
The code is completely written in Fortran90, and running scripts are written in shell (using gnu-awk for input datafiles processing). The required software is a Fortran 95 compiler (g95 and gfortran are both free and efficient, but Makefiles with Intel's ifort compiler options are also provided). The required libraries are NetCDF (either 3.6.x or 4.x.x), MPI (see below), and GRIB API (associated to the use of the ECMWF meteorological datasets). The

model includes tools that can help the user to configure the model's Makefiles for the libraries already installed. The model computation time for one AMDx64 node of 16 CPUs is 1h30min for 1 month of simulation for the Paris area, at 15 km resolution, the domain size being 45x48x8 with a time step of 360 seconds on average. CHIMERE uses the distributed memory scheme, and MPI message passing library. It is maintened for Open MPI (recommended) and LAM/MPI, but works, with minor changes in the scripts, with MPICH or other MPI compatible parallel environments. The model parallelism results from a Cartesian division of the main geographical domain into several sub-domains, each one being processed by a worker process. Each worker performs the model integration in its geographical sub-domain as well as boundary condition exhanges with its neighbours. In addition a master process performs initialisations and file input/output. To configure the parallel sub-domains, the user has to specify two parameters in the model parameter file: the number of sub-domains for the zonal and meridional directions. The total number of CPUs used is therefore the product of these two numbers, plus one CPU for the master process.
For graphical postprocessing, simple interfaces are available using either the GMT 5 or the GrADS 6 free software. Also an additional graphical user interface (GUI) software CHIMPLOT is provided. It allows making various 1D or 2D plots (e.g., longitude-latitude or time-altitude maps, vertical slices, time series, vertical profiles). One can also overlay multiple fields (e.g., O_3 concentrations, wind vectors, and pressure contours) and perform simple operations such as calculating daily maxima, daily means, vertical or horizontal averaging or integrations.

1.4 Last changes in this version *chimere 2014b*

Version ***chimere 2014b*** contains the following improvements:

- Processes
  - ◇ Added the *FastJ* radiative transfer model to compute photolysis reaction rates. This makes it possible to extend the model domain vertically beyond 500 hPa. An automatic calculation of optical depth (for clouds and aerosols) is also done.
  - ◇ Added possible read of fires emissions fluxes (if provided by the user)
  - ◇ Added SAPRC-07-A chemical mechanism
  - ◇ Updated ISOROPIA V2006
- Numerics/Software
  - ◇ Activated adaptive CFL condition. This speeds up computations.
  - ◇ Improved deep convection calculation. This speeds up computations and yields more realistic ozone land-sea interfaces.
  - ◇ **diagmet**, **diagbio**, and **diagdust** programs are put in the model core.
  - ◇ Improved calculations of boundary conditions (with new datasets built with LMDz-INCA, GOCART and MACC global climatologies)
  - ◇ Optimized calculations of vertical levels

1.5 About this documentation

This documentation describes the last version of the CHIMERE chemistry-transport model named ***chimere 2014b***. The model and associated source codes are freely available on a web site:

http://www.lmd.polytechnique.fr/chimere/

In this documentation:

- ◇ Chapter 2 explains how to install the model from scratch and perform a first run using the prepared test case 'Heat Wave summer 2003 over Europe'.

- ◇ Chapter 3 (p.31) presents the model sources documentation including the pre- and post-processing interfaces.
- ◇ Chapter 4 (p.47) and 5 (p.53), explain how the user may define its own model geometry (domain and landuse) and its own configuration for chemistry (gas and/or aerosols, tracers etc.)
- ◇ Chapters 6 (p.59), 8 (p.77), 9 (p.83), 10 (p.93) describe the treatment (processes and numerics) of the emissions, boundary conditions, meteorology and chemistry.
- ◇ Appendix presents "how-to" files explaining the way to install libraries such as netCDF and LAM/MPI, and the format of all files used by the model.
- ◇ A list of published papers about studies using CHIMERE is displayed in chapter A, p.137.

For further questions, please send an e-mail to the developers at chimere@lmd.polytechnique.fr.

Chapter 2

First CHIMERE simulation

In the case of a user who never used the CHIMERE model before, this chapter presents how to:

- Install all softwares prerequisites, §2.1
- Perform a simulation with the pre-defined test case available on the CHIMERE web site, §2.2, with a complete description of the model top-calling script, §2.3
- See the results, §2.4, post-process the concentrations fields §2.5.

2.1 Main sources installation

The CHIMERE model has only been tested on GNU/Linux systems with LAM-MPI and Open MPI message passing libraries. However it should be working on most UNIX systems provided the following software is installed. The foreseenable changes should be related to **shell**, **awk** and **make** syntax, to the **MPI** library used, and also to unformatted binary files which may have to be converted.
The model requires:

- a **Fortran 95** compiler (e.g., **gfortran**)
- GNU **bash** Bourne shell, **awk** and **make**
- Unidata **NetCDF** library (free)
- **Open MPI** (`http://www.open-mpi.org`) or **LAM-MPI** (Indiana University) software (free)
- The NCO libraries (free)

The installation process of NetCDF and MPI is fully described in **§D, p.155** and **§E, p.161**. **The NetCDF library must be compiled with the same compiler as CHIMERE model.**
If no **bash** is installed, the model may work with a baseline Bourne-shell, but the user may have to edit the scripts to take in account some syntactic features specific to **bash** . The same remark apply to the **awk** and **make** utilities.
The model has been tested with the following compilers: gfortran, g95, ifort and pgf90.
In the following examples, the **wget** utility is used for downloading, because it is a robust and powerful downloading tool. However, if **wget** is not installed on your system, you can obviously use your favorite browser to download files.
The Table 2.1 reports useful URL adresses for the development and the use of the CHIMERE model and its modules

2.2 The first run tutorial

For the first CHIMERE run, we propose to simulate the particulate matter pollution event occurred over Northern Europe in March 2009.

Models	
WRF model (free)	http://www.wrf-model.org/index.php
MM5 model (free)	http://box.mmm.ucar.edu/mm5
NCAR	http://ncar.ucar.edu
ISORROPIA	http://nenes.eas.gatech.edu/ISORROPIA
Librairies	
Unidata NetCDF library (free)	http://www.unidata.ucar.edu/
Open MPI library (free)	http://www.open-mpi.org
Fortran compilers	
gfortran compiler (free)	http://gcc.gnu.org/wiki/GFortran
ifort compiler	http://www.intel.com/cd/software/products/asmo-na/eng/compilers/index.htm
g95 compiler (free)	http://g95.sourceforge.net/
pgf90 compiler	www.pgroup.com
Databases	
EMEP	http://www.emep.int
Global Land Cover Facility (GLCF)	http://glcf.umiacs.umd.edu/data/landcover
GlobCover Portal	http://ionia1.esrin.esa.int
LAI from NASA/EOSDIS	http://www.daac.ornl.gov

Table 2.1: *Useful URL adresses for the development and the use of the CHIMERE model and its modules*

This Test Case simulation is over the European domain called *CONT5* (defined in **domains/domainlist.nml**, see below) and lasts 8 days starting from March 12 2009. The PM pollution event occurs on March 19 with a maximum at 14h. To drive CHIMERE, WRF model meteorological fields have been prepared. The WRF simulation was driven by the 6-hourly NCEP/AVN analyses with the spectral "nudging" option (grid FDDA). You can see the detailed list of WRF simulation parameters in the output file wrfout*. The model domain covers the Western Europe with a horizontal resolution of 45km and 30 vertical levels.

2.2.1 Download required data and programs

To perform this test case, you need to download the model and some input data archives. To access the source files and databases for the first time, you need to register by filling out the form in the downloads section of the CHIMERE web site: [http://www.lmd.polytechnique.fr/chimere/download.php]. Your data will be examined and if approved you will receive your login/password to access the download page.
The script chimere-download.sh is provided to simplify CHIMERE installation. You need to download the script from the web site and to launch it from the directory where you wish to install Chimere.
The script does the following:

1. Prompts you to specify the directory where you would like to store large data files. Creates the model directory and subdirectories for the big files, emissions, output, and the meteorology
2. Downloads the CHIMERE source code and data for the test case: EMEP emissions[1] preprocessed for July and August and MM5 meteorological output for the 5 days of test simulation.
3. Downloads emission data for other months and the complete emiSURF preprocessor
4. Downloads the boundary and initial conditions
5. Decompresses the downloaded archives to the appropriate directories
6. Moves the archives to the ARCH directory

[1]For the use of these emissions data, please acknowledge EMEP (Yearly totals), IER (Time variations), TNO (Aerosol emissions), UK Dept of Environment (VOC speciation, Passant, 2002).

2.2.2 Simulation configuration

Once the code is downloaded and the mandatory libraries NetCDF and MPI are installed, the next step is to configure CHIMERE for your system.
CHIMERE uses configuration files that reflect user's requirements and environment. These files reside in ***chimere 2014b*** top directory:

- [Makefile.hdr] is a symbolic link to a preformated file, specific to a given compiler. It contains all the informations pertinent to your execution environment: compiler options, libraries, and so on. *Makefile.hdr* is included by all subsequent makefiles in CHIMERE source tree, to ensure a consistent compilation.
- [mychimere.sh] contains PATHs to the system software used by CHIMERE: NetCDF and MPI libraries, Fortran compiler, the *Makefile.hdr* version to use, and the compilation mode (debugging or performance, see below). This file simplifies model portability between different computers, system library versions and Fortran compilers. Once you generated a version of mychimere.sh for a particular system/compiler, you can easily change between them just by changing the symbolic link mychimere.sh to mychimere.sh.[sofware_version].
- [chimere.par] is an ASCII file that unites by topic all main parameters of CHIMERE simulations, such as data file locations, domain definitions, physical and numerical options. It also accepts comments (started with '#'), valid bash commands like

  ```
  $(date -u -d "${di} ${ndays} days" +%Y-%m-%d)
  ```

  and supports simplified date arithmetic, e.g.,

  ```
  (($di - 1))
  ```

  instead of

  ```
  $(date -u -d "$di 1 days ago" +%Y-%m-%d)
  ```

  A copy of this file is given in the §2.3, p.20.

To configure CHIMERE:

- Run config.sh.

  ```
  ./config.sh mychimere.sh.gfortran_MyLinuxCluster
  ```

  This will generate a version of mychimere.sh corresponding to

  - ◇ location of your Fortran compiler
  - ◇ location of your NetCDF package
  - ◇ location of your MPI library and executables
  - ◇ if needed, location of your gribex library (for interfaces to meteorologcal datasets in the grib format)

  It will also create a symbolic link mychimere.sh to the newly generated version of the file. Later, during CHIMERE compilation with the compile script and when running the top-calling script chimere.sh, an appropriate symbolic link *Makefile.hdr* will be created. You can then manually edit mychimere.sh to specify the complilation mode: DEVEL for debugging or PROD for performance.
- Edit chimere.par to :
  - ◇ set up the time span of a run
  - ◇ set the cartesian division of the domain (nzdoms and nmdoms)
  - ◇ tell CHIMERE the location of pertinent files and directories including the input data that you downloaded:
    - ◇ domain geometry
    - ◇ species list

- ◇ emission files
- ◇ boundary conditions files
- ◇ meteo file
- ◇ working directory
- ◇ output directory

◇ choose model options

The current Chimere version has been tested with Open MPI. The latter does **not** need to be booted, you can just launch mpirun with your executable. If you are still using LAM MPI, see p. 165.

- Compile all programs:
  `make clean`
  `./compile` - this should be used instead of **make**, since it *sources* the current mychimere.sh making the parameters defined there visible to the system during model compilation and linking.
  Then you can execute the top-calling script chimere.sh. For instance for the proposed test case:
  `chimere.sh`
  and see the messages on the screen to check if installation was correctly done.

2.3 Main options of *chimere.par*

Notes to the top-calling script **chimere.sh** and the parameter file chimere.par:

- The first optional argument of the script **chimere.sh** is the starting date. For example, for the tutorial test case, the user could launch the script using `chimere.sh 20090312`. The parameter 'di' would have the value '20090312' in this case. The starting date 'di' can be also specified in chimere.par for each of nested simulations. If the 'di' parameter is specified as the argument of **chimere.sh** it has a priority over those given in chimere.par.
- Most of the parameters visible to CHIMERE are specified in chimere.par in the format

  ```
  [$parameter_name] This parameter description  : Value1, Val2,..  ValN
  ```

  All parameters initialized this way will be visible to the scripts of CHIMERE during simulations.
- Simulation parameters, such as lab, nested, dom, etc., are given as comma-separated values after the colon character (":") in chimere.par. Each column of values corresponds to a different simulation. The user can run multiple simulations with a single call to **chimere.sh**. The script will subsequently run simulations with parameters defined by the columns whose numbers are listed in the "RUNS" line in the beginning of chimere.par. This is useful when running nested simulations: e.g., the first column corresponds to a course domain, while the second one specifies the fine domain. If for some parameter the number of comma-separated values is less than the number of the simulation requested, the last comma-separated value will be used for that simulation. For instance, you would typically save concentrations to the restart file *end....nc* at the same frequency for all your simulations, thus having only one value of the *$nsconcs* parameter.
- Analysis or forecast mode? ($forecast = 0 or 1) If simulation timing parameters (di, de, dib, deb, dim, dem, dibm, debm) are set to 0 in chimere.par, they will be automatically redefined in **scripts/check-dates.sh** according to the value of the *$forecast* parameter.
  - ◇ In the analysis mode ($forecast = 0), the run duration is 'ndays', from 'di' to 'di'+'ndays'-1. If a previous simulation is used to force the current one (with initial conditions), it is assumed to have the same duration 'ndays' and to span from 'di'-'ndays' to 'di'-1.
  - ◇ In the forecast mode ($forecast = 1), 'ndays' refers to the maximum forecast time, and the whole simulation period is from 'di' to 'di'+'ndays', i.e., 'ndays'+1. The previous simulation used to force the current one spans from 'di'-1 to 'di'+'ndays'-1.
  - ◇ Typical 'ndays' value is 5 days for an analysis run and 4 days for a forecast simulation.

- Compilation and execution flags. The user specifies whether to run various CHIMERE components using the following flags :

Flag	Action	Script in the **scripts/** directory	Chimere component(s)
imakecompil	Model compilation	chimere-compil.sh	
imakemeteo	Meteorological interface	chimere-meteo.sh	interf-<meteo> and chimere.e
imakeaemis	Anthropogenic emissions	chimere-aemis.sh	prepemis.e
imakedust	Dust emissions	chimere-run.sh	chimere.e
imakefemis	Fire emissions	chimere-aemis.sh	prepemis.e
iusebound	Inititial and boundary conditions	chimere-bound.sh	prep_bc.e/prep_chimere.e
imakerun	Running Chimere	chimere-run.sh	chimere.e

These flags can be either 1 or 0 meaning to launch or not the corresponding pre-processor.
Besides, most of the flags can also have the value of 2. In this case the pre-processor will be launched only if its output file is required and does not already exist. These output files and directories are also specified in chimere.par.
The directory specified by the $datadir parameter can be used to store dynamic pre-processor files ($exdomout, $fnemisa, $fnemisb, etc.).
The $iusebemis and $iusedust flags determine whether the simulation needs biogenic emissions and dust species, respectively. The $imakedust flag determines whether to generate dust emissions in the model core (chimere.e). Note that $iusebemis and $iusedust flags along with the $imakerun flag use the same model component (chimere.e). They are related to different parts of the code and are independent. For instance, setting $iusedust to 1 and $imakerun to 0 will launch **chimere-run.sh** and chimere.e, so that dust emissions will be computed, but not the model time integration loop.

Here is the listing of the parameter file chimere.par:

```
#=======================================================================
#    CHIMERE Modeling System Configuration file
#    For model code & data downloads, updates, news, and documentation
#    see http://www.lmd.polytechnique.fr/chimere
#=======================================================================
# => The variables mentioned here with the '$' sign (e.g., $dom) can be further used in expressions
#  - given they have been defined BEFORE they are used ! Otherwise -> empty string instead!
#
# => For dates arithmetic, you can use expressions like (($di + 1)) or (($deb - 1)).
#    They will be replaced by valid bash "date" commands with the %Y%m%d format
#
# => Valid bash commands can also be used, e.g., $(date -u -d "${di} ${ndays} days" +%Y-%m-%d)
#
# => ${chimere_root} is where your source chimere files are
#
# List the simulations to run separated by whitespace in the next line:
#-----------------------------
      runs :  1
#-----------------------------
#-------------------------------------------
#  Separate parameters for multiple runs with commas, e.g., Nested... : no, yes
#  If there are less values than run number (e.g., 2 columns but run 3 is requested) -> last given
#  So be careful!
#-------------------------------------------
   # Date/Time management
   [$forecast] Forecast(1) or analysis(0) run                 : 0
   [$di]       CHIMERE run Start Date                         : 20090312 # Overridden by chimere.s
   [$ndays]    CHIMERE run Duration (0 = auto)                : 8
   [$de]       CHIMERE run End Date (0 = auto)                : 0
   [$dib]      CHIMERE prev. run Start Date (0 = auto)        : 0
   [$deb]      CHIMERE previous run End Date (0 = auto)       : 0
   [$dim]      Meteo driver Start Date  (0 = auto)            : (($di - 1))
   [$dem]      Meteo driver End Date  (0 = auto)              : (($de + 1))
```

```
[$dibm]     Meteo drv prev run Strt Date (0 = auto)         : (($dib - 2))
[$debm]     Meteo drvr prev run End Date (0 = auto)         : (($deb + 2))

# CHIMERE Simulation Domain
[$nested]               Nested run? (yes/no)                : no, yes
[$tonest]               Output will be used for nesting?    : no, no
[$dom]                  CHIMERE domain                      : CONT5, IDF15C
[$nzdoms]               Number of parallel zonal subdomains : 5
[$nmdoms]               Number of parallel merid subdomains : 3
[$nlayer_chimere]       Number of vertical layers           : 8
[$top_chimere_pressure] Top layer pressure (mbar)           : 500
[$first_layer_pressure] First layer pressure (sigma * 1e3)  : 997

# Meteorology Driver
[$online]   on-line [1] or off-line [0] modeling            : 0
[$meteo]    Meteo driver (WRF,MM5,ecm)                      : WRF
[$metdom]   Meteo driver domain                             : d01, d02

# Simulation Output Files
[$lab]      Simulation label                                : Test, TestNest
# Test case for winter-time PM pollution episode
[$clab]     Coarse domain label                             : none, Test
[$lab1]     Simulation label (to use its data)              : #
[$levout]   Number of layers in output file                 : 8
[$accur]    Output species detailed (low/full)              : low
[$nsconcs]  Conc. save freq. (hr), file end...              : 24
[$nsdepos]  - Cumulated deposition, file dep...             : 12
[$sim]      Current run label (output files' ending)        : ${di}_${de}_${lab}
[$sim1]     Label of the run to use its data                : ${di}_${de}
[$psim]     Previous run label                              : ${dib}_${deb}_${lab}

# Emissions
[$emis]               Anthropogenic emission source         : emep, emep
[$surface_emissions]     Use surface emissions? (1/0)       : 1, 1
[$point_emissions]       Use point emissions?   (1/0)       : 0
[$fire_emissions]        Use fire emissions?    (1/0)       : 0
[$iusebemis]             Need biogenic emissions? (1/0)     : 1
[$allow_afr]          Africa: dust by wind erosion? (1/0)   : 1
# Warning: the European dust production model was fit using MM5 meteo files. Becareful when u
[$iopt_eros]          Europe: dust by wind erosion? (1/0)   : 0
[$icuth]              u* threshold estimation              : 1
[$ifluxv]             saltation/sandblasting scheme       : 2

# Boundary conditions
[$iusebound]  Use and build Initial & Boundary conditions?  : 1 #   0 - do not use; 1 - use a
                                                               #   2 - check if files exist
# Chemistry Options
[$mecachim]  Chemistry mechanism (0..3)                     : 2, 2
[$aero]      Chemically-active aerosols (1/0)               : 1
[$nbins]     Number of aerosol size sections                : 10
[$seasalt]   Include sea salts? (1/0)                       : 1
[$pops]      Include POPs? (1/0)                            : 0
[$carb]      Include carboneceous species?                  : 1
[$iusedust]  Include dust species and emissions? (1/0)      : 1
[$soatyp]    Secondary organic aerosol scheme (0..2)        : 2
[$trc]       Include tracers?                               : 0
[$nequil]    ISORROPIA coupling (1) / tabulation (0)        : 0
[$npeq]      - equilibrium calc freq (phys steps, < 5)      : 1

# Numerical solution parameters
[$phys]      Physical time steps per hour                   : 6
```

```
[$step]      Chemical steps per 1 phys. step                : 2, 4
[$ngs]       Number of Gauss-Seidel iterations              : 1, 1
[$nsu]        - during spinup                               : 5
[$irs]        - number of spinup hours                      : 1
[$iadv]      Advection scheme (0..2)                        : 2
[$iadvv]     Vertical advection scheme (0..1)               : 1

# Radiative processes
[$ifastj]   0 for old photorates 1 for fastj                : 1

# CHIMERE Subgrid Processes
[$ideepconv]   Deep convection activation (1/0)             : 1
[$urbancorr]   Urban correction [1] or not [0]              : 0

# Flags whether to run individual dynamic interfaces and the Core
[$imakecompil] Compile dynamic interfaces & core ?  : 1  #   Attention: if you change nzdoms or
[$imakemeteo]  Run meteo interface? (0-2)           : 1 #   0 - do not run; 1 - run; 2 - run onl
[$imakeaemis]  Build anthropogenic emissions? (0-2) : 1 #   0 - do not build; 1 - build; 2 - bui
[$imakefemis]  Build fire emissions? (0-2)          : 0 #   0 - do not build; 1 - build; 2 - bui
[$imakedust]   Build dust emissions? (0-1)          : 1 #   0 - do not build; 1 - build
[$imakerun]    Run Chemistry-Transport? (0-1)       : 1

#-------------------------------------------------------------------------------------------
#         Directories and files (Absolute PATHs here! No stuff like ../../OUTPUTS !!)
#-------------------------------------------------------------------------------------------

# ---------------- Simulation Output -----------------
[$simuldir]      Simulation output                        : ${chimere_root}/../BIGFILES/OUTPUTS/
[$csimuldir]     Course run output (for nested run BC)    : ${simuldir}/../${clab}
[$psimuldir]     Previous run output (if continue)        : $simuldir
[$tmplab]        Label for date/time of script run        : $(date +%Y%m%d_%H-%M)
[$chimere_tmp]   Temporary directory                      : ${simuldir}/tmp${di}-${lab}_${tmplab

# ------------------- Static Data ------------------------

[$bigfilesdir]   Big files (AEROMIN.bin, etc)             : ${chimere_root}/../BIGFILES
[$iland_cover]   Land Cover DB, GLCF(1)/Globcover(2)      : 1
[$landcover_dir] Land Cover directory                                 : ${bigfilesdir}/LANDCOV
[$megan_data]    MEGAN data root                                      : ${bigfilesdir}/MEGAN
[$bcdir]         Boundary conditions                                  : ${bigfilesdir}
[$bcgas]         BC Gaseous Species                                   : LMDz4_INCA3_96x95x19_v
[$bcgasdt]       No gas bc (0), Climatological (1) or time varying  (2) : 1
[$bcaer]         BC non-dust  Aerosols                                : LMDz4_INCA3_96x95x19_v
[$bcaerdt]       No aer bc (0), Climatological (1) or time varying  (2) : 1
[$bcdust]        BC Dusts                                             : GOCART
[$bcdustdt]      No dust bc (0), Climatological (1), time varying  (2)  : 1

# ------------- Dynamic Pre-processors' Data  ------------

## --------------- INPUT -----------------------------------
[$meteo_DIR]        Meteo driver output dir              : ${bigfilesdir}/TEST/METEO
[$meteo_file]       Meteo file                           : # ${meteo_DIR}/wrfout_${metdom}_$(da
[$meteo_nfile]      -"- next file (if WRF continuous run) : # ${meteo_DIR}/wrfout_${metdom}_$(da
[$emissdir]         Anthropic emission Dir (from Stage 1) : ${bigfilesdir}/TEST/EMIS
[$fire_emissdir]    FIRE emission Dir (from Stage 1)      : ${bigfilesdir}/FIREMIS

## --------------- OUTPUT (and possibly input for future runs)
[$datadir]          Pre-processors input/output directory : ${simuldir}/data_${dom}_${lab}
[$metdir]           Dir to store exdomout file            : ${simuldir}/../METEO.${dom}
[$fnmeteo]          Meteo out file on chimere 3D grid     : ${simuldir}/meteo.${sim}.nc
[$exdomout]         METEO file name                       : ${metdir}/exdomout.${sim1}.nc
```

```
   [$aemisdir]         Dir to store anthrpc emiss (stage 2)  : ${simuldir}/../AEMIS
   [$fnemisa]          Anthropic emiss. File (from Stage 2)  : ${aemisdir}/AEMISSIONS.${sim1}.nc
   [$fnemisf]          Fires emiss. File (from Stage 2)      : ${datadir}/FEMISSIONS.${sim}.nc
   [$fnemisb]          Biogenic emission File                : ${datadir}/BEMISSIONS.${sim}.nc
   [$fnemisd]          Dust emission File                    : ${datadir}/DEMISSIONS.${sim}.nc
   [$iniboundir]       Dir to store INI/BOUND fileS          : ${simuldir}/../INIBOUN.${dom}.${n
   [$fnbounconc]       Bondary concentrations file           : ${iniboundir}/BOUN_CONCS.${sim1}.
   [$fniniconc]        Initial concentrations file           : ${iniboundir}/INI_CONCS.${sim1}.n

   # ------------ Miscellaneous -----------------------------
   [$garbagedir]       Log files (compilation)               : ${chimere_root}/compilogs
   [$clean]            Clean mode                            : full # full, light, or none

#=====================================================================
#                          CHIMERE PARAMETERS SHORT DESCRIPTION
#                        SEE CHIMERE DOCUMENTATION FOR MORE DETAIL
#                          ---------------------------
#  SOFTWARE REQUIRED: gawk, gmake, netcdf, lam-mpi or openmpi
#   A Fortran 90 compiler: CHIMERE has been tested with:
#    ifort, pgf90, g95, xlf95
#
#  *** TESTED on architectures: i386/GNU-Linux, x86_64/GNU-Linux, IA64/GNU-Linux
#       and power4/AIX-5L
#
#=====================================================================
# emis=std
#       Anthropic emission interface: std only available at present
#       User can define its own interface. This assumes the
#       definition of command lines added below below the
#       comment "Hourly anthropic emissions"
#       std emissions are given for each model species in an ascii
#       files containing 3 types of day per month and 12 months.
#=====================================================================
# Management of the temporary directory:   chimere_tmp
#       All operations are done in a temporary directory.
#       CHIMERE_TMP is the temporary directory. Give a name where
#       there is a lot of temporary disk space
#       The size of the directory is typically 100 mo but
#       can be much more in high-resolution simulations
#       CHIMERE is executed in this directory.
#       !!!! This name must be an absolute path (not ./mydir ...) !!!!
#       By setting a CHIMERE_TMP directory name that depends
#       on process number ($$) or current date/time (by default),
#       it is possible to perform several simulations simultaneously
#       without undesired interactions
########################################
# Chemical parameters of the simulation #
########################################
# mecachim:
#  [0] : no gas phase chemistry
#  [1] : melchior complete
#  [2] : melchior reduced
#  [3] : SAPRC-07A
# accur=low or full  can be used for nesting
#  low resolution (main components with families)
#  full resolution (all components with families. used for nesting)
# nbins: How many bins for aerosols
#    The cut off diameters 2.5 and 10 um are respected.
#    You can change the parameter dmax in ./chemprep/chemprep.univ.sh in order to adapt the
#    size distribution. This script is adapted for nbins=4, 6, 12 (nbins=6 is recommanded)
# Aerosols: aero flag
```

```
#  [0] : no NO3, NH4, SO4, PPM, Sec. Org. Aer., WATER
#  [1] : Minimal configuration with NO3, NH4, SO4, PPM, Sec. Org. Aer., WATER
# Sea salt aerosols: seasalt flag
#  [0] : none
#  [1] : inert sea salts
#  [2] : active sea salts (reaction with chemistry), not fully validated
# iusedust flag:
#  [0] : none
#  [1] : yes, these dusts are considered as emitted within the domain
# pops flag: Persistent Organic Pollutants: =1 only if mecachim>0 and aero=1
#  [0] : none
#  [1] : yes , only three PAHs available : BaP, BbF, BkF (not fully validated)
# Output species accuracy
# soatyp flag: Secondary Organic Chemistry chemistry
# [0] : no SOA chemistry
# [1] : simple scheme
# [2] : medium scheme
# [3] : complex scheme
# carb flag: Primary carbonaceous species (OCAR  : Organic material, BCAR : Black carbon)
#  [0] : no
#  [1] : yes
# soatyp flag: Secondary Organic Chemistry chemistry
#      soatyp>0 only if aero = 1
########################################
# Physical parameters
# phys=6        Frequency of physics calculation (number per hour)
#               It could be automatically optimized during the preprocessing stage
# step=1        Refined time step relative to physics calculation
#               1/(phys*step) is the time step in hours
#               Down to 1/4 degree resolution, phys=6 and step=1 is fine
#               For finer grids (5-10 kms), take at least step=4
#               For grids of 2-5 kms, try step=6 or more
#               nzdoms: number of MPI subdomains in zonal direction, in case of parallel execution
#               nmdoms: number of MPI subdomains in meridian direction.
# lab           Choose a label to uniquely identify this run
# clab          Same for coarse domain if necessary
# meteo         Type of meteo
# metdom        Name of the meteorological domain
# nested        "yes" if your simulation needs a coarse CHIMERE run
# tonest        "yes" if your simulation drives a nest run
# dom           Name of the CHIMERE domain as specified in file names of the "domains" directory
# phys          Frequency of physics calculation (number per hour)
# ideepconv
#      0 : No deep convection; 1 : Select deep convection automatically according resolution
# iadv=2    horizontal advection    0 : For upwind, 1 : for PPM, 2 : for VanLeer
# iadvv=1   vertical advection      0 : for upwind, 1 : for VanLeer
########################################
# simuldir = output directory
#    If this run is a continuation one, initial conditions will be
#    obtained from the "end" file in this directory in the directory "psimuldir"
########################################
```

2.4 Direct run outputs

2.4.1 The output on screen

The outputs on screen give the correct reading of input file or not, shows the meteorological pre-processing phase and the Chimere simulation itself by printing some variables to give informations about the run. The

choices of outputs are:

- The current date in format `yyyymmddhh`
- The first two species defined in the **OUTPUT_SPECIES** file
- The 2m temperature (in Kelvin)
- The boundary layer height (in meters)
- The vertical wind speed (in m/s) of the first vertical level (typically between 0 to 30 m AGL).
- The integration time-step (in mn)
- The percentage of simulation done (in %)
- The CPU used for each hour of simulation (in mn)

All these values are given for a cell located at the middle of the horizontal domain. The results is something like:

```
DATE           O3      NO2     T_2m(K)     PBLH(m)    w(m/s)     DT(mn)     run(%)     CPU(mn)
2013062600    52.3     0.0       30.5       472.    0.69E-03        5.         0.       13.4
2013062601    52.3     0.0       30.0       470.    0.74E-03       10.         1.       75.8
```

2.4.2 The output files

Four different output files are delivered:

- **out**.nc**: contains concentrations fields
- **meteo**.nc**: contains meteorology regridded on the CHIMERE mesh
- **dep**.nc**: contains dry and wet deposition fluxes
- **ini**.nc** and **end**.nc**: for initialization and restart

They are encoded in the NetCDF format, which presents the following advantages:

- portability among different architectures of computers
- self-documentation since a lot of meta-data are included in the file itself
- direct access
- compatibility with many free or commercial post-processing tools

Moreover, CHIMERE uses a NetCDF convention derived from the one used in NCAR'S WRF mesocscale modelling system, simplifying the toolset for post-processing.

The chemical fields outputs on file "out.[label].nc"

Three-dimensional chemical fields are written in an output **out.[label].nc** file. The selected species correspond to those listed in the **OUTPUT_SPECIES** parameter file. Default concentrations values are expressed in ppb. These values may be transformed into μg.m^{-3} if the molar mass of each species is added as a second column in the parameter files *OUTPUT_SPECIES...* located in the chemprep directory (the default value is zero). In case of use of FastJX for the photolysis rates, an output of the optical depth for clouds and aerosols is automatically added as output in the **out.[label].nc** file.
example: In the file **chemprep/data/output_species/OUTPUT_SPECIES...**: If the line is "`O3 0`", ozone results will be in ppb. If the line is "`O3 48`", the results will be in μg.m^{-3}.

Selected meteorological and turbulence related fields "meteo.[label].nc"

Hourly 2-D and 3-D meteorological and turbulence related fields calculated on the CHIMERE grid are provided in the output *meteo* file. For an "off-line" run meteorological fields are calculated with the corresponding meteorological model (e.g. WRF) and then interpolated on the CHIMERE grid. Turbulence related fields are

calculated with the "diagmet" program now embedded in the CHIMERE core. The variables included in the *meteo* file are listed in Table 2.2.

Model Variable	Variable Description	Units
Times	Date string	NA
lon	Longitude	degrees-east
lat	Latitude	degrees-north
2-D Variables		
hght	Boundary Layer Height	m
usta	Friction Velocity u_*	m/s
uwta	Convection Velocity w_* m/s	
aerr	Aerodynamic Resistance	s/m
sshf	Surface Heat Flux	W/m^2
slhf	Surface Latent Heat Flux	W/m^2
u10m	10m Zonal Wind Speed	m/s
v10m	10m Meridional Wind Speed	m/s
w10m	10m Vertical Wind Speed	m/s
tem2	2m Temperature	K
soim	Soil Moisture	m^3/m^3
sreh	Surface relative humidity	%
pscf	Surface Pressure	Pa
swrd	Short Wave Radiation	W/m^2
atte	Radiation Attenuation Coefficient	[0-1]
copc	Convective precipitation	kg/m^2/h
lspc	Large Scale precipitation	kg/m^2/h
toppc	Total precipitation	kg/m^2/h

Model Variable	Variable Description	Units
3-D Variables		
hlay	Top of Layers' Height	m
thlay	Layers' Thickness	m
winz	Zonal Wind Speed	m/s
winm	Meridional Wind Speed	m/s
winw	Vertical Wind Speed	m/s
temp	Temperature	K
pres	Pression	Pa
airm	Air Density	kg/m^3
sphu	Specific Humidity	kg/kg
clwc	Liquid (+ice) Water Content	kg/kg
cliq	Cloud Liquid Water Mixing Ratio	kg/kg
cice	Ice Liquid Water Mixing Ratio	kg/kg
rain	Rain Water Mixing Ratio	kg/kg
kzzz	Vertical Diffusion Coefficient	m^2/s^2
Deep convection related fields		
dpeu	Entrainement in Updraft	kg/m^2/s
dped	Entrainement in Downdraft	kg/m^2/s
dpdu	Detrainement in Updraft	kg/m^2/s
dpdd	Detrainement in Downdraft	kg/m^2/s
flxu	Upward Mass Flux	kg/m^2/s
flxd	Downward Mass Flux	kg/m^2/s

Table 2.2: *Variables in the METEO output file.*

The deposition fields outputs on file "dep.[label].nc"

This file contains fluxes integrated over the chemical time-step duration. The calculations are done in the model core and are written in independent files. For the dry deposition flux, only the first vertical cell is taken into account. On the other hand, for the wet deposition, fluxes are sumed up the whole column since, in the model, each vertical level may contribute to a net sink. Units of these two integrated fluxes are g/cm^2.

The restart fields outputs on file "end.[label].nc"

The structure of this file is described in **Appendix G.7, p.175**. The main goal of this file is to save all concentrations fields every 24h. For example, for a second run following in time the first one, this "end..." file will be link to a "ini..." file and thus used to give realistic initial conditions during the restart.

2.5 Post-processing the results

Apart some configuration files and static data files written in ASCII code, all the input and output files of the model are written in the NetCDF format, using conventions similar to the WRF conventions. Thus the tools described below may be used to process almost any CHIMERE NetCDF file, including meteo files. CHIMERE NetCDF files are suffixed with **.nc**.
You can use the *CHIMPLOT* program to visualize your data, either interactively or producing plots automatically. Interactive visualization is done using a simple graphical user interface running *chimplot.py*. To automate your work you can save a *Template* after plotting a figure and then run a command-line version *chimplotcm.py* with a datafile of interest and the generated *Template*. There are multiple options running *chimplotcm.py*. Please refer to the *CHIMPLOT* web site for installation and usage guidelines:

`http://www.lmd.polytechnique.fr/chimplot`.

2.6 Some figures to validate your first CHIMERE simulation for the 2009 Test Case

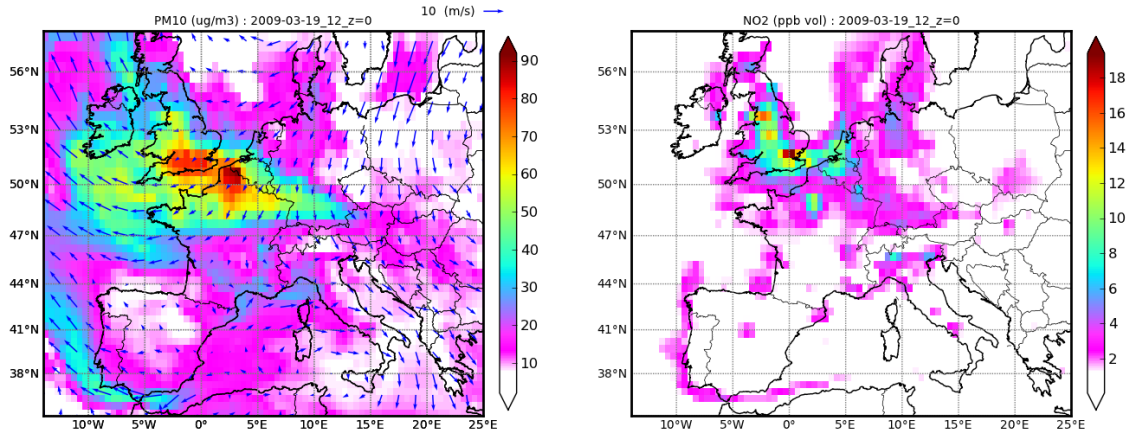
Here we present some figures from the March 2009 test case described in §2. If you used the data available on the CHIMERE website for this test case (the TEST directory when using the chimere-download.sh script), and the simulation parameters set by default in chimere.par, then you should obtain the same figures. The figures shown here were made with *CHIMPLOT*.
To quickly plot these figures with *CHIMPLOT* you can execute the following few lines of *bash* code from the main CHIMPLOT directory ***chimplot***. The code runs the command-line utility *chimplotcm.py*. Sample *CHIMPLOT* Templates PM10_test.par and wind_test.par are provided with the Test Case and can be downloaded on the CHIMERE download page `http://www.lmd.polytechnique.fr/chimere/download.php`.

```
chimfile=OUTPUTS/Test/out.20090312_20090319_Test.nc
metfile=OUTPUTS/Test/meteo.20090312_20090319_Test.nc
chimplotcm.py -fig PM10.png "$chimfile $metfile" "PM10_test.par wind_test.par"
```

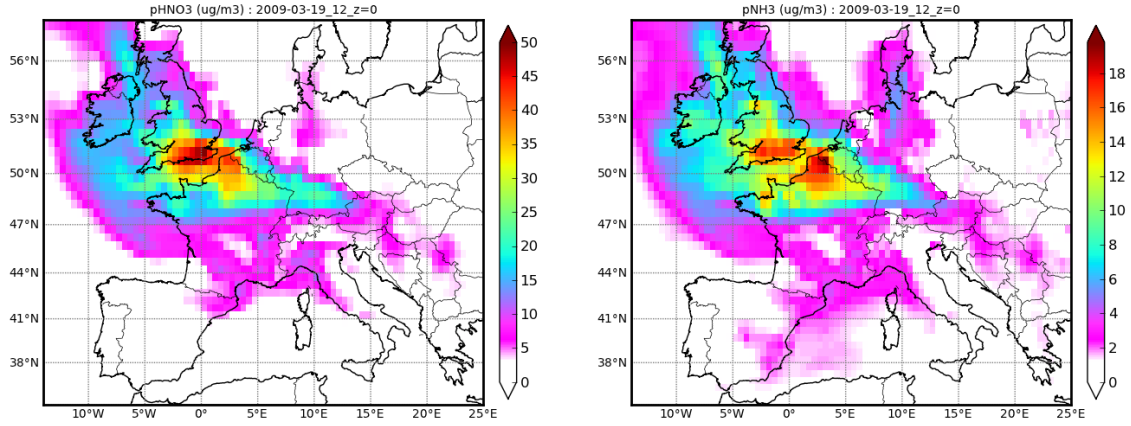
To make other plots automatically from the template PM10_test.par:

```
for v in NO2 pHNO3 pNH3 pH2SO4 pPPM ; do
   chimplotcm.py -varname "['${v}']" -fig ${v}.png ${chimfile} PM10_test.par
done
```

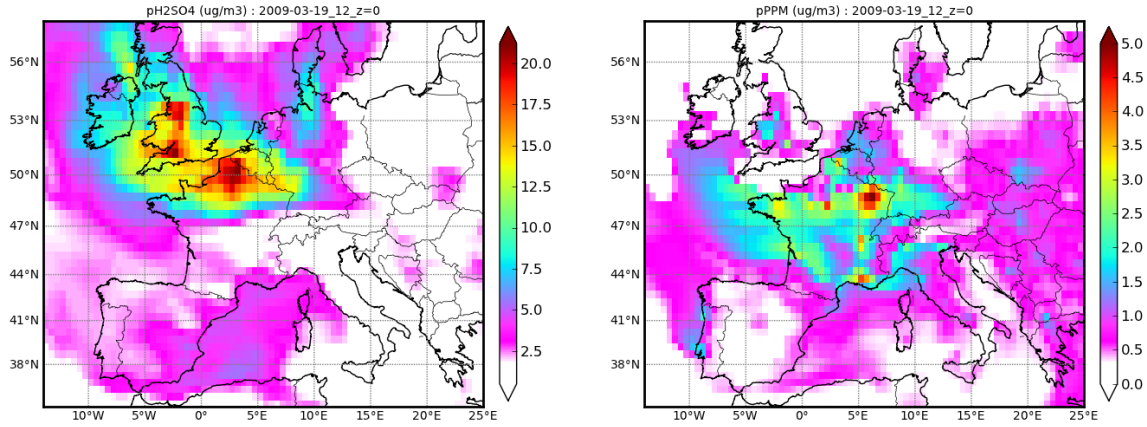
The code above supposes you put the CHIMPLOT template into the BIGFILES directory containing the OUTPUT directory where the out.*nc file is written.
Note: the "-varname" option can only be used with a single template at a time, therefore the second of the above examples (the one with a loop over species) will plot concentration maps without wind vectors. If you wanted to automate the first of the above examples, please check the templates/mk_templ.py script for template generation.



(a) PM_{10} (μg m^{-3}) and NO_2 (ppb) concentrations on March 19, 2009 at 12h



(b) HNO_3 and NH_3 concentrations (μg m^{-3}) on March 19, 2009 at 12h



(c) $H2SO_4$ and PPM concentrations (μg m^{-3}) on March 19, 2009 at 12h

Figure 2.1: Figures to validate the March 2009 Test Case simulation

Chapter 3

CHIMERE model source code

3.1 CHIMERE general code structure

The general structure of the CHIMERE model is shown in Figure 3.1. Before running the model core (chimere.e executable), a few pre-processors need to prepare the model input data. These are:

- Data generated once per simulation domain ${dom} and put to the **domains/${dom}** directory:
  - ◇ Domain horizontal and vertical coordinates (**domains/HCOORD/COORD_${dom}** and **domains/VCOORD/VCOORD_${nlayer_chimere}_${first_layer_pressure}_${top_chimere_pressure}**, see p. 47)
  - ◇ Land-use categories: (**LANDUSE_[database]_${dom}** in ascii format used in chimere and **LANDUSE_[database]_${dom}.nc** to visualize, see p. 48)
  - ◇ Biogenic emission factors and leaf-area indices to generate the biogenic emissions with the MEGAN model parameterizations (**EFMAP_LAI_${dom}.nc**, see p. 62)
- Data generated once per specified chemistry/aerosol configuration
  - ◇ Chemistry and aerosol parameters (the **chemprep/inputdataXXXX.X** directory, see p. 53)
- Data from the dynamic pre-processors, often generated for every CHIMERE simulation, but any of them can be re-used for further simulations by adjusting appropriate flags in the top calling script chimere.sh. The following data are put to the CHIMERE data directory **${datadir}** :
  - ◇ Emissions: biogenic (**BEMISSIONS.${sim}.nc**, p. 62), anthropogenic (**AEMISSIONS.${sim}.nc**, p. 59), fire emissions (**FEMISSIONS.${sim}.nc**, p. 62) and dust (**DEMISSIONS.${sim}.nc**, p. 63)
  - ◇ Meteorological variables (**exdomout.${sim}.nc**, p. 83)
  - ◇ Boundary and initial conditions: **BOUN_CONCS.${sim}.nc-*** for boundary (p. 77) and **INI_CONCS.${sim}.nc-*** or **end.${sim}.nc** in output directory for initial conditions, depending on whether or not the simulation starts from a restart file (p. 82)

CHIMERE simulation output consists of four NetCDF files in **${simuldir}**:

- Output concentrations **out.${sim}.nc**
- Restart concentrations **end.${sim}.nc**
- Depositions **dep.${sim}.nc**
- Meteorological fields diagnosed by CHIMERE **meteo.${sim}.nc** (p. 83)

Each pre-processor prepares its data on the CHIMERE grid and for the time period and region to simulate. The meteorological pre-processor is separated from the rest of the CHIMERE code and is found in the **meteo/** directory. It prepares meteorological data in the CHIMERE format on horintal grid (see p. 83). The domain preprocessor is also separated and is found in the **domains/** directory (see p. 47). The chemical preprocessor is located in the **chemprep/** directory (see p. 53). The rest of the CHIMERE code is in the **src/** directory. The model core organization is described below. The main FORTRAN program **src/main/chimere.F90** initializes and reads all data and then integrates the model for the required time period. The output files are then

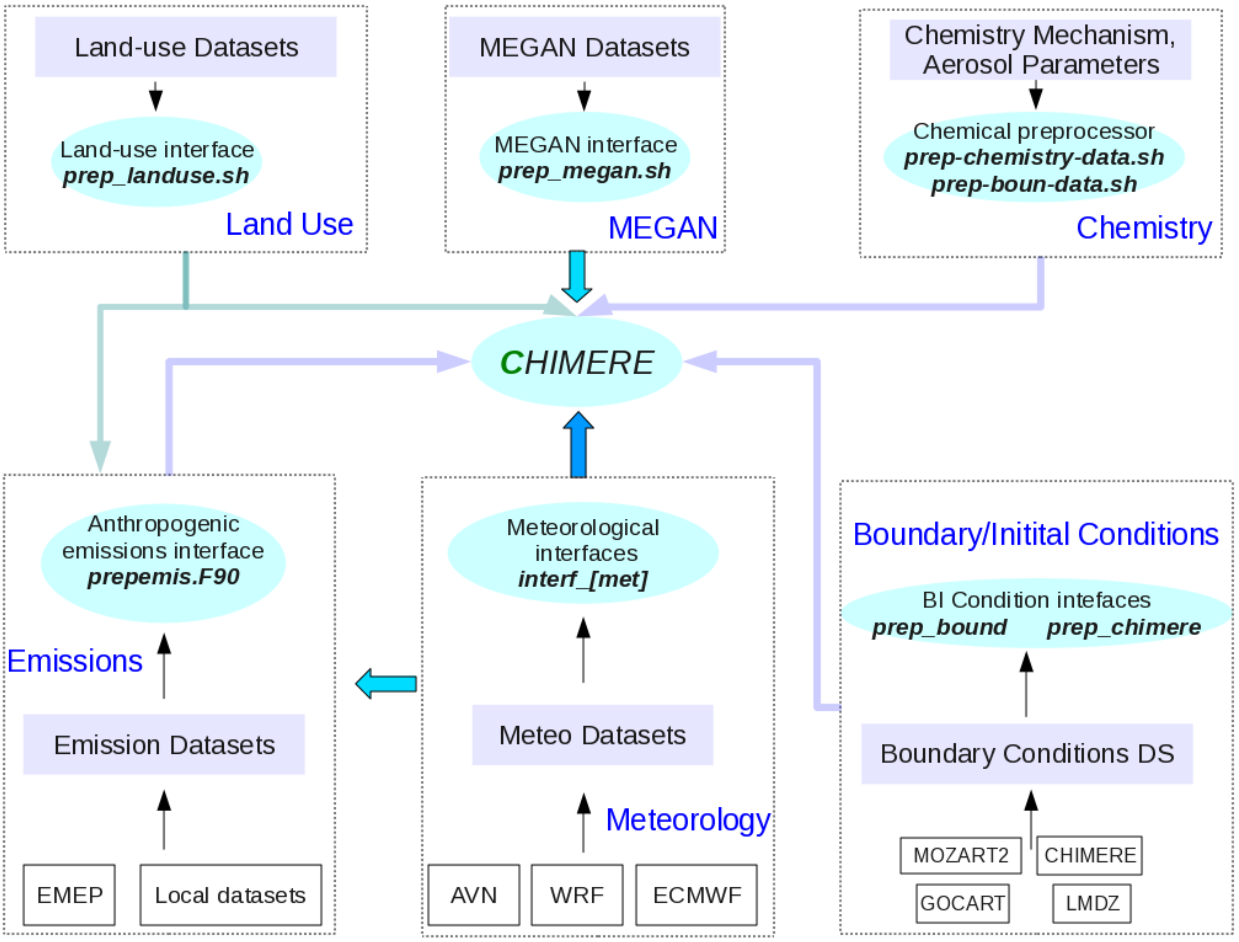


Figure 3.1: *General structure of CHIMERE model*

available for post-processing. The whole system is driven by the top calling script chimere.sh, which :

- reads parameters of the simulation
- links all necessary files into a **temporary directory** where all programs are executed
- compiles all necessary code
- runs the 3 dynamic pre-processors (meteo, emission and boundary conditions)
- runs the model itself

Before running the top calling script, it must be edited to specify model options and directories.
Model directories are specified in two different files: data directories are given in chimere.par, while system directories, such as PATHs to NetCDF and MPI libraries, are given in the file mychimere.sh. The latter is activated with a *source* command inside the top calling script chimere.sh and the compile script. This is done to simplify the model portability between different computers: the user can create one mychimere.[System/Compiler].sh version for each computer, each with its own system PATHs and architecture parameters, and then just create a symbolic link mychimere.sh -> mychimere.[System/Compiler].sh every time one needs to run CHIMERE on one of those computers. This allows to avoid editting system parameters every time the model is run on a different computer or with a different compiler or MPI library.
The script config.sh automates the task of editing mychimere.sh by searching the installed libraries and Fortran compilers and guiding the User to choose between available versions. When making the choices **rougeit is up**

to User to ensure that all the components are compiled with the same Fortran compiler! After the script has finished its work a new version of mychimere.sh is created corresponding to the desired configuration.

3.2 CHIMERE time integration

CHIMERE model is splitted into two main parts: a general initialization phase and the time integrations of all chemistry-transport equations over the whole simulation duration (Figure 3.2).

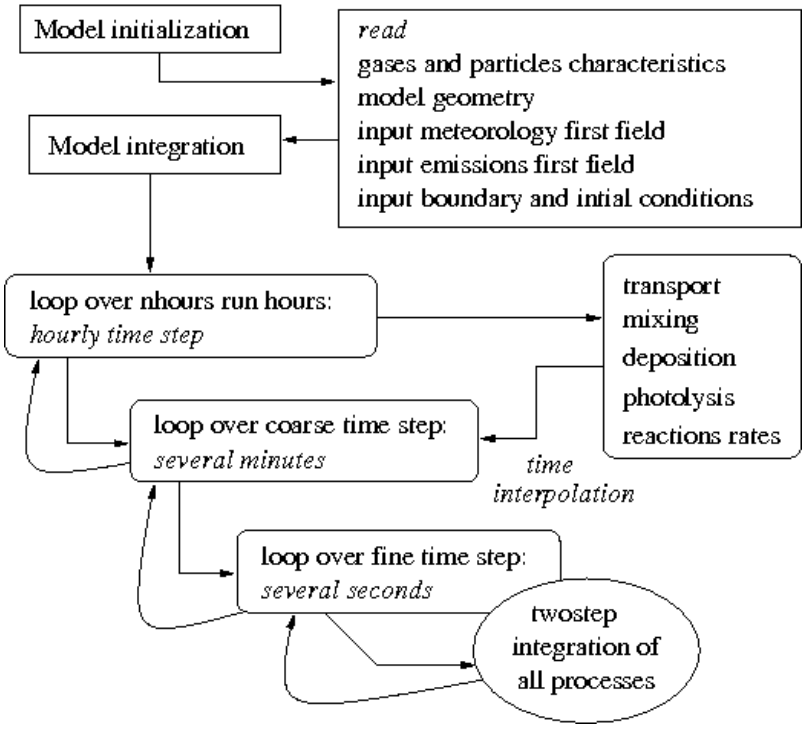


Figure 3.2: *General CHIMERE structure for time integration of all processes*

- The **initialization phase** is dedicated to the read of all inpout parameters as well as the two first meteorological and emissions fields (in order to start the run with realistic meteorological and concentrations fields).
- The **time integration** phase is itself splitted into three parts:
  - A predefined **hourly time-step**. This time step is fixed and is due to the fact that meteorological and emissions data have to be, at least, hourly provided.
  - A **user's defined coarse time step 'nphour'**, corresponding to the time interpolation of "physical" parameters, such as wind, temperature, reactions rates etc. A second time-step is dynamically estimated in the meteorological pre-processor. Using the horizontal wind field, the vertical velocity and the entrainment in the updraft (in case of deep convection), a recommended time step is estimated. During the run, if the user time step is too low, the model time integration is increase to reach the recommended value. Figure 3.3 presents preconised 'number of model integration per hor' for the CFL estimated only with the horizontal wind (u), the vertical wind (w) and the entraiment in the updraft (up). For a test run over the CONT5 domain and 10 vertical levels (from surface to 500hPa), with a user time step of 10mn (i.e nphour=6), we can see than deep convection requires to increase the time resolution up to 6mn (i.e nphour=10). If the user's defined time-step is lower that the recommended one, the user's choice is applied (even if this is not the optimal choice).

- A **user's defined "fine" time step 'ichemstep'**: this corresponds to the integration of the chemical mechanism, including delta concentrations due to all processes. This is achieved by the two-step scheme. Due to the stiffness of the chemical system to solve, this time step must be at least 30s (or less if possible).

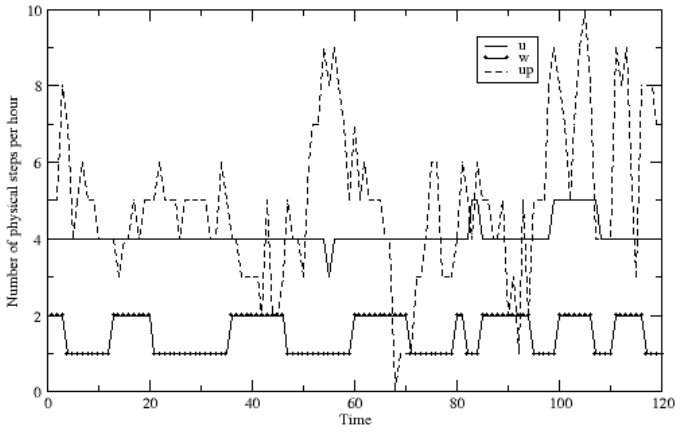


Figure 3.3: *Calculation of the number of integration steps per hour to respect the CFL over a complete 120 hours simulation.*

3.3 Directories

The ***chimere 2014b*** top directory contains individual files, the test case top calling script and subdirectories. These subdirectories are :

- chemprep : Contains data files for gas, aerosols and chemical mechanisms.
- domains/ : A subdirectory where coordinate files COORD_${dom} and land-use files LANDUSE_${dom} must be placed for each CHIMERE model domain. This directory contains also the file **domainlist.nml** where each line corresponds to a model domain.
- makefiles.hdr/ : Contains examples of Makefile headers suited for several architectures and compilers.
- meteo/ : This directory contains all the elements for the first step of meteo interfaces, *i.e.* the horizontal/time interpolation and reformatting of data. When the user starts from a new meteorological data set, a new shell script named **interf-${meteo}** along with a read/interpolate fortran routine named **prep${meteo}.F90** and the associated **Makefile-${meteo}** should be created by the user and placed in this directory. It is recommended to start from **interf-wrf**, **prepwrf.F90** and **Makefile-wrf** as templates to help creating these interface programs.
- scripts/ : Contains families of scripts pointed to by the top level script. While the top level script mainly defines variables, execution scripts in this directory perform the low-level tasks.
- src/ : Contains the source code of CHIMERE.
- util/ : Contains some utility programs.

There are other directories created when running the model:

- exe-${dom}.${nzdoms}.${nmdoms}-${nlayers} : This is where all executable files are copied. This directory used to not recompile the CHIMERE code at each run.

- tmpdir/: CHIMERE *temporary directory* defined by *$chimere_tmp* in chimere.sh. This allows several simultaneous simulations to be launched from a unique directory, provided the name of the temporary directory *$chimere_tmp* contains a unique process number (**$$** in Bourne Shell) or script execution date and time (default option in **chimere.sh**). Depending on the *clean* option in **chimere.sh**, this directory can be left after a model simulation (especially when debugging) or removed at the end of the top calling script execution. A temporary directory is created for each model run.
  Hint for developpers :
  You can `cd` to **tmpdir** to modify the model code and test your modifications. The model environment and parameters are defined in files **chimere.nml** (also known as INFOS in previous versions) and **chimere_params.F90** which remain until you erase **tmpdir**. To perform a model run, without the overhead of replaying all the meteo and boundary conditions stuff, just type:
  ```
  make && time mpirun -np N -ssi rpi sysv ./chimere.e
  ```
  with N = number of subdomains + 1
- outdir/: An *output* directory where simulation output files are placed during the run. The address of this directory is given in the top calling script (variable **$simuldir**. It does not need to be created before the run.

3.4 Model Files

3.4.1 Scripts

There is three main steps when the top-calling script chimere.sh is launched.

1. Preparation of landuse and chemical data files:
   - chimere-domain.sh prepares the domain data generated by the static pre-processors
   - util/define_geom is an utility script that defines the vertical grid. It outputs a file with hybrid sigma-p coefficients defining the grid.
   - scripts/define_params.sh calls read-params.sh and check-dates.sh to inititalize simulation parameters. It is called by chimere.sh
   - chemprep/prep-chemistry-data.sh, prep-tracer-data.sh, check_consistency.sh, and copy-chemresults.sh rebuild a chemical mechanism (see explanations p.53)
   - scripts/make-chemistry.sh is called by chimere.sh and prepares chemistry files (if not already done)
2. The sequential part scripts/chimere-step1.sh:
   - scripts/chimere-init.sh inherits the variables defined in chimere.sh and initializes other simulation parameters used by other scripts.
   - scripts/chimere-compil.sh is called to compile the model code.
   - scripts/chimere-bound.sh launches the initial / boundary conditions interfaces.
   - scripts/chimere-meteo.sh launches the meteorological interfaces.
   - scripts/chimere-aemis.sh, chimere-bemis.sh, and chimere-dust.sh perform some sanity checks and launch anthropogenic, biogenic, and dust emission interfaces, respectively.
   - scripts/chimere-run1.sh launches the model core execution for the sequantial part
3. The parallel part scripts/chimere-step1.sh:
   - scripts/chimere-step2.sh calls the parallel part of CHIMERE that requires several processors. The separation onto sequential and parallel parts is done to avoid the loss of computing time by requesting many processors on a cluster to run sequential programs.

3.4.2 Makefiles

The compilation process of most of the code in the distribution is driven by Makefiles. To ensure consistency, all Makefile call a unique top level header, **Makefile.hdr**, which deals with all the user installation details.

Makefile.hdr is in fact a symbolic link to one of the predefined headers located in **makefiles.hdr** subdirectory.

3.4.3 Meteo interface - 1st stage

The interface discribed below is for WRF, MM5 and ECMWF (noted ecm in ${meteo} in chimere.par) mesoscale modelling systems. Note that the WRF interface does not require COORD_${medom} files, since domain grid coordinates can be found in WRF output NetCDF files and ECMWF interface requires LSMORO file as described below.

I. meteo/

- compile-meteo.sh: script to compile the meteorological interface
- interf-${meteo}: scripts to run the meteorological interface

I-1. meteo/domains/MM5

- COORD_MM5${metdom}: contains the "cross" coordinates of the MM5 file.
- COORD_MM5${metdom}_DOT: contains the "dot" coordinates of the MM5 file.

I-2. meteo/domains/ecm

- LSMORO_ecm${metdom}.GRB: contains the coordinates of the ecm file, Geopotentiel and Land_sea mask at ground.

I-3. meteo/src/

- ${meteo}_consts.F90: define uniquely the physical constants used by **prepi${meteo}.F90**.
- prep${meteo}.F90: read MM5,WRF or emcwf standard output files and perform interpolations to the horizontal CHIMERE model grid. Compiled to **prep${meteo}.e** and called by the scripts **interf-${meteo}**.
- ${meteo}_par.F90: describes input and output variables for interf-${meteo}. Should be edited depending on the available variables in the meteo output file.
- prep_bilin.F90: bilinear interpolation subroutine used in the meteo interface **prep${meteo}.F90**.
- Makefile-${meteo}: Makefiles for the meteo interface compilation.
- subs.F90: contains various helper subroutines (symbolic link to ${chimere_root}/src/tools/subs.F90).
- interp_tools.F90: subroutines to calculate the weighting coefficients for horizontal interpolation (symbolic link to ${chimere_root}/modules/interp_tools.F90).
- io.F90: I/O subroutines (symbolic link to ${chimere_root}/src/tools/io.F90).
- calendar.F90: calendar subroutines (symbolic link to ${chimere_root}/src/tools/calendar.F90).
- ncvar.F90: netcdf I/O subroutines (symbolic link to ${chimere_root}/src/modules/ncvar.F90).

II. tmpdir/

- ${chimere_tmp}/meteo/metargs-${meteo}: ASCII files generated by the top calling script (**scripts/chimere-meteo.sh**). Passed to **meteo/interf-${meteo}**. Contain parameters to drive **prep${meteo}.e**.
- ${chimere_tmp}/meteo/prep${meteo}.nml: namelist generated by **meteo/interf-${meteo}** to drive **prep${meteo}.e**.
- ${datadir}/meteo/exdomout.${sim}.nc: output NetCDF file generated by **meteo/interf-${meteo}**. Contains meteo variables interpolated to CHIMERE horizontal grid.

III. util/

- make_mm5_coord: utility script allowing to extract coordinates and terrain altitude, in longitude/latitude format, of a MM5 **TERRAIN** file. Edit the script itself for giving information. The output files are **COORD_MM5${domain}** and **COORD_MM5${domain}_DOT** used by **interf-MM5**.

3.4.4 Source directories

All the model sources are available in the **src/** directory. Some sub-directories are present as follows:

1. src/ contains source subdirectories and template files
   - chimere_params.F90.sed module is a template used to build **chimere_params.F90**. It will hold compile-time parameters of the "master" namespace. Each parameter is defined by a macro, which is subsituted before compile time by the top level script.
   - worker_params.F90.sed module is a template used to build **worker_params.F90**. It will hold compile-time parameters of the 'worker' namespace. Each parameter is defined by a macro, which is subsituted before compile time by the top level script.
2. src/main contains top level programs
   - chimere.F90 is the main program. Compiled to **chimere.e** and called by the execution script.
   - integrun.F90 is the main subroutine called by **chimere.F90** for the "master" process
   - master_locvalues.F90 is a subroutine used to calculate time interpolated values in the "master" side
3. src/modules contains master-side modules
   - chimere_common.F90 module holds all the variables shared in the "master" namespace, type definitions and allocation subroutines
   - chimere_consts.F90 module holds most of the physical and mathematical constants used throughout the model
   - master_message_subs.F90 module contains a bunch of message passing subroutines, used by the "master" side
   - message_defs.F90 module holds constant indexes for message passing between master and workers
4. src/initio contains the initialization and I/O subroutines
   - ini*.F90 are initialization subroutines executed once by the "master" process
   - readhour.F90, renewhour.F90 provide the model with hourly meteo and boundary conditions, under "master" control
   - outprint.F90, write*.F90 periodically save the model results to files, under "master" control
   - other..*.F90 are helpers for initialization subroutines
5. src/model contains the code for the "workers"
   - worker.F90 is the main subroutine called by **chimere.F90** for the "worker" processes
   - worker_common.F90 module holds all the variables shared in the "worker" namespace, type definitions and allocation subroutines
   - worker_message_subs module contains a bunch of message passing subroutines, used by the "worker" side
   - other..*.F90 are the core of CHIMERE model

   Despite the capability of Fortran 95 to perform dynamic memory allocation, CHIMERE still uses static allocation, and 'common' declarations, because it proved to be significantly faster at run time.
6. src/iso contains the ISORROPIA thermodynamic model. Unmodified ISORROPIA library. Called by workers, but has its own namespace.
7. src/fastjx70b contains the Fast-JX model. Called by workers, but has its own namespace.
8. src/tools contains helpers. Some helpers, used both by master and workers.
9. src/prep contains the code to prepare emissions and boundary conditions before core model run
   - prepemis.F90 is the standard emission interface. Compiled to **prepemis.e** and called by the top calling script.
   - prep_bc.F90 is the boundary and initial conditions interface for the coarse (non-nested) runs. Compiled to **prep_bc.e** and called by the top calling script.

- prep_chimere.F90 is the boundary and initial conditions interface for the nested runs. Compiled to **prep_chimere.e** and called by the top calling script.
- prep_mie.F90 used to intialize (read inputfile) the Fast-JX model. Compiled to **prep_mie.e** and called by the top calling script

3.4.5 Dynamic files generated at runtime

All these files are created and moved into the tmpdir/ directory.

1. Dynamic parameters All these files are created and moved into the tmpdir/ directory.
   - ${chimere_tmp}/prep_bc.nml: namelist generated by the top calling script to drive **prep_bound.e**.
   - ${chimere_tmp}/prep_chimere.nml: namelist generated by the top calling script to drive **prep_chimere.e**.
   - ${chimere_tmp}/prepemis.nml: namelist generated by the top calling script to drive **prepemis.e**.
   - ${chimere_tmp}/prep_mie.nml: namelist generated by the top calling script to drive **prep_mie.e**.
   - ${chimere_tmp}/chimere.nml: namelist containing most of the runtime parameters for the model. This file was the file named INFOS in previous model versions
2. Dynamic data files All these files are created into the datadir/ directory.
   - ${datadir}/exdomout.${sim}.nc: NetCDF file generated by the first stage of the meteo interface. Contains meteo parameters interpolated to the model grid.
   - ${datadir}/AEMISSIONS.${sim}.nc: NetCDF file generated by the anthropogenic emissions interface. Contains timely anthropogenic emissions.
   - ${datadir}/BEMISSIONS.${sim}.nc: NetCDF file generated in CHIMERE to save biogenic emissions calculated during the simulation.
   - ${datadir}/FEMISSIONS.${sim}.nc: NetCDF file generated in CHIMERE to save biogenic emissions calculated during the simulation.
   - ${datadir}/BOUN_CONCS.${sim}.nc-*: NetCDF file(s) generated by the boundary/initial conditions interface. Contain timely lateral and top concentrations.
   - ${datadir}/INI_CONCS.${sim}.nc-*: NetCDF file(s) generated by the boundary/initial conditions interface. Contain initial concentrations.

3.5 Routine calls sequence

The general schematic diagram of calls of the CHIMERE model **chimere.F90** is given in Figure 3.4. Only major routines are cited, not the utility ones.

1. The main program **chimere.F90** first calls all initialization routines (in **inichimere.F90** and further calls) where all "static data" data are read and many variables defined.
2. Then it calls the integration routines **integrun.F90** and **worker.F90** which then
   (a) reads hourly data every hour (routine **readhour.F90**
   (b) loops on the coarse time step,
   (c) outputs results on files (routine **outprint.F90**) and
   (d) shifts hourly data (routine **renewhour**).
3. At each model step, one needs hourly data for the start and the end of the hour in order to linearly interpolate, for meteo data, boundary conditions and biogenic emissions. The code keeps only these two instants in memory as explained in Figure 3.5. Within the coarse time step, a call to routine **physics.F90** is made, in order to define all variables that will be taken as constants during the time step (linear interpolation of meteo data, calculation of reaction rates etc...), and a loop on the fine time step is carried out, with a call to the numerical solver **twostep.F90**.

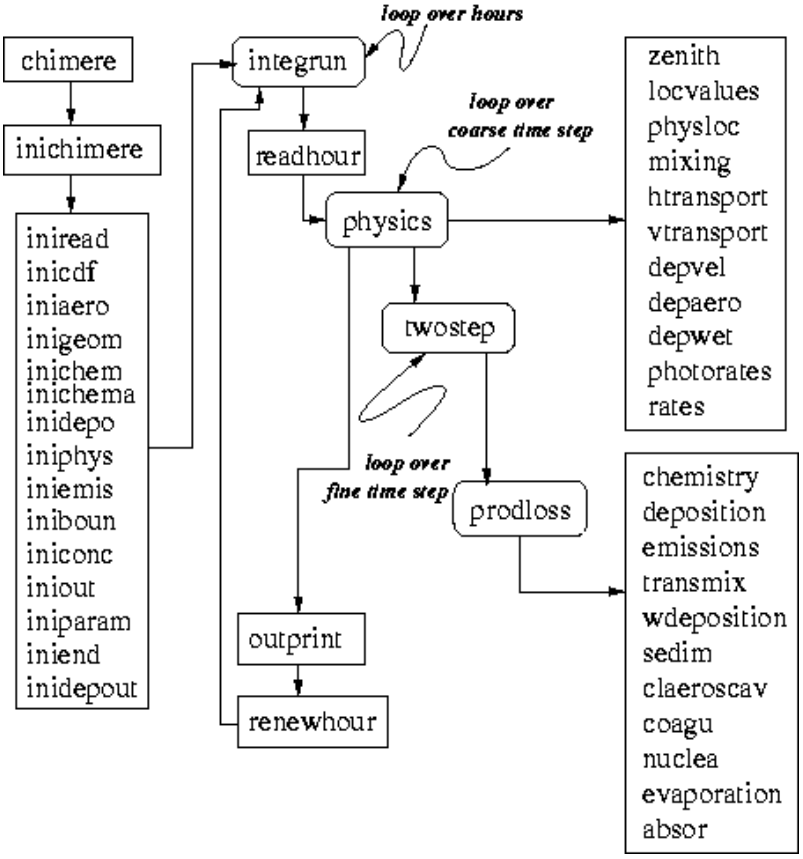


Figure 3.4: *Detailed list of CHIMERE routines and time loops*

4. The **twostep.F90** routine calls the core routine **prodloss.F90** which calculates, for all processes, the loss and production fluxes and sums them. Thus **prodloss.F90** calls **emissions.F90** (emission fluxes), **transmix.F90** (transport and mixing fluxes), **chemistry.F90** (chemical fluxes) and **deposition.F90** (deposition fluxes). The routine **transmix.F90** calculates the PPM concentrations at the boundaries with routines contained in the **ppm.F90** package.

3.6 Parallelism

3.6.1 Domains division

Only the core of the model (chimere.e) has been parallelized. The meteo and preparation interfaces remain sequential tasks.
To allow for a parallel execution of CHIMERE by several processors, the main domain is horizontally divided in rectangular subdomains. This cartesian division is performed in the main execution script, which takes as inputs the user-defined parameters **nzdoms** and **nmdoms**, numbers of subdomains in each dimension. Then the main execution script launches **nzdoms*nmdoms+1** chimere.e processes in parallel, through the MPI command

```
mpirun -np nzdoms*nmdoms+1 ./chimere.e
```

One of these processes will be called the **master**, the others will be **workers**. There are as many workers as CHIMERE subdomains.

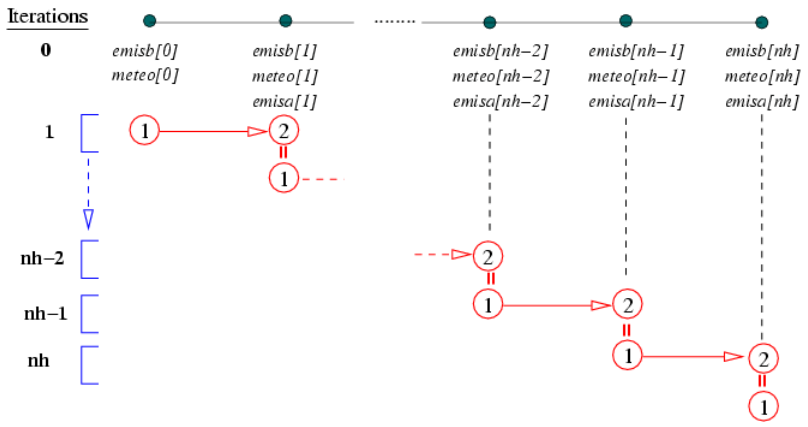


Figure 3.5: *Time processing in CHIMERE*

Remark: Only **nzdoms*nmdoms** processors are required to execute the code, because the master process is very light, and is generally working when workers are sleeping. Unless you are not limited in CPU number, don't waste a CPU for the master and declare only **nzdoms*nmdoms** in your hostlist file.

In a first order analysis, we could consider that :

1. the master performs all initializations
2. the master sends to each worker its share of data, corresponding to its subdomain
3. the workers work ...
4. the workers send their results to the master
5. the master gathers results, and saves that to output files
6. the master sends new boundary conditions to workers

This would be a beautiful simple world, with birds and flowers ...

In a second order analysis, we realize that a worker process requires not only the share of data corresponding to its subdomains, but also a stripe of boundary data belonging to its neighbours. The reason is that to calculate a target value at point **i**, you need source values at point **i-3, i-2, i-1, i, i+1, i+2, i+3** . In two dimensions, of course.
So, the algorithm becomes :

1. the master performs all initializations
2. the master sends to each worker its share of data, corresponding to its subdomain, plus a surrounding "halo"
3. the workers work, and at each fine time step, update their halo by getting it from their neighbour
4. the workers send their results to the master
5. the master gathers results, and saves that to output files
6. the master sends new boundary conditions to workers

Not so complicated, isn't it ? Let us see where the Devil is hidden ...

In fact, to calculate a target value at point **i** and time **tn+1**, you need source values at point **i-3, i-2, i-1**, at time **tn+1**, and source values **i, i+1, i+2, i+3** at time **tn**. You cannot simply calculate target values at time **tn+1** from a set of source values at time **tn**. That is, to start the calculation of the 5th line of a subdomain,

you need to know the new values of the 3 last pixels of the 5th line of its left neighbour. This is realized by setting a dependancy relationship between lines, and by copying the 3 last pixels of a line to the halo of the corresponding line in the right-hand subdomain. This copy occurs for each line of each subdomain, thus at a frequency much higher than the fine time step.

Last, and hopefully least :
What we have just explained in the previous paragraph for the **i** direction also applies to the **j** direction. The dependancy relationship in both directions leads to a straightforward conclusion : *it is impossible to parallelize CHIMERE*.
We have practically solved the problem by starting the computation of each row of subdomains as if it were an independant domain, with no upper and lower neighbour, exactly as we do for the main domain in the sequential scheme. But at the end of each fine time step, we update their upper and lower halos. This provides a reasonnable smoothing between subdomains, albeit not being numerically identical to the sequential scheme. This leads to an imperceptible numerical difference between the results of the sequential model and those of the parallel model, showing patterns parallel to the X direction when we display the difference. The amplitude of the discrepancy is negligible, it damps very quickly, and we have never observed the development of numerical instabilities from these patterns.

3.6.2 Recommendations

The optimal number of subdomains **nzdoms*nmdoms** results from a tradeoff between the true computing time and the time wasted in message passing between processes. The message passing time is roughly proportional to the perimeters of the subdomains, and the true computation time to their area. For a 80*80 domain and the gas version, you will waste CPU time in message passing if you go beyond 4*4 subdomains. On the other hand, the same 80*80 simulation with the aerosols version, sea salts and 3 Gauss-Seidel iterations should still be efficient with 8*8 subdomains.
It is the user's responsibility to try with an increasing number of subdomains (and an increasing number of processors, of course) on a typical forecast configuration, and to decide of the best choice.
Another technical point of detail, which may have severe impacts on performance, is the type of process locking used for collective communications. Suppose that you have divided your domain in 4 subdomains, and you run on 4 processors (defined in your MPI hostlist file). The main calling script will spawn 5 processes: one master, and 4 workers. One processor, generally the first in your hostfile, will be overbooked with the master anf the first worker. This is generally not a problem, because master and worker do not work at the same time. But suppose the following case : the master has called the 4 workers, and they have a rendez-vous (synchronization) somewhere in the code. The workers work, and the master sleeps until the program reaches the rendez-vous. No problem, if the master process is really sleeping: the load of the fisrt processor will be 1, produced either by the master, or by the first worker. But if your MPI library has choosen what they call *spin-lock* process locking, the master process will not sleep waiting. It will poll continuously to check if the workers have reached the rendez-vous. In that case, the load of the first processor will be 2: master (polling) and worker1(working) and the whole computing time will be roughly multiplied by 2. With LAM/MPI, this situation is avoided by selecting the **sysv** System Services Interface. This is the rationale of the command

```
mpirun -np \$((\$nzdoms*\$nmdoms+1)) -ssi rpi sysv ./chimere.e
```

found at the end of the main execution script.
If you have the opportunity to use many processors for CHIMERE, you can "waste" a processor for the master process. That is, for the 4 subdomains case, you will list 5 processors in your MPI hostlist file. In that case, and only in that case, you can let MPI choose spin-locking for collective communications : it will be faster to have the master polling continuously than awaking it from a real sleep. This is achieved, with LAM/MPI, with this command replacing the previous one:

```
mpirun -np \$((\$nzdoms*\$nmdoms+1)) -ssi rpi usysv ./chimere.e
```

3.7 The 'chimere.nml' model namelist

A CHIMERE run consists in several actions which are performed in the top calling script:

- running the interfaces,
- building the namelists and
- executing **./chimere.e**.

For the model execution, many input files are necessary. After running the interfaces, they are listed in the **chimere.nml** model namelist. This list also contains the output files names and directories.
This section describes all files and users choices listed in this namelist. All these input files must be present in the temporary directory before running the executable **chimere.e**. The top calling script copies and constructs these files in the temporary directory automatically. We also list the corresponding internal file names used during the run. In the following list, we define:

- $modeldir: the model directory
- $tmpdir: the simulation directory
- $outputdir: the output results directory
- $inputdata: an example of chemistry data directory automatically produced by the chemprep script. Note this directory is always produced before a run and always put in the directory $modeldir/chemprep/inputdata
- DOM: an example of simulation horizontal domain
- d1_d2: the starting and ending dates of the simulation
- lab: the name of the simulation

The necessary parameters and input files are listed below. For each file, we describe its "common name", the complete path and its function.

Parameter	Value	Type
version	'chimere'	The model version
idatestart	2008062100	The starting date of the simulation
nhourrun	240	The number of hours of the simulation
iopinit	1	The use of initial conditions
imakerun	1	Make the run or not
iusebemis	1	Build biogenic emissions or not
iusedust	1	Build dust emissions or not
iusebound	1	Build and use boundary conditions or not
ifastj	0	Use on-line fastJ scheme or not
iopt_eros	0	use local erosion in Europe
allo_afr	1	Allow emissions of dust in Europe
icuth	1	The ustar threshold parameterization
ifluxv	2	The sandblasting flux parameterization
nlong	95	Number of values in longitude for the dust data
nlat	24	Number of values in latitude for the dust data

These parameters are integer and describes the starting date and duration (in hours) of the simulation. The other flags are the choices to make the initial conditions, biogenic emissions, mineral dust emissions, the use of boundary conditions, the use of the on-line FastJ module, and the parameterizations included in the mineral dust module.

Parameter	Value	Type
fnoutspec	'$inputdata/OUTPUT_SPECIES.full'	Name of output species (here, if the user wants all species in output)
fnspec	'$inputdata/ACTIVE_SPECIES'	all active species names
fnchem	'$inputdata/CHEMISTRY'	preprocessed reactions
fnstoi	'$inputdata/STOICHIOMETRY'	stoichiometric coefficients
fnrates	'$inputdata/REACTION_RATES'	tables of reaction rates
fnfamilies	'$inputdata/FAMILIES'	Definition of families
fnphot	'$inputdata/PHOTO_PARAMETERS'	Tabulated zenithal angles
fnaerosol	'$inputdata/AEROSOL'	aerosols; number of bins, molar weights
fnaeromin	'$inputdata/AEROMIN.bin'	Parameters for ISORROPIA scheme for aerosols
fnaeroorg	'$inputdata/AEROORG.bin'	Parameters for the SOA scheme
fnprim	'$inputdata/PRIMARY'	Size distribution of aerosols
fnsemivol	'$inputdata/SEMIVOL'	Semivolatile aerosols parameters
fnanthro	'$inputdata/ANTHROPIC'	List of anthropic emitted species
fnfires	'$inputdata/FIRES'	List of fires emitted species
fnbiogen	'$inputdata/BIOGENIC'	List of biogenic emitted species
fndepoespe	'$inputdata/DEPO_SPEC'	coefficients for calculation of resistances / species
fndepopars	'$inputdata/DEPO_PARS'	landuse coefficients for dry deposition
fnwetd	'$inputdata/WETD_SPEC'	wet deposition species and parameters

The files in the '$inputdata/' directory are produced by the chemprep program during the first model iteration. This includes the active species names, the output species, the stoichiometric coefficients, tables of reaction rates, definition of families, the tabulated zenithal angles, the number of bins, molar weights of aerosols. The specific `AEROMIN.bin` and `AEROORG.bin` are binary files for the ISOROPIA and SOA chemical schemes respectively.

Parameter	Value	Type
fnlanduse	'$modeldir/domains/DOM/LANDUSE_GLCF_DOM'	Landuse in the CHIMERE classes
fniVCO	'$modeldir/domains/VCOORD/VCOORD_8_997_500'	Verticla coordinates coefficients
fniMGNEF	'$modeldir/domains/DOM/EFMAP_LAI_DOM.nc'	Leaf Area Index for MEGAN
fnisolspe	'$modeldir/chemprep/dustdata/dustdata-soil.asc'	Soil data for dust emissions
fnisurface	'$modeldir/chemprep/dustdata/dustdata-surf.asc'	Surface data for dust emissions

The files in the domains directory depends only of the horizontal grid. They are automatically generated when the use launch a simulation.

Parameter	Value	Type
fnmetraw	'$outputdir/data_DOM_lab/exdomout.d1_d2_lab.nc'	Input: Meteo fields on the native meteo model vertical grid
fnbounconc	'$outputdir/data_DOM_lab/BOUN_CONCS.d1_d2_lab.nc'	Input: boundary conditions
fnemisa	'$outputdir/data_DOM_lab/AEMISSIONS.d1_d2_lab.nc'	Input: antrhopogenic emissions
fnemisf	'$outputdir/data_DOM_lab/FEMISSIONS.d1_d2_lab.nc'	Input: Fires emissions
fnoBIO	'$outputdir/data_DOM_lab/BEMISSIONS.d1_d2_lab.nc'	Output: Biogenic emissions
fnoDUST	'$outputdir/data_DOM_lab/DEMISSIONS.d1_d2_lab.nc'	Output: Mineral dust emissions
fninit	'$outputdir/ini.d1_d2_lab.nc'	Output: Initial conc fields
fniniex	'$outputdir/iex.d1_d2_lab.nc'	Output: Initial conc fields for POPs
fnout	'$outputdir/out.d1_d2_lab.nc'	Output: Simulation conc fields
fnexc	'$outputdir/exc.d1_d2_lab.nc'	Output: Additional conc fields in soil and water
fnmeteo	'$outputdir/meteo.d1_d2_lab.nc'	Output: Meteo fields on the chimere grid
fnconcs	'$outputdir/end.d1_d2_lab.nc'	Output: Last conc fields (used for restart)
fnendex	'$outputdir/exe.d1_d2_lab.nc'	Output: Final backup of concentrations in soil, vegetation and sea
fndepos	'$outputdir/dep.d1_d2_lab.nc'	Output: Deposition fluxes

Note that the complete format of the main output files is more precisely described in §2.4.2,p.26.

3.8 How to add a variable in the code?

3.8.1 From the master to workers

Using previous versions of the model, to add a new parameter was an easy task. With the parallelized version, this is a little bit more complicated. If you need to know a value in the core model, but using some data estimated with the pre-processors, you need to transfer informations from the master to the workers. Basically, 5 subroutines have to be updated if you want a new variable (real or integer, scalar or array). We present an example based on the deep convection implementation: to know if we are in a convective cell or not, we use a flag named 'ideep(nzonal,nmerid)'. This array has to be hourly updated in the 'locvalues.F90' subroutine (for the estimation of variables at the chemical time-step).

1. src/modules/message_defs.F90:

```
integer,parameter :: ias_ideep   =__LINE__
```

2. src/modules/master_message_subs.F90:
   From the master to the worker in send_frac_hourly_int_arrays(ip,dom(ip))

```
integer,dimension(:,:),allocatable :: ibuf2

allocate(ibuf2(nzcount,nmcount))
ibuf2=ideep(izstart:izend,imstart:imend)
call mpi_send(ibuf2,                          &
     nzcount*nmcount,                         &
     mpi_integer,ip,                          &
     ias_ideep,                               &
     mpi_comm_world,ierr)
deallocate(ibuf2)
```

3. src/modules/chimere_common.F90:

```
integer,dimension(nzonal,nmerid)         :: ideep
```

4. src/model/worker_common.F90:

```
integer,dimension(nzonalmax,nmeridmax)   :: ideep
```

5. src/model/worker_message_subs.F90:
   The worker receives the information from the master in recv_frac_hourly_int_arrays

```
integer,dimension(:,:),allocatable :: ibuf2

allocate(ibuf2(nzonal,nmerid))
call mpi_recv(ibuf2, nzonal*nmerid, mpi_integer,0, ias_ideep, &
                       mpi_comm_world,mpi_status_ignore,ierr)
ideep(1:nzonal,1:nmerid) = ibuf2(:,:)
deallocate(ibuf2)
```

3.8.2 From workers to the master

If you need to know the values of a variable calculated in the core worker model (i.e., to write values to an output file), you need to transfer information from the worker to the master, as only the master includes the appropriate subroutines for writing output files. Four source files have to be modified if you want to pass a variable from workers to the master (real or integer, scalar or array).
Consider an example of a photolysis rates variable (phrate worker array) that could be computed in a radiation scheme. Array values are updated hourly, based on clear-sky values per photolysis reaction included in the PHOTO_PARAMETERS file, the zenith angle calculated by the model, and the altitude. Therefore, a 4-dimensional array phrate(nphotmax,nzonal,nmerid,nverti) (nphotmax is the maximum number of photolysis reactions considered in CHIMERE, nzonal is the number of zonal cells for each worker core, nmerid is the

number of meridian cells for each worker core, and nverti is the number of vertical layers) is calculated every hour. With this convention, source files that we need to modify are the following,

1. src/modules/chimere_common.F90:
   Define an array in the master COMMON, with the same type and dimensions as the phrate array,

   ```
   real(kind=8), dimension(nphotmax,nzonal,nmerid,nverti) :: phrate
   ```

   The name of this array can be either the same as in the worker (as in this example, phrate) or a different one.
2. src/modules/message_defs.F90:
   Define an integer index for receiving the array by the master:

   ```
   integer,parameter :: iar_phrate      =__LINE__
   ```

3. src/modules/master_message_subs.F90:
   We usually want to receive the new variable by the master every time it is updated. This updating frequency is essential in order to decide in which master subroutine we should receive the new variable. In this example, phrate is updated hourly so, following the master data flow (see **src/main/integrun.F90**), the most appropriate master subroutine is,

   ```
   subroutine recv_locvalues(ip,dom)
   ```

   Since we need a 4-dimensional array buffer, we have to include in this subroutine:

   ```
   real(kind=8), dimension(:,:,:,:), allocatable :: dbuf4
   ```

   Then we call mpi_recv as follows:

   ```
    allocate(dbuf4(nphotmax,nzcount,nmcount,nverti))
    call mpi_recv(dbuf4, nphotmax*nzcount*nmcount*nverti,  &
        mpi_double_precision,ip, iar_phrate,            &
        mpi_comm_world,status,ierr)
    phrate(1:nphotmax, izstart:izend, imstart:imend,1:nverti) = dbuf4
    deallocate(dbuf4)
   ```

4. src/model/worker_message_subs.F90:
   We have to send the original phrate array values from the worker. Again, following the worker data flow (see **src/model/worker.F90**), the most appropriate subroutine to do that in the worker in our example is:

   ```
   subroutine worker_send_locvalues
   ```

   We have to include in this subroutine:

   ```
    real(kind=8), allocatable, dimension(:,:,:,:) :: dbuf4
   ```

   Then we call mpi_send as follows:

   ```
    allocate(dbuf4(nphotmax,nzonal,nmerid,nverti))
    dbuf4(:,:,:,:) = phrate(1:nphotmax,1:nzonal,1:nmerid,1:nverti)
    call mpi_send(dbuf4, nphotmax*nzonal*nmerid*nverti, &
        mpi_double_precision, 0, iar_phrate,            &
        mpi_comm_world,ierr)
    deallocate(dbuf4)
   ```

We highly recommend to understand both **integrun.F90** and **worker.F90** data flows before applying any of those changes.

3.8.3 Write variable into outfile

Consider the same example as before. Phrate worker array is reveived by master. To write this array into outfile, we need to modify three routines.

1. src/initio/iniconc.F90:
   We need to initialise the phrate array because at the first time step of the simulation this array is not calculated by worker.

```
phrate(:,:,:,:)=dzero
```

2. src/modules/chimere_common.F90:
   We have to include in this subroutine:

```
integer :: out_phrate_varid
```

3. src/initio/iniout.F90:
   We have to include in this subroutine:

```
integer :: out_nphot_dimid
```

   Then we have to define the new dimension *nphotmax* into netcdf file:

```
subroutine create_dims_out
ncstat=nf90_def_dim(out_ncid,'nphotmax', nphotmax,out_nphot_dimid)
NCERR(__LINE__)
```

   Then we have to define the new variable into netcdf file:

```
! phrate
    ncstat=nf90_def_var(out_ncid,'phrate',NF90_FLOAT,                                    &
         (/out_nphot_dimid,out_zonal_dimid,out_merid_dimid,out_layers_dimid,out_time_dimid/), &
         out_phrate_varid)
    NCERR(__LINE__)
    ncstat=nf90_put_att(out_ncid,out_phrate_varid,'units','K')
    NCERR(__LINE__)
    ncstat=nf90_put_att(out_ncid,out_phrate_varid,'long_name','Temperature')
    NCERR(__LINE__)
```

4. src/initio/outprint.F90:
   We have to include in this subroutine:

```
    real(kind=8), allocatable, dimension(:,:,:,:) :: toprint4d
```

   Then we have to write the new variable into netcdf file:

```
  allocate(toprint4d(nphotmax,nzonal,nmerid,nivout))
  toprint4d(:,:,:)=phrate(1:nphotmax,1:nzonal,1:nmerid,1:nivout)
  ncstat=nf90_put_var(out_ncid,out_phrate_varid,toprint4d,  &
  (/1,1,1,1,iprint+1/),(/nphotmax,nzonal,nmerid,nivout,1/))
  NCERR(__LINE__)
  deallocate(toprint4d)
```

Chapter 4

[domains]: Domains and landuse

To create a new CHIMERE domain, the User can run either chimere-domain.sh or just the main script chimere.sh, which will call chimere-domain.sh.
Every time you need a new domain, the following steps generally need to be done.

1. Define a new coordinate file **domains/HCOORD/COORD_$dom**, where $dom is the name of the simulation domain defined in chimere.par.
   - If the new domain is regular in terms of latitude and longitude, just add a line to the *domains/domainlist.nml* file (see below)
   - Otherwise generate yourself the *domains/HCOORD/COORD_$dom* file. This file has two columns: "lon lat", and the longitude changes first. You can see the examples in the *domains/HCOORD* directory.
2. Run chimere-domain.sh. This will
   - Create all landuse data files needed for depositions and biogenic emissions (work done automatically by domains/prep_landuse.sh)
   - Create MEGAN biogenic emission factors and leaf-area indices on the domain grid (work done automatically by domains/prep_megan.sh) for further generation of biogenic emissions by the **src/diag/diagbio.F90** program (see p. 62)
3. Create anthropogenic emission files, either on your own, or using the EMEP emissions interface (see p. 59)

The landuse data are automatically calculated. During the first run over a domain, the landuse programs will be launched by the scripts/chimere-domain.sh script and will create all data files for CHIMERE in the **domains/$dom** directory, where $dom is the name of the simulation domain.

4.1 The *domains/domainlist.nml* file

If the simulation domain is regular in terms of latitude and longitude, the file **domains/HCOORD/COORD_$dom** is created automatically from a single line of domain parameters specified by the user in the domains/domainlist.nml file. If the domain already exists, the run continues. Otherwise scripts/chimere-domain.sh calls the domains/makeCOORDdomains.sh script that generates the domain horizontal coordinates in the **domains/HCOORD/COORD_$dom** file.
For example, the line describing the CHIMERE 'CONT3' domain corresponds to the mesh displayed in the Figure 4.1. The first column, the $dom is a name given by the user to the model horizontal grid/domain. The other columns are the number of cells in the x-direction, the number of cells in the y-direction, and the coordinates of the South-West cell center, as follows:

```
domain      NX  NY  DX    DY    XMIN    YMIN
CONT1       65  33  0.5   0.5   -10.0   40.5
CONT3       67  46  0.5   0.5   -10.5   35.0
CONT4       70  44  0.5   0.5   -10.5   36.0
CONT5       79  47  0.5   0.5   -14.0   35.0
FRA10      101 111 0.15   0.1    -5.0   41.0
```

If, however, the simulation domain is not regular in terms of latitude and longitude, the user has to provide himself a correct **domains/HCOORD/COORD_$dom** file. Note that a domain that is regular in terms of distance (e.g., 3x3 km) is **not** regular in terms of latitude/longitude.

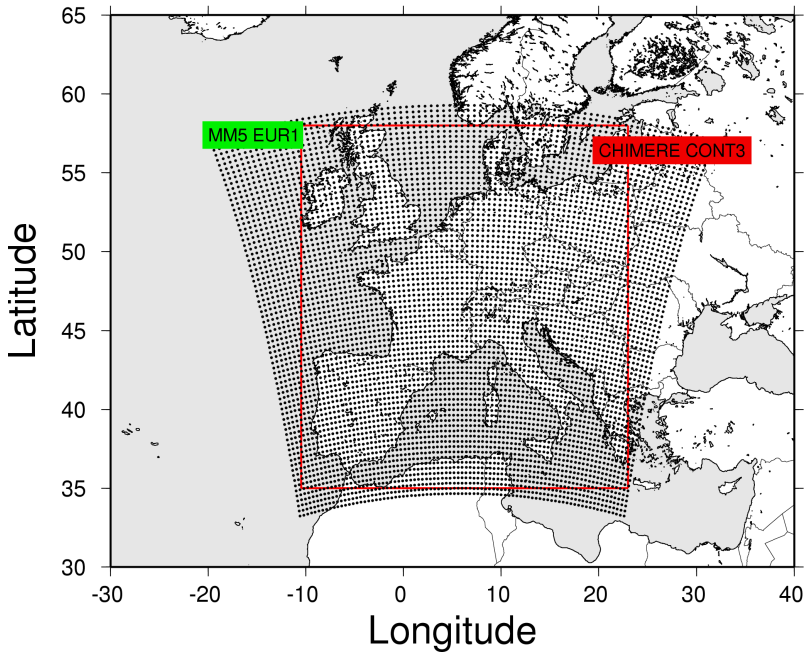


Figure 4.1: *Examples of horizontal domains. The dots represent the MM5 EUR1 grid cells centers and the rectangle represents the boundaries of the CHIMERE CONT3 domain.*

4.2 Land Use Types, Data, and Interface

Land use types, or categories, are needed by CHIMERE to calculate a number of processes, such as deposition, biogenic emissions, or surface layer momentum and heat transfer. Land use files need to be constructed only once per model domain. There are currently 9 land use categories in CHIMERE. Those categories are calculated from available global land use databases, which can contain different number of classes. The *chimere 2014b* version comes with land use data and interfaces to two databases: **GLCF** and **GlobCover** (see below). The 9 CHIMERE land use types are described in Table 4.1, with the correspondance to the GLCF (University of Maryland) data base.

An additional class "inland water" has been added to the classifications in both land cover databases to distinguish between the sea water and fresh water. This was needed to avoid model emissions of sea salt over the fresh water surfaces. The separation was done using a land-sea mask. So instead of the original 14 GLCF and 22 GlobCover classes, CHIMERE land use pre-processor takes 15 and 23 classes for GLCF and GlobCover, respectively (see Table 4.2 and Table 4.3).

Category Number	**Description**	[**0:13**]	**Corresponding GLCF**
1	Agricultural land / crops	[11]:	Cropland
2	Grassland	[10]+1/2[7]:	Grassland+1/2Wooded grassland
3	Barren land/bare ground	[12]:	Bare ground
4	Inland Water		
4	Urban	[13]:	Urban and built-up
6	Shrubs	[8]+[9]:	Shrublands
7	Needleaf forest	[1]+[3]+1/2([5]+[6])+1/4[7]	
8	Broadleaf forest	[2]+[4]+1/2([5]+[6])+1/4[7]	
9	Ocean	[0]:	Water

Table 4.1: *Landuse categories used in CHIMERE*

0	Water
1	Evergreen Needleleaf Forest
2	Evergreen Broadleaf Forest
3	Deciduous Needleleaf Forest
4	Deciduous Broadleaf Forest
5	Mixed Forest
6	Woodland
7	Wooded Grassland
8	Closed Shrubland
9	Open Shrubland
10	Grassland
11	Cropland
12	Bare Ground
13	Urban and Built
14	Inland Water

Table 4.2: *GLCF land cover types used in CHIMERE*

The Global Land Cover Facility (GLCF)

The Global Land Cover Facility (GLCF[1]) is 1km$\times$1km resolution[2] database from the University of Maryland, following the methodology of [Hansen and Reed, 2000]. This global land cover classification is based on the imagery from the AVHRR satellites analyzed to distinguish 14 land cover classes. Table 4.2 shows the 15 GLCF land cover classes used in CHIMERE.

GlobCover Land Cover

The GlobCover Land Cover is a global land cover map at 10 arc second (300 meter) resolution [Bicheron et al., 2011]. It contains 22 global land cover classes defined within the UN Land Cover Classification System (LCCS). GlobCover database is based on the ENVISAT satellite mission's MERIS sensor (Medium Resolution Image Spectrometer) Level 1B data acquired in Full Resolution (FR) mode with a spatial resolution of 300 meters. GlobCover LC was derived from an automatic and regionally-tuned classification of a time series of MERIS FR composites covering the period December 2004-June 2006. Table 4.3 shows

[1] `http://glcf.umiacs.umd.edu/data/landcover`
[2] Actually, the resolution of the source files used is 0.08°

1	Post-flooding or irrigated cropland
2	Rainfed cropland
3	Mosaic cropland (50-70%) / vegetation (20-50%)
4	Mosaic vegetation (50-70%) / cropland (20-50%)
5	Broadleaved evergreen or semi-deciduous forest (>5m)
6	Closed broadleaved deciduous forest (>5m)
7	Open broadleaved deciduous forest/woodland (>5m)
8	Closed needleleaved evergreen forest (>5m)
9	Open needleleaved deciduous or evergreen forest (>5m)
10	Closed to open mixed broadleaved and needleleaved forest
11	Mosaic forest or shrubland (50-70%) / grassland (20-50%)
12	Mosaic grassland (50-70%) / forest or shrubland (20-50%)
13	Shrubland
14	Herbaceous vegetation
15	Sparse (<15%) vegetation
16	Closed to open broadleaved forest regularly flooded
17	Closed broadleaved forest / shrubland permanently flooded
18	Grassland / woody vegetation regularly flooded
19	Urban areas >50%
20	Bare areas
21	Water bodies
22	Permanent snow and ice
23	Inland water

Table 4.3: *GlobCover land cover types used in CHIMERE*

the 22 GlobCover classes, together with the additional "Inland water" class, to derive the 9 CHIMERE land use categories.

4.2.1 Land use interface

When the **LANDUSE_$dom** file is not found in the **domains/$dom** directory, **chimere-domain.sh** script runs the land use interface to generate this file.
The scripts and programs are:

- domains/prep_landuse.sh. Runs **extract_landuse.e** program.
- domains/src/extract_landuse.F90: Extracts original GLCF or GlobCover land cover classes data for the specified Chimere domain from the global data files **glcf_world.nc** and **globcover.nc**. Then it calculates the 9-category fractions on the CHIMERE grid from the GLCF or GlobCover classes. It creates **LANDUSE_$dom** file containing the fraction of land use per grid cell (numbers between 0 and 1, see Table 4.1) .

The global land cover NetCDF files **glcf_world.nc** and **globcover.nc** are provided in a separate directory. This directory is given by the variable $landcover_dir in the top-calling script chimere.sh. The choice of a land cover Database is made using the script variable $iland_cover : iland_cover=1 for GLCF, land_cover=2 for GlobCover.
ASCII files domains/src/LAND_AGGREGATION_GLCF and domains/src/LAND_AGGREGATION_GLOBCOVER contain the matrix of correspondance between the 15 GLCF classes and the 23 GlobCover classes, respectively, with the 9 CHIMERE categories used by **extract_landuse.F90**.
The interface contains a new interpolation algorithm that greatly saves computation time when the model

domain grid is rectilinear.

4.3 Details on output files

4.3.1 Horizontal domain COORD

Model domains are entirely defined by their grid cell centres description. It is given in the **COORD_$dom** file which must be placed in the **domains/** directory. The **COORD_$dom** file contains lines with a longitude (in decimal degree) and a latitude (in decimal degree). Each pair of coordinates stands for a grid cell centre, described (from top to bottom of file) from West to East then from South to North.
In the definition of a new CHIMERE domain, the user must check carefully whether the domain is quasi-rectangular. Most projection systems work, even a regular grid in geographic coordinates (longitude-latitude) provided the resolution is not too coarse (say > 2 degree).
Model grids can be any quasi-rectangular grid, with weakly varying spatial step. It is assumed, in particular for the Parabolic Piecewise Method for tranpsort that locally (over 5 consecutive cells) the grid size is constant in each direction, with sizes equal to that of the locally central cell. Sphericity effects are taken into account, but therefore linearized. It is important to note that the COORD file for CHIMERE is absolutly not the same that the one used for MM5 (or others meteorological inputs). An example is displayed in the Figure 4.1. If the user wants to define his own horizontal grid, we propose a script described in §C.1, p.153.

4.3.2 Vertical grid VCOORD

Structure The model uses any number of vertical layers, described in hybrid sigma-p coordinates. The pressure in hPa at the top of each layer k is given by the following formula:

$$P_k = a_k 10^5 + b_k P_{surf}.$$

P_{surf} is the surface pressure and the coefficients a_k and b_k are calculated by the geom.awk script, called from chimere-domain.sh via define_geom.sh. The a_k and b_k coefficients ($1 \leq k \leq nlayer$) are written to the VCOORD file which is then stored in the domains/VCOORD/ directory of the chimere root directory, and in the domains/ subdirectory of the temporary chimere directory.
The generation of the VCOORD file depends on three parameters of the chimere.par file :

```
[$nlayer_chimere]       Number of vertical layers           : 20
[$top_chimere_pressure] Top layer pressure (mbar)           : 200
[$first_layer_pressure] First layer pressure (sigma * 1e3)  : 997
```

`$nlayer_chimere` is the number of vertical layers needed,
`$top_chimere_pressure`is the pressure of the top of the domain, and
`$first_layer_pressure` is the pressure of the top of the lowest chimere level, *expressed in* $\sigma * 10^3$ *units*.
For example, if `$first_layer_pressure` is set to 997, the thickness of the first layer (in pressure) will be equal to $(1 - 0.997)\, P_{surf} \simeq 3\,\mathrm{hPa}$.

Placing the vertical levels Since version 2014, the algorithm for positioning the vertical levels have changed : up to version 2013b, the layer thickness was increasing exponentially from ground level to the top of model. Even though this permitted to have a good resolution within the PBL, layers inside the free troposphere had thicknesses reaching several kilometers, which hinders the representation of long-range transportation of anthropogenic of natural contamination plumes (e.g. dust layers). Since version 2014, the algorithm coded in `geom.awk` produces a VCOORD file in which the thickness of the layers increase exponentially with height in the lowest $200\,\mathrm{hPa}$ of the atmosphere, and have constant thickness (in pressure coordinates) from $200\,\mathrm{hPa}$ to the top of the model. The number n_{200} of layers in the lowest $200\,\mathrm{hPa}$ of the model is determined so that:

- No layer is thicker than its upper neighbour. Since the layer thickness increase exponentially from $k = 1$ to $k = n_{200}$ and is constant from $k = n_{200}+1$ to $k =$`$nlayer_chimere`, this condition is equivalent to imposing that layer n_{200} is not thicker than layer $n_{200} + 1$
- n_{200} is the highest possible value such that condition 1 is verified

These two conditions are coded in `geom.awk` and produce a VCOORD file that ensures a fine vertical resolution for the lowest atmospheric layers while not having too thick layers close to model top. Another script `geom-verbose.awk` is also provided in order to make a (relatively) user-friendly output on the screen so that the user can check whether the vertical resolution obtained with their parameters is reasonable. A sample output of `geom-verbose.awk` is as follows:

```
Vertical layers will be as follows :
lowest model layer will be  5 hPa thick
will have  6  layers below 800 hPa
           2  layers from 800 hPa to  500 hPa
k     ca        cb         p(hPa)       thk(hPa)
  1   0.00000   0.99500    995.00000      5.00000
  2   0.00902   0.97705    986.07113      8.92887
  3   0.02513   0.94500    970.12617     15.94496
  4   0.05389   0.88777    941.65206     28.47411
  5   0.10525   0.78555    890.80371     50.84835
  6   0.19697   0.60303    800.00000     90.80371
  7   0.34848   0.30152    650.00000    150.00000
  8   0.50000   0.00000    500.00000    150.00000
-----------------------------------------------
```

Users may want to generate their own VCOORD files depending on their modelling priorities (long-range transport, urban boundary layer ...). To do that, the easiest possibility is to modify the `geom.awk` script according to one's needs.

Chapter 5

[chemprep]: The chemical preprocessor

This is how the chemical preprocessor works.

- When the script chimere.sh is launched, the availability of chemistry input files coresponding to the specific simulation is checked. If the data already exist, the run continues. If not, the script chemprep/make-chemistry.sh creates all prerequesite files.
- This script will create a new directory in the main directory chemprep and called something like inputdata.2110011210.6 where the arguments follwing the string inputdata. correspond to the simulation options. In this new directory, all input files required by CHIMERE for a simulation are stored.
- If a new simulation with the same options is launched or in case of a restart, the files will be used as it. If the main run options change, the script will be automatically launched again to create new files.

5.1 Options available in *chimere.par*

These options are listed in chimere.par (p.20) under section "Chemistry Options" as follows:

mecachim	option for the gas-chemistry mechanism. No gas phase chemistry [0]; melchior complete [1]; melchior reduced [2] SAPRC-07-A [3]
accur	option for the output species accuracy for aerosols[1]. Possible values are: low, full,
nbins	option for the aerosols bins number. The cut off diameters 2.5 and 10 um are respected. You can change the parameter dmax in ./chemprep/prep-chemistry-data.sh in order to adapt the size distribution. This script is adapted for nbins=4 and nbins=6.
aero	options for simulation of aerosols or not. [0=no; 1=yes] (if yes : Minimal configuration with NO3, NH4, SO4, PPM, Sec. Org. Aer., WATER)
seasalt	option for the sea salts simulation. none=0, inert=1, active=2. "active" means sea salts react with chemistry
iusedust	Mineral dusts are included as active species and emitted within the domain.

[0] if not,
[1] if yes.

pops — Persistent Organic Pollutants.
pops=1 only if mecachim>0 and aero=1

carb — Primary carbonaceous species
[0=no; 1=yes]
(if yes, OCAR and BCAR are used)

trc — Tracers
[0=no; 1=yes]
(if yes, both gaseous and particulate tracers can be used)

soatyp — SOA chemistry:
no SOA chemistry [0],
simple [1],
medium [2]
Note that soatyp>0 only possible if aero = 1

With these options, the script scripts/make-chemistry.sh is launched.

5.2 The first-level script *make-chemistry.sh*

This script checks if input data files are already existing or not. If not, new ones are created. The "label" for the output directory is built in this script as follows:

labchem=$mecachim $aero $seasalt $pops $carb $gtrc $soatyp $iusedust $iadv $iadvv .$nbins

For example and for a simulation with only gas-phase chemistry and no aerosols, but with a passive tracer, the directory created will be with the label **"1000001000.0".**

5.3 The second-level scripts

The script chemprep/prep-chemistry-data.sh calls the programs in the directory chemprep/src:

- chemprep-distrib.f: Program for the calculation of aerosol size distribution. Note that the minimum and maximum value of the aerosols diameters are fixed with the values: D_{pmin}=0.001μm and D_{pmax}=40μm. The user may easily change these values in the *prep-chemistry-data.sh* script.
- chemprep-families.f: Reads all species and builds the file containing the name and contents of families.

The script prep-tracer-data.sh adds parameters of gaseous and particulate tracers to the data files describing parameters of the chemistry mechanism, depositions, and output: REACTIONS, ANTHROPIC, FAMILIES, DEPO_SPEC, WETD_SPEC, ACTIVE_SPECIES, OUTPUT_SPECIES.full, OUTPUT_SPECIES.low, REACTION_RATES, CHEMISTRY (see below).

5.4 Manual changes of the mechanism

The chemical preprocessing scripts allows to modify reactions, add reactions or even completely change the chemical mechanism. It allows an easy writing of reactions and from two initial input files **REACTIONS** and **PHOTORATES** produces other files which are read by **chimere**. Once the two input files are prepared by the user, the preprocessor is invoked by running the make-chemistry.sh script.
The conditions for the set of reactions to be used are listed below:

- Only reactions of the type A1(+B1(+C1....)->(a*)A2+(b*)B2+... are accepted. Letters with index 1 denote the reactants and those with index 2 the products. a, b, (if any) are stoichiometric coefficients. If omitted they are considered to equal 1. Negative stoichiometric coefficients are accepted, but not recommended since it can lead to negative concentrations. Stoichiometry in the reactants is not allowed.
- Only species which are *consumed* at least once in the mechanism will be considered as **active species** in the Chimere model. If the user intends to use a species which results of chemical reactions but is not a reactant in any reaction, she (he) should add an artificial reaction to the mechanism, for instance A->X (A is the concerned product), with a negligible reaction rate, i. e. k=1e-10 (s-1).
- There are special species whose concentration is only prescribed in the model. These are H2O (water vapor), N2 (molecular nitrogen), O2 (molecular oxygen) and M (80% N2 + 20% O2). Their values are given by the meteo data. Reaction with these species is possible with no constraint. Changes in these "prescribed species" imply several modifications in the Chimere code and are not an easy issue.
- Reactions have a maximum of 4 reactant species and as many products as desired (less than 1000!). To increase the number of reactants one needs just to change the parameter **nreactamax** in the header files **src/chimere_params.f90.sed** and **src/worker_params.f90.sed**.
- It may be desirable that stoichiometric coefficients vary with some parameters like temperature. This is however not possible here in this version.
- All reactions will be processed by the solver in an equivalent manner. There is no family grouping (like often used for the QSSA solver) available.
- Clear sky photolysis rates must be precalculated by the user, and depend only on the zenith angle Z. No dependence on height is allowed, even in the presence of clouds. The proposed tabulated values correspond to an average value between 0 and 1000m. This should be a good compromise for the boundary layer. Introducing a dependence with height will be considered in a future model version. The 12 Tabulated J values must correspond to zenith angles of (in degree) 90,88,86,83,80,75,70,60,45,30,15,0
- There is a possibility of defining *families*. These are groups of species whose concentration sum can be output in the model. However these families are only used in outputs, not in the chemistry itself. See syntax in the next section.
- The mathematical expressions for reaction rates (the K's and J's) can take 20 forms, but here only a limited number is available. The table below shows the available possibilities, together with associated syntax.

Type number	Name	Math	syntax in REACTIONS file
1	Constant K	K	k=*value*
2	Simplified Arrhenius	K=Aexp(-B/T)	k(T)=Aexp(-B/T), A=*value*, B=*value*
3	Arrhenius	K=Aexp(-B/T)(300/T)**N	k(T)=Aexp(-B/T)(300/T)**N, A=*value*, B=*value*, N=*value*
4	Troe or Falloff	K=K_0*f**Z/(1+M*(K_0/K_∞)) K_0=A_0exp(-B_0/T)(300/T)**N_0 K_∞=A_∞exp(-B_∞/T)(300/T)**N_∞ Z=1/(1+(Log10(M*K_0/K_∞))**2) M=air-density	K(T,M)=troe(A_0,B_0,N_0,A_∞,B_∞,N_∞,f)
5	Photolysis	J=J(Z)	J(Z)=photorate(*label*)[2].
6	Special type	K=K_1*K_2/(1+K_2) K_1=A_1exp(-B_1/T) K_2=A_2exp(-B_2/T)	k(T)=SPECIAL_1(A_1, B_1, A_2, B_2)[3]

[2] *label* is a label standing for recognition of **chemprep** in the **PHOTORATES** file. All photolysis rates must appear tabulated in this latter file, the tabulated values corresponding to specific zenith angles (see above)

[3] * Special form for radical recombination (not used in this mechanism)

7	Special type	K=K_1/(1+K_2) K_1=A_1exp(-B_1/T) K_2=A_2exp(-B_2/T)	k(T)=SPECIAL_2(A_1, B_1, A_2, B_2)
8	Special type	K=2*sqrt(f1*f2*f3*f4/((1+f3)*(1+f4))) f1=A_1exp(-B_1/T) f2=A_2exp(-B_2/T) f3=A_3exp(-B_3/T) f4=A_4exp(-B_4/T)	k=SPECIAL_3(A_1,B_1,A_2,B_2,A_3,B_3,A_4,B_4)
9	Special type	K=2*sqrt(f1*f2)*(1-sqrt(f3*f4))*(1-f4)/(2-f3-f4) f1=A_1exp(-B_1/T) f2=A_2exp(-B_2/T) f3=A_3exp(-B_3/T) f4=A_4exp(-B_4/T)	k=SPECIAL_3(A_1, B_1, A_2, B_2, A_3, B_3, A_4, B_4)
10 to 12	Not used [4]		
13	Aggregated ozone photolysis	J=J0*H2O/(H2O+M*(0.02909*exp(70/T) +0.06545*exp(110d0/T))) H2O=water vapor (molec/cm3) M=air density (molec/cm3)	J(T,Z,H2O)=photorate(O3) [5]
14	Modified Troe [6]	Like Type #4 (Troe) but: Z=1/(1+((Log10(M*K_0/K_∞)-0.12)/1.2)**2)	K(T,M)=troe(A_0,B_0,N_0,A_∞,B_∞,N_∞,f)
15	NO2/HONO Heterogeneous reaction	ks=0.5*depo(NO2) at level 1	ks=0.5*depo(NO2)
16 to 20	Not used [7]		
26	Special type	k(T)=k_0(T)+k_3(T)[M]/(1+k_3(T)[M]/k_2) k_0(T)=A1exp(-B_0/T) k_2(T)=A1exp(-B_2/T) k_3(T)=A1exp(-B_3/T) M=air-density	k(T)=saprc_2(A_0, B_0, A_2, B_2, A_3, B_3)
27	Special type	k(T)=k_1(T)+k_2(T)[M] k_1(T)=A1exp(-B_1/T) k_2(T)=A1exp(-B_2/T) M=air-density	k(T)=saprc_1(A_1, B_1, A_2, B_2)
29	Troe or Falloff for SAPRC	K=K0*f**Z/(1+M*(K0/K_∞)) K0=A0exp(-B0/T)(300/T)**N0 K_∞=A_∞exp(-B_∞/T)(300/T)**N_∞ Z=1/(1+(Log10(M*K0/K_∞)/N)**2) M=air-density	K(T,M)=troe_saprc(A_0,B_0,N_0,A_∞,B_∞,N_∞,f,N)

5.5 Syntax of the REACTIONS file

Following are the rules for writing the REACTIONS file

- Each line is considered as a reaction except blank lines or lines starting with a "#" sign (left for comments).
- Species names must contain at most 15 characters.
- A reaction is written as: **A1(+A2(+A3(+A4)))->(a1*)B1+(a2*)B2+(a3*)B3...** *Rate expression* where **Ai** are the reactants (max=4), **Bi** the products and **ai** are possible stoichiometric (written if different from

[4] User can define a new type. Changes must be done in **chemprep.awk** (recognition of a new syntax), **Binichem.awk** (define the number of constant **ltabrate**, and in **Brates.f** (new math expression)

[5] Aggregation of the ozone photolysis with reactions with atomic oxygen. The photolysis rates must be those of ozone only, hence the budget reaction is O3->2*OH.

[6] Fall-off specific to NO2+OH+M->HNO3

[7] User can define a new type. Changes must be done in **chemprep.awk** (recognition of a new syntax), **Binichem.awk** (define the number of constant **ltabrate**, and in **Brates.f** (new math expression).

1).

- *Rate expression* follows the syntax rules defined in the above table.
- Reactants can also be one (or several) of the prescribed species (H2O, N2, O2 or M).
- A1+A1(+A1)...->... are allowed (repetition of the same reactant, like HO2+HO2...
- Syntax like A1+A2-A3 is NOT allowed
- Negative stoichiometric coefficients are allowed, but not recommended (correctness of results not garanteed because never tested). In that case, however, use the syntax ±a1*B1 in the products.
- Families are defined using the syntax:
  FAM=A1+A2+A3...
  Ai must be active species, and can be repeated as many times as desired. There is no limitation to the number of family elements.

5.6 Syntax of the PHOTORATES file

The syntax is very simple: Each line contains information for one photolysis reaction. There can be more photolysis reactions than in the **REACTIONS** file. The unused ones are ignored. There must be an exact correpsondence between the **labels** of the photolysis reactions defined in the **REACTIONS** file. This label is the first column. The other columns contain the 12 tabulated photolysis rate values for the zenith angles from 90 to 0 degrees (see above table).

Chapter 6

Emissions

CHIMERE accounts for four types of emissions:

- **Anthropogenic emissions** that need pre-processing by the user either with an inventory and model of his/her own or, for emissions over Europe with the stand-alone model developed and distributed by the CHIMERE team (Sect. 6.1).
- **Biogenic and natural emissions** that if not provided by the user may be automatically calculated with the embedded CHIMERE pre-processor based on landuse data (Sect. 6.2).
- **Dust emissions** that may also be estimated with the embedded CHIMERE pre-processor (Sect. 6.3)
- **Fire emissions** that need pre-processing by the user following a stand-alone procedure (Sect. 6.4)

6.1 Anthropogenic surface emissions

There are two options on how anthropogenic emissions may be handled by the CHIMERE model. The user can pre-process anthropogenic emissions from an inventory of his/her own choice and input directly the "AEMISSIONS.${sim}.nc" ready-to-read netCDF file to CHIMERE (see **Appendix G.4, p.172**) (Sect. 6.1.1). Alternatively, CHIMERE team develops and distributes an anthropogenic surface emission pre-processing model called emiSURF that based on a top-down approach estimates hourly emission fluxes on the CHIMERE grid and the period of the simulation from the EMEP data over Europe (Sect. 6.1.2). The output of this model may be processed by the anthropogenic emission pre-processor embedded in CHIMERE ("prepemis.F90"), which compiles the "AEMISSIONS.${sim}.nc" file.

6.1.1 User's precompiled emissions

The user should compile his/her own AEMISSIONS.nc file. This file must contain hourly emission fluxes, projected on the CHIMERE 3-D grid for all gases and aerosol species involved in the chemical mechanism of the CHIMERE simulation (MELCHIOR or SAPRC) in molecules·cm^{-2}·s^{-1} (see Table 6.1 for the list of the required species may). Aerosol fluxes should also be converted in"molecule-like" units in this anthropogenic emission input file considering a fictitious molar mass equal to 100g·mol^{-1}. The conversion coefficient from mass unit to CHIMERE model unit is 6.022×10^{23} mol^{-1}/(100g·mol^{-1}). In this case the user should set the [$imakeaemis] flag at 0, so that "prepemis.F90" program does not run, and provide the appropriate [$aemisdir] and [$fnemisd] paths pointing to the AEMISSIONS.${sim}.nc file in the "chimere.par" file.

6.1.2 The emiSURF interface

For simulations over Europe, the starting point are annual national emission totals from the EMEP database (EMEPCWEST [V. Vestreng, 2005]) available at the web site `http://www.emep.int`. Additional data for benzo(a)pyrene, benzo(k)fluoranthene and benzo(b)fluoranthene (respectively BaP, BkF and BbF) can

MELCHIOR2

NO	Nitrogen monoxide
NO2	Nitrogen dioxide
HONO	Nitrous acid
SO2	Sulphur dioxide
NH3	Ammoniac
CO	Carbon monoxide
CH4[1]	Methane
C2H6	Ethane
NC4H10	n-Butane
C2H4	Ethene
C2H6	Ethane
C3H6	Propene
C5H8	Isoprene
OXYL	o-Xylene
HCHO	Formaldehyde
CH3CHO	Acetaldehyde
CH3COE	Methyl ethyl Ketone
APINEN	α-pinene

AEROSOLS

PPM_fin[2]	Primary particulate matter
PPM_coa[3]	Primary particulate matter
PPM_big[4]	Primary particulate matter
H2SO4_fin[5]	Primary sulfuric acid
BaP_fin [5]	Benzo(a)pyrene
BbF_fin[5]	Benzo(b)fluoranthene
BkF_fin[5]	Benzo(b)fluoranthene
OCAR_fin[5]	Primary organic carbon
BCAR_fin[5]	Primary black carbon

SAPRC

CH4[1]	Methane
CO	carbon monoxide
HONO	Nitrous acid
NO	itrogen monoxide
NO2	itrogen dioxide
SO2	Sulphur dioxide
ACET	Acetone
ALK1	Ethane
ALK2	Propane
ALK3	Alkans 2.5x10^3 <k_{OH}< 5x10^3
ALK4	Alkans 5x10^3<k_{OH}<1x10^4
ALK5	Alkans 1x10^4<k_{OH}
ARO1	Aromatiques k_{OH}<2x10^4
ARO2	Aromatiques k_{OH}>2x10^4
BALD	Aromatic aldehydes
CCHO	Acetaldehyde
C2H4	Ethen
GLY	Glyoxal
HCHO	Formaldehyde
MEOH	Methanol
MACR	Methacrolein
OLE1	Alkens k_{OH}<7x10^4
OLE2	Alkens k_{OH}>7x10^3
CRES	Phenols and Cresols
PRD2	Ketones (k_{OH}>0.7x10^4 ppm^{-1}.mn^{-1})
RCHO	Lumped C3+ Aldehydes
C5H8	Isoprene
APINEN	α-pinene
ACYE	Acetylen
BENZ	Benzen
AACD	Acetic Acid
IPRD	Lumped isoprene product species
NH3	Amoniac

[1] Zero in this model version
[2] $\phi < 2.5\ \mu$m
[3] $2.5 < \phi < 10\ \mu$m
[4] $\phi > 10\ \mu$m
[5] Assumed to be in the fine mode

Table 6.1: *Gas and particle emissions required for MELCHIOR and SAPRC*

be requested on the EMEP-MSCEAST web site http://www.msceast.org. Annual totals for European countries are provided per SNAP sector in Mg·year^{-1}·grid cell area^{-1} over the 0.5^{o}x05^o resolution EMEP grid. The following pollutants are available: NO_x, SO_x, NMVOC, CO, NH_3, PM_{coarse} and $PM_{2.5}$, where PM_{coarse}=PM_{10}-$PM_{2.5}$. Inventory data are provided for each year and can be found in the annual-EMEP05x05/data_expert directory. The processing of the annual totals to obtain hourly fluxes over the CHIMERE 3-D grid for all the chemical species of the corresponding mechanism consists in three main steps in the emiSURF model (Figure 6.1).

Step 1 [emep_preproc.sh]
This bash shell program reads the annual inventory data and creates one file per pollutant: NO_x, SO_x, NMVOC, CO, NH_3, PPM2 = PM_{coarse} and PPM3 = $PM_{2.5}$. The header of these files reads: COUNTRY_ID, WE_EMEP_cell_ID, SN_EMEP_cell_ID,SNAP1,...SNAP10. Emission fluxes are in Mg·year^{-1}·EMEP grid cell area^{-1}.

Step 2 [source2chimere.F90]

- Spatial allocation of surface emissions on the CHIMERE grid is based on landuse data. Two databases

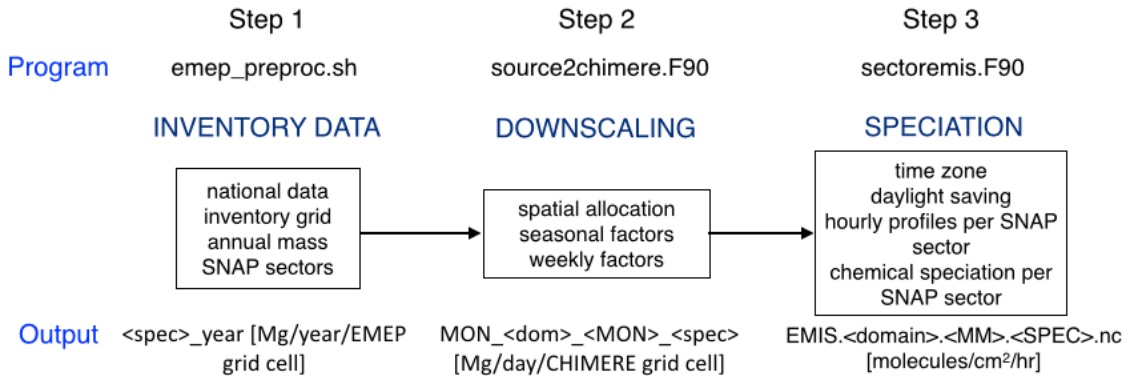


Figure 6.1: *Top-down processing of EMEP anthropogenic emissions with the emiSURF interface*

are implemented in the current version of emiSURF: glcf data at 1km resolution developed by the University of Maryland Department of Geography (http://www.landcover.org) and globcover at 10 arc second (≈300m) resolution developed under the European Space Agency initiative (http://due.esrin.esa.int/globcover/). In both cases emiSURF spatially allocates emissions based on a classification among four landuse types: urban, crop, water or forest.

- Annual data for each inventory pollutant are allocated on the twelve months of the year based on seasonal factors provided by the Institute of Energy Research for each country and SNAP sector (see the inputdata/SEASONAL-FACS_<POL> file).
- A second temporal allocation is applied to account for day-of-week variation, per pollutant, country and SNAP sector (see the inputdata/WEEKLY-FACS_<POL> files), where columns read from Monday through Sunday. These variations follow the guidelines provided by the Institute for Energy Economics and Rational Use of Energy, University of Stuttgart; [Ebel et al., 1994]

Step 3 [sectoremis.F90]

- A time-shift on the data is applied to take into account the time zone and daylight saving information for each country.
- 24-hour profiles for each day of week and for each SNAP sector are applied over the emissions to obtain hourly data.
- Hourly emissions from all SNAP sectors, gridded over the CHIMERE simulation domain are aggregated to a single flux per emitted pollutant.
- Chemical speciation operates on the emitted pollutants at two stages. "Inventory" pollutants (i.e PPM2, PPM3, NO_x, CO, SO_x, NH_3, CH_4 and NMVOC) split into "real" compounds with ratios depending on the SNAP activity sector. At a second stage, "real" compounds split into "model" compounds depending on the chemical mechanism (Melchior or SAPRC). This process is described in the AGGREGATION_$mechanism files found in the "inputdata" directory. Differences between the two chemical mechanisms apply only to the NMVOC species.
  NO_x: For all SNAP sectors 90% of NO_x emissions is assigned to NO_2, 9.2% to NO and 0.8% to HONO [R. Kurtenbach, 2001]. Depending on the country, NO_x emissions in the EMEP inventory may include soil NO biogenic emissions in the "Agriculture" sector. The user should be carful not to doublecount NO soil emissions when running the biogenic emissions pre-processor embedded in the CHIMERE model (Sect. 6.2).
  SO_x: For all SNAP sectors, 99% of SO_x is assigned to SO_2 and 1% to sulphuric acid (H_2SO_4) in the particulate phase.
  NMVOC: For both mechanisms (Melchior and SAPRC) NMVOC emissions first split into 221 "real" compounds of the british PORG speciation depending on the SNAP sector [Passant, 2002]. Then, a two-step procedure aggregates "real" VOC compounds to a smaller set of VOC classes which correspond

directly to the specific compounds of the MELCHIOR or SAPRC chemical mechanism, following the Middleton methodology [Middleton et al., 1990]. Following this procedure, "real" compounds are lumped together into "model" compounds using a reactivity weighting factor which depends on the relative OH radical rate constants of the "real" and "model" compounds. The user should bear in mind that the same reactivity weighting factors are used on emissions for all countries, which represents a significant source of uncertainty in the spatial distribution of VOC emissions.
AEROSOLS: The coarse and fine fractions of particles (PPM2 and PPM3 respectively) split into PPM_coa and PPM_fin, BCAR_coa and BCAR_fin and OCAR_coa and OCAR_fin at ratios depending on the SNAP activity sector. **NEW:** The speciation of the carbonaceous species has changed in chimere2014. When the $carb parameter is set to 1 in chimere.par, the anthropogenic species are separated into PPM, OCAR, and BCAR in CHIMERE. Otherwise, if carb=0, the non-carbonaceous species PPM are mixed with OCAR and BCAR resulting in the species called TPPM. For all the activity sectors H_2SO_4 emissions (1% of the total SO_x) is attributed to the fine mode H_2SO_4_fin.

6.2 Biogenic emissions

6.2.1 The biogenic emitted species

In the complete version of the model, the model needs:

- NO ..... Nitrogen monoxide
- APINEN ..... α-pinene
- LIMONE ..... Limonene
- OCIMEN ..... Ocimene (Lumped class)
- NA_coa ..... Sodium fraction of sea salts
- H2SO4_coa ..... Sulfate fraction of sea salts
- C5H8 ..... Isoprene
- BPINEN ..... β-pinene
- TERPEN ..... Terpene (Lumped class)
- HUMULE ..... Humulene (Lumped class)
- SALT_coa ..... Total dry sea salts
- HCL_coa ..... Chloride fraction of sea salts
- WATER_coa ..... Water fraction of sea salts

Emissions of six Chimere species: isoprene, α-pinene, β-pinene, limonene, ocimene, and NO, are calculated using the MEGAN model data and parameterizations. The new MEGAN model ([Guenther et al., 2006], v. 2.04) exploits most recent measurements in a gridded and canopy scale approach, more appropriate for use in CTMs since it estimates the effective burden of gases that mix and react in the boundary layer. Estimates of biogenic VOCs from vegetation and NO emissions are calculated as :

$$ER_i = EF_i \times \gamma_i(T, PPFD, LAI) \times \rho_i \tag{6.1}$$

where ER_i ($\mu g.m^{-2}.h^{-1}$) is the emission rate of species i, EF_i ($\mu g.m^{-2}.h^{-1}$) is an emission factor at canopy standard conditions, γ_i (unitless) is an emission activity factor that accounts for deviations from canopy standard conditions, and ρ_i is a factor that accounts for production/loss within canopy. The canopy standard conditions relevant for this study are defined as: air temperature (T) of 303 K, photosynthetic photon flux density (PPFD) of 1500 $\mu mol.m^{-2}.s^{-1}$ at the top of the canopy, leaf area index (LAI) of 5 $m^2.m^{-2}$ and a canopy with 80% mature, 10% growing and 10% old foliage. The MEGAN model parameterizes the bulk effect of changing environmental conditions using three time-dependent input variables specified at top of the canopy: temperature (T), radiation (PPFD), and foliage density (LAI). The production/loss term within canopy is assumed to be unity ($\rho = 1$). The equation can then be expanded as :

$$ER_i = EF_i \times \gamma_{T,i} \times \gamma_{PPFD} \times \gamma_{LAI} \tag{6.2}$$

The MEGAN model provides input EF and LAI data over a global grid, herefater projected on the CHIMERE model grid. The current available choice for EFs is restricted to following species: isoprene, α-pinene, β-

pinene, myrcene, sabinene, limonene, δ^3-carene, ocimene, and nitrogen oxide. EF's are static and refer to years 2000-2001. They are obtained summing up over several plant functional types (e.g. broadleaf and needle trees, shrubs, etc...). LAI database is given as a monthly mean product derived from MODIS observations, referred to base year 2000. Hourly emissions are calculated using 2-m temperature and short-wave radiation from a meteorological model output. The optimal choice for this work is the 150" resolution products proposed in the MEGAN inventory. The daily PPFD and temperature, which are representative values of the simulation, are set to the fixed values of 400. $\mu mol.m^{-2}.s^{-1}$ and 297 K, respectively.
Terpene and humulene emissions are not calculated in this model version and are set to zero.
Sea salt emissions are calculated by [Monahan, 1986] :

$$\frac{dF}{dr} = 1.373 U_{10}^{3.41} r^{-3} (1 + 0.057 r^{1.05}) 10^{1.19 e^{-B^2}} \tag{6.3}$$

$$B = \frac{0.38 - log(r)}{0.65} \tag{6.4}$$

F is the flux of sea salt particle number in particles m^{-2} s^{-1} μm^{-1}, **r** the particle radius in μm and $\mathbf{U_{10}}$ is the wind speed at 10 m in m s^{-1}.

6.2.2 Biogenic emission interface

The **BEMISSIONS.nc** required by the model file should contain 2D hourly biogenic emissions with Isoprene, Terpenes and Nitrogen Monoxide. It is created by the **src/initio/write_bemis.F90** program. The format of the **BEMISSIONS.nc** netCDF file is given in **Appendix G.5, p.174**, with 2D records containing the biogenic emission rates in molec/cm2/s.

- The program **remap_ef.F90** called by **prep_megan.sh** interpolates original global MEGAN emission factors and LAI data on the Chimere grid for the required domain. **prep_megan.sh** is called by **make-chemgeom.sh**, so these calculations can be done only once for a given domain. Original emission factor data are netcdf files called **<spec>all200021.nc** corresponding to the period 2000–2001 with <spec> referring to a given species. Those files must be stored in the $bigfilesdir/MEGAN/NETCDF_150sec/EF/EFMT21b directory. LAI data are 12 netcdf files of the format **laivyyyymm.nc** each file corresponding to one month of the year. The files must be stored in the $bigfilesdir/MEGAN/NETCDF_150sec/LAI/LAI20 directory. The output file is called **EFMAP_LAI_<domain>.nc** and is put to the **domains** directory. It contains emission factors for each MEGAN species, as well as 12 LAIs for each month as 2D variables on the Chimere grid for the given domain.
- Module **diagbio_megan** in **src/model/diagbio_megan.F90** contains subroutine *megan_bioemis* called from **src/model/worker_bio.F90** that calculates emission rates for the nine afore-mentioned MEGAN species (redistributed into the six Chimere species) using parameterizations of the original MEGAN code [Guenther et al., 2006]. The module also contains the data used for the calculations.
- Biogenic emissions for sea salts are calculated in the *calculate_bioemissions* subroutine from **src/model/diagbio_science.F90** module, which is called by **src/model/worker_bio.F90**. The file **LANDUSE_<domain>** that contains land use fractions (see Table 4.1) is required for sea salt calculations by *calculate_bioemissions*.

6.3 Mineral dust emissions

This CHIMERE model version may be viewed as an intermediate one concerning a complete mineral dust emissions calculation over Europe and Africa. Historically, there was no dust emissions in CHIMERE before 2005.
Between 2005 and 2008, two model developments were done in parallel:

- a **simple dust emissions scheme for Europe**, in order to close the aerosol mass budget for air quality studies ([Vautard et al., 2005b]). This development was done over Europe only due to the availability of anthropogenic emissions (EMEP only for the CHIMERE version previous to 2008). The parameterization were chosen to be simple in order to ensure fast calculations considering that all gaseous and particles species are calculated. The main goal was not to have the best emissions schemes but a scheme able to unbiase the modelled aerosols masses over Europe, and enough robust and stable to make confident forecasts.
- the **transport model CHIMERE-dust** dedicated to long range transport of dust over the northern hemisphere ([Menut et al., 2005, Menut et al., 2007, Menut, 2008, Menut et al., 2013]). This model was developed for studies of mineral aerosols processes (emissions and transport) over the Northern Atlantic.

In 2010, the development of CHIMERE-dust was frozen. Its specific parameterizations were implemented into CHIMERE (specific dry deposition velocities, saltation and sandblasting, Weibull distribution for wind speed used for emissions, the Tiedke deep convection scheme). The current model version thus proposed the two models into a single one. However, the developments are not yet finished: the mineral dust database used is only valid for arid and semi-arid areas oner Africa (Figure 6.2) and the erosion scheme over Europe remains simple. For the next years, developments will be done to ensure an homogeneous mineralogic and soil database over the globe and a single saltation and sandblasting scheme.

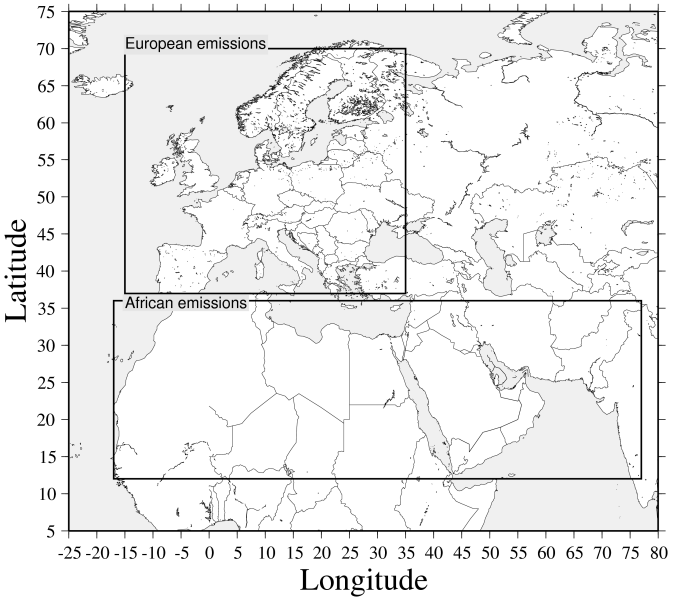


Figure 6.2: *Domains of mineral dust emissions estimations.*

Dust emissions are calculated by the **src/model/worker_dust.F90** program. The latter uses **diag-dust_science.F90** module.

6.3.1 Dust emissions over Africa

We used the scheme presented by [Alfaro and Gomes, 2001] to compute the dust fluxes and the size distribution. The calculations are numerically optimized following the developments in [Menut et al., 2005]. Table 6.2 displays notations, their values (if constants) and related units we used for the calculations. This model described the dust emission process as a balance between the kinetic energy provided by the saltating soil grains and the cohesion energy of the dust particles. The complete dust emission model proposed by [Alfaro and Gomes, 2001] is a coupling of the saltation flux calculation proposed by [Marticorena and Bergametti, 1995], and the sandblasting model developed by [Alfaro et al., 1998].

Parameter	Notation	Unit
Surface layer dynamic parameters		
Wind speed at 10 meters AGL	$\overline{U}_{10m}$	m.s^{-1}
Saltation roughness length	z_0	m
Smooth erodible roughness length	z_0^s	m
Saltation friction velocity	u_*	m.s^{-1}
Threshold saltation friction velocity	u_*^T	m.s^{-1}
Soil characteristics		
Soil particle density [quartz grains]	ρ_p	kg.m^{-3}
Air density	ρ_{air}	kg.m^{-3}
Soil aggregate particle size diameter	D_p	m
Particle kinetic energy	e_c	kg.m^2.s^{-2}
Multimodal aerosol size (with i values*)		
Mean Mass Diameter	$d_{m,i}$	m
Geometric standard deviation	σ_i	ad.
Binding energy	e_i	kg.m^2.s^{-2}
Fluxes (with j values*)		
Aerosol bin mass diameter	$d_{m,j}$	m
Horizontal (saltation) flux	F_h	kg.m^{-1}.s^{-1}
Mass vertical (sandblasting) flux	$F_{v,m}$	kg.m^{-2}.s^{-1}
Number vertical (sandblasting) flux	$F_{v,n}$	m^{-2}.s^{-1}
Sandblasting efficiency (for mass) F_v/F_h	α	m^{-1}
Adaptative constant	β	m.s^{-2}

Table 6.2: *Notations used to describe the saltation and sandblasting processes. * i=3 in this case.*

6.3.1.1 Saltation flux

As described in [Marticorena and Bergametti, 1995], [Alfaro and Gomes, 2001], [Gomes et al., 2003], the vertically integrated saltation flux is estimated using the [White, 1986]'s equation:

$$F_h(D_p) = \frac{K\rho_{air}}{g\ u_*^3}\left(1-\frac{u_*^T}{u_*}\right)\left(1+\frac{u_*^T}{u_*}\right)^2 \tag{6.5}$$

where u_* is the "saltation" friction velocity, i.e the friction velocity calculated using the roughness length, z_0, following [Marticorena and Bergametti, 1995]. u_*^T is the threshold friction velocity depending on the soil particle diameter size D_p and z_0. Following [Marticorena and Bergametti, 1995], we consider the air density as constant with ρ_{air}=1.227 kg.m^{-3}, and used the constant value $K = 1$. The parameterization used for the calculation of u_{*T} is the one proposed by [Shao and Lu, 2000]:

$$u_*^T(D_p) = \sqrt{a_n\left(\frac{\rho_p g D_p}{\rho_{air}} + \frac{\gamma}{\rho_{air} D_p}\right)} \tag{6.6}$$

with the constant parameters $a_n = 0.0123$ and γ=300 kg.m^{-2}. The particle density, ρ_p=2.65 10^3 kg.m^{-3} is chosen to be representative of quartz grains clay minerals.
The threshold friction velocities u_*^T may be modified by the drag partioning and the soil moisture. In this study, we used the drag partitioning proposed by [Marticorena and Bergametti, 1995] without soil moisture influence.
The saltation flux F_h is non-zero only if $u_* > u_*^T(D_p)$ for a given soil particle diameter D_p. The total saltation flux is thus obtained by integrating F_h over the soil size distribution from D_p^{min}=10^{-6}m to D_p^{max}=2. 10^{-2}m.

This interval is chosen in order to cover the whole range of possible soil sizes.

6.3.1.2 Sandblasting flux

The sandblasting fluxes is computed based on the partitioning of the kinetic energy of individual saltating aggregates and the cohesion energy of the dust particles. This model assumed that dust emitted by sandblasting is characterized by three modes whose proportion depends on the wind friction velocity. From wind tunnel measurements performed on two natural soils from semi arid regions, [Alfaro et al., 1998] consider these three modes as independent of the soil types. They described the three modes using log-normal distributions with diameters d_1=1.5 10^{-6}m, d_2=6.7 10^{-6}m and d_3=14.2 10^{-6}m and their associated standard deviation, respectively σ_1=1.7, σ_2=1.6 and σ_3=1.5. Based on this model, as soil aggregate size or wind speed increases, kinetic energy becomes able to release first particles of the coarsest mode that are associated with the lowest cohesion energy, then particles from the intermediate population, and finally the finest particles. It also implied that for a specific wind speed and soil size distribution, the dust flux may be zero even if the saltation process occurs. In order to apportion the available kinetic energy between the three modes, a constant cohesion energy e_i is associated to each mode values. The numerical values of e_i were determined by adjusting the predicted aerosols size distribution to those measured in wind tunnel under different wind conditions, using an iterative least square routine, as described in [Alfaro et al., 1998]. Depending on the description of the soil size distribution (measured or fitted), this procedure leads to different values of the cohesion energy [Alfaro et al., 1998]. [Alfaro and Gomes, 2001] recommend the use of the following values: e_1=0.376, e_2=0.366 and e_3=0.346 kg.m^{2}s^{-2}.

	p_1	p_2	p_3
$e_c < e_3$	0	0	0
$e_3 < e_c < e_2$	0	0	1
$e_2 < e_c < e_1$	0	$\frac{e_c - e_2}{e_c - e_3}$	1-p_2
$e_1 < e_c$	$\frac{e_c - e_1}{e_c - e_3}$	$(1-p_1)\frac{e_c - e_2}{e_c - e_3}$	1-p_2 − p_1

Table 6.3: *Fractions (p_i) of the kinetic energy for the three binding energies e_i, after [Alfaro et al., 1997]*

The kinetic energy is expressed, as a function of the soil particle diameter after [Alfaro et al., 1997] and [Shao and Lu, 2000]:

$$e_c = \rho_p \frac{100\pi}{3} D_p^3 \left(u_*^s\right)^2 \tag{6.7}$$

It is compared to cohesion energy of the three aerosol modes in order to compute the proportion $p_i(D_p)$ of these three modes to the total dust size-distribution (Table 6.3). The variations of $p_i(D_p)$ as a function of the available kinetic energy are illustrated in Figure 6.3 . Once the kinetic energy exceed e_3, the coarse mode is release and p_3 remains equal to 1 when the kinetic energy increase until it reaches e_2. Then p_3 exhibit a sharp decrease for any further increase of the kinetic energy. On the opposite, p_2 increase rapidly from 0 to 0.60 between e_2 and e_1. The decrease of p_2 once e_1 has been reached is not so severe than for p_3.
The dust flux is assumed to be proportional to the horizontal saltation flux $F_h(D_p)$. After [Alfaro and Gomes, 2001], summing the Equation 6.8 over the three aerosols modes, the total sandblasting flux may be written:

$$F_{v,m,i}(D_p) = \sum_{k=1}^{N_{class}} \frac{\pi}{6} \rho_p \beta \frac{p_i(D_{p,k}) d_{m,i}^3}{e_i} dF_h(D_{p,k}) \tag{6.8}$$

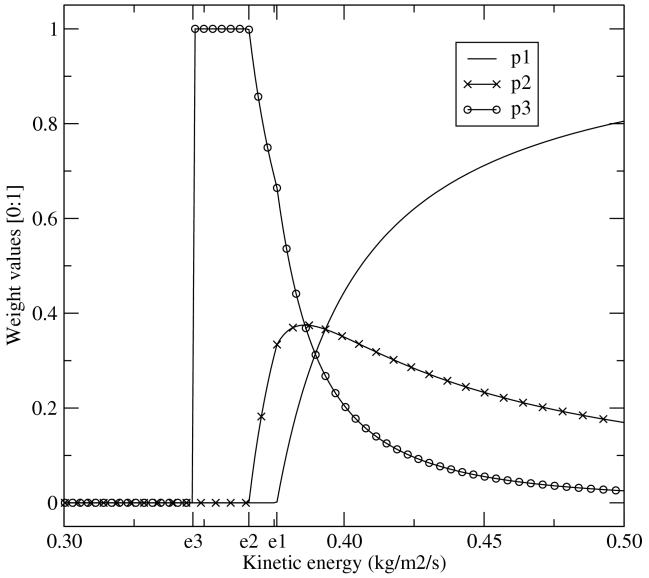


Figure 6.3: *Estimation of weights as a function of the prescribed binding energies* e_1, e_2 *and* e_3.

where N_{class} is the number of intervals discretizing the soil size distribution in the range $[D_p^{min} : D_p^{max}]$ and $d_{m,i}$ the mean mass diameter.
Finally, these three mass fluxes contributions are redistributed into the aerosols bins. The discretization chosen for aerosol size distribution ranged from 10^{-7}m to 10^{-4}m with 100 bins for this work. The corresponding mass fraction is distributed using a log-normal distribution, [Seinfeld and Pandis, 1998].

6.3.1.3 Weibull distribution for 10m wind speed

The interest of the specific Weibull distribution to represent wind speed variability was extensively discussed by numerous authors such as [Pavia and O'Brien, 1986], [Pryor et al., 2005] and [Cakmur et al., 2004]. In order to build a distribution for a chosen wind speed value, representing the mean value for a specific area and period, the probability density function is expressed as:

$$p(|U|) = \frac{k}{A}\left(\frac{|U|}{A}\right)^{k-1} exp\left[-\left(\frac{|U|}{A}\right)^{k}\right] \tag{6.9}$$

where k is a dimensionless shape parameter (in our case $k = 4$) and A is a scale parameter related to the mean of the distribution (in our case the modelled wind speed for each cell and each modelled hour).

6.3.1.4 The smooth roughness length and drag partition factor

The smooth roughness length, z_{0s}, is calculated only for coarse sand, fine-medium sand and silt because clay is too fine and does not represent erodible material. It is defined, for each soil type as the maximum among the three diameters (coarse sand, fine-medium sand and silt) and which have a non-zero mineral fraction, divided by 30. The smooth roughness length is required in the drag partition factor computation [Marticorena and Bergametti, 1995].

6.3.2 Dust emissions over Europe

The goal for dust over western Europe was not to develop a sophisticated erosion scheme for temperate regions as described in [Vautard et al., 2005b]. The parameterization follows the classical approach of dust emission

modelling in a simplified manner. The dust vertical flux (in g.m^2.s^{-1}) F is modelled with a functional approach similar to that of [Zender et al., 2003], which itself is based on the [Marticorena and Bergametti, 1995] approach and the [White, 1986] formula:

$$F = \alpha C u_{*s} \left(u_{*s}^2 - u_{*t}^2\right) \tag{6.10}$$

where u_{*s} denotes the saltation friction velocity, u_{*t} the threshold friction velocity and C is a coefficient that may depend on several surface factors. The sandblasting efficiency, α; describes the ratio of the vertical flux to the horizontal saltation flux. The saltation friction velocity us corresponds to that encountered on erodible parcels of the model grid cell, usually smoother than typical vegetated surfaces found in Europe. It is calculated by using the 10m wind field, a saltation roughness length of 5.10^{-4}m and the assumption of neutral stability as in most previous studies. In order to keep the formulation simple, the threshold friction velocity is assumed to depend only on gravimetric soil moisture w. This dependence uses the [Fecan et al., 1999] formulation:

$$u_{*t} = f_w u_{*0} \tag{6.11}$$

where u_{*0} is the minimal friction velocity for dust entrainment over dry soil, and is taken to be uniformly constant. The soil moisture factor f_w is given by

$$\begin{cases} w < w_t & f_w = 1 \\ w > w_t & f_w = \sqrt{1 + 1.21(100(w - w_t))^{0.68}} \end{cases} \tag{6.12}$$

where w_t is the gravimetric soil moisture content (in kg.kg^{-1}) above which entrainment is inhibited by soil moisture. This threshold is usually calculated as a function of the fraction of clay, in a rather empirical manner. In Europe during the summer season, the volumetric soil moisture provided by the NCEP GFS analyses and MM5 drops below 0.15 (gravimetric equivalent of about 0.10) only after several weeks without precipitation. We take here the uniform constant value w_t=0.1 kg.kg^{-1} throughout the model domain, which corresponds to a large clay fraction ([Fecan et al., 1999]).

The independence of threshold friction velocity on soil type is a strong assumption, since our aim is only to test the impact of introducing erosion processes. [Iversen and White, 1982] and [Shao and Lu, 2000] have proposed formulations linking the threshold velocity to the soil particle distribution. In both cases a minimal value of 0.2 m.s^{-1} is found, related to soil particles with a mean diameter of 0.1 mm. According to [Xuan, 2004], threshold friction velocities adjusted to wind tunnel observations are too large as they do not account for subgrid scale turbulence. Following this argument we divided the previous minimal threshold by 2 and take u_{*0}=0.1 m.s^{-1}.

The sandblasting efficiency is taken as $\alpha = 510^{-5} m^{-1}$ an order of magnitude obtained from the measurements, over Northern Spain and Niger, of [Gomes et al., 2003], and it is again kept uniformly constant, although its dependence can be made explicit as a function of clay content ([Marticorena and Bergametti, 1995]).

In the ideal case of a bare, non crusted soil, the factor C has been taken equal to ([Zender et al., 2003]):

$$C_i = \frac{2.61 \rho_{air}}{g} \tag{6.13}$$

In practice, the soil is covered with vegetation, snow or water over most of Western Europe and is very often crusted. We, therefore, define:

$$C = f_b f_c C_i \tag{6.14}$$

where f_c is the crustation factor, which has been found from field studies to lie in the 0.001-0.1 range ([Goossens, 2003]; [Gomes et al., 2003]), and f_b is the fraction of bare ground where dust is available for entrainment. In practice, the product $f_c f_b$ is taken here uniformly constant over land and is tuned to optimize

the model/observation correlations while keeping the average mineral dust fraction close to that found in the climatological observations of [Putaud et al., 2004]. This leads to $f_c f_b = 410^{-3}$: This strong assumption of a uniform factor leads to a large uncertainty. However, our results remain valid if other factors of the same order of magnitude are taken. Due to this uncertainty, our results should be considered in a qualitative manner only, which is enough for a sensitivity study. The [Fecan et al., 1999] parameterization of the effect of soil moisture was unable to inhibit dust erosion in sporadic events of fall wind and rain storms over Western Europe under wet conditions. Dust emissions are therefore set to zero when gravimetric soil moisture exceeds 0.2, and kept as the scheme calculates them only when it is below 0.16, a linear interpolation being performed between these two values.
The above emissions are assumed to be total emissions. Since emissions of mineral dust occurs primarily in the coarse mode, one assumes half of emissions in the 10-40 μm mode, 45% of emissions in the 2.510 μm mode and the remaining 5% are distributed in the fine mode using the same distribution as for anthropogenic.

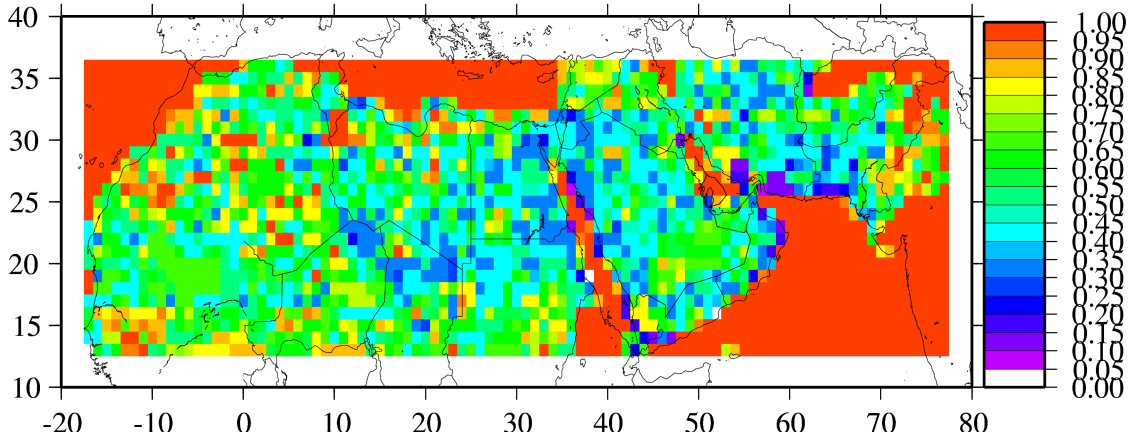


Figure 6.4: *Relative part of the most important soil class for each model cell. A value of 0.5 means that the most present soil represents 50% of the model cell.*

6.3.3 Data used for the mineral dust emissions calculations

The model parameters presented in Table 6.4 are mandatory to estimate mineral dust emissions fluxes.

Parameters	Units	Time variability
mandatory		
Soil composition (over Africa only)	% clay, % silt, % sand	constant
Aeolian roughness length z_0 (over Africa only)	cm	constant
Erodibility (over Africa only)	%	constant
10m wind speed	m/s	variable

Table 6.4: *Needed parameters for the mineral dust emissions fluxes calculations*

The soil is represented by relative percentages of sand, silt and clay for each model cell. Over Africa, data are built using ERS scatterometer data for *z0*, USGS and STATSGO-FAO data for landuse and soil properties. The spatial coverage is limited to the Northern Africa as displayed in Figure 6.4. The data are available in the CHIMERE file: chemprep/dustdata/dustdata-surf.asc.
For each soil type, mineralogical properties are defined as:

- coarse sand: D_p=0.069 μm, σ=1.6

- fine medium sand: D_p=0.021 μm, σ=1.8
- silt: D_p=0.0125 μm, σ=1.6
- clay: D_p=0, σ=0

These parameters are not dependent on time nor meteorology and are considered as constant. Based on these primary soil properties, more refined soil species are defined as explained in Table 6.5. An α factor is also defined, leading to estimate the vertical dust flux using the [Marticorena and Bergametti, 1995] scheme but not the explicit [Alfaro and Gomes, 2001]. However, it is strongly recommended to use [Alfaro and Gomes, 2001] to retrieve realistic vertical fluxes. These data are available in the input CHIMERE data file: chemprep/dustdata-soil.asc.

[Marticorena and Bergametti, 1995] soiltypes

Category	% CS	% FMS	% silt	% clay	% salt	α	z_{0s}	Soiltype
1	0	62.5	37.5	0	0	6.15e-06	7.00e-04	silty fine sand
2	80	20	0	0	0	1.25e-06	2.30e-03	medium sand
3	100	0	0	0	0	1.00e-06	2.30e-03	coarse sand
4	90	10	0	0	0	1.12e-06	2.30e-03	coarse medium sand
5	0	100	0	0	0	3.04e-06	7.00e-04	fine sand
6	31.25	31.25	37.5	0	0	4.35e-06	2.30e-03	silty medium sand
7	0	0	20	0	80	4.04e-06	1.73e-03	salty medium sand
8	0	0	8	0	92	3.18e-06	1.73e-03	salty silt fort
9	0	0	0	100	0	0.0e+00	2.30e-03	Clayey soil
10	0	0	50	0	50	7.35e-06	1.73e-03	Salt waste
11	0	0	100	0	0	1.99e-05	4.17e-04	Agricultural soil
12	0	50	10	0	40	3.50e-06	1.73e-03	Salty fine sand
13	60	0	40	0	0	3.31e-06	2.30e-03	Silty Coarse Sand
21	0	0	0	0	0	0.0	0.0	Mountains, cities
22	0	0	0	0	0	0.0	0.0	Rivers
23	0	0	0	0	0	0.0	0.0	Cultures
24	0	0	0	0	0	0.0	0.0	Inland water
99	0	0	0	0	0	0.0	0.0	Ocean

Table 6.5: *Description of soil types. CS= Coarse sand; FMS=Fine medium sand.*

6.4 Fire emissions

To account for fire emissions in the CHIMERE simulations, the following lines need to informed in chimere.par:

- $fire_emissions should be set to 1;
- $fire_emissdir is the name of the directory where fire emissions are stored;
- $fnemisf is the name of the output emission file.

Species list is the same as the anthropogenic one in the current version.
Fire emissions have to be provided in the following file format:

- One netcdf file per species and per month;
- Hourly emissions gridded on the simulation domain;
- Emissions are only provided for grid cells with non zero values, as a list of sources
- List of variables:
  - lon: Longitude grid (2D)
  - lat: latitude grid (2D)
  - ilatsources: latitude index of non-zero sources (1D=sources)
  - ilonsources: longitude index of non-zero sources (1D=sources)
  - SPEC: hourly emissions for species SPEC (3D=hours,days,sources) in molecule/cm2/s

Example netcdf file header for CO is given in **Appendix G.8**.

Chapter 7

Depositions and resuspension

7.1 Dry deposition

7.1.1 For gases :

Dry deposition is considered for model gas species i and is parameterized as a downward flux $F_{d,i} = -v_{d,i}c_i$ out of the lowest model layer with c_i being the concentration of species i. The deposition velocity is, as commonly, described through a resistance analogy ([Wesely, 1989]):

$$v_{d,i} = \frac{1}{R_a + R_{b,i} + R_{c,i}} \tag{7.1}$$

Stable case

$$R_a = \frac{1}{ku_*}\left[ln\left(\frac{z}{z_0}\right) + 4.7(\zeta - \zeta_0)\right] \tag{7.2}$$

Neutral case

$$R_a = \frac{1}{ku_*}\left[ln\left(\frac{z}{z_0}\right)\right] \tag{7.3}$$

Unstable case

$$R_a = \frac{1}{ku_*}\left[ln\left(\frac{z}{z_0}\right) + ln\left(\frac{(\eta_0^2+1)(\eta_0+1)^2}{(\eta_r^2+1)(\eta_r+1)^2}\right) + 2\left(tan^{-1}\eta_r - tan^{-1}\eta_0\right)\right] \tag{7.4}$$

where $\eta_0 = (1 - 15\zeta_0)^{1/4}$, $\eta_r = (1 - 15\zeta_r)^{1/4}$ and $\zeta_0 = z_0/L$, **L** is the Obukov length, k the von Karman constant and z_0 is the dynamical roughness length. z_0 depends on the fraction of land-use for each category and on the season. See Section on land-use and on meteorology for more details.
According to [Hicks et al., 1987] the quasi laminar resistance R_b, i is calculated as:

$$R_{b,i} = \frac{2}{ku_*}\left(\frac{Sc_i}{Pr}\right)^{2/3} \tag{7.5}$$

where Sc_i and P_r are the Schmidt and Prandtl number, respectively, k the von Karman's constant and u_* the friction velocity.
The formulation of the surface resistance R_c follows [Erisman et al., 1994]. It uses a number of different other resistances accounting mainly for stomatal and surface processes which are again dependent on the land use type and season. Necessary chemical parameters for the calculation of R_c are also taken from [Erisman et al., 1994] except for carbonyls ([Sander et al., 1999]; [Baer and Nester, 1992]) and peroxide

species ([Hall et al., 1999]). All species-related parameters are gathered in the DEPO_SPEC file located in all chemprep/inputdata directories related to the simulation.
In the DEPO_SPEC parameter file:

```
O3      48      0.01    1       2000
SO2     64      1e5     0       1e-20
NO2     46      0.01    0.1     2000
NO      30      2e-3    0       2000
NH3     17      1e+5    0       1e-20
.....................................
```

These columns are read and used in the **initio/inidepo.f90** subroutine. The parameters are:
1. charspec: species name
2. dMx: molar mass of the model species
3. dHx: effective Henry's law constant (M atm^{-1}) for the gas
4. df0: a normalized (0 to 1) reactivity factor for the dissolved gas
5. rRwat: parameter is not used
In **initio/inidepo.f90**, dHx and df0 are used for the mesophyllic resistance value (definition in [Seinfeld and Pandis, 1998], p.973) as:

- Mesophylle resistance Rm factor

```
do nd=1,ndepo
   Rm(nd)=1d-2/((dHx(nd)/3d3)+(1d2*df0(nd)))
enddo
```

- Quasi-laminary boundary layer resistance Rb factor

```
do nd=1,ndepo
   DH2O_Dx=sqrt(dMx(nd)/18d0)
   factRb(nd) = ((rNu/(DH2O*prandtl))                &
        &               * DH2O_Dx)**(2d0/3d0)        &
        &               * 2d0/vkarm
enddo
```

Here DH2O and DH2O_Dx are the molecular diffusivity of water and gaseous species, respectively.
The main land/seasonal parameters can be found in the file DEPO_LAND file which can be found in all chemprep/inputdata directories. Seasonal variations of resistances are taken from 3 Wesely Seasons:

- #1 (summer with full vegetation), from may to october. In August, September and October, however, LAI, stomatal resistance and deposition height are divided by two for the CROPLAND category in order to take into account harvested fields.
- #3 (winter without frost) from november through march.
- #5 (transitional season with short annuals) for April.

Most land parameters are taken from [Wesely, 1989], but LAI are drawn from the NASA/EOSDIS Oak Ridge National Laboratory using average LAI field measurements, for Summer.
Dry deposition (for gases) parameters are initialized in routine **src/initio/inidepo.f90**. At the coarse time step frequency, deposition velocities are calculated in routine **src/model/depvel.f90**. Deposition fluxes are calculated at the fine time step frequency in routine **src/model/deposition.f90**.

7.1.2 For aerosols:

Dry deposition for aerosols also makes use of a resistance scheme. The dry deposition velocity is expressed as :

$$v_d = v_s + \frac{1}{r_a + r_b + r_a r_b v_s} \tag{7.6}$$

where v_s is the sedimentation velocity expressed as in [Seinfeld and Pandis, 1998], R_a the aerodynamic resistance and R_b the quasi-laminar resistance for particles.
The aerodynamic resistance R_a is calculated as the integral of the inverse of the diffusivity coefficient K(z) up to the middle of the model surface layer, which can be estimated using the analytical formulae of the surface-layer similarity profiles for K ([Seinfeld and Pandis, 1998]).
Over vegetal canopies, corrections have been implemented according [Zhang et al., 2001], [Giorgi, 1986] and [Peters and Eiden, 1992]. A complete discussion on mecanistic processes of dry deposition is available in [Petroff, 2005].

7.2 Wet scavenging

When the aerosol option is selected, scavenging for gas/aerosols in clouds or rain droplets is taken into account. Wet scavenging is formulated as follows:

- For **gases** in **clouds**: Nitric acid, ammonia in the gas phase are scavenged by cloud droplets. This process is assumed to be revertible. Moreover, for in-cloud scavenging, dissolved gases in a non precipitating cloud can reappear in the gas phase due to cloud dissipation. Equilibrium between dissolved gases concentration and gas-phase concentrations follow Seinfeld and Pandis (1998).
- For **gases** in **rain droplets below the clouds**: Dissolution of gases in precipitating drops is assumed to be irrevertible, both for HNO_3 and NH_3. The scavenging coefficient is expressed as:

$$\Gamma = \frac{pD_g}{6.10^5 u_g D^2}(2 + 0.6R_e^{1/2}S_c^{1/3}) \tag{7.7}$$

  p being the precipitation rate (mm h^{-1}), D_g the molecular diffusion coefficient (m^2s^{-1}), u_g the raindrop velocity (m s^{-1}), Re and Sc respectively the Reynolds and Schmidt numbers of drops. [Mircea and Stefan, 1998] and references therein give relationships between u_g and hydrometeor diameter for various types of precipitation. In the model, sulfur dioxide and hydrogen peroxide are also scavenged by precipitation.
- For **particles** in **clouds** : Particles can be scavenged either by coagulation with cloud droplets or by precipitating drops. Particles also act as cloud condensation nuclei to form new droplets. This latter process of nucleation is the most efficient one in clouds. According to [Tsyro, 2002] and [Guelle et al., 1998], the deposition flux is written as:

$$\left[\frac{dQ_l^k}{dt}\right] = -\frac{\epsilon_l P_r}{w_l h} Q_l^k \tag{7.8}$$

  with p_r being the precipitation rate released in the grid cell (g cm^{-2} s^{-1}), w_l the liquid water content (g cm^{-3}), h the cell thickness (cm) and eipsilon an empirical uptake coefficient (in the range 0 - 1) depending on particle composition. l and k are respectively the bin and composition subscripts.
- For **particles** in **rain droplets below the clouds** : Particles are scavenged by raining drops, the deposition flux of particles being:

$$\left[\frac{dQ_l^k}{dt}\right] = -\frac{\alpha p E_l}{u_g} Q_l^k \tag{7.9}$$

  with a being an empirical coefficient, p the precipitation rate in the grid cell (g cm^{-2} s^{-1}), E a collision efficiency coefficient between particles and raining drops ([Loosmore and Cederwall, 2004]) and u_g the falling drop velocity (cm s^{-1}).

7.3 Resuspension of particulate matter

Text published in [Vautard et al., 2005b]

Saltation, which is necessary to transfer small mineral particles from the soil into the atmosphere, is not the only natural aerosol upward entrainment process. Resuspension of freshly deposited small particles lying at the surface by turbulent wind is a distinct process, their extraction resulting from the imbalance between adhesive and lifting forces (see e.g. [Reeks and Hall, 2001]. Such particles can originate from the atmosphere or the biosphere, and are particularly easy to extract shortly after deposition ([Loosmore, 2003]). They can be made of vegetal debris obtained from the mechanical or biological degradation of canopy elements, spores, pollens, etc. ([Simoneit and Mazurek, 1982]). The evidence of the presence of biogenic non mineral compounds in the continental aerosols has been reported several times (see e.g. [Andreae and Crutzen, 1997], for instance in the form of "humic matter", consisting in carbonaceous polymers (see [Gelencser et al., 2002] and references therein), and cellulose ([Kunit and Puxbaum, 1996]). As shown by [Gelencser et al., 2002], some of these aerosols could be of secondary nature.

However, for the sake of simplicity, we assume that this biogenic aerosol component is of primary origin. In order to represent these processes, we use a bulk formulation based on the simple resuspension rate empirical formula of [Loosmore, 2003], which was shown to provide a very good fit to the available resuspension measurement data:

$$\lambda = 0.01 \frac{u_*^{1.43}}{\tau^{1.03}} \tag{7.10}$$

where λ is the resuspension rate (in s^{-1}) and τ is the time after the start of resuspension. In the experiments used by the previous authors, the particles are first deposited then resuspended. In reality, deposition and resuspension are simultaneous, and the available dust concentration on the ground is governed by resuspension, washout by runoff and absorption by soil water, production by deposition and other biological or mechanical processes. The detail of all these processes is essentially unknown, and we assume here that the available concentration of dust does only depend on the wetness of the surface. In this empirical view, the resuspension flux is governed by:

$$F = P f(w) u_*^{1.43} \tag{7.11}$$

where $f(w)$ is a function of the soil water content and P is a constant tuned in order to approximately close the PM10 mass. The soil water modulation factor is vanishing for wet soil (gravimetric soil water content of 0.2 or more, as before, and is equal to 1 for dry soil, w less than 0.1). A linear relation is assumed between these values. The resuspension flux is found to be F=1800 $\mu g m^{-2} h^{-1}$ for a dry soil and for a friction velocity of 1 $m.s^{-1}$. In Northern Europe the typical MM5 value for volumetric soil water content is 25%, and 0.5 $m.s^{-1}$ for the friction velocity. This leads to a mass flux of about 170 $\mu g m^{-2} h^{-1}$ and then about 1.4 $ton.km^{-2}$ and per year, which is much larger than the anthropogenic emissions in most remote rural areas, but an order of magnitude smaller than that in urban areas. Finally, in the absence of any information the reentrained PM10 particle mass is supposed to be distributed in a standard atmospheric size distribution: $2/3$ of the mass as PM2.5 and $1/3$ as coarse PM1-PM2.5. Within PM2.5, particles are distributed as for the anthropogenic emissions.

Chapter 8

Initial and boundary conditions

8.1 Chemical boundary conditions

This section includes information for both initial and boundary conditions, both of which are treated in the same process although initial conditions extracted from a coarse scale simulation are only used for non-chained Chimere simulations.

8.1.1 Boundary conditions from global models

While some regional chemistry transport model rely on observation-based boundary concentrations, the Chimere strategy relies exclusively on simulations from global models. The added value in geographical and temporal variability as well as the larger number of chemical species available argue in favour of this second option, despite the increased sensitivity of the limited area CTM to any bias in the large scale forcing data. In order to cope with possible limitations in the global model forcing, we choose to increase the modularity of the global to regional nesting by allowing the use of several sources of boundary conditions (i.e. simulations from different models), or even combinations of such sources.
Three sources of boundary conditions were kindly made available by global chemistry-transport modelling groups to Chimere users. Their main characteristics are summarised below. The users are invited to take good care of acknowledging the work of their global modelling colleagues in their products and publications.
All the global fields provided for download are monthly climatologies (ie. averages over several years for a given month of the year) but the code has the capacity to use time-varying boundary conditions if the user has such fields available (see section 8.1.4).

8.1.1.1 Available source of input data

MACC The global chemical reanalysis produced as part of the MACC II project (Monitoring Atmospheric Composition and Climat II, www.copernicus-atmosphere.eu) is also made available. The global MACC service provides a 5-yr reanalysis for the period 2004-2009 of trace gases and aerosol concentrations. A global monthly climatology at a resolution of 1.125^o is made available to Chimere users.
The MACC modelling system relies on the coupled IFS-Mozart [Horowitz, 2003] modelling and assimilation system for reactive gases and on the MACC prognostic aerosol module for particulate matter.
Detailed validation of the MACC reanalysis can be found at:
`http://www.copernicus-atmosphere.eu/services/aqac/global_verification/validation_reports/`.
For users, in case of publication using these MACC data, please add in your acknowledgements: *This data set was provided by the MACC-II project, which is funded through the European Union Framework 7 programme. It is based on the MACC-II reanalysis for atmospheric composition; full access to and more information about this data can be obtained through the MACC-II web site (*`http://www.copernicus-atmosphere.`

eu).
The list of chemical species available in the MACC reanalysis is given in the list below.

- BC ..... Black carbon
- BIGALK ..... Lumped alkans C>3
- BIGENE ..... Lumped alkenes C>3
- C10H16 ..... lumped monoterpense
- C2H6 ..... Ethane
- CH2O ..... Formaldehyde
- CH3CHO ..... Acetaldehyde
- CH4 ..... Methane
- CO ..... Carbon monoxide
- DUST1 ..... Desert dusts (0.03-0.55 μm)
- DUST2 ..... Desert dusts (0.55-0.9 μm)
- DUST3 ..... Desert dusts (0.9-20 μm)
- GLYOXAL ..... Glyoxal
- H2O2 ..... Hydrogen peroxide
- HNO3 ..... Nitric acid
- ISOP ..... Isoprene
- NH3 ..... Ammonia
- NO2 ..... Nitrogen dioxide
- O3 ..... Ozone
- OM ..... Particulate organic matter (0.1-1 μm)
- PAN ..... Peroxy acetyl nitrate
- SO2 ..... Sulfur dioxide
- SO4 ..... Sulfate
- TOLUENE ..... Toluene

LMDz-INCA The historical and still commonly used set of boundary conditions is provided by the LMDz-INCA model (Laboratoire de Météorologie Dynamique General Circulation Model coupled with INCA: Interaction with Chemistry and Aerosols). The original INCA model is described in ([Hauglustaine et al., 2004] and [Folberth et al., 2006]) while developments related to aerosol modelling are presented in ([Bauer et al., 2004], [Schulz et al., 2006] and [Balkanski et al., 2007]). The specific version presented here is LMDZ4-INCA3 with the nitrate chemistry introduced in [Hauglustaine et al., 2014]. It has 96x96 horizontal grid points and 19 vertical levels.
The list of chemical species available in the LMDz4-INCA3 model is given below. An example of surface ozone concentrations modelled with LMDz-INCA and MACC is presented in Figure 8.1.

- ALKAN ..... Lumped alkans C > 3
- AROM ..... Lumped aromatics
- BC ..... Black carbon
- C2H4 ..... Ethylene
- C2H6 ..... Ethan
- C3H6 ..... Propen
- CH2O ..... Formaldehyde
- CH3CHO ..... Acetaldehyde
- CH4 ..... Methane
- CNO3 ..... Coarse Nitrate (2.5-5 μm)
- CO ..... Carbon monoxide
- DUST ..... Desert dusts (1-10 μm)
- H2O2 ..... Hydrogen peroxide
- HNO3 ..... Nitric acid
- NH3 ..... Ammonia
- NH4 ..... Particulate ammonium (0.1-1 μm)
- NO2 ..... itrogen dioxide
- NO3 ..... Particulate nitrate (0.1-1 μm)
- O3 ..... Ozone
- OC ..... Particulte organic carbon (0.1-1 μm)
- PAN ..... Peroxy acetyl nitrate
- SO2 ..... Sulfur dioxide
- SO4 ..... Sulfate

GOCART The Global model GOCART (NASA,[Ginoux et al., 2001]) was historically the only source of boundary conditions for particulate matter, it can still be used in combination with other sources for gaseous boundary conditions.
The list of chemical species available in the GOCART model is given in the list below. For each species, the size distribution is given in μm. An example of surface mineral dust concentrations modelled with GOCART and MACC is presented in Figure 8.2.

- DUST1 ..... Desert dusts (0.2-0.36)
- DUST2 ..... Desert dusts (0.36-0.6)
- DUST3 ..... Desert dusts (0.6-1.2)
- DUST4 ..... Desert dusts (1.2-2)
- DUST5 ..... Desert dusts (2-3.6)
- DUST6 ..... Desert dusts (3.6-6)

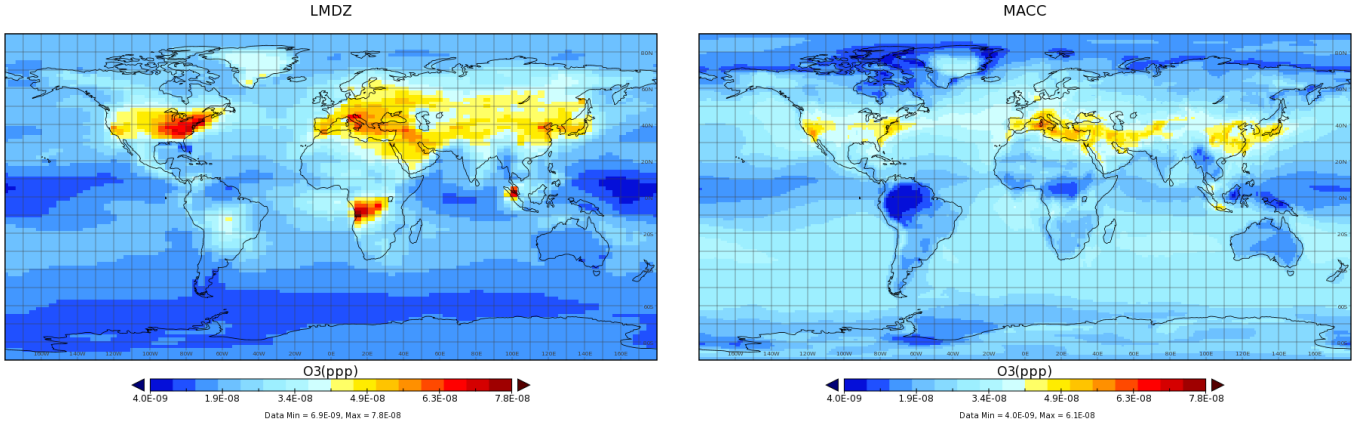


Figure 8.1: *Surface ozone concentrations modelled with LMDz-INCA and MACC for july.*

- DUST7 . . . . . Desert dusts (6-12)
- HBBC1 Hydrophobic black carbon (0.02-0.06)
- HBBC2 Hydrophobic black carbon (0.06-0.18)
- HBBC3 Hydrophobic black carbon (0.18-0.54)
- HBBC4 Hydrophobic black carbon (0.54-1.62)
- HBBC5 Hydrophobic black carbon (1.62-4.86)
- HBBC6 Hydrophobic black carbon (4.86-14.58)
- HBOC1 . . . . . Hydrophobic organic carbon (0.02-0.06)
- HBOC2 . . . . . Hydrophobic organic carbon (0.06-0.18)
- HBOC3 . . . . . Hydrophobic organic carbon (0.18-0.54)
- HBOC4 . . . . . Hydrophobic organic carbon (0.54-1.62)
- HBOC5 . . . . . Hydrophobic organic carbon (1.62-4.86)
- HBOC6 . . . . . Hydrophobic organic carbon (4.86-14.58)
- HLBC1 . Hydrophylic black carbon (0.02-0.06)
- HLBC2 . Hydrophylic black carbon (0.06-0.18)
- HLBC3 . Hydrophylic black carbon (0.18-0.54)
- HLBC4 . Hydrophylic black carbon (0.54-1.62)
- HLBC5 . Hydrophylic black carbon (1.62-4.86)
- HLBC6 Hydrophylic black carbon (4.86-14.58)
- HLOC1 . . . . . Hydrophylic organic carbon (0.02-0.06)
- HLOC2 . . . . . Hydrophylic organic carbon (0.06-0.18)
- HLOC3 . . . . . Hydrophylic organic carbon (0.18-0.54)
- HLOC4 . . . . . Hydrophylic organic carbon (0.54-1.62)
- HLOC5 . . . . . Hydrophylic organic carbon (1.62-4.86)
- HLOC6 . . . . . Hydrophylic organic carbon (4.86-14.58)
- SULF1 . . . . . Sulfates (0.02-0.06)
- SULF2 . . . . . Sulfates (0.06-0.18)
- SULF3 . . . . . Sulfates (0.18-0.54)
- SULF4 . . . . . Sulfates (0.54-1.62)
- SULF5 . . . . . Sulfates (1.62-4.86)
- SULF6 . . . . . Sulfates (4.86-14.58)

8.1.2 Structure of the boundary conditions from global models

All global forcing data are given in netcdf format with one file per month. Additional information on the input data are provided in the netcdf attributes for each variable. The most important attributes are "unit":

- **ppp** for part per part (mixing ratio),
- **ppb** for part per billion of 1e9 ppp,
- **ug** for micro-gram per cubic meter)

"typ" indicates if the variable is a gas ("gas"), desert dust ("dust") or non-dust aerosol ("aer"). The molar mass as used in the global model should also be provided.

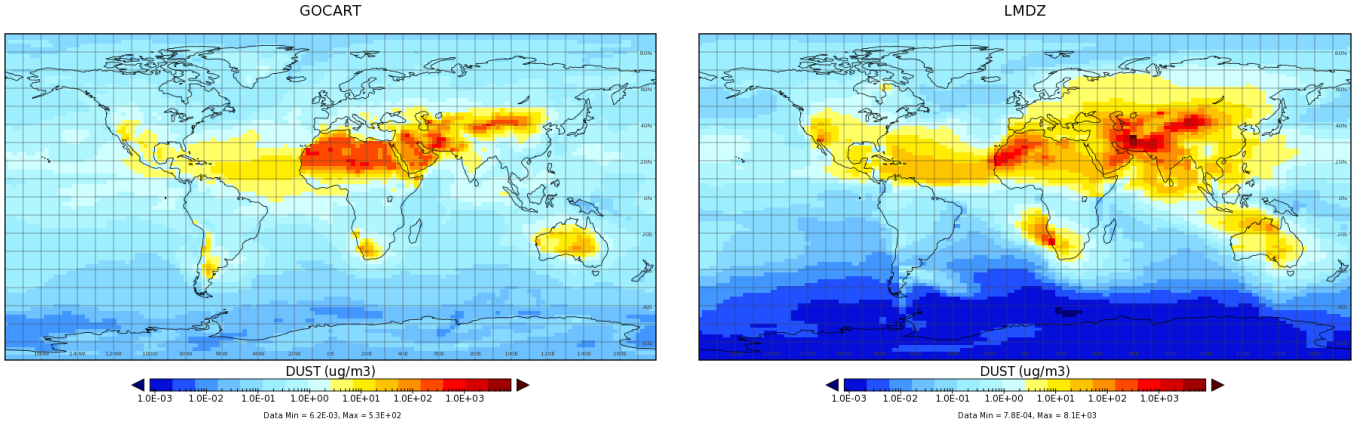


Figure 8.2: *Surface mineral dust concentrations modelled with GOCART and LMDzINCA for july.*

In addition to concentration fields, the input files have latitude and longitude coordinates as well as the vertical grid (either 3D pressure on model levels or surface pressure + alpha and beta coefficients for the sigma-p grid). Would some conversion be required to provide concentrations in ppb to Chimere from the native unit in the global model (e.g. μg m^{-3}), the 3D temperature field is also requested in order to derive air density. Alternatively a constant and 3D uniform temperature of 15^{o}C is used.
The correspondence between the chemical species of the global model and Chimere is handled in the chemprep part of the code. This way, it is possible to use any source of input data for any of the chemical mechanism of Chimere.
The file **XXX_builder** (XXX is the name of a global concentrations dataset, GOCART, LMDZ-INCA or MACC at the moment) is used to build the interface between XXX and CHIMERE species. These files are split in 5 files types.

- For gas species : XXX_builder.meca where meca represents the chemical mechanism name (SAPRC/MELCHIOR1/MELCHIOR2)
- For SOA : XXX_buider.aer.soa where soa represents the SOA mechanism used (simple/medium/complex)
- For dust : XXX_buider.dust if the DUST specie are taken into account
- For primary aerosol species : XXX.car if the carbonaceous species are taken into account and ppmcarb if there are no carbonaceous species.
- For sea salts : xxx_builder.nacl if the sea salts are taken into account

Should any modification be added to the chemical scheme, these builders have to be modified accordingly.
For example, the builder for LMDz-INCA and the SAPRC chemical mechanism is:
chemprep/boundaries_spec/INCAv2012_builder.saprc

```
# Coarse species, typde, number of corresponding CHIMERE species,
# and for each species: name, molar mass, conversion factor
ALKAN  gas  1 ALK3   59. 1.
AROM   gas  1 ARO2  119. 1.
C2H4   gas  1 C2H4   28. 1.
C2H6   gas  1 ALK1   30. 1.
C3H6   gas  1 OLE1   72. 1.
CH2O   gas  1 HCHO   30. 1.
CH3CHO gas  1 CH3CHO 44. 1.
CH4    gas  1 CH4    16. 1.
CO     gas  1 CO     28. 1.
H2O2   gas  1 H2O2   34. 1.
```

```
HNO3    gas  1 HNO3    63. 1.
NH3     gas  1 NH3     17. 1.
NO2     gas  1 NO2     46. 1.
O3      gas  1 O3      48. 1.
PAN     gas  1 PAN    100. 1.
SO2     gas  1 SO2     64. 1.
```

8.1.3 Adding new sources of input data

Basic netcdf manipulation using nco or cdo tools should allow advanced users to convert any global model fields into the appropriate format following the structure of the existing forcings and keeping one file per month, even if high frequency data are available. A new builder also needs to be written for each type of forcing. Apart from that, all the processing described in section 8.1.4, should work without distinction for any type of input data.

8.1.4 Boundary conditions interface

8.1.4.1 Chimere parameter file

In the chimere.par file, the user is invited to provide the path to its Boundary Conditions data (bcdir) together with a label pointing towards the relevant source (INCA, MACC, GOCART) as the name of the subdirectory where global data where extracted. The source of boundary data can be a composite of several global models for gas, dust and non-dust aerosol by using the right flags: bcgas, bcdust, and bcaer. And for each of these flag the user can indicate whether climatological data (monthly means) are desired (with bcgasdt, bcaerdt, or bcdustdt = 0), or if a higher temporal frequency is available (setting these flags to 1) in that case the fortan code extract automatically the highest available temporal resolution.

8.1.4.2 scripts/chimere-bound.sh

By reading the arguments in the chimere.par file, this script will link towards the right type of input data for each type of compound (gas, aer, dust). If several sources are required, the boundary condition extraction will be performed sequentially before being merged into a single file. In the case of time varying data, the script will try to locate the boundary conditions of the relevant years. Otherwise, for climatological data, the code looks for monthly data in the "clim" subdirectory. The boundary condition year is then handled as "0000".

8.1.4.3 src/prep/prep_bc.F90

The geometrical extraction as well as unit conversion is ultimately performed in the fortran part of the pre-processor. This code is generic an ignores the origin of the input data as long as the correct input format is provided. It can handle any temporal resolution of the boundary conditions and makes the difference between climatological and time-varying fields by checking whether the boundary condition year is "0000".

8.1.4.4 Output

The prep_bc.F90 program generates two groups of files: BOUN_CONCS.nc-* and INI_CONCS.nc-*. The files in each group are arranged by species types: gaseous ("-gas" suffix), aerosols ("-aer" suffix), and mineral dust ("-dust" suffix). **prep_bc** also generates the corresponding ASCII files with the ".lst" extension listing the actual *.nc files created by the program. The BOUN_CONCS.nc-* files contain trace species concentration on the outskirts of the Chimere domain for all the simulation time steps. The INI_CONCS.nc-* files contain initial conditions in the 3D limited-area domain; they are used if the model cannot find a previous Chimere run (see section 8.2).

8.1.5 Internal boundary conditions

Boundary conditions can be either "external" (see previous sections) or given by a coarse-resolution CHIMERE simulation. When a coarse-resolution simulation is available, i.e., when the **out.[coarse-label].nc** file exists, the **prep_chimere.F90** interface in the **src/prep** directory is used to generate the lateral and top boundary conditions to a nested run. This option is indicated by switching on the nest flag in chimere.par.

8.2 Initial concentrations

8.2.1 Initial concentrations species

There are two possible initialisation modes:

- Initialisation by reading initial concentrations in a restart file. This file must contain the "end" concentrations of a previous simulation, as provided in the **end.[label].nc** (and **exe.[label].nc** if the **pops** flag is activated). The species list is contained in the **end.[label].nc** file itself and is read by CHIMERE during initialisation.
- Initialisation by interpolating global concentration fields. This is the most common option used for a first initialisation.
- Initialisation by interpolating boundary conditions. Because of technical limitations, it is used only when the pops flag is activated (pops=1)

The top calling script checks the existence and non-emptiness of a file called **ini.[label].nc** (and **iex.[label].nc** if the **pops** flag is activated) in the simulation directory, which can be a copy of an "end" file. If it exists and is nonempty, then the initial conditions are used. In the other case, initial conditions are interpolated from boundary conditions. Initial conditions are read and put into arrays **conc** and **conco** in routine **src/initio/iniconc.F90**.

8.2.2 Initial concentrations interface

There are two types of initial conditions that can be used for CHIMERE : Initialized concentrations and non initialized concentrations. In the first case a file named **ini.[label].lst** is placed in the simulation directory (the same as where the CHIMERE output files **out.[label].nc**, **par.[label]** and **end.[label]** are). In the second case there is no need to provide a file; initial conditions will be taken from interpolated global fields, layer by layer. The initial concentration files **INI_CONCS.nc-*** generated by **prep_bc.e** are listed in the ASCII file **INI_CONCS.list**. When no restart files are available for the current run, the latter is linked to the initialisation file **ini.[label].lst** in the output directory. The **ini.[label].lst** file is used to initialise the simulation.
When the restart file **end.[label].nc** from the previous simulation is available, it is linked to the **ini.[label].nc** file. This is automatically done in the **scripts/chimere-run1.sh** script. The format of the **ini.[label].nc** file is exactly the same as that of the **end.[label].nc** file. It contains the concentrations encoded in the netCDF format, described in **Appendix G.7, p.175**.
Initialisation is important for large-scale simulations (domains larger than about 500 Km $\times$ 500 km). Under extremely stagnant conditions, spin-up of one or two days may also be necessary at local (100 Km) scale. At regional scale, the spin-up time should be of the order of 4-5 days (for ozone and precursors).

Chapter 9

Meteorology

The meteorological data are used three different times in CHIMERE:

- §9.1: Input data: CHIMERE being an off-line model, input meteorological fields are necessary. These input data have to be reformatted to be read by CHIMERE.
- §9.2: Diagnostic parameters: Many meteorological parameters are required for a CHIMERE simulation. Depending on the input meteorological driver, they are not always available as input. Thus, in CHIMERE, a diagnostic program may be activated to parameterize the necessary but not provided parameters.
- §9.3: Transport and mixing: Once all meteorological data are available, they are used to mix and transport chemical species during the simulation.

9.1 Meteorological input data

CHIMERE is driven by meteorological fields from regional models, such as WRF or MM5 or global models such as ECMWF-IFS. To use these meteorological fields, available in various data format, CHIMERE contains several pre-processors to homogeneize these data and deliver a standard meteorological file to be read by the CHIMERE core: the NetCDF file **exdomout.nc**.

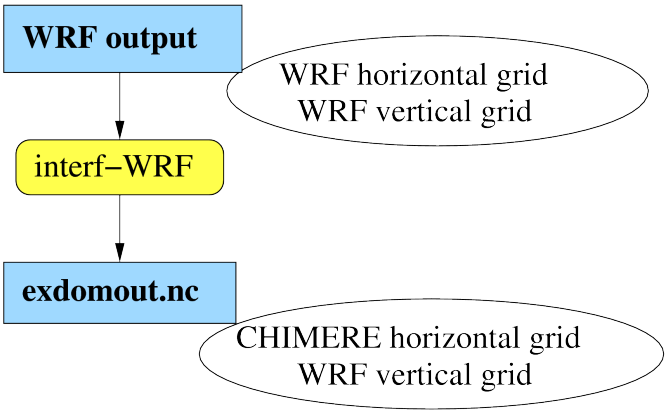


Figure 9.1: *Flow chart of the meteorological CHIMERE pre-processor. WRF model is shown as an example of a weather forecast model driving CHIMERE. Programs are shown in yellow and NetCDF files in blue.*

The top calling script of CHIMERE calls a program named **interf-[metname]** in the **meteo** directory. This program (usually a bourne shell script) has to be written by the user.
One example is given : *interf-wrf* which is a generic interface to WRF. Figure 9.1 displays an example of

the pre-processor. The *prepwrf* interface takes a WRF output netcdf file wrfout... given by the 'meteo_file' variable in *chimere.sh* and then by 'fn_wrf' in *prepwrf.nml*. The list of WRF variables to process and their parameters are specified in the structure variable 'varmeta' and are initialized in subroutine *initvars*. You might need to adjust this initialization (and the corresponding definitions of the parameters between IFIRST and ILAST in the beginning of the program), if your WRF output has variables additional to those specified in 'varmeta'. The domain coordinate files *COORD_WRF*, *COORD_WRF_U*, and *COORD_WRF_V* are created by *prepwrf* from the WRF output netcdf files, so in contrast to MM5 you do not have to use an additional program for it. The 'metdom' variable specified in *chimere.sh* is not used by the WRF interface.
This script *interf-wrf* calls a Fortran program, *prepwrf-interp.F90*. This program made several operations on the data:

- It transforms original meteorological variables given on the meteo model grid, at a frequency that is not necessarily one hour, to standard variables given on the CHIMERE horizontal grid as hourly values.
- The operations performed are horizontal and temporal interpolation, wind vector rotation, transformation from perturbation and mean values to the total ones, etc., depending on the original data format.
- Note there is no vertical interpolation (from the meteo file to CHIMERE) to conserve the full vertical resolution, for a better accuracy on turbulent diagnostics made later in CHIMERE (see §9.2)

At the end, a generic meteo file is created, **exdomout.nc**, with a dedicated CHIMERE format. In this file, some variables are mandatory, some others are optional. The file structure is entirely defined by the header listing in **Appendix G.2, p.168**. Table 9.1 lists these variables which must or can be output by the interpolation stage.

File Name	Variable	Dimension	Units
Mandatory Variables			
lon	longitude of gridpoints	2D	degrees_east
lat	latitude of gridpoints	2D	degrees_north
alti	Altitude of half layer	3D	m
winz	Zonal component of the wind	3D	m/s
winm	Meridional component of the wind	3D	m/s
temp	Temperature	3D	K
sphu	Specific humidity	3D	kg/kg
pres	Pressure	3D	Pa
cliq	Cloud liquid water content (excluding rain water)	3D	Kg/Kg
swrd	Short Wave Radiation	2D	W/m^2
lwrd	Long Wave Radiation	2D	W/m^2
psfc	Surface pressure	2D	Pa
tem2	2m Temperature	2D	K
rh2m	2m Relative humidity	2D	0-1
weas	Water equiv. accum. snow depth	2D	mm
copc	Convective Precipitation	2D	kg/m^2/hour
lspc	Large-scale Precipitation	2D	kg/m^2/hour
Optional Variables			
rain	rain water profile	3D	Kg/Kg
cice	ice profile	3D	Kg/Kg
sshf	Surface sensible heat flux	2D	W/m2
slhf	Surface latent heat flux	2D	W/m2
usta	Friction velocity	2D	m/s
hght	Boundary layer height	2D	m
lowc	Low cloud fraction	2D	m
medc	Medium cloud fraction	2D	m
higc	High cloud fraction	2D	m

Table 9.1: *Mandatory and optional variables in* **exdomout.nc** *meteo file. Note that all meteorological 3D variables must be provided at half-layers levels.*

The programs are provided for MM5, WRF and IFS/ECMWF. If other meteorological data have to be

used, the user should give it a name, [metname], and write the *interf-[metname]* bash program and the *prep[metname].F90* fortran program. The user should also change the **"meteo="** line in the top calling script.

9.2 Diagnostics of parameters:

The second stage of the meteorological fields treatment is directly in the CHIMERE model, and during the hourly integration phase. Note that compared to the previous versions of CHIMERE, all these programs replace the *diagmet* programs.
All programs are called by the *integrun.F90* routine and are:

- *readmetro*: routine for the hourly reading of the *exdomout.nc* file
- *calc_turb*: calculation of turbulence on raw meteo profiles
- *calc_winw*: calculation of the vertical wind speed on chimere profiles
- *calc_deepconv*: calculation of deep convection fluxes (if required by the user)
- *checkcfl*: Estimation of the adaptative time-step
- *outprint*: Save meteo data (high vertical resolution) to the *meteo.$sim.nc* file.
- *met2chim*: Conversion of units from the meteo format to the specifc CHIMERE format (molecules, centimeters and seconds).

9.2.1 Management of additional parameters

These calculations are done in the *calc_turb* routine. The first calculation is done to estimate several meteorological parameters, mandatory for CHIMERE but not always available with the meteorological input files. These parameters correpond to the optional parameters listed in Table 9.1. The calculations are done using the meteorological fields provided in the *exdomout.nc* file, i.e already projected on the horizontal CHIMERE grid but still on the native meteo model vertical grid.
The availability of these parameters is checked during the reading of the *exdomout.nc* file. If the parameters exist, they are not recalculated, contrarily to the previous versions of CHIMERE where it was a user's option. Indeed, we consider that if the variables exist, they correspond to recent parameterization in the meteorological model used and are consistent with other variables. They thus have to be keep.
If they are not available, the following parameters are diagnosed:

- If **boundary layer height** is not available from meteo data, it will be calculated. The boundary layer height is considered as the maximum of the [Troen and Mahrt, 1986] boundary layer height calculated from the Richardson number profile, as the lowest altitude where R_i = 0.5, and a more convectively-based boundary layer height calculation. The latter is based on a simplified and diagnostic version of the approach of [Cheinet and Teixeira, 2003]. It consists in the resolution of the (dry) thermal plume equation with diffusion. The in-plume vertical velocity and buoyancy equations are solved and the boundary layer is taken as the height where vertical velocity stops. Thermals are initiated with a non-vanishing vertical velocity and potential temperature departure, depending on the turbulence similarity parameters in the surface layer.
- The **friction velocity** u_* is used for deposition and calculation of diffusivities. It is a particularly sensitive parameter for ozone in Summer through the calculation of aerodynamic resistance R_a. It should strongly depend on land use type, which are critical to deposition. In meteorological models, especially large-scale, roughness lengths are sometimes estimated too roughly for the application to high-resolution deposition. The recalculation of u_* which is proposed uses the [Louis et al., 1982] formulation which is particularly robust and gave satisfactory results.
- **Heat fluxes** are also used for the calculation of w_* and therefore mixing, and the height of the boundary layer. In fact only the virtual heat flux is required, which can be recalculated from an empirical formula

[Priestley, 1949] using temperatures in the first meteorological model layers. This formula is not very accurate.

- The **vertical turbulent diffusivity** K_z. Horizontal turbulent fluxes are not considered. Vertical turbulent mixing takes place only in the boundary-layer. The formulation uses K-diffusion following the parameterization of [Troen and Mahrt, 1986], without counter-gradient term. In each model column, diffusivity K(z) is calculated as:

$$K_z = k w_s z \left(1 - \frac{z}{h}\right)^{1/3} \tag{9.1}$$

where w_s is a vertical scale given by similarity formulae.

- In the stable case (surface sensible heat flux < 0): $w_s = u_*/(1 + 4.7z/L)$
- in the unstable case: $w_s = (u_*^3 + 2.8ew_*^3)^{1/3}$

where e = max(0.1,z/h), **L** is the Obukhov Length, w_* is the convective velocity scale, u_* the friction velocity and h the boundary layer height. A minimal K(z) is assumed, with a value of 0.01 m^2/s.

Finally, all three-dimensional meteorological fields are averaged over the CHIMERE vertical grid. Note that several fixed parameters are present in this *calc_turb* routine. They were chosen are the more realistic as possible and it is not recommended to modify these values. These constant valeus are listed in Table 9.2.

Variable	Value	Description
pblmin	20.	Minimum PBL height
vkminup	0.1	Minimum Kz above PBL (m2/s)
z10m	10.	10 meters above ground level
soimdef	1.0	Default Soil Moisture (no resuspension/erosion)
woff	0.5	Wind offset to smooth Richardson numbers (m/s)
crhx	0.90	Min RH for cloud BLH enhancement
vkmax	500.	Maximum Kz
odclw	0.18e3	Optical depth rate for liquid water
odcic	0.06e3/0.9	Optical depth rate for ice
topcldmax	1000.	Maximum altitude of low clouds top
cloh	1	High cloud option for attenuation
crhh	0.95	High cloud option for attenuation
cloh2	0.005	High clouds optical depth /m for RH=1
ztherm	25.0	Height of thermals start
ric	0.5	Troen and Mahrt suggestion for critical Ri for BL top
dvsca	1000.0	Entrain./Detrain. first guess vertical scale (m)
vkmindry	0.01	Minimum Kz in the dry boundary layer (m2/s)
vkminwet	1.0	Minimum Kz in cloudy boundary layer (m2/s)
rlam	150.	Upper air mixing length

Table 9.2: *Constant values used for the calculation of additionnal parameters in the routine calc_turb.*

9.2.2 Estimation of the vertical velocity

This calculation is done in the *calc_winw* routine. The vertical velocity is diagnosed by using the horizontal fluxes. A simple momentum conservation relation is applied to calculate the vertical flux for the top of each model box (assuming that the first one, near the ground, is zero).

9.2.3 Deep convection fluxes

These calculations are done in the *calc_deepconv* routine. The calculation of deep convection fluxes is done only if the user defined the corresponding flag as ideepconv=1 in the *chimere.par* namelist file.

The deep convection scheme describes effects of subgrid scale clouds on tropospheric convection, after [Tiedtke, 1989]. Deep convection occurs when cumulus or cumulo-nimbus clouds (referenced as convective clouds) are present. These clouds are formed when air masses are unstable, when warm air is at the surface or cold air is transported in upper layers (cold front). High vertical wind speed are observed leading to vertically extended cloud structures. On the other hand, when clouds are only due to mechanical forcings (mountains, warm fronts), they are named stratiform clouds and generally exhibit low vertical speed values.

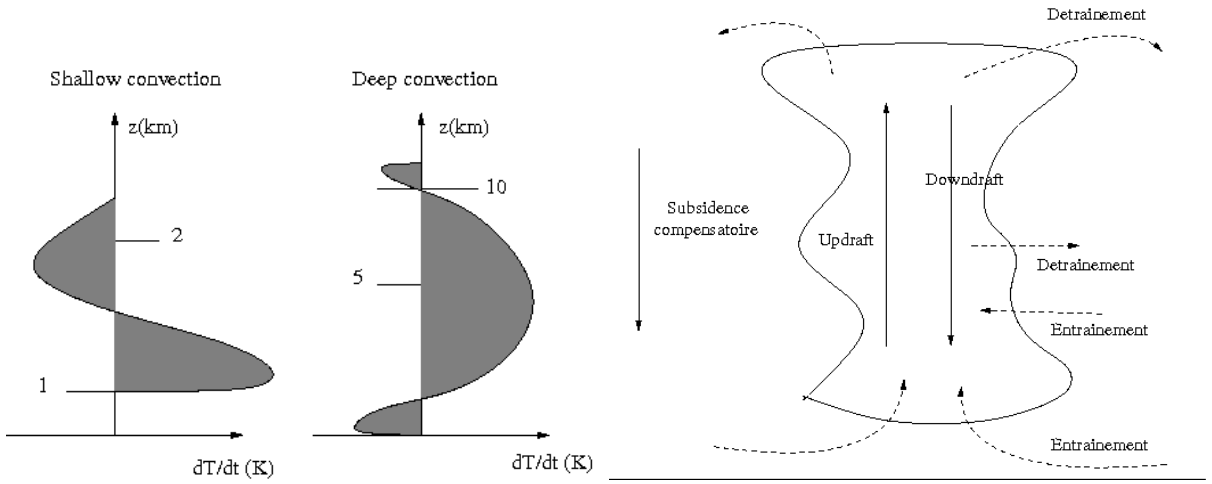


Figure 9.2: *[left] Temperatures changes due to shallow and deep convection and [right] Schematic view of a convective cloud*

Air masses may be quickly mixed in the troposphere when convective unstabilities occured under a cloud. To describe this phenomenon, schemes generally consider a cloud (and the whole column including this cloud) and the environment. In the major part of deep convection parameterizations, the hypothesis of small cloud surface compared to the total studied surface is done.
Under the cloud, updrafts and downdrafts are observed, Figure 9.2. The updraft originates from air masses lighter than their environment when downdrafts represent fall of colder air (often with rain). In the updraft and the downdraft, air may be exchange between the cloud and the environment: if air of environment flows to the cloud, this is the **entrainment** and if air of clouds flows towards environment, this is the **detrainment**. In order to ensure mass conservation, a compensatory **subsidence** is observed in the environment.
In CHIMERE, the Tiedtke scheme is implemented. The main goal of this scheme is to estimated a convection mass flux:

$$M(z) = \rho(z)(a_{up}\overline{w_{up}(z)} + a_{dw}\overline{w_{dw}(z)}) = -\rho(z)a_{env}\overline{w_{env}(z)} \tag{9.2}$$

with $\overline{w_{up}(z)} > 0$, $\overline{w_{dw}(z)} < 0$ et $\overline{w_{ent}(z)} < 0$ the vertical wind speed in the updrafts, downdrafts and environment, respectively. The vertical gradient of this mass flux is:

$$\frac{\partial M(z)}{\partial z}(z) = E(z) - D(z) \tag{9.3}$$

with $E(z) > 0$ et $D(z) > 0$, the entrainment and detrainment fluxes. This equation works both for updrafts and downdrafts, with, for example for the updraft:

$$E(z) = E_{up}(z) + E_{dw}(z) \text{ and } D(z) = D_{up}(z) + D_{dw}(z) \tag{9.4}$$

An example of estimated fluxes are displayed in the Figure 9.3.
These fluxes are used to estimates chemical concentrations fluxes as:

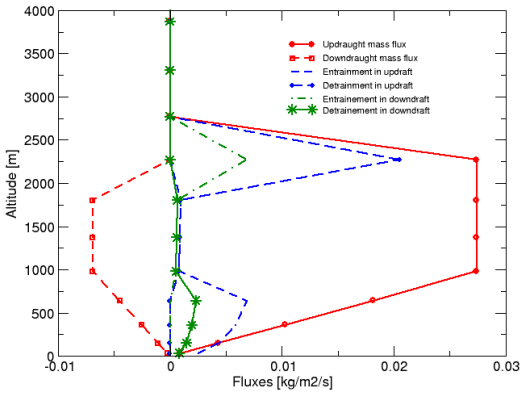


Figure 9.3: *Entrainment and detrainment fluxes in the updrafts and downdrafts.*

$$\frac{\partial M_{up}(z)c_{up}(z)}{\partial z} = E_{up}(z)c_{env} - D_{up}(z)c_{up} \tag{9.5}$$

$$\frac{\partial M_{dw}(z)c_{dw}(z)}{\partial z} = E_{dw}(z)c_{env} - D_{dw}(z)c_{dw} \tag{9.6}$$

with the concentrations c_{up}, c_{dw} and c_{env} in the updraft, downdraft and environment, respectively. The parametrization is designed with the parameter names such as in the Figure 9.4.
The net flux is first estimated in the **locvalues.f90** routine. At this stage, the fluxes are in molecules.cm^{-2}.s^{-1} (after conversion in **iniphys.f90**). For each grid cell, the Equation 9.3 is applied to give 'updraught mass flux' (flxuloc) and 'downdraught mass flux' (flxdloc). The calcualtion is done from surface to top domain in order to ensure mass conservation following the relation:

$$\begin{aligned} FLXU(z) = & \frac{\partial M_{up}(z)}{\partial z}(z) = E_{up}(z) - D_{up}(z) + FLXU(z-1) \\ FLXD(z) = & \frac{\partial M_{dw}(z)}{\partial z}(z) = E_{dw}(z) - D_{dw}(z) + FLXD(z-1) \end{aligned} \tag{9.7}$$

The top level of the cloud and the detrainment (when $E_{dw}(z) > 0$) are estimated separately and names 'nvcloudtop' and 'nvdettop', respectively.
These fluxes are used in the **transmix.f90** routine. One have to note that the 'concu', 'concd' parameters are not concentrations but ratios of pollutants molecules number on air molecules number. This conversion is done to ensure 'trpr' and 'trlo' production and loss fluxes terms in molecule.cm^{-3}.s^{-1}. 'concu' and 'cond' are estimated using the mass conservation relation, as for example:

$$\begin{aligned} FLXU(nv) \times concu(nv) = & FLXU(nv-1) \times concu(nv-1) \\ & + dpeu(nv) \times conc(nv) \\ & - dpdu(nv) \times concu(nv) \end{aligned} \tag{9.8}$$

and we have:

$$concu(nv) = \frac{FLXU(nv-1) \times concu(nv-1) + dpeu(nv) \times conc(nv)}{dpdu(nv) + FLXU(nv)} \tag{9.9}$$

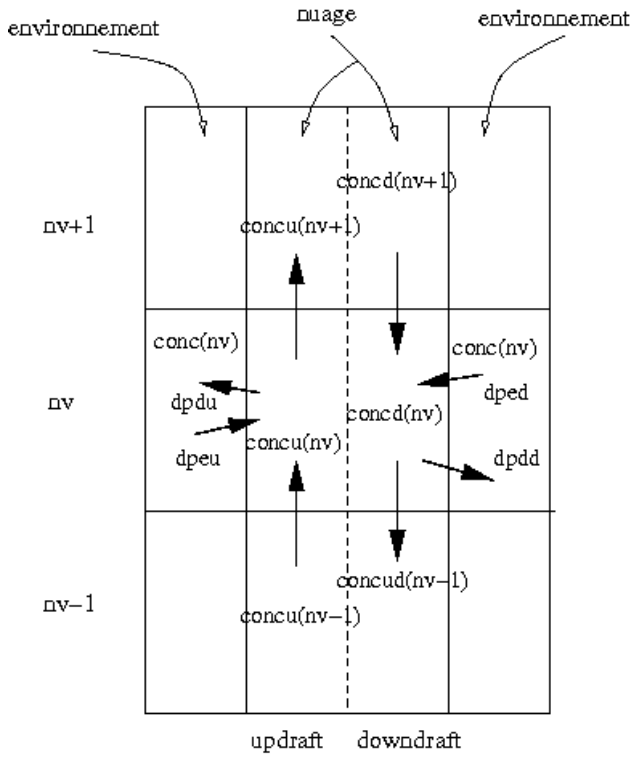


Figure 9.4: *Convective atmopsheric column and its environment*

9.3 Transport and mixing

9.3.1 Horizontal transport

Three schemes for horizontal transport of chemical concentrations in the model are now available. The choice between the three may be done species by species by changing the second column flag in the **ACTIVE_SPECIES** file. The schemes are:

- A simple first-order upwind scheme named **upwind** in the model: low computational cost but not very accurate and very diffusive.
- The second-order **Van Leer** scheme: low computational cost and good accuracy for transport of high concentrations in plumes.
- The third-order **PPM** scheme (PPM stands for 'Parabolic Piecewise Method'), proposed by [Colella and Woodward, 1984]): high computational cost but more accurate for long-live species, naturally diffusive in a chemistry-transport model

These three schemes are all defined and used in the **src/model/transmix.f90** program. We consider the following conservation equation:

$$\frac{\partial u}{\partial t} + \frac{\partial F_i(u)}{\partial x_i} = 0 \tag{9.10}$$

where $u = (\rho, \rho v_x, \rho v_y, \rho v_z, e)$ the physical conserved quantities (spatially) and $F(u)$ the corresponding flux. Each values and associated fluxes are represented at the center of each cell, $u_n = u(x_n)$; F_n. Of course, for a more realistic approach, we would represent these fluxes at each cells interface ($F_{n+1/2}$): thus, the problem of the advection schemes is to represent these interfaces fluxes by using only the known mean values fluxes. Formally, we can estimate the next time step u with the following equation:

$$u_n^{t+\Delta t} = u_n^{t+\Delta t} - \left(\frac{F^t_{n+1/2} - F^t_{n-1/2}}{\Delta x} \right) \Delta t \tag{9.11}$$

This equation is exact because it ensures the mass conservation between inside and outside fluxes for each directions. To estimate the value of $F^t_{n+1/2}$, we have to use the known values of F_n et F_{n+1}. The way we use all these adjacent fluxes defines the "centered" or "advanced" scheme type and induces its numerical stability or not.
The following scheme is named "upwind" because it follows the advected flux. By the way, we choose the flux value we use as a function of the place we are and the direction we want to go, as:

$$F^t_{n+1/2} = \begin{cases} F^t_n & \text{if } v > 0 \\ F^t_{n+1} & \text{if } v < 0 \end{cases} \tag{9.12}$$

This scheme is clearly asymmetrical. In addition, numerical experiments showed it is very diffusive. To avoid these effects, more complex schemes were developped: they are using more cells and thus are able to limit numerical errors due to too crude interpolations between cells. In the CHIMERE model, we implemented two advection schemes recognized for their good numerical accuracy: the VanLeer scheme in the **src/model/vanleer.f90** program and the PPM scheme in the **src/model/ppm.f90**.
Horizontal mass fluxes (independent of species, first order) are calculated first at each coarse time step in routine **src/model/htransport.f90**, then the complete calculation using the species concentration and PPM is performed at each fine time step in routine **src/model/transmix.f90**.

9.3.2 Vertical transport

Vertical transport is assumed to balance horizontal mass divergence. Two schemes are implemented: the first-order upwind scheme and the second-order VanLeer scheme (**NEW** in *chimere 2014b*).
The vertical mass flux of dry air is calculated columnwise for each cell interface in the vertical direction, successively from model bottom to model top, in the following way :

- In the lowest layer, the lateral mass imbalance is calculated by summing up all the incoming mass fluxes at the lateral boundaries of the cell and substracting the outgoing mass fluxes at lateral boundaries, the wind at the upper interface of the lowest model layer is then calculated in order to compensate this mass imbalance by an opposite flux at the cell's upper boundary. This calculation is performed at the first order, assuming that the density of the air crossing a cell boundary is equal to the average density of the upstream cell, both for horizontal and vertical transport.
- The same calculation is then performed successively for each cell in all the column up to the model top, balancing the total imbalance of the mass flux from lateral and lower boundaries by an opposite mass flux at the upper boundary. These vertical transport mass fluxes (independent of species) are calculated first at each coarse time step in routine **src/model/vtransport.f90**

The calculation of the concentration tendancies due to vertical transport for each model species is then performed at each fine time step in routine **src/model/transmix.f90**, performing first-order upwind vertical transport if parameter **iadvv** is set to **0** in **chimere.par**, and the second-order monotonous Van Leer I vertical transport scheme if **iadvv** is set to **1** in **chimere.par**. As the latter transport scheme needs two concentration values upstream of the considered boundary and one concentration value downstream, and this can not be secured next to model bottom and model top, CHIMERE switches back to upwind vertical transport for the cells where only one value of upstream concentration is available within the vertical simulation domain (including the boundary condition at model top).

9.3.3 Turbulent mixing

At each interface between layers k and k+1, one calculates an equivalent turbulent vertical velocity V_k and vertical mixing is expressed in layer k by the mass flux:
Net Flux = $\mathbf{V}_k(\mathbf{C}_{k+1}.\mathbf{D}_k/\mathbf{D}_{k+1} - \mathbf{C}_k)/\mathbf{H}_k$,
where **C** denotes concentrations, **D** densities and **H** layer thicknesses. Density ratios are applied since turbulent mixing must conserve mass in each model cell. An equivalent formula is used for the upper layer. The turbulent velocity V_k is deduced from K(z) using:

$$V_k = \frac{K_z}{(\frac{1}{2}(H_k + H_{k+1}))} \tag{9.13}$$

When the top of the boundary layer is above the model top, H_{k+1} is replaced by h - <model-top> in the previous equation.
The K(z) profile is calculated in routine **src/model/mixing.f90**, as well as the turbulent velocity profile. Vertical mixing mass fluxes (independent of species, first order) are calculated first at each coarse time step in routine **src/model/vtransport.f90**, then the complete calculation using the species concentration is performed at each fine time step in routine **src/model/transmix.f90**.

Chapter 10

Chemistry

10.1 The TWO-STEP time numerical solver

The numerical method for the temporal solution of the stiff system of partial differential equations is adapted from the second-order TWOSTEP algorithm originally proposed by [Verwer, 1994] for gas phase chemistry only. It is based on the application of a Gauss-Seidel iteration scheme to the 2-step implicit backward differentiation (BDF2) formula:

$$c^{n+1} = \frac{4}{3}c^n - \frac{1}{3}c^{n-1} + \frac{2}{3}\Delta t R(c^{n+1}), \tag{10.1}$$

with c^n being the vector of chemical concentrations at time t_n, Δt the time step leading from time t_n to $t_n + 1$ and $R(c) = \dot{c} = P(c) - L(c)c$ the temporal evolution of the concentrations due to chemical production and emissions (P) and chemical loss and deposition (L). Note that L is a diagonal matrix here. After rearranging and introducing the production and loss terms this equation reads

$$c^{n+1} = \left(I + \frac{2}{3}\Delta t L(c^{n+1})\right)^{-1} \left(\frac{4}{3}c^n - \frac{1}{3}c^{n-1} + \frac{2}{3}\Delta t P(c^{n+1})\right). \tag{10.2}$$

The implicit nonlinear system obtained in this scheme can be solved pertinently with a Gauss-Seidel method (Verwer, 1994).

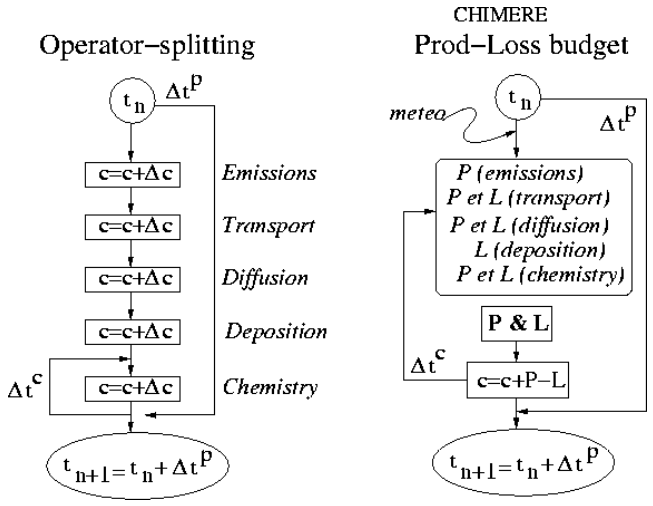


Figure 10.1: *Principle of 'operator-splitting' versus Chimere integration*

In CHIMERE the production and loss terms P and L in equation 10.2 are replaced by the modified terms

$\tilde{P} = P + P_h + P_v$ and $\tilde{L} = L + L_h + L_v$, respectively. P_h and P_v denote the temporal evolution of the concentrations due to horizontal (only advection) and vertical (advection and diffusion) inflow into the concerned grid box,
L_h and L_v the temporal evolution due to the respective outflow divided by the concentration itself. With this integration scheme, at each time step all physical and chemical processes are updated simultaneously. The "operator splitting" technique (see e.g. [McRae et al., 1982], which is still a standard way of solving the 3D transport-chemistry-problem, and the associated "splitting error" are therefore avoided. Further advantages of the scheme are its stability even for quite long time steps due to the implicitness of the formulation and the simplicity of the code which facilitates the development of secondary models (adjoint, tangent linear) enormously.
In practice, time stepping has two time steps: A **coarse time step**, where all physical variables are calculated, and a **fine step** (refined step in order to gain accuracy on chemistry. During loops over fine steps, physical variables are maintained constant.
In the provided version for the continental models, we chose a "very quick formulation", with a 10-minute physical step, no sub-chemical steps, i.e. all processes are stepped to 10 minutes, with only 1 Gauss-Seidel iteration. **It is STRONGLY recommended**, in order to have more accurate results, to use 2 Gauss-Seidel iterations, which increases by 2 the computer time. This change affects mostly concentrations during morning. However, for values of ozone concentration, the proposed version does not appear to degrade simulations, especially during afternoon hours.
The TWOSTEP formulae and loops are performed in module **src/model/twostep_mod.f90**.

10.2 Gas-phase chemistry

10.2.1 Chemical mechanisms (gas phase)

CHIMERE offers the option to include different gas phase chemical mechanisms. The original, complete scheme ([Lattuati, 1997]), hereafter called MELCHIOR1, describes more than 300 reactions of 80 gaseous species.
The hydrocarbon degradation is fairly similar to the EMEP gas phase mechanism ([Simpson, 1992]). Adaptations are made in particular for low NO_x conditions and NO_x-nitrate chemistry. All rate constants are updated according to [Atkinson et al., 1997] and [De Moore et al., 1994].
Heterogeneous formation of HONO from deposition of NO2 on wet surfaces is now considered, using the formulation of [Aumont et al., 2003]. In order to reduce the computing time a reduced mechanism with less than species and about 120 reactions is derived from MELCHIOR ([Derognat et al., 2003]), following the concept of "chemical operators" ([Carter, 1990]). This reduced mechanism is called MELCHIOR2 hereafter.
A third gas phase chemical mechanism is now available : SAPRC-07-A ([Carter, 2010], `http://www.engr.ucr.edu/~carter/SAPRC/`). It describes more than 275 reactions of 85 species and it is the most recent mechanism of mechanisms proposed in CHIMERE.
The base chemical mechanisms files are placed in **chemprep/data**, the mecanisms are automatically generated and placed in the **chemprep/inputdata** directories. New mechanisms can be implemented, in this case a work on the **chemprep/chemprep.awk** is required in adequation with the **REACTIONS** file for a new set of reactions. Not all forms of reactions are allowed. Arrhenius, Troe, photolysis and few other classical reaction rate types are only allowed. Introducing other types implies some recoding. See the technical documentation (the chemprep preprocessor). A file with altitude-dependent photolysis rates must also be provided, named **PHOTO_PARAMETERS.[meca]** in **chemprep/data**.
Photolysis rates are calculated under clear sky conditions as a function of height using the TUV model ([Madronich et al., 1998]). Then clouds are taken into account in a highly parameterized fashion.
Important notice: Photolysis rates are estimated only up to 13000m. If you want to use the model with higher vertical levels, you have to remember CHIMERE results would be correct for transport (with z_{max}=14 000m) but NOT for gas chemistry.

Gas-phase chemistry constants is read in initialization routine **src/initio/inichem.f90**. Then rates are calculated at the coarse time step in routine **src/model/rates.f90**, but chemical fluxes are calculated for all species at the fine time step in routine **src/model/chemistry.f90**.

10.2.2 Species list of the reduced MELCHIOR1 gas-phase chemical mechanism

Species	Definition
Inorganic compounds	
O3	ozone
H2O2	hydrogen peroxide
OH	hydroxy radical
HO2	hydroperoxy radical
NO	nitric oxide
NO2	nitrogen dioxide
NO3	nitrogen trioxide
N2O5	dinitrogen pentoxide
HONO	nitrous acide
HNO3	nitric acide
HNO4	pernitric acide
CO	carbon monoxide
SO2	sulfur dioxide
H2SO4	sulfuric acid
Hydrocarbon species [1]	
CH4	methane
C2H6	ethane
NC4H10	n-butane
C2H4	ethene
C3H6	propene
OXYL	o-xylene
C5H8	isoprene
APINEN	α-pinene
BPINEN	β-pinene
LIMONE	limonene
TERPEN	terpenes (lumped class)
HUMULE	Humulene (lumped class)
OCIMEN	Ocimene (lumped class)
Alcohol species	
C2H5OH	ethanol
CH3OH	methanol
Carbonyls	
HCHO	formaldehyde
CH3CHO	acetaldehyde
CH3COE	methyl ethyl ketone
CH3COY	dimethyl glyoxal
MEMALD	4-oxo-2-pentenal
MAC	methacroleine
MVK	methyl vinyl ketone
GLYOX	glyoxal
MGLYOX	methyl glyoxal
OFURAN	5-methyle-3H-furan-2-one
Organic nitrates	
CH3NO3	methyl nitrate
ETNO3	ehtyl nitrate
BUNO3	n-butyl-2-nitrate
ISNI	unsaturated nitrate from RO2P1
CARNIT	nitrate carbonyl taken as α-nitrooxy acetone
ORNIT1	α-hydroperox nitrate
ORNIT2	α-hydroperoxy nitrate from C5H8 and APINEN
(Per)oxy radicals	
C2H5O2	perxoy ethyl
CH2O2C	ethyl hydroperoxy
CH3O2	methyl peroxy
CH3COO	peroxy acetyl radical
CH3CHX	propyl hydroperoxy
CH3COX	peroxy from butan-2-one
CH3COZ	peroxy from MACO2+NO reaction
SECBUO	2-oxy butyl
SECC4H	peroxyl butyl
OXYL1	peroxy radical from OXYL
RO2IP1	peroxy radical from C5H8+OH reaction
MEMAL1	adition of OH on MEMALD
MEMAL2	formed from the abstraction of an hydrogen in alpha position
MACO2	peroxy radical from MAC+OH reaction
MVKO2	peroxy radical from MVK
APIOH	Peroxy radical from APINEN+OH reaction
Peroxy nitrates	
RNC2H4	peroxy ethyl nitrate
RNC3H6	peroxy propyl nitrate
RNC5H8	peroxy from C5H8+NO3 reaction
ROXYL1	peroxy from OXYL+NO3 reaction
ISNIR	peroxy from ISNI+OH reaction
APINO3	Peroxy radical from APINEN+NO3 reaction
Pernitrates	
PAN	peroxyacetyl nitrate
MACPAN	peroxy acyl nitrate from MAC
CH3NO4	methyl pernitrate
MEMPAN	peroxy acyl nitrate from MEMAL2
Peroxide	
APIO2H	hydroperoxyde from APINENOH+HO2 reaction
BUO2H	Butyl hydroperoxyde
CH3O2C	hydroxyethyl hydroperoxide
CH3O2H	methyl hydroperoxide
CH4CHX	hydroxypropyl hydroperoxide
CH4COX	butan-2-one-3-hydroperoxide
CH4COZ	hydroperoxide from CH3COZ+HO2 reaction
ETO2H	ethyl hydroperoxide
MACO2H	hydroperoxy from MACO2+HO2 reaction
MEMAH2	hydroperoxy from MEMAL2+HO2 reaction
MEMALH	hydroperoxy from MEMAL1+HO2 reaction
MVKO2H	hydroperoxy from MVKO2+HO2 reaction
OXYLH1	hydroperoxy from OXYL1+HO2 reaction
PEROX	hydroperoxy from RO2P1+HO2 reaction
PPA	peroxy acetyl acid

[1] Hydrocarbon model species (except for CH4 and C2H4) represent groups of hydrocarbons with similar reactivity. As "definition" a typical representative of this group is given. This is also true for the degradation products.

Reaction list of the reduced MELCHIOR1 chemical mechanism

Reactions	Kinetic constants
Inorganic	
O3+NO→NO2	k(T)=A$e^{-B/T}$,A=1.8e-12,B=1370
O3+NO2→NO3	k(T)=A$e^{-B/T}$,A=1.2e-13,B=2450
O3+OH→HO2	k(T)=A$e^{-B/T}$,A=1.9e-12,B=1000
O3+HO2→OH	k(T)=A$e^{-B/T}$,A=1.4e-14,B=600
NO+HO2→OH+NO2	k(T)=A$e^{-B/T}$,A=3.7e-12,B=-240
NO2+OH+M→HNO3	k(T,M)=mtroe(3.4e-30,0,3.2,4.77e-11,0,1.4,0.30)
HO2+OH→H2O	k(T)=A$e^{-B/T}$,A=4.8e-11,B=-250
H2O2+OH→HO2	k(T)=A$e^{-B/T}$,A=2.9e-12,B=160
HNO3+OH→NO3	k(T)=A$e^{-B/T}$,A=7.2e-15,B=-785
HNO3+OH+M→NO3	k(T,M)=troe(1.9e-33,-725,0,4.1e-16,-1440,0,1)
CO+OH→HO2+CO2	k(T)=A$e^{-B/T}$(300/T)^N,A=1.3e-13,B=0,N=1
CO+OH+M→HO2+CO2	k=3.21e-33
H2+OH→HO2	k(T)=A$e^{-B/T}$,A=7.7e-12,B=2100
HO2+HO2→H2O2	k(T)=A$e^{-B/T}$,A=2.2e-13,B=-600
HO2+HO2+M→H2O2	k(T)=A$e^{-B/T}$,A=1.7e-33,B=-1000
HO2+HO2+H2O→H2O2	k(T)=A$e^{-B/T}$,A=3.22e-34,B=-2800
HO2+HO2+H2O+M→H2O2	k(T)=A$e^{-B/T}$,A=2.38e-54,B=-3200
NO3+HO2→NO2+OH	k=4e-12
NO3+H2O2→HNO3+HO2	k=2e-15
NO3+O3→NO2	k=1e-17
NO3+NO→2*NO2	k(T)=A$e^{-B/T}$,A=1.8e-11,B=-110
NO3+NO3→2*NO2	k(T)=A$e^{-B/T}$,A=8.5e-13,B=2450
NO2+NO3→NO+NO2	k(T)=A$e^{-B/T}$,A=4.5e-14,B=1260
NO2+NO3+M→N2O5	k(T,M)=troe(2.7e-30,0,3.4,2e-12,0,-0.2,0.33)
N2O5+M→NO3+NO2	k(T,M)=troe(1e-3,11000,3.5,9.7e14,11080,-0.1,0.33)
NO2+HO2+M→HNO4	k(T,M)=troe(1.8e-31,0,3.2,4.7e-12,0,0,0.6)
HNO4+M→HO2+NO2	k(T,M)=troe(5e-6,10000,0,2.6e15,10900,0,0.6)
HNO4+OH→NO2	k(T)=A$e^{-B/T}$,A=1.5e-12,B=-360
NO+OH+M→HONO	k(T,M)=troe(7.e-31,0,2.6,1.5e-11,0,0.5,0.6)
HONO+OH→NO2	k(T)=A$e^{-B/T}$,A=1.8e-11,B=390
NO2→HONO+NO2	ks=0.5*depo(NO2)
SOx	
SO2+CH3O2→H2SO4+HCHO+HO2	k=4e-17
SO2+OH+M→H2SO4+HO2	k(T,M)=troe(4e-31,0,3.3,2e-12,0,0,0.45)
OH	
CH4+OH→CH3O2	k(T)=A$e^{-B/T}$,A=2.3e-12,B=1765
C2H6+OH→C2H5O2	k(T)=A$e^{-B/T}$,A=7.9e-12,B=1030
C2H4+OH+M→CH2O2C	k(T,M)=troe(7e-29,0,3.1,9e-12,0,0,0.7)
C3H6+OH+M→CH3CHX	k(T,M)=troe(8e-27,0,3.5,3e-11,0,0,0.5)
CH3OH+OH→HCHO+HO2	k(T)=A$e^{-B/T}$,A=3.1e-12,B=360
C2H5OH+OH→CH3CHO+HO2	k(T)=A$e^{-B/T}$,A=4.1e-12,B=70
OH	
HCHO+OH→CO+HO2	k(T)=A$e^{-B/T}$,A=8.6e-12,B=-20
CH3CHO+OH→CH3COO	k(T)=A$e^{-B/T}$,A=5.6e-12,B=-310
CH3COE+OH→CH3COX	k(T)=A$e^{-B/T}$(300/T)^N,A=2.92e-13,B=-414,N=-2
MEMALD+OH→MEMAL1	k=5.6e-11
GLYOX+OH→2*CO+HO2	k=1.1e-11
MGLYOX+OH→CH3COO+CO	k=1.5e-11
OFURAN+OH→MVKO2	k=6.9e-11
MAC+OH→0.5*MACO2	k(T)=A$e^{-B/T}$,A=1.86e-11,B=-175
MVK+OH→MVKO2	k(T)=A$e^{-B/T}$,A=4.1e-12,B=-453
CH3O2H+OH→CH3O2	k(T)=A$e^{-B/T}$,A=1.9e-12,B=-190

Reactions	Kinetic constants
ETO2H+OH→C2H5O2	k(T)=A$e^{-B/T}$,A=1.9e-12,B=-190
PPA+OH→CH3COO	k(T)=A$e^{-B/T}$,A=1.9e-12,B=-190
BUO2H+OH→SECC4H	k(T)=A$e^{-B/T}$,A=1.9e-12,B=-190
CH4COX+OH→CH3COX	k(T)=A$e^{-B/T}$,A=1.9e-12,B=-190
CH3O2C+OH→CH2O2C	k(T)=A$e^{-B/T}$,A=1.9e-12,B=-190
CH4CHX+OH→CH3CHX	k(T)=A$e^{-B/T}$,A=1.9e-12,B=-190
OXYLH1+OH→OXYL1	k(T)=A$e^{-B/T}$,A=1.9e-12,B=-190
MEMALH+OH→MEMAL1	k(T)=A$e^{-B/T}$,A=1.9e-12,B=-190
MEMAH2+OH→MEMAL2	k(T)=A$e^{-B/T}$,A=1.9e-12,B=-190
PEROX+OH→RO2IP1	k(T)=A$e^{-B/T}$,A=1.9e-12,B=-190
MACO2H+OH→MACO2	k(T)=A$e^{-B/T}$,A=1.9e-12,B=-190
MVKO2H+OH→MVKO2	k(T)=A$e^{-B/T}$,A=1.9e-12,B=-190
CH4COZ+OH→CH3COZ	k(T)=A$e^{-B/T}$,A=1.9e-12,B=-190
APIO2H+OH→APIOH	k(T)=A$e^{-B/T}$,A=1.9e-12,B=-190
CH3O2H+OH→HCHO+OH	k(T)=A$e^{-B/T}$,A=1.e-12,B=-190
ETO2H+OH→CH3CHO+OH	k(T)=A$e^{-B/T}$(300/T)^N,A=1.30e-13,B=-1176,N=-2
BUO2H+OH→CH3COE+OH	k(T)=A$e^{-B/T}$(300/T)^N,A=6.1e-14,B=-1681,N=-2
CH4COX+OH→CH3COY+OH	k(T)=A$e^{-B/T}$(300/T)^N,A=6.1e-14,B=-1533,N=-2
CH3O2C+OH→2*HCHO+OH	k(T)=A$e^{-B/T}$(300/T)^N,A=1.30e-13,B=-1238,N=-2
CH3O2C+OH→2*HCHO+OH	k(T)=A$e^{-B/T}$(300/T)^N,A=4.05e-13,B=-688,N=-2
CH4CHX+OH→HCHO+CH3CHO+OH	k(T)=A$e^{-B/T}$(300/T)^N,A=4.05e-13,B=-688,N=-2
CH4CHX+OH→HCHO+CH3CHO+OH	k(T)=A$e^{-B/T}$(300/T)^N,A=6.1e-14,B=-1681,N=-2
OXYLH1+OH→MEMALD+MGLYOX+OH	k=1.44e-10
MEMALH+OH→GLYOX+MGLYOX+OH	k(T)=A$e^{-B/T}$(300/T)^N,A=1.71e-13,B=-1403,N=-2
MEMAH2+OH→MALEIC+CH3O2	k=1.27e-11
PEROX+OH→0.43*MAC+0.57*MVK+HCHO+OH	k=8.22e-11
MACO2H+OH→CH3COZ	k=1.28e-11
MVKO2H+OH→0.28*HCHO+0.28*MGLYOX+0.28*OH+0.72*CH3CHO +0.72*CH3COO	k(T)=A$e^{-B/T}$(300/T)^N,A=4.05e-13,B=-1032,N=-2
MVKO2H+OH→0.28*HCHO+0.28*MGLYOX+0.28*OH+0.72*CH3CHO +0.72*CH3COO	k(T)=A$e^{-B/T}$(300/T)^N,A=6.1e-14,B=-1595,N=-2
CH4COZ+OH→CH3COE+OH	k=5.14e-11
APIO2H+OH→CH3CHO+CH3COE+OH	k(T)=A$e^{-B/T}$(300/T)^N,A=1.91e-13,B=-1193,N=-2
APIO2H+OH→CH3CHO+CH3COE+OH	k(T)=A$e^{-B/T}$(300/T)^N,A=3.82e-13,B=-882,N=-2
NO3	
CH4+NO3→CH3O2+HNO3	k=4e-19
C2H6+NO3→C2H5O2+HNO3	k=8e-18
NC4H10+NO3→SECC4H+HNO3	k=5.5e-17
C2H4+NO3→RNC2H4	k=2e-16
C3H6+NO3→RNC3H6	k=9.45e-15
OXYL+NO3→ROXYL1+HNO3	k=3.7e-16
C5H8+NO3→RNC5H8	k=7.8e-13
CH3OH+NO3→CH3O2+HNO3	k(T)=A$e^{-B/T}$,A=1.3e-12,B=2560
C2H5OH+NO3→C2H5O2+HNO3	k=9e-16
HCHO+NO3→CO+HNO3+HO2	k=5.8e-16
CH3CHO+NO3→CH3COO+HNO3	k=2.8e-15
CH3O2+NO3→HCHO+HO2+NO2	k=1.2e-12
C2H5O2+NO3→CH3CHO+NO2+HO2	k=1.2e-12
CH3COO+NO3→CH3O2+NO2+CO2	k=4e-12
CH2O2C+NO3→2*HCHO+NO2+HO2	k=1.2e-12
SECC4H+NO3→SECBUO+NO2	k=1.2e-12
CH3COX+NO3→CH3COY+NO2+HO2	k=1.2e-12
CH3CHX+NO3→HCHO+CH3CHO+NO2+HO2	k=1.2e-12
OXYL1+NO3→MEMALD+MGLYOX+NO2+HO2	k=1.2e-12
MEMAL1+NO3→GLYOX+MGLYOX+NO2+HO2	k=1.2e-12
MEMAL2+NO3→MALEIC+NO2+CH3O2	k=4e-12
MACO2+NO3→CH3COZ+NO2+CO2	k=4e-12

Reactions	Kinetic constants
RO2IP1+NO3→0.38*MAC+0.50*MVK+0.88*HCHO+0.12*RO2IP1 +0.88*HO2+NO2	k=1.2e-12
MVKO2+NO3→0.28*MGLYOX+0.28*HCHO+0.72*CH3CHO +0.72*CH3COO+0.28*HO2+NO2	k=1.2e-12
CH3COZ+NO3→CH3COE+HO2+NO2	k=1.2e-12
APIOH+NO3→CH3CHO+CH3COE+NO2+HO2	k=1.2e-12
RNC2H4+NO3→0.5*CARNIT+HCHO +1.5*NO2+0.5*HO2	k=1.2e-12
RNC3H6+NO3→0.5*CARNIT+0.5*CH3CHO+0.5*HCHO +1.5*NO2+0.5*HO2	k=1.2e-12
ROXYL1+NO3→BENZAL+NO2+HO2	k=1.2e-12
ISNIR+NO3→0.95*CH3CHO+0.475*CH3COE+0.475*MGLYOX +0.05*ISNI+0.05*HO2+1.9*NO2	k=1.2e-12
RNC5H8+NO3→0.85*ISNI+0.1*MAC+0.05*MVK+0.15*HCHO +1.1*NO2+0.8*HO2	k=1.2e-12
APINO3+NO3→CH3CHO+CH3COE+2*NO2	k=1.2e-12
O3	
C2H4+O3→HCHO+0.12*HO2+0.13*H2+0.44*CO	k(T)=Ae$^{-B/T}$,A=9.1e-15,B=2580
C3H6+O3→0.53*HCHO+0.5*CH3CHO+0.31*CH3O2+0.28*HO2 +0.15*OH+0.065*H2+0.4*CO+0.7*CH4	k(T)=Ae$^{-B/T}$,A=5.5e-15,B=1880
C5H8+O3→0.67*MAC+0.26*MVK+0.55*OH+0.07*C3H6+0.8*HCHO +0.06*HO2+0.05*CO+0.3*O3	k(T)=Ae$^{-B/T}$,A=1.2e-14,B=2013
MAC+O3→0.8*MGLYOX+0.7*HCHO+0.215*OH+0.275*HO2 +0.2*CO+0.2*O3	k(T)=Ae$^{-B/T}$,A=5.3e-15,B=2520
MVK+O3→0.82*MGLYOX+0.8*HCHO+0.04*CH3CHO+0.08*OH +0.06*HO2+0.05*CO+0.2*O3	k(T)=Ae$^{-B/T}$,A=4.3e-15,B=2016
PEROX+O3→0.7*HCHO	k=8e-18
organic	
CH3O2+NO→HCHO+NO2+HO2	k(T)=Ae$^{-B/T}$,A=4.2e-12,B=-180
C2H5O2+NO→CH3CHO+NO2+HO2	k=8.7e-12
CH3COO+NO→CH3O2+NO2+CO2	k=2e-11
CH2O2C+NO→2*HCHO+NO2+HO2	k=9e-12
SECC4H+NO→SECBUO+NO2	k=4e-12
SECC4H+NO+M→SECBUO+NO2	k(T,M)=troe(-3.76e-32,0,0,-3.3e-12,0,8.1,0.41)
SECBUO+M→CH3COE+HO2	k(T)=Ae$^{-B/T}$,A=3.0e-14,B=200
SECBUO→CH3CHO+C2H5O2	k(T)=Ae$^{-B/T}$,A=7.20e+12,B=5780
CH3COX+NO→CH3COY+NO2+HO2	k=4e-12
CH3CHX+NO→HCHO+CH3CHO+NO2+HO2	k=4e-12
OXYL1+NO→MEMALD+MGLYOX+NO2+HO2	k=4e-12
MEMAL1+NO→GLYOX+MGLYOX+NO2+HO2	k=4e-12
MEMAL2+NO→MALEIC+NO2+CH3O2	k=1.4e-11
MACO2+NO→CH3COZ+NO2+CO2	k=1.4e-11
RO2IP1+NO→0.32*MAC+0.42*MVK+0.74*HCHO+0.14*ISNI +0.12*RO2IP1+0.78*HO2+0.86*NO2	k(T)=Ae$^{-B/T}$,A=1.4e-11,B=180
MVKO2+NO→0.266*MGLYOX+0.266*HCHO+0.684*CH3CHO +0.684*CH3COO+0.05*ISNI+0.266*HO2+0.95*NO2	k(T)=Ae$^{-B/T}$,A=1.4e-11,B=180
CH3COZ+NO→CH3COE+HO2+NO2	k(T)=Ae$^{-B/T}$,A=1.4e-11,B=180
APIOH+NO→0.8*CH3CHO+0.8*CH3COE+0.8*NO2+0.8*HO2+0.2*ISNI	k=4e-12
organic	
CH3O2+HO2→CH3O2H	k(T)=Ae$^{-B/T}$,A=4.1e-13,B=-790
C2H5O2+HO2→ETO2H	k(T)=Ae$^{-B/T}$,A=2.7e-13,B=-1000
CH3COO+HO2→0.67*PPA+0.33*O3	k(T)=Ae$^{-B/T}$,A=4.3e-13,B=-1040
SECC4H+HO2→BUO2H	k(T)=Ae$^{-B/T}$,A=2.7e-13,B=-1000
CH3COX+HO2→CH4COX	k(T)=Ae$^{-B/T}$,A=2.7e-13,B=-1000
CH2O2C+HO2→CH3O2C	k(T)=Ae$^{-B/T}$,A=2.7e-13,B=-1000
CH3CHX+HO2→CH4CHX	k(T)=Ae$^{-B/T}$,A=2.7e-13,B=-1000
OXYL1+HO2→OXYLH1	k(T)=Ae$^{-B/T}$,A=2.7e-13,B=-1000
MEMAL1+HO2→MEMALH	k(T)=Ae$^{-B/T}$,A=2.7e-13,B=-1000

Reactions	**Kinetic constants**
MEMAL2+HO2→MEMAH2	k(T)=Ae$^{-B/T}$,A=2.7e-13,B=-1000
RO2IP1+HO2→PEROX	k(T)=Ae$^{-B/T}$,A=2.7e-13,B=-1000
MACO2+HO2→MACO2H	k(T)=Ae$^{-B/T}$,A=2.7e-13,B=-1000
MVKO2+HO2→MVKO2H	k(T)=Ae$^{-B/T}$,A=2.7e-13,B=-1000
CH3COZ+HO2→CH4COZ	k(T)=Ae$^{-B/T}$,A=2.7e-13,B=-1000
APIOH+HO2→APIO2H	k(T)=Ae$^{-B/T}$,A=2.7e-13,B=-1000
CH3O2+CH3O2→2*HCHO+2*HO2	k(T)=SPECIAL_1(1.1e-13,-365,25,1165)
CH3O2+CH3O2→HCHO+CH3OH	k(T)=SPECIAL_2(1.1e-13,-365,25,1165)
C2H5O2+CH3O2→CH3CHO+HCHO+2*HO2	k(T)=SPECIAL_3(6.4e-14,0,1.1e-13,-365,10.2,533,25,1165)
C2H5O2+CH3O2→CH3CHO+CH3OH	k(T)=SPECIAL_4(6.4e-14,0,1.1e-13,-365,10.2,533,25,1165)
C2H5O2+CH3O2→C2H5OH+HCHO	k(T)=SPECIAL_4(6.4e-14,0,1.1e-13,-365,25,1165,10.2,533)
CH3COO+CH3O2→CH3O2+CO2+HCHO+HO2	k(T)=SPECIAL_1(5.1e-12,-272,4.4e5,3910)
CH3COO+CH3O2→MECOOH+HCHO	k(T)=SPECIAL_2(5.1e-12,-272,4.4e5,3910)
SECC4H+CH3O2→SECBUO+HCHO+HO2	k(T)=SPECIAL_3(1.2e-12,1500,1.1e-13,-365,50,1165,25,1165)
SECC4H+CH3O2→CH3COE+CH3OH	k(T)=SPECIAL_4(1.2e-12,1500,1.1e-13,-365,50,1165,25,1165)
SECC4H+CH3O2→CH3COE+HCHO	k(T)=SPECIAL_4(1.2e-12,1500,1.1e-13,-365,25,1165,50,1165)
CH3COX+CH3O2→CH3COY+HCHO+2*HO2	k(T)=SPECIAL_3(5.5e-11,1500,1.1e-13,-365,50,1165,25,1165)
CH3COX+CH3O2→CH3COY+CH3OH	k(T)=SPECIAL_4(5.5e-11,1500,1.1e-13,-365,50,1165,25,1165)
CH3COX+CH3O2→CH3COY+HCHO	k(T)=SPECIAL_4(5.5e-11,1500,1.1e-13,-365,25,1165,50,1165)
CH2O2C+CH3O2→3*HCHO+2*HO2	k(T)=SPECIAL_3(2.3e-12,0,1.1e-13,-365,50,1165,25,1165)
CH2O2C+CH3O2→2*HCHO+CH3OH	k(T)=SPECIAL_4(2.3e-12,0,1.1e-13,-365,50,1165,25,1165)
CH2O2C+CH3O2→3*HCHO	k(T)=SPECIAL_4(2.3e-12,0,1.1e-13,-365,25,1165,50,1165)
CH3CHX+CH3O2→CH3CHO+2*HCHO+2*HO2	k(T)=SPECIAL_3(1.3e-10,2200,1.1e-13,-365,50,1165,25,1165)
CH3CHX+CH3O2→CH3CHO+HCHO+CH3OH	k(T)=SPECIAL_4(1.3e-10,2200,1.1e-13,-365,50,1165,25,1165)
CH3CHX+CH3O2→CH3CHO+2*HCHO	k(T)=SPECIAL_4(1.3e-10,2200,1.1e-13,-365,25,1165,50,1165)
RNC3H6+CH3O2→0.5*CARNIT+1.5*HCHO+0.5*CH3CHO +0.5*NO2+1.5*HO2	k(T)=SPECIAL_3(1.3e-10,2200,1.1e-13,-365,50,1165,25,1165)
RNC3H6+CH3O2→CARNIT+CH3OH	k(T)=SPECIAL_4(1.3e-10,2200,1.1e-13,-365,50,1165,25,1165)
RNC3H6+CH3O2→ORNIT1+HCHO	k(T)=SPECIAL_4(1.3e-10,2200,1.1e-13,-365,25,1165,50,1165)
OXYL1+CH3O2→MEMALD+MGLYOX+HCHO+2*HO2	k(T)=SPECIAL_3(2.1e-13,-600,1.1e-13,-365,50,1165,25,1165)
OXYL1+CH3O2→MEMALD+MGLYOX+CH3OH	k(T)=SPECIAL_4(2.1e-13,-600,1.1e-13,-365,50,1165,25,1165)
OXYL1+CH3O2→MEMALD+MGLYOX+HCHO	k(T)=SPECIAL_4(2.1e-13,-600,1.1e-13,-365,25,1165,50,1165)
MEMAL1+CH3O2→GLYOX+MGLYOX+HCHO+2*HO2	k(T)=SPECIAL_3(1.3e-11,800,1.1e-13,-365,50,1165,25,1165)
MEMAL1+CH3O2→GLYOX+MGLYOX+CH3OH	k(T)=SPECIAL_4(1.3e-11,800,1.1e-13,-365,50,1165,25,1165)
MEMAL1+CH3O2→GLYOX+MGLYOX+HCHO	k(T)=SPECIAL_4(1.3e-11,800,1.1e-13,-365,25,1165,50,1165)
MEMAL2+CH3O2→MALEIC+CH3O2+HCHO+HO2	k(T)=SPECIAL_1(5.1e-12,-272,4.4e5,3910)
MEMAL2+CH3O2→MAA+HCHO	k(T)=SPECIAL_2(5.1e-12,-272,4.4e5,3910)

Reactions	**Kinetic constants**
RO2IP1+CH3O2→0.3*MVK+0.3*MAC+1.6*HCHO+2*HO2	k(T)=SPECIAL_3(1.3e-11,800,1.1e-13,-365,50,1165,25,1165)
RO2IP1+CH3O2→0.3*MVK+0.3*MAC+0.6*HCHO+CH3OH	k(T)=SPECIAL_4(1.3e-11,800,1.1e-13,-365,50,1165,25,1165)
RO2IP1+CH3O2→0.3*MVK+0.3*MAC+1.6*HCHO	k(T)=SPECIAL_4(1.3e-11,800,1.1e-13,-365,25,1165,50,1165)
RNC5H8+CH3O2→0.6*ISNI+HCHO+2*HO2	k(T)=SPECIAL_3(1.3e-11,800,1.1e-13,-365,50,1165,25,1165)
RNC5H8+CH3O2→0.6*ISNI+CH3OH	k(T)=SPECIAL_4(1.3e-11,800,1.1e-13,-365,50,1165,25,1165)
RNC5H8+CH3O2→0.6*ISNI+HCHO	k(T)=SPECIAL_4(1.3e-11,800,1.1e-13,-365,25,1165,50,1165)
MACO2+CH3O2→CH3COZ+CO2+HCHO+HO2	k(T)=SPECIAL_1(5.1e-12,-272,4.4e5,3910)
MACO2+CH3O2→MAA+HCHO	k(T)=SPECIAL_2(5.1e-12,-272,4.4e5,3910)
MVKO2+CH3O2→MGLYOX+2*HCHO+2*HO2	k(T)=SPECIAL_3(5.5e-11,1500,1.1e-13,-365,50,1165,25,1165)
MVKO2+CH3O2→MGLYOX+HCHO+CH3OH	k(T)=SPECIAL_4(5.5e-11,1500,1.1e-13,-365,50,1165,25,1165)
MVKO2+CH3O2→MGLYOX+2*HCHO	k(T)=SPECIAL_4(5.5e-11,1500,1.1e-13,-365,25,1165,50,1165)
APIOH+CH3O2→CH3CHO+CH3COE+HCHO+2*HO2	k(T)=SPECIAL_3(1.8e-11,2200,1.1e-13,-365,1e9,0,25,1165)
APIOH+CH3O2→CH3CHO+CH3COE+HCHO	k(T)=SPECIAL_4(1.8e-11,2200,1.1e-13,-365,1e9,0,25,1165)
APINO3+CH3O2→CH3CHO+CH3COE+NO2+HCHO+HO2	k(T)=SPECIAL_3(1.8e-11,2200,1.1e-13,-365,1e9,0,25,1165)
APINO3+CH3O2→ORNIT2+HCHO	k(T)=SPECIAL_4(1.8e-11,2200,1.1e-13,-365,1e9,0,25,1165)
CH3COO+CH3COO→2.*CH3O2+2.*CO2	k(T)=Ae$^{-B/T}$,A=2.8e-12,B=-530
C2H5O2+CH3COO→CH3CHO+CH3O2+CO2+HO2	k(T)=SPECIAL_3(6.4e-14,0,2.8e-12,-530,10.2,533,1e9,0)
C2H5O2+CH3COO→CH3CHO+MECOOH	k(T)=SPECIAL_4(6.4e-14,0,2.8e-12,-530,1e9,0,10.2,533)
SECC4H+CH3COO→SECBUO+CH3O2+CO2	k(T)=SPECIAL_3(1.2e-12,1500,2.8e-12,-530,1e9,0,50,1165)
SECC4H+CH3COO→CH3COE+MECOOH	k(T)=SPECIAL_4(1.2e-12,1500,2.8e-12,-530,1e9,0,50,1165)
CH3COX+CH3COO→CH3COY+CH3O2+CO2+HO2	k(T)=SPECIAL_3(5.5e-11,1500,2.8e-12,-530,1e9,0,50,1165)
CH3COX+CH3COO→CH3COY+MECOOH	k(T)=SPECIAL_4(5.5e-11,1500,2.8e-12,-530,1e9,0,50,1165)
CH2O2C+CH3COO→2*HCHO+CH3O2+CO2+HO2	k(T)=SPECIAL_3(2.3e-12,0,2.8e-12,-530,1e9,0,50,1165)
CH2O2C+CH3COO→2*HCHO+MECOOH	k(T)=SPECIAL_4(2.3e-12,0,2.8e-12,-530,1e9,0,50,1165)
CH3CHX+CH3COO→CH3CHO+HCHO+CH3O2+CO2+HO2	k(T)=SPECIAL_3(1.2e-10,2200,2.8e-12,-530,1e9,0,50,1165)
CH3CHX+CH3COO→CH3CHO+HCHO+MECOOH	k(T)=SPECIAL_4(1.2e-10,2200,2.8e-12,-530,1e9,0,50,1165)
RNC3H6+CH3COO→0.5*CARNIT+0.5*HCHO+0.5*CH3CHO+0.5*NO2+CH3O2+CO2+0.5*HO2	k(T)=SPECIAL_3(1.2e-10,2200,2.8e-12,-530,1e9,0,50,1165)
RNC3H6+CH3COO→ORNIT1+MECOOH	k(T)=SPECIAL_4(1.2e-10,2200,2.8e-12,-530,1e9,0,50,1165)
OXYL1+CH3COO→MEMALD+MGLYOX+CH3O2+CO2+HO2	k(T)=SPECIAL_3(2.1e-13,-600,2.8e-12,-530,1e9,0,50,1165)
OXYL1+CH3COO→MEMALD+MGLYOX+MECOOH	k(T)=SPECIAL_4(2.1e-13,-600,2.8e-12,-530,1e9,0,50,1165)
MEMAL1+CH3COO→GLYOX+MGLYOX+CH3O2+CO2+HO2	k(T)=SPECIAL_3(1.3e-11,800,2.8e-12,-530,1e9,0,50,1165)
MEMAL1+CH3COO→GLYOX+MGLYOX+MECOOH	k(T)=SPECIAL_4(1.3e-11,800,2.8e-12,-530,1e9,0,50,1165)
MEMAL2+CH3COO→MALEIC+2*CH3O2+CO2	k(T)=Ae$^{-B/T}$,A=5.6e-12,B=-530
RO2IP1+CH3COO→0.3*MVK+0.3*MAC+0.6*HCHO+HO2+CH3O2+CO2	k(T)=SPECIAL_3(1.3e-11,800,2.8e-12,-530,1e9,0,50,1165)

Reactions	Kinetic constants
RO2IP1+CH3COO→0.3*MVK+0.3*MAC+0.6*HCHO+MECOOH	k(T)=SPECIAL_4(1.3e-11,800,2.8e-12,-530,1e9,0,50,1165)
RNC5H8+CH3COO→0.6*ISNI+CH3O2+CO2	k(T)=SPECIAL_3(1.3e-11,800,2.8e-12,-530,1e9,0,50,1165)
RNC5H8+CH3COO→0.6*ISNI*+MECOOH	k(T)=SPECIAL_4(1.3e-11,800,2.8e-12,-530,1e9,0,50,1165)
MACO2+CH3COO→CH3O2+CH3COZ+2*CO2	k(T)=$Ae^{-B/T}$,A=5.6e-12,B=-530
MVKO2+CH3COO→MGLYOX+HCHO+HO2+CH3O2+CO2	k(T)=SPECIAL_3(5.5e-11,1500,2.8e-12,-530,1e9,0,50,1165)
MVKO2+CH3COO→MGLYOX+HCHO+MECOOH	k(T)=SPECIAL_4(5.5e-11,1500,2.8e-12,-530,1e9,0,50,1165)
APIOH+CH3COO→CH3CHO+CH3COE+HO2+CH3O2+CO2	k(T)=$Ae^{-B/T}$,A=1.4e-11,B=835
APINO3+CH3COO→CH3CHO+CH3COE+NO2+CH3O2+CO2	k(T)=$Ae^{-B/T}$,A=1.4e-11,B=835
C2H5O2+C2H5O2→2*CH3CHO+2*HO2	k(T)=SPECIAL_1(6.4e-14,0,10.2,533)
C2H5O2+C2H5O2→CH3CHO+C2H5OH	k(T)=SPECIAL_2(6.4e-14,0,10.2,533)
SECC4H+SECC4H→2*SECBUO	k(T)=SPECIAL_1(1.2e-12,1500,50,1165)
SECC4H+SECC4H→2*CH3COE	k(T)=SPECIAL_2(1.2e-12,1500,50,1165)
CH3COX+CH3COX→2*CH3COY+2*HO2	k(T)=SPECIAL_1(5.5e-11,1500,50,1165)
CH3COX+CH3COX→2*CH3COY	k(T)=SPECIAL_2(5.5e-11,1500,50,1165)
CH2O2C+CH2O2C→4*HCHO+2*HO2	k(T)=SPECIAL_1(2.3e-12,0,50,1165)
CH2O2C+CH2O2C→4*HCHO	k(T)=SPECIAL_2(2.3e-12,0,50,1165)
CH3CHX+CH3CHX→2*HCHO+2*CH3CHO+2*HO2	k(T)=SPECIAL_1(1.3e-10,2200,50,1165)
CH3CHX+CH3CHX→2*HCHO+2*CH3CHO	k(T)=SPECIAL_2(1.3e-10,2200,50,1165)
RNC3H6+RNC3H6→CARNIT+HO2+HCHO+CH3CHO+NO2	k(T)=SPECIAL_1(1.3e-10,2200,50,1165)
RNC3H6+RNC3H6→CARNIT+ORNIT1	k(T)=SPECIAL_2(1.3e-10,2200,50,1165)
OXYL1+OXYL1→2*MEMALD+2*MGLYOX+2*HO2	k(T)=SPECIAL_1(2.1e-13,-600.,50,1165)
OXYL1+OXYL1→2*MEMALD+2*MGLYOX	k(T)=SPECIAL_2(2.1e-13,-600.,50,1165)
MEMAL1+MEMAL1→2*GLYOX+2*MGLYOX+2*HO2	k(T)=SPECIAL_1(1.3e-11,800,50,1165)
MEMAL1+MEMAL1→2*GLYOX+2*MGLYOX	k(T)=SPECIAL_2(1.3e-11,800,50,1165)
MEMAL2+MEMAL2→2*MALEIC+2*CH3O2	k(T)=$Ae^{-B/T}$,A=2.8e-12,B=-530
RO2IP1+RO2IP1→0.6*MVK+0.6*MAC+1.2*HCHO+1.2*HO2	k(T)=SPECIAL_1(1.3e-11,800,50,1165)
RO2IP1+RO2IP1→0.6*MVK+0.6*MAC+1.2*HCHO	k(T)=SPECIAL_2(1.3e-11,800,50,1165)
RNC5H8+RNC5H8→1.2*ISNI+1.2*HO2	k(T)=SPECIAL_1(1.3e-11,800,50,1165)
RNC5H8+RNC5H8→1.2*ISNI	k(T)=SPECIAL_2(1.3e-11,800,50,1165)
MACO2+MACO2→2*CH3COZ+2*CO2	k(T)=$Ae^{-B/T}$,A=2.8e-12,B=-530
MVKO2+MVKO2→2*MGLYOX+2*HCHO+2*HO2	k(T)=SPECIAL_1(5.5e-11,1500,50,1165)
MVKO2+MVKO2→2*MGLYOX+2*HCHO	k(T)=SPECIAL_2(5.5e-11,1500,50,1165)
APIOH+APIOH→2*CH3CHO+2*CH3COE+2*HO2	k(T)=$Ae^{-B/T}$,A=1.8e-11,B=2200
APINO3+APINO3→2*CH3CHO+2*CH3COE+2*NO2	k(T)=$Ae^{-B/T}$,A=1.8e-11,B=2200
organic	
CH3O2+NO→CH3NO3	k(T)=$Ae^{-B/T}$,A=2.1e-14,B=-180
CH3NO3+OH→HCHO+HNO3+HO2	k(T)=$Ae^{-B/T}$,A=1.e-14,B=-1060
C2H5O2+NO→ETNO3	k=1.25e-13
ETNO3+OH→CH3CHO+HNO3+HO2	k(T)=$Ae^{-B/T}$,A=4.4e-14,B=-720
SECC4H+NO+M→BUNO3	k(T,M)=troe(3.76e-32,0,0,3.3e-12,0,8.1,0.41)
BUNO3+OH→RNC3H6	k=6.7e-13
RNC2H4+NO→0.5*CARNIT+HCHO+1.5*NO2+0.5*HO2	k=8.9e-12
RNC3H6+NO→0.5*CARNIT+0.5*CH3CHO+0.5*HCHO +1.5*NO2+0.5*HO2	k=4e-12
ROXYL1+NO→BENZAL+NO2+HO2	k=4e-12
ISNI+OH→ISNIR	k=3.4e-11
ISNI+O3→0.5*ISNI+0.5*HCHO+0.5*MGLYOX+0.5*NO2 +0.08*OH+0.2*O3	k=5e-18
ISNIR+NO→0.95*CH3CHO+0.475*CH3COE+0.475*MGLYOX +0.05*ISNI+0.05*HO2+1.9*NO2	k(T)=$Ae^{-B/T}$,A=1.4e-11,B=180
RNC5H8+NO→0.85*ISNI+0.1*MAC+0.05*MVK+0.15*HCHO +1.1*NO2+0.8*HO2	k(T)=$Ae^{-B/T}$,A=1.4e-11,B=180
APINO3+NO→CH3CHO+CH3COE+2*NO2	k=4e-12
RNC5H8+HO2→ORNIT2	k(T)=$Ae^{-B/T}$,A=2.7e-13,B=-1000

Reactions	Kinetic constants
RNC2H4+HO2→ORNIT1	k(T)=A$e^{-B/T}$,A=2.7e-13,B=-1000
RNC3H6+HO2→ORNIT1	k(T)=A$e^{-B/T}$,A=2.7e-13,B=-1000
ROXYL1+HO2→BENZYL	k(T)=A$e^{-B/T}$,A=2.7e-13,B=-1000
ISNIR+HO2→ORNIT2	k(T)=A$e^{-B/T}$,A=2.7e-13,B=-1000
APINO3+HO2→ORNIT2	k(T)=A$e^{-B/T}$,A=2.7e-13,B=-1000
CH3COO+NO2+M→PAN	k(T,M)=troe(2.7e-28,0,7.1,1.2e-11,0,0.9,0.3)
PAN+M→CH3COO+NO2	k(T,M)=troe(4.9e-3,12100,0,5.4e16,13830,0,0.3)
PAN+OH→HCHO+NO3+CO2	k(T)=A$e^{-B/T}$,A=9.5e-13,B=650
MACO2+NO2+M→MACPAN	k(T,M)=troe(2.7e-28,0,7.1,1.2e-11,0,0.9,0.3)
MACPAN+M→MACO2+NO2	k(T,M)=troe(4.9e-3,12100,0,5.4e16,13830,0,0.3)
MACPAN+OH→CH3COE+NO3+O3+CO2	k(T)=A$e^{-B/T}$,A=3.25e-13,B=-500
MEMAL2+NO2+M→MEMPAN	k(T,M)=troe(2.7e-28,0,7.1,1.2e-11,0,0.9,0.3)
MEMPAN+M→MEMAL2+NO2	k(T,M)=troe(4.9e-3,12100,0,5.4e16,13830,0,0.3)
MEMPAN+OH→CH3COE+NO3+CO2	k(T)=A$e^{-B/T}$,A=3.25e-13,B=-500
CH3O2+NO2+M→CH3NO4	k(T,M)=troe(2.5e-30,0,5.5,7.5e-12,0,0,0.36)
CH3NO4+M→CH3O2+NO2	k(T,M)=troe(9e-5,9690,0,1.1e16,10560,0,0.36)
ORNIT1+OH→CARNIT+OH	k(T)=A$e^{-B/T}$(300/T)^N,A=6.1e-14,B=-1743,N=-2
ORNIT1+OH→RNC3H6	k(T)=A$e^{-B/T}$,A=1.9e-12,B=-190
ORNIT2+OH→0.95*CH3CHO+0.475*CH3COE+0.475*MGLYOX +0.05*ISNI+0.05*OH+0.95*NO2	k(T)=A$e^{-B/T}$(300/T)^N,A=6.1e-14,B=-1743,N=-2
ORNIT2+OH→ISNIR	k(T)=A$e^{-B/T}$,A=1.9e-12,B=-190
photolytic	
O3→2*OH	J(T,Z,H2O)=photorate(O3)
NO2→NO+O3	J(Z)=photorate(NO2)
NO3→NO2+O3	J(Z)=photorate(NO3-2)
H2O2→2*OH	J(Z)=photorate(H2O2)
HNO3→NO2+OH	J(Z)=photorate(HNO3)
HCHO→CO+2*HO2	J(Z)=photorate(HCHO-1)
HCHO→CO+H2	J(Z)=photorate(HCHO-2)
CH3CHO→CH3O2+HO2+CO	J(Z)=photorate(CH3CHO)
CH3COE→CH3COO+C2H5O2	J(Z)=photorate(CH3COE)
CH3COY→2*CH3COO	J(Z)=photorate(CH3COY)
MGLYOX→CH3COO+HO2+CO	J(Z)=photorate(MGLYOX)
GLYOX→0.6*HO2+2*CO+1.4*H2	J(Z)=photorate(GLYOX)
MEMALD→0.5*OFURAN+0.5*MEMAL2+0.5*HO2	J(Z)=photorate(MEMALD)
NO3→NO	J(Z)=photorate(NO3-1)
N2O5→NO2+NO3	J(Z)=photorate(N2O5)
CH3O2H→HCHO+OH+HO2	J(Z)=photorate(CH3O2H)
ETO2H→CH3CHO+OH+HO2	J(Z)=photorate(CH3O2H)
BUO2H→CH3COE+OH+HO2	J(Z)=photorate(CH3O2H)
CH4COX→CH3COY+OH+HO2	J(Z)=photorate(CH3O2H)
CH3O2C→2*HCHO+OH+HO2	J(Z)=photorate(CH3O2H)
CH4CHX→HCHO+CH3CHO+OH+HO2	J(Z)=photorate(CH3O2H)
OXYLH1→MEMALD+MGLYOX+OH+HO2	J(Z)=photorate(CH3O2H)
MEMALH→GLYOX+MGLYOX+OH+HO2	J(Z)=photorate(CH3O2H)
MEMAH2→MALEIC+OH+CH3O2	J(Z)=photorate(CH3O2H)
PEROX→0.14*RO2IP1+0.488*CH3COE+0.372*MAC+0.86*HCHO +0.9*HO2+OH	J(Z)=photorate(CH3O2H)
MACO2H→CH3COZ+OH+CO2	J(Z)=photorate(CH3O2H)
MVKO2H→0.28*HCHO+0.28*MGLYOX+0.28*HO2+0.72*CH3CHO +0.72*CH3COO+OH	J(Z)=photorate(CH3O2H)
CH4COZ→CH3COE+OH+HO2	J(Z)=photorate(CH3O2H)
APIO2H→CH3CHO+CH3COE+OH+HO2	J(Z)=photorate(CH3O2H)
PPA→CH3O2+CO2+OH	J(Z)=photorate(PPA)
HNO4→HO2+NO2	J(Z)=photorate(HNO4)
HONO→NO+OH	J(Z)=photorate(HONO)
CH3NO4→CH3O2+NO2	J(Z)=photorate(HNO4)
CH3NO3→HCHO+HO2+NO2	J(Z)=photorate(CH3NO3)
ETNO3→CH3CHO+HO2+NO2	J(Z)=photorate(ETNO3)

Reactions	Kinetic constants
BUNO3→CH3COE+HO2+NO2	J(Z)=photorate(BUNO3)
PAN→CH3COO+NO2	J(Z)=photorate(PAN)
CARNIT→CH3COO+HCHO+NO2	J(Z)=photorate(CH3CHO)
ORNIT1→CH3CHO+HCHO+NO2+OH	J(Z)=photorate(CH3O2H)
ORNIT2→0.95*CH3CHO+0.475*CH3COE+0.475*MGLYOX+0.05*ISNI +0.05*HO2+0.95*NO2+OH	J(Z)=photorate(CH3O2H)
APINEN+NO3→APINO3	k(T)=A$e^{-B/T}$,A=1.19e-12,B=-490
BPINEN+NO3→APINO3	k(T)=A$e^{-B/T}$,A=1.19e-12,B=-490
LIMONE+NO3→APINO3	k(T)=A$e^{-B/T}$,A=1.19e-12,B=-490
OCIMEN+NO3→APINO3	k(T)=A$e^{-B/T}$,A=1.19e-12,B=-490
TERPEN+NO3→APINO3	k(T)=A$e^{-B/T}$,A=1.19e-12,B=-490
HUMULE+NO3→APINO3	k(T)=A$e^{-B/T}$,A=1.19e-12,B=-490
APINEN+OH→APIOH	k(T)=A$e^{-B/T}$,A=1.21e-11,B=-444
BPINEN+OH→APIOH	k(T)=A$e^{-B/T}$,A=1.21e-11,B=-444
LIMONE+OH→APIOH	k(T)=A$e^{-B/T}$,A=1.21e-11,B=-444
OCIMEN+OH→APIOH	k(T)=A$e^{-B/T}$,A=1.21e-11,B=-444
TERPEN+OH→APIOH	k(T)=A$e^{-B/T}$,A=1.21e-11,B=-444
HUMULE+OH→APIOH	k(T)=A$e^{-B/T}$,A=1.21e-11,B=-444
APINEN+O3→0.65*CH3CHO+0.53*CH3COE+0.14*CO+0.2*C2H5O2 +0.42*CH3CHX+0.85*OH+0.1*HO2	k(T)=A$e^{-B/T}$,A=1.0e-15,B=736
BPINEN+O3→0.65*CH3CHO+0.53*CH3COE+0.14*CO+0.2*C2H5O2 +0.42*CH3CHX+0.85*OH+0.1*HO2	k(T)=A$e^{-B/T}$,A=1.0e-15,B=736
LIMONE+O3→0.65*CH3CHO+0.53*CH3COE+0.14*CO+0.2*C2H5O2 +0.42*CH3CHX+0.85*OH+0.1*HO2	k(T)=A$e^{-B/T}$,A=1.0e-15,B=736
TERPEN+O3→0.65*CH3CHO+0.53*CH3COE+0.14*CO+0.2*C2H5O2 +0.42*CH3CHX+0.85*OH+0.1*HO2	k(T)=A$e^{-B/T}$,A=1.0e-15,B=736
OCIMEN+O3→0.65*CH3CHO+0.53*CH3COE+0.14*CO+0.2*C2H5O2 +0.42*CH3CHX+0.85*OH+0.1*HO2	k(T)=A$e^{-B/T}$,A=1.0e-15,B=736
HUMULE+O3→0.65*CH3CHO+0.53*CH3COE+0.14*CO+0.2*C2H5O2 +0.42*CH3CHX+0.85*OH+0.1*HO2	k(T)=A$e^{-B/T}$,A=1.0e-15,B=736
C5H8+OH→RO2IP1	k(T)=A$e^{-B/T}$,A=2.55e-11,B=-410
NC4H10+OH→SECC4H	k(T)=A$e^{-B/T}$(300/T)^N,A=1.36e-12,B=-190,N=-2
OXYL+OH→OXYL1	k=1.37e-11

- The reactions O_3+hν→O(1D), O(1D)+H_2O→2OH, O(1D)+M→O(3P)+M and O(3P)+O_2+M→O_3+M have been combined to reaction O_3+hν→ O(1D) by taking into account H_2O and M concentrations in order to adjust the photolysis frequency.
- Due to lack of data, photolysis frequencies of higher organic peroxides are taken as that of CH_3OOH.
- Three body Troe reactions [1], given in the form :

$$k = \frac{k_0[M]}{1+\frac{k_0[M]}{k_\infty}} f^Z$$

with

$$Z = \frac{1}{1+\left(log_{10}\left(\frac{k_0(T)[M]}{k_\infty(T)}\right)\right)^2}$$

$$k_0 = A_0 e^{\left(-\frac{B_0}{T}\right)}\left(\frac{T}{300}\right)^{-n}, \text{ and } k_\infty = A_\infty e^{\left(-\frac{B_\infty}{T}\right)}\left(\frac{T}{300}\right)^{-m},$$

The parameters are given in the order $A_0, B_0, n, A_\infty, B_\infty, m, f$

- The reaction NO2+OH :

$$k = \frac{k_0[M]}{1+\frac{k_0[M]}{k_\infty}} f^Z$$

with

$$Z = \frac{1}{1 + \left(\frac{log_{10}\left(\frac{k_0(T)[M]}{k_\infty(T)} - 0.12\right)}{1.2} \right)^2}$$

$$k_0 = A_0 e^{\left(-\frac{B_0}{T}\right)} \left(\frac{T}{300}\right)^{-n}, \text{ and } k_\infty = A_\infty e^{\left(-\frac{B_\infty}{T}\right)} \left(\frac{T}{300}\right)^{-m},$$

The parameters are given in the order $A_0, B_0, n, A_\infty, B_\infty, m, f$

- Radical recombinations SPECIAL_1 :

$$k\left(T\right) = k_1\left(T\right) \times \frac{k_2\left(T\right)}{1 + k_2\left(T\right)}$$

The parameters are given in the order A_1, B_1, A_2, B_2

- Radical recombinations SPECIAL_2 :

$$k\left(T\right) = \frac{k_1\left(T\right)}{1 + k_2\left(T\right)}$$

The parameters are given in the order A_1, B_1, A_2, B_2

- Radical recombinations SPECIAL_3 :

$$k\left(T\right) = 2 \times \sqrt{\frac{k_1\left(T\right) \times k_2\left(T\right) \times k_3\left(T\right) \times k_4\left(T\right)}{\left(1 + k_3\left(T\right)\right) \times \left(1 + k_4\left(T\right)\right)}}$$

The parameters are given in the order $A_1, B_1, A_2, B_2, A_3, B_3, A_4, B_4$

- Radical recombinations SPECIAL_4 :

$$k\left(T\right) = 2 \times \sqrt{k_1\left(T\right) \times k_2\left(T\right)} \times \frac{1 - \sqrt{\frac{k_3(T)}{1+k_3(T)} \times \frac{k_4(T)}{1+k_4(T)}} \times \left(1 - \frac{k_4(T)}{1+k_4(T)}\right)}{2 - \frac{k_3(T)}{1+k_3(T)} - \frac{k_4(T)}{1+k_4(T)}}$$

The parameters are given in the order $A_1, B_1, A_2, B_2, A_3, B_3, A_4, B_4$

10.2.3 Species list of the reduced MELCHIOR2 gas-phase chemical mechanism

Species	Definition
Inorganic compounds	
O3	ozone
H2O2	hydrogen peroxide
OH	hydroxy radical
HO2	hydroperoxy radical
NO	nitric oxide
NO2	nitrogen dioxide
NO3	nitrogen trioxide
N2O5	dinitrogen pentoxide
HONO	nitrous acide
HNO3	nitric acide
CO	carbon monoxide
SO2	sulfur dioxide
H2SO4	sulfuric acid
Hydrocarbon species[2]	
CH4	methane
C2H6	ethane
NC4H10	n-butane
C2H4	ethene
C3H6	propene
OXYL	o-xylene
C5H8	isoprene
APINEN	α-pinene
BPINEN	β-pinene
LIMONE	limonene
TERPEN	terpenes (lumped class)
HUMULE	Humulene (lumped class)
OCIMEN	Ocimene (lumped class)

[2]Hydrocarbon model species (except for CH4 and C2H4) represent groups of hydrocarbons with similar reactivity. As "definition" a typical representative of this group is given. This is also true for the degradation products.

Carbonyls

HCHO ..... formaldehyde
CH3CHO ..... acetaldehyde
CH3COE ..... methyl ethyl ketone
GLYOX ..... glyoxal
MGLYOX ..... methyl glyoxal
CH3COY ..... dimethyl glyoxal
MEMALD ..... unsaturated dicarbonyls, reacting like 4-oxo-2-pentenal
MVK ..... methyl vinyl ketone
MAC ..... methacroleine

Organic nitrates

PAN ..... peroxyacetyl nitrate
CARNIT ..... nitrate carbonyl taken as α-nitrooxy acetone
ISNI ..... unsaturated nitrate from isoprene degradation

Organic peroxides

CH3O2H ..... methyl hydroperoxide
PPA ..... peroxy acetyl acid

(Per)oxy radicals

CH3O2 ..... methyl peroxy radical
CH3COO ..... peroxy acetyl radical

Operators [3]

oRO2 ..... representing peroxy radicals from OH attack to C2H5, NCHH10, C2H4, C3H6, OXYL, CH3COE, MEMALD, and MVK
oROOH ..... representing organic peroxides from oRO2+HO2 reactions
obio ..... representing peroxy radicals produced by C5H8 and APINEN + OH reaction
obioH .representing biogenic organic peroxides from obio+HO2 and obio+obio reactions
oPAN ..representing PAN homologue compounds (except PAN)
PANH .....representing results from oPAN+HO2 reaction
toPAN ... representing results from oPAN+NO2 reaction oRN1 representing organic nitrate peroxy radicals from NO3 attack to C2H4, C3H6, C5H8, APINEN, BPINEN, LIMONE, TERPEN, OCIMEN, HUMULE and OH attack to ISNI

Reaction list of the reduced MELCHIOR2 chemical mechanism

Reactions	Kinetic constants	Ref.
Inorganic chemistry		
O3+NO→NO2	$Ae^{-B/T}$,A=1.8e-12,B=1370	[1]
O3+NO2→NO3	$Ae^{-B/T}$,A=1.2e-13,B=2450	[1]
O3+OH→HO2	$Ae^{-B/T}$,A=1.9e-12,B=1000	[1]
O3+HO2→OH	$Ae^{-B/T}$,A=1.4e-14,B=600	[1]
NO+HO2→OH+NO2	$Ae^{-B/T}$,A=3.7e-12,B=-240	[1]
NO2+OH+M→HNO3	troe(3.4e-30,0,3.2,4.77e-11,0,1.4,0.30)	[2], n9
HO2+OH→H2O	$Ae^{-B/T}$,A=4.8e-11,B=-250	[1]
H2O2+OH→HO2	$Ae^{-B/T}$,A=2.9e-12,B=160	[1]
HNO3+OH→NO3	$Ae^{-B/T}$,A=5.5e-15,B=-985	[3], n1
CO+OH→HO2+CO2	$Ae^{-B/T}(300/T)^{N}$, A=2e-13, B=0, N=1	[3], n1
HO2+HO2→H2O2	$Ae^{-B/T}$,A=2.2e-13,B=-740	[1], n1
HO2+HO2+H2O→H2O2	$Ae^{-B/T}$,A=4.52e-34,B=-2827	[1], n1
NO3+HO2→NO2+OH	4e-12	[1]
NO3+H2O2→HNO3+HO2	2e-15	[3]
NO3+NO→2*NO2	$Ae^{-B/T}$,A=1.8e-11,B=-110	[1]
NO2+NO3→NO+NO2	$Ae^{-B/T}$,A=4.5e-14,B=1260	[3]
NO2+NO3+M→N2O5	troe(2.7e-30,0,3.4,2e-12,0,-0.2,0.33)	[1], n9
N2O5+M→NO3+NO2	troe(1e-3,11000,3.5,9.7e14,11080,-0.1,0.33)	[1], n9
N2O5+H2O→2*HNO3	2.6e-22	[4]
N2O5+H2O+H2O→2*HNO3	2e-39	[4]
NO+OH+M→HONO	troe(7.e-31,0,2.6,1.5e-11,0,0.5,0.6)	[1], n9
HONO+OH→NO2	$Ae^{-B/T}$,A=1.8e-11,B=390	[1]
NO+NO+O2→2*NO2	$Ae^{-B/T}$,A=3.30E-39,B=-530.0	[1]
NO2→HONO	0.5*depo(NO2)	[18]
SOx chemistry		

[3] For the concept of "chemical operators" see Carter (1990) and Aumont et al. (1997)

Reactions	Kinetic constants	Ref.
SO2+CH3O2→H2SO4+HCHO+HO2	4e-17	[3]
SO2+OH+M→H2SO4+HO2	troe(4e-31,0,3.3,2e-12,0,0,0.45)	[3], n9
OH attack to hydrocarbons		
CH4+OH→CH3O2	$Ae^{-B/T}$,A=2.3e-12,B=1765	[1]
C2H6+OH→CH3CHO+oRO2	$Ae^{-B/T}$,A=7.9e-12,B=1030	[1]
NC4H10+OH→0.9*CH3COE+0.1*CH3CHO+0.1*CH3COO+0.9*oRO2	$Ae^{-B/T}(300/T)^N$,A=1.36e-12, B=-190, N=-2	[5]
C2H4+OH+M→2*HCHO+oRO2	troe(7e-29,0,3.1,9e-12,0,0,0.7)	[1], n9
C3H6+OH+M→HCHO+CH3CHO+oRO2	troe(8e-27,0,3.5,3e-11,0,0,0.5)	[1], n9
OXYL+OH→ MEMALD+MGLYOX+oRO2	1.37e-11	[5]
C5H8+OH→0.32*MAC +0.42*MVK +0.74*HCHO +obio	$Ae^{-B/T}$, A=2.55e-11, B=-410	[1]
APINEN+OH→0.8*CH3CHO+0.8*CH3COE+obio	$Ae^{-B/T}$, A=1.21e-11, B=-444	[17]
BPINEN+OH→0.8*CH3CHO+0.8*CH3COE+obio	$Ae^{-B/T}$, A=1.21e-11, B=-444	[17]
LIMONE+OH→0.8*CH3CHO+0.8*CH3COE+obio	$Ae^{-B/T}$, A=1.21e-11, B=-444	[17]
HUMULE+OH→0.8*CH3CHO+0.8*CH3COE+obio	$Ae^{-B/T}$, A=1.21e-11, B=-444	[17]
OCIMEN+OH→0.8*CH3CHO+0.8*CH3COE+obio	$Ae^{-B/T}$, A=1.21e-11, B=-444	[17]
TERPEN+OH→0.8*CH3CHO+0.8*CH3COE+obio	$Ae^{-B/T}$, A=1.21e-11, B=-444	[17]
OH attack to carbonyls and peroxides		
HCHO+OH→CO+HO2	$Ae^{-B/T}$,A=8.6e-12,B=-20	[1]
CH3CHO+OH →CH3COO	$Ae^{-B/T}$,A=5.6e-12,B=-310	[1]
MEMALD+OH →GLYOX+MGLYOX+oRO2	5.6e-11	[1]
CH3COE+OH →CH3COY+oRO2	$Ae^{-B/T}(300/T)^N$, A=2.92e-13, B=-414, N=-2	[1]
GLYOX+OH→2*CO+HO2	1.1e-11	[1]
MGLYOX+OH→CH3COO+CO	1.5e-11	[1]
MVK+OH→0.266*MGLYOX +0.266*HCHO+0.684*CH3CHO +0.684*CH3COO+0.05*ISNI+0.95*oRO2	$Ae^{-B/T}$,A=4.1e-12,B=-453	[6]
MAC+OH→0.5*CH3COE+0.5*CO2+0.5*oPAN	$Ae^{-B/T}$,A=1.86e-11,B=-175	[6]
CH3O2H+OH→CH3O2	$Ae^{-B/T}$,A=1.9e-12,B=-190	[1]
PPA+OH→CH3COO	$Ae^{-B/T}$,A=1.9e-12,B=-190	n2
CH3O2H+OH→HCHO+OH	$Ae^{-B/T}$,A=1.e-12,B=-190	[1]
oROOH+OH→0.8*OH+0.2*oRO2	$Ae^{-B/T}$,A=4.35e-12,B=-455	n2
obioH+OH→OH	8e-11	n2
PANH+OH→0.2*oPAN	1.64e-11	n2
CARNIT+OH→CH3CHO+CO+NO2	k(T)=$Ae^{-B/T}$,A=5.6e-12,B=-310	
NO3 attack to hydrocarbons and aldehydes		
C2H4+NO3→0.5*CARNIT+HCHO+oRN1	2e-16 [1]	
C3H6+NO3→0.5*CARNIT+1.5*HCHO+0.5*CH3CHO +0.5*HO2+oRN1	9.45e-15	[1]
APINEN+NO3→CH3CHO+CH3COE+oRN1	$Ae^{-B/T}$,A=1.19e-12,B=490	[8]
BPINEN+NO3→CH3CHO+CH3COE+oRN1	$Ae^{-B/T}$,A=1.19e-12,B=490	[8]
LIMONE+NO3→CH3CHO+CH3COE+oRN1	$Ae^{-B/T}$,A=1.19e-12,B=490	[8]
OCIMEN+NO3→CH3CHO+CH3COE+oRN1	$Ae^{-B/T}$,A=1.19e-12,B=490	[8]
HUMULE+NO3→CH3CHO+CH3COE+oRN1	$Ae^{-B/T}$,A=1.19e-12,B=490	[8]
TERPEN+NO3→CH3CHO+CH3COE+oRN1	$Ae^{-B/T}$,A=1.19e-12,B=490	[8]
C5H8+NO3→0.85*ISNI+0.1*MAC+0.05*MVK+0.15*HCHO +0.8*HO2+oRN1	7.8e-13	[6]
HCHO+NO3→CO+HNO3+HO2	5.8e-16	[1]
CH3CHO+NO3→CH3COO+HNO3	2.8e-15	[9]
CH3O2+NO3→HCHO+HO2+NO2	1.2e-12	[10]
CH3COO+NO3→CH3O2+NO2+CO2	4e-12	[10]
oRO2+NO3→NO2+HO2	1.2e-12	[10]
obio+NO3→NO2+HO2	1.2e-12	[10]
oPAN+NO3→NO2+HO2	4e-12	[10]

Reactions	Kinetic constants	Ref.
oRN1+NO3→1.5*NO2	1.2e-12	[10]
O3 attack to unsaturated hydrocarbons		
C2H4+O3→HCHO+0.12*HO2+0.13*H2+0.44*CO	$Ae^{-B/T}$,A=9.1e-15,B=2580	[1]
C3H6+O3→0.53*HCHO+0.5*CH3CHO+0.31*CH3O2 +0.28*HO2+0.15*OH+0.065*H2+0.4*CO+0.7*CH4	$Ae^{-B/T}$,A=5.5e-15,B=1880	[1]
C5H8+O3→0.67*MAC+0.26*MVK+0.55*OH+0.07*C3H6 +0.8*HCHO +0.06*HO2+0.05*CO+0.3*O3	$Ae^{-B/T}$,A=1.2e-14,B=2013	[6]
MAC+O3→0.8*MGLYOX+0.7*HCHO+0.215*OH+0.275*HO2 +0.2*CO+0.2*O3	$Ae^{-B/T}$,A=5.3e-15,B=2520	[6]
MVK+O3→0.82*MGLYOX+0.8*HCHO+0.04*CH3CHO +0.08*OH+0.06*HO2+0.05*CO+0.2*O3	$Ae^{-B/T}$,A=4.3e-15,B=2016	[6]
APINEN+O3→1.27*CH3CHO+0.53*CH3COE+0.14*CO +0.62*oRO2+0.42*HCHO+0.85*OH+0.1*HO2	$Ae^{-B/T}$,A=1.0e-15,B=736	[8]
BPINEN+O3→1.27*CH3CHO+0.53*CH3COE+0.14*CO +0.62*oRO2+0.42*HCHO+0.85*OH+0.1*HO2	$Ae^{-B/T}$,A=1.0e-15,B=736	[8]
LIMONE+O3→1.27*CH3CHO+0.53*CH3COE+0.14*CO +0.62*oRO2+0.42*HCHO+0.85*OH+0.1*HO2	$Ae^{-B/T}$,A=1.0e-15,B=736	[8]
TERPEN+O3→1.27*CH3CHO+0.53*CH3COE+0.14*CO +0.62*oRO2+0.42*HCHO+0.85*OH+0.1*HO2	$Ae^{-B/T}$,A=1.0e-15,B=736	[8]
OCIMEN+O3→1.27*CH3CHO+0.53*CH3COE+0.14*CO +0.62*oRO2+0.42*HCHO+0.85*OH+0.1*HO2	$Ae^{-B/T}$,A=1.0e-15,B=736	[8]
HUMULE+O3→1.27*CH3CHO+0.53*CH3COE+0.14*CO +0.62*oRO2+0.42*HCHO+0.85*OH+0.1*HO2	$Ae^{-B/T}$,A=1.0e-15,B=736	[8]
organic radical conversion		
CH3O2+NO→HCHO+NO2+HO2	$Ae^{-B/T}$,A=4.2e-12,B=-180	[1]
CH3COO+NO→CH3O2+NO2+CO2	2e-11	[1]
oRO2+NO→NO2+HO2	4e-12	n3
obio+NO→0.86*NO2+0.78*HO2+0.14*ISNI	$Ae^{-B/T}$,A=1.4e-11,B=180	[6]
oPAN+NO→NO2+HO2	1.4e-11	n3
oRN1+NO→1.5*NO2	4e-11	n3
organic radical recombination		
CH3O2+HO2→CH3O2H	$Ae^{-B/T}$,A=4.1e-13,B=-790	[1]
CH3COO+HO2→0.67*PPA+0.33*O3	$Ae^{-B/T}$,A=4.3e-13,B=-1040	[1]
oRO2+HO2→ oROOH	$Ae^{-B/T}$,A=2.7e-13,B=-1000	n4
obio+HO2→obioH	$Ae^{-B/T}$,A=2.7e-13,B=-1000	n4
oPAN+HO2→PANH	$Ae^{-B/T}$,A=2.7e-13,B=-1000	n4
oRN1+HO2→X	$Ae^{-B/T}$,A=2.7e-13,B=-1000	n4
CH3O2+CH3O2→1.35*HCHO+0.7*HO2	$Ae^{-B/T}$,A=1.13e-13,B=-356	[1], n5
CH3COO+CH3O2→0.5*CH3O2+0.5*CO2+HCHO+0.5*HO2	$Ae^{-B/T}$,A=3.34e-12,B=-400	[1], n5
oRO2+CH3O2→0.65*HCHO+0.8*HO2+0.35*CH3OH	$Ae^{-B/T}$,A=1.5e-13,B=-220	n5
obio+CH3O2→0.8*HO2+0.5*HCHO	$Ae^{-B/T}$,A=2.44e-11,B=223	n5
oPAN+CH3O2→HCHO+0.5*HO2	$Ae^{-B/T}$,A=7.9e-12,B=-140	n5
CH3COO+CH3COO→2.*CH3O2+2.*CO2	$Ae^{-B/T}$,A=2.8e-12,B=-530	[1], n5
oRO2+CH3COO→0.8*CH3O2+0.8*CO2+0.8*HO2	$Ae^{-B/T}$,A=8.6e-13,B=-260	n5
obio+CH3COO→0.5*HCHO+1.5*HO2+0.7*CO2	$Ae^{-B/T}$,A=1.18e-11,B=127	n5
oPAN+CH3COO→CH3O2+CO2+HO2	$Ae^{-B/T}$,A=3.34e-12,B=-400	n5
oRO2+oRO2→1.3*HO2	6.4e-14	n5

Reactions	Kinetic constants	Ref.
organic nitrates and pernitrates		
CH3COO+NO2+M→PAN	troe(2.7e-28,0,7.1,1.2e-11,0,0.9,0.3)	[1], n9
oPAN+NO2+M→toPAN	troe(2.7e-28,0,7.1,1.2e-11,0,0.9,0.3)	n6 , n9
PAN+M→CH3COO+NO2	troe(4.9e-3,12100,0,5.4e16,13830,0,0.3)	[1], n9
toPAN+M→oPAN+NO2	troe(4.9e-3,12100,0,5.4e16,13830,0,0.3)	n6 , n9
PAN+OH→HCHO+NO3+CO2	$Ae^{-B/T}$,A=9.5e-13,B=650	[1]
toPAN+OH→NO3+CO2	$Ae^{-B/T}$,A=3.25e-13,B=-500	n6
ISNI+OH→0.95*CH3CHO+0.475*CH3COE+0.475*MGLYOX +0.05*ISNI+0.05*HO2+oRN1	3.4e-11	[6]
photolytic reactions		
O3→2*OH	photorate	[3], n7
NO2→NO+O3	photorate	[3]
NO3→NO2+O3	photorate	[3], [11]
NO3→NO	photorate	[3], [11]
N2O5→NO2+NO3	photorate	[3]
H2O2→2*OH	photorate	[3]
HNO3→NO2+OH	photorate	[3]
HONO→NO+OH	photorate	[3]
HCHO→CO+2*HO2	photorate	[3]
HCHO→CO+H2	photorate	[3]
CH3CHO→CH3O2+HO2+CO	photorate	[1]
CH3COE→CH3COO+CH3CHO+oRO2	photorate	[11], [12]
CH3COY→2*CH3COO	photorate	[13], [14]
MGLYOX→CH3COO+HO2+CO	photorate	[1]
GLYOX→0.6*HO2+2*CO+0.7*H2	photorate	[13], [14]
MEMALD→0.5*MVK+0.5*MALEIC+0.5*oPAN+0.5*HCHO +0.5*HO2	photorate	[15]
CH3O2H→HCHO+OH+HO2	photorate	[3]
PPA→CH3O2+CO2+OH	photorate	n8
oROOH→OH+HO2	photorate	n8
obioH→OH+HO2	photorate	n8
PANH→OH+HO2	photorate	n8
PAN→CH3COO+NO2	photorate	[3]

- [1] Atkinson et al., 1997
- [2] Donahue et al., 1997
- [3] DeMore et al., 1997
- [4] Mentel et al., 1996
- [5] Atkinson, 1990
- [6] Paulson and Seinfeld, 1992
- [7] Le Bras, 1997
- [8] Atkinson et al., 1994
- [9] DeMore et al., 1990
- [10] Canosa-Mas et al., 1996
- [11] Johnston et al., 1996
- [12] Martinez et al., 1992
- [13] Jenkins et al., 1997
- [14] Plum et al., 1983
- [15] Bierbach et al., 1994
- [16] Lightfoot et al., 1996
- [17] Kirchner and Stockwell, 1996
- [18] Aumont, 2002

- n1 : Rate constants containing a density dependent term in a minor reaction channel have been simplified by putting an average boundary layer molecular density of $2.5*10^{19}$ molecules/cm^3.
- n2 : For operator reactions with OH, oROOH is interpreted as 2-butyl hydrogen peroxide, obioH as a peroxide from isoprene degradation, PANH represents unsaturated organic peroxides; due to lack of data, the rate constants of these compounds and of peroxy acetyl acid have been estimated using structure reactivity relationships in Kwok and Atkinson (1995).
- n3 : The rate constant of the operator reaction oRO2+NO has been set to that of the i-C3H7O2+NO

reaction given in [16], that of oPAN+NO to that of CH3COO2+NO [1], the rate constant for oRO2NO+NO is taken from that of ISNIR (nitrate peroxy radicals from isoprene degradation) + NO [6].

- n4 : The rate constants for the operator reactions oRO2, obio, RO2NI+HO2 have been set to that of the reaction C2H5O2+HO2 [1], that of oPAN+HO2 has been taken from CH3COO2+HO2 [1].
- n5 : Radical conserving and terminating pathways are combined to single reactions; rate constants in operator reactions are affected by interpreting oRO2 as 2-butyl peroxy radical [16], obio as a peroxy radical from isoprene degradation [6] and oPAN as CH3COO2.
- n6 : Reaction rates of the operators oPAN and OPAN have been set to those of the peroxy acetyl radical and PAN, respectively.
- n7 : The reactions O3+hν→O(1D), O(1D)+H2O→2OH, O(1D)+M→O(3P)+M and O(3P)+O2+M→O3+M have been combined to reaction O3+hν→O(1D) by taking into account H2O and M concentrations in order to adjust the photolysis frequency.
- n8 : Due to lack of data, photolysis frequencies of higher organic peroxides are taken as that of CH3OOH.
- n9 : Three body Troe reactions [1], given in the form:

$$k = \frac{k_0[M]}{1 + \frac{k_0[M]}{k_\infty}} f^Z$$

with

$$Z = \frac{1}{1 + \left(log_{10}\left(\frac{k_0(T)[M]}{k_\infty(T)}\right)\right)^2}$$

$$k_0 = A_0 e^{\left(-\frac{B_0}{T}\right)} \left(\frac{T}{300}\right)^{-n}, \text{ and } k_\infty = A_\infty e^{\left(-\frac{B_\infty}{T}\right)} \left(\frac{T}{300}\right)^{-m},$$

The parameters are given in the order $A_0, B_0, n, A_\infty, B_\infty, m, f$

10.2.4 Species list of the SAPRC-07-A gas-phase chemical mechanism

Species	Definition
Inorganic compounds	
O3	ozone
H2O2	hydrogen peroxide
OH	hydroxy radical
HO2	hydroperoxy radical
NO	nitric oxide
NO2	nitrogen dioxide
NO3	nitrogen trioxide
N2O5	dinitrogen pentoxide
HONO	nitrous acide
HNO3	nitric acide
CO	carbon monoxide
SO2	sulfur dioxide
Hydrocarbon species	
CH4	Methane
C2H4	Ethen
ACYE	Acetylen
BENZ	Benzen
C5H8	Isoprene
APINEN	α-pinene
BPINEN	β-pinene
LIMONE	limonene
lumped class	
TERPEN	terpenes
HUMULE	Humulene
OCIMEN	Ocimene
ALK1	Ethane
ALK2	Propane
ALK3	Alkans 2.5x10^3 <k$_{OH}$< 5x10^3
ALK4	Alkans 5x10^3<k$_{OH}$<1x10^4
ALK5	Alkans 1x10^4<k$_{OH}$
ARO1	Aromatiques k$_{OH}$<2x10^4
ARO2	Aromatiques k$_{OH}$>2x10^4
OLE1	Alkens k$_{OH}$<7x10^4
OLE2	Alkens k$_{OH}$>7x10^3
AFG1	Lumped photoreactive monounsaturated dicarbonyl aromatic fragmentation products that photolyze to form radicals
AFG2	Lumped photoreactive monounsaturated dicarbonyl aromatic fragmentation products that photolyze to form non-radical products

AFG3 ..... Lumped diunsaturatred dicarbonyl aromatic fragmentation product
RNO3 ..... Lumped Organic Nitrates

PAN and PAN analogues

PAN ..... Peroxy Acetyl Nitrate
PAN2 ..... PPN and other higher alkyl PAN analogues
PBZN ..... PAN analogues formed from Aromatic Aldehydes
MAPAN ..... PAN analogues formed from Methacrolein

Carbonyls

HCHO ..... Formaldehyde
MEK .... Ketones and other non-aldehyde oxygenated products that react with OH radicals faster than $5x10^{-13}$ but slower than $5x10^{-12}$ $cm^3.molec^{-2}.s^{-1}$
GLY ..... Glyoxal
MACR ..... Methacrolein
MVK ..... Methyl Vinyl Ketone
CCHO ..... Acetaldehyde
RCHO ..... Lumped C3+ Aldehydes
ACET ..... Acetone
BACL ..... Biacetyl
BALD ..... Aromatic aldehydes
CRES ..... Phenols and Cresols
PRD2 ..... Ketones (k_{OH}>$0.7x10^4$ $ppm^{-1}.mn^{-1}$)
NPHE ..... Nitrophenols
IPRD ..... Lumped isoprene product species
MEOH ..... Methanol

Organic peroxides

XOOH ..... Lumped organic hydroperoxide structure, used to represent the effect of photolysis of the hydroperoxide group in the SAPRC-99 peroxy radical representation (Carter, 2000).
COOH ..... Methyl Hydroperoxide
FACD ..... Formic Acid
PACD ..... Higher organic acids
AACD ..... Acetic Acid

(Per)oxy radicals

TBUO ..... t-Butoxy Radicals
RCO3 ..... Peroxy Propionyl and higher peroxy acyl Radicals
MEO2 ..... Methyl Peroxy Radicals
MECO3 ..... Acetyl Peroxy Radicals
MACO3 .... Peroxyacyl radicals formed from methacrolein and other acroleins
BZCO3 .. Peroxyacyl radical formed from Aromatic Aldehydes
BZO ..... Phenoxy Radicals

Operators [1]

RO2N . Peroxy Radical Operator representing NO consumption with organic nitrate formation
RO2R ..... Peroxy Radical Operator representing NO to NO2 conversion with HO2 formation
R2O2 ..... Peroxy Radical Operator representing NO to NO_2 conversion without HO_2 formation

Reaction list of the SAPRC-07-A chemical mechanism

Reactions	Kinetic constants
Inorganic chemistry	
O3+NO→NO2	k(T)=A$e^{-B/T}$,A=3.00e-12,B=1500
O3+NO2→NO3	k(T)=A$e^{-B/T}$,A=1.40e-13,B=2470
NO+NO3→2*NO2	k(T)=A$e^{-B/T}$,A=1.80e-11,B=-110
NO+NO+O2→2*NO2	k(T)=A$e^{-B/T}$,A=3.30e-39,B=-530
NO2+NO3+M→N2O5	k(T,M)=saprc_troe(3.60e-30,-4.10,0.,1.90e-12,0.20,0.,0.35,1.33)
N2O5+M→NO2+NO3	k(T,M)=saprc_troe(1.30e-03,-3.50,11000,9.70e+14,0.10,11080,0.35,1.33)
N2O5+H2O→2*HNO3	k=2.50e-22
N2O5+H2O+H2O→2*HNO3	k=1.80e-39
NO2+NO3→NO+NO2	k(T)=A$e^{-B/T}$,A=4.50e-14,B=1260
OH+NO+M→HONO	k(T,M)=saprc_troe(7.00e-31,-2.60,0.,3.60e-11,-0.10,0.,0.60,1.0)
OH+HONO→NO2	k(T)=A$e^{-B/T}$,A=2.50e-12,B=-260
OH+NO2+M→HNO3	k(T,M)=saprc_troe(1.80e-30,-3.00,0.,2.80e-11,0.,0.,0.60,1.0)
OH+NO3→HO2+NO2	k=2.00e-11
OH+HNO3→NO3	k(T)=saprc_2(2.40e-14,-460,2.70e-17,-2199,6.50e-34,-1335)
OH+CO→HO2+CO2	k(T)=saprc_1(1.44e-13,0.,3.43e-33,0.)
OH+O3→HO2	k(T)=A$e^{-B/T}$,A=1.70e-12,B=940
HO2+NO→OH+NO2	k(T)=A$e^{-B/T}$,A=3.60e-12,B=-270
HO2+NO2+M→HNO4	k(T,M)=saprc_troe(2.00e-31,-3.40,0.,2.90e-12,-1.10,0.,0.60,1.0)

[1] For the concept of "chemical operators" see Carter (1990) and Aumont et al. (1997)

Reactions	Kinetic constants
HNO4+M→HO2+NO2	k(T,M)=saprc_troe(3.72e-05,-2.40,10650,5.42e+15,-2.30,11170,0.60,1.0)
HNO4+OH→NO2	k(T)=Ae$^{-B/T}$,A=1.30e-12,B=-380
HO2+O3→OH	k(T)=Ae$^{-B/T}$(300/T)^{N},A=2.03e-16,B=-693,N=-4.57
HO2+HO2→H2O2	k(T)=saprc_1(2.20e-13,-600,1.90e-33,-980)
HO2+HO2+H2O→H2O2	k(T)=saprc_1(3.08e-34,-2800,2.66e-54,-3180)
NO3+HO2→0.8*OH+0.8*NO2+0.2*HNO3	k=4.00e-12
NO3+NO3→2*NO2	k(T)=Ae$^{-B/T}$,A=8.50e-13,B=2450
H2O2+OH→HO2	k=1.80e-12
OH+HO2→H2O	k(T)=Ae$^{-B/T}$,A=4.80e-11,B=-250
OH+H2→HO2	k(T)=Ae$^{-B/T}$,A=7.70e-12,B=2100
SOx chemistry	
OH+SO2+M→HO2+H2SO4	k(T,M)=saprc_troe(3.30e-31,-4.30,0.,1.60e-12,0.,0,0.60,1.0)
RO$_2$X operator	
RO2R+NO→NO2+HO2	k(T)=Ae$^{-B/T}$,A=2.60e-12,B=-380
RO2R+HO2→XOOH	k(T)=Ae$^{-B/T}$,A=3.80e-13,B=-900
RO2R+NO3→NO2+HO2	k=2.30e-12
RO2R+MEO2→HO2+0.75*HCHO+0.25*MEOH	k=2e-13
RO2R+RO2R→HO2	k=3.50e-14
RO2N+NO→RNO3	k(T)=Ae$^{-B/T}$,A=2.60e-12,B=-380
RO2N+HO2→XOOH+PRD2	k(T)=Ae$^{-B/T}$,A=3.80e-13,B=-900
RO2N+NO3→NO2+HO2+PRD2	k=2.30e-12
RO2N+MEO2→HO2+0.25*MEOH+PRD2+0.75*HCHO	k=2e-13
RO2N+RO2R→HO2+PRD2	k=3.50e-14
RO2N+RO2N→HO2+2*PRD2	k=3.50e-14
MECO3+RO2R→MEO2+CO2	k(T)=Ae$^{-B/T}$,A=4.40e-13,B=-1070
MECO3+RO2N→MEO2+CO2+HO2+PRD2	k(T)=Ae$^{-B/T}$,A=4.40e-13,B=-1070
MACO3+RO2R→CO2+HCHO+MECO3	k(T)=Ae$^{-B/T}$,A=4.40e-13,B=-1070
MACO3+RO2N→CO2+HCHO+MECO3+HO2+PRD2	k(T)=Ae$^{-B/T}$,A=4.40e-13,B=-1070
R2O2+RO2R→RO2R	k=3.50e-14
R2O2+RO2N→RO2N	k=3.50e-14
R2O2+R2O2→X	k=3.50e-14
R2O2+MECO3→MECO3	k(T)=Ae$^{-B/T}$,A=4.40e-13,B=-1070
R2O2+RCO3→RCO3	k(T)=Ae$^{-B/T}$,A=4.40e-13,B=-1070
R2O2+BZCO3→BZCO3	k(T)=Ae$^{-B/T}$,A=4.40e-13,B=-1070
R2O2+MACO3→MACO3	k(T)=Ae$^{-B/T}$,A=4.40e-13,B=-1070
RCO3+RO2R→CO2+RO2R+CCHO	k(T)=Ae$^{-B/T}$,A=4.40e-13,B=-1070
RCO3+RO2N→RO2R+CCHO+CO2+HO2+PRD2	k(T)=Ae$^{-B/T}$,A=4.40e-13,B=-1070
BZCO3+RO2R→CO2+BZO+R2O2	k(T)=Ae$^{-B/T}$,A=4.40e-13,B=-1070
BZCO3+RO2N→CO2+BZO+R2O2+HO2+PRD2	k(T)=Ae$^{-B/T}$,A=4.40e-13,B=-1070
OH attack to hydrocarbons	
AFG1+OH→0.521*RO2R+0.201*MECO3+0.217*MACO3 +0.06*RO2N+0.202*R2O2+0.334*CO+0.407*RCHO+0.129*MEK +0.107*GLY+0.267*MGLY+0.284*XC	k=7.40e-11
AFG2+OH→0.521*RO2R+0.201*MECO3+0.217*MACO3 +0.06*RO2N+0.202*R2O2+0.334*CO+0.407*RCHO+0.129*MEK +0.107*GLY+0.267*MGLY+0.284*XC	k=7.40e-11
AFG3+OH→0.561*RO2R+0.117*MECO3+0.206*MACO3 +0.117*RO2N+0.172*R2O2+0.114*CO+0.274*GLY+0.153*MGLY +0.019*BACL+0.231*IPRD+0.195*AFG1+0.195*AFG2+0.938*XC	k=9.35e-11
CH4+OH→MEO2	k(T)=Ae$^{-B/T}$,A=1.85e-12,B=1690
C2H4+OH+M→RO2R+1.61*HCHO+0.195*CCHO	k(T,M)=saprc_troe(1.00e-28,-4.50,0.,8.80e-12,-0.85,0.,0.60,1.0)
C5H8+OH→0.907*RO2R+0.093*RO2N+0.079*R2O2+0.624*HCHO +0.23*MACR+0.32*MVK+0.357*IPRD+-0.167*XC	k(T)=Ae$^{-B/T}$,A=2.54e-11,B=-410

Reactions	Kinetic constants
ACYE+OH+M→0.3*HO2+0.7*OH+0.3*CO+0.3*FACD+0.7*GLY	k(T,M)=saprc_troe(5.50e-30,-2.00,0.,8.30e-13,0.,0.,0.60,1.0)
BENZ+OH→0.57*HO2+0.29*RO2R+0.116*OH+0.024*RO2N +0.29*GLY+0.57*CRES+0.029*AFG1+0.261*AFG2+0.116*AFG3+-0.976*XC	k(T)=A$e^{-B/T}$,A=2.33e-12,B=193
ALK1+OH→RO2R+CCHO	k(T)=A$e^{-B/T}$(300/T)^N,A=1.34e-12,B=499,N=-2
ALK2+OH→0.965*RO2R+0.035*RO2N+0.261*RCHO+0.704*ACET+-0.105*XC	k(T)=A$e^{-B/T}$(300/T)^N,A=1.49e-12,B=87,N=-2
ALK3+OH→0.695*RO2R+0.236*TBUO+0.07*RO2N+0.558*R2O2 +0.026*HCHO+0.445*CCHO+0.122*RCHO+0.024*ACET+0.332*MEK+-0.046*XC	k(T)=A$e^{-B/T}$,A=1.51e-12,B=-126
ALK4+OH→0.83*RO2R+0.01*MEO2+0.011*MECO3+0.149*RO2N +0.933*R2O2+0.002*CO+0.029*HCHO+0.438*CCHO+0.236*RCHO +0.426*ACET+0.106*MEK+0.146*PRD2+-0.119*XC	k(T)=A$e^{-B/T}$,A=3.75e-12,B=-44
ALK5+OH→0.647*RO2R+0.353*RO2N+0.958*R2O2+0.04*HCHO +0.106*CCHO+0.209*RCHO+0.071*ACET+0.086*MEK +0.407*PRD2+2.004*XC	k(T)=A$e^{-B/T}$,A=2.70e-12,B=-374
OLE1+OH→0.904*RO2R+0.001*MEO2+0.095*RO2N+0.234*R2O2 +0.7*HCHO+0.301*CCHO+0.47*RCHO+0.005*ACET+0.119*PRD2 +0.026*MACR+0.008*MVK+0.006*IPRD+0.822*XC	k(T)=A$e^{-B/T}$,A=6.18e-12,B=-501
OLE2+OH→0.914*RO2R+0.086*RO2N+0.052*R2O2+0.209*HCHO +0.788*CCHO+0.481*RCHO+0.136*ACET+0.076*MEK+0.022*PRD2 +0.027*MACR+0.002*MVK+0.037*IPRD+0.111*XC	k(T)=A$e^{-B/T}$,A=1.26e-11,B=-488
ARO1+OH→0.166*HO2+0.482*RO2R+0.284*OH+0.068*RO2N +0.077*PRD2+0.218*GLY+0.138*MGLY+0.166*CRES+0.049*BALD +0.164*AFG1+0.193*AFG2+0.284*AFG3+0.002*XC	k=6.15e-12
ARO2+OH→0.108*HO2+0.58*RO2R+0.202*OH+0.11*RO2N +0.035*PRD2+0.116*GLY+0.286*MGLY+0.104*BACL+0.108*CRES +0.039*BALD+0.217*AFG1+0.21*AFG2+0.282*AFG3+1.486*XC	k=2.57e-11
OH attack to carbonyls and peroxides	
GLY+OH→0.63*HO2+0.37*RCO3+1.26*CO+-0.37*XC	k=1.10e-11
MGLY+OH→MECO3+CO	k=1.50e-11
CRES+OH→0.8*RO2R+0.2*BZO+0.25*MGLY+5.05*XC	k(T)=A$e^{-B/T}$,A=1.70e-12,B=-950
NPHE+OH→BZO+XN	k=3.50e-12
BALD+OH→BZCO3	k=1.20e-11
MACR+OH→0.5*RO2R+0.5*MACO3+0.416*CO+0.084*HCHO +0.416*MEK+0.084*MGLY+-0.416*XC	k(T)=A$e^{-B/T}$,A=8.00e-12,B=-380
MVK+OH→0.3*RO2R+0.675*MECO3+0.025*RO2N+0.675*R2O2 +0.3*HCHO+0.675*RCHO+0.3*MGLY+-0.725*XC	k(T)=A$e^{-B/T}$,A=2.60e-12,B=-610
IPRD+OH→0.67*RO2R+0.289*MACO3+0.041*RO2N+0.336*CO +0.055*HCHO+0.129*CCHO+0.013*RCHO+0.15*MEK+0.332*PRD2 +0.15*GLY+0.174*MGLY+-0.504*XC	k=6.19e-11
PRD2+OH→0.472*HO2+0.379*RO2R+0.029*MECO3+0.049*RCO3 +0.071*RO2N+0.094*R2O2+0.213*HCHO+0.084*CCHO+0.545*RCHO +0.115*MEK+0.336*PRD2+0.877*XC	k=1.55e-11
MEOH+OH→HO2+HCHO	k(T)=A$e^{-B/T}$,A=2.85e-12,B=345
FACD+OH→HO2+CO2	k=4.50e-13
AACD+OH→0.491*RO2R+0.509*MEO2+0.509*CO2+0.491*MGLY+-0.491*XC	k(T)=A$e^{-B/T}$,A=4.20e-14,B=-855
PACD+OH→RO2R+0.143*CO2+0.142*CCHO+0.4*RCHO +0.457*BACL+-0.455*XC	k=1.20e-12
COOH+OH→0.3*OH+0.7*MEO2+0.3*HCHO	k(T)=A$e^{-B/T}$,A=3.80e-12,B=-200
ACET+OH→MECO3+R2O2+HCHO	k(T)=A$e^{-B/T}$(300/T)^N,A=4.56e-14,B=-429,N=-3.65
RCHO+OH→0.035*RO2R+0.965*RCO3+0.035*CO+0.035*CCHO	k(T)=A$e^{-B/T}$,A=5.10e-12,B=-405
CCHO+OH→MECO3	k(T)=A$e^{-B/T}$,A=4.4e-12,B=-365
HCHO+OH→HO2+CO	k(T)=A$e^{-B/T}$,A=5.4e-12,B=-135
MEK+OH→0.376*RO2R+0.51*MECO3+0.074*RCO3+0.039*RO2N +0.591*R2O2+0.088*HCHO+0.504*CCHO+0.376*RCHO+0.3*XC	k(T)=A$e^{-B/T}$(300/T)^N,A=1.3e-12,B=25,N=-2

Reactions	Kinetic constants
XOOH+OH→OH	k=2.50e-11
organic nitrates and pernitrates	
RNO3+OH→0.189*HO2+0.305*RO2R+0.332*NO2+0.175*RO2N +0.671*R2O2+0.011*HCHO+0.429*CCHO+0.037*RCHO+0.004*ACET +0.18*MEK+0.039*PRD2+0.494*RNO3+0.174*XN+0.04*XC	k=7.20e-12
PAN+M→MECO3+NO2	k(T,M)=saprc_troe(4.90e-03,0.,12100,4.00e+16,0.,13600,0.30,1.41)
PAN2→RCO3+NO2	k(T)=Ae$^{-B/T}$,A=8.30e+16,B=13940
PBZN→BZCO3+NO2	k(T)=Ae$^{-B/T}$,A=7.9e+16,B=14000
MAPAN→MACO3+NO2	k(T)=Ae$^{-B/T}$,A=1.6e+16,B=13486
MECO3+NO2+M→PAN	k(T,M)=saprc_troe(2.70e-28,-7.10,0.,1.21e-11,-0.90,0.,0.30,1.41)
RCO3+NO2→PAN2	k(T)=Ae$^{-B/T}$(300/T)^{N},A=1.21e-11,B=0,N=1.07
BZCO3+NO2→PBZN	k=1.37e-11
MACO3+NO2→MAPAN	k(T)=Ae$^{-B/T}$(300/T)^{N},A=1.21e-11,B=0,N=1.07
TBUO+NO2→RNO3+-2*XC	k=2.4e-11
BZO+NO2→NPHE	k(T)=Ae$^{-B/T}$,A=2.3e-11,B=-150
NO_3 attack	
MEO2+NO3→HCHO+HO2+NO2	k=1.30e-12
MECO3+NO3→MEO2+CO2+NO2	k=2.3e-12
RCO3+NO3→NO2+CCHO+RO2R+CO2	k=2.30e-12
BZCO3+NO3→NO2+CO2+BZO+R2O2	k=2.30e-12
MACO3+NO3→NO2+CO2+HCHO+MECO3	k=2.30e-12
R2O2+NO3→NO2	k=2.30e-12
HCHO+NO3→HNO3+HO2+CO	k(T)=Ae$^{-B/T}$,A=2e-12,B=2431
CCHO+NO3→MECO3+HNO3	k(T)=Ae$^{-B/T}$,A=1.40e-12,B=1860
RCHO+NO3→RCO3+HNO3	k(T)=Ae$^{-B/T}$,A=1.40e-12,B=1601
GLY+NO3→0.63*HO2+0.37*RCO3+HNO3+1.26*CO+-0.37*XC	k(T)=Ae$^{-B/T}$,A=2.80e-12,B=2376
MGLY+NO3→MECO3+HNO3+CO	k(T)=Ae$^{-B/T}$,A=1.40e-12,B=1895
CRES+NO3→BZO+HNO3+XC	k=1.40e-11
BALD+NO3→BZCO3+HNO3	k(T)=Ae$^{-B/T}$,A=1.34e-12,B=1860
MACR+NO3→0.5*RO2R+0.5*MACO3+0.5*HNO3+0.5*CO +0.5*XN+1.5*XC	k(T)=Ae$^{-B/T}$,A=1.50e-12,B=1815
IPRD+NO3→0.799*RO2R+0.15*MACO3+0.051*RO2N+0.15*HNO3 +0.572*CO+0.227*HCHO+0.218*RCHO+0.008*MGLY+0.572*RNO3 +0.278*XN+-0.815*XC	k=1.00e-13
C2H4+NO3→RO2R+RCHO+XN+-1*XC	k(T)=Ae$^{-B/T}$(300/T)^{N},A=3.3e-12,B=2880,N=-2
OLE1+NO3→0.824*RO2R+0.176*RO2N+0.488*R2O2+0.009*CCHO +0.002*RCHO+0.024*ACET+0.546*RNO3+0.454*XN+0.572*XC	k(T)=Ae$^{-B/T}$,A=4.73e-13,B=1047
OLE2+NO3→0.423*RO2R+0.409*NO2+0.033*MEO2+0.136*RO2N +0.762*R2O2+0.074*HCHO+0.546*CCHO+0.154*RCHO+0.11*ACET +0.002*MEK+0.026*MVK+0.007*IPRD+0.322*RNO3 +0.269*XN+0.114*XC	k(T)=Ae$^{-B/T}$,A=2.20e-13,B=-382
ozonolysis	
AFG1+O3→0.522*HO2+0.826*OH+0.652*RCO3+0.652*R2O2 +0.522*CO+0.174*CO2+0.652*HCHO+0.432*GLY+0.568*MGLY+-0.872*XC	k=9.66e-18
AFG2+O3→0.522*HO2+0.826*OH+0.652*RCO3+0.652*R2O2 +0.522*CO+0.174*CO2+0.652*HCHO+0.432*GLY+0.568*MGLY+-0.872*XC	k=9.66e-18
AFG3+O3→0.554*HO2+0.095*RO2R+0.471*OH+0.013*MECO3 +0.163*RCO3+0.007*RO2N+0.163*R2O2+0.58*CO+0.19*CO2 +0.163*HCHO+0.366*GLY+0.279*MGLY+0.003*MACR+0.004*MVK +0.003*IPRD+0.35*AFG1+0.35*AFG2+0.139*AFG3+-0.575*XC	k=1.43e-17
MVK+O3→0.064*HO2+0.05*RO2R+0.164*OH+0.05*RCO3 +0.475*CO+0.124*CO2+0.1*HCHO+0.351*FACD+0.95*MGLY+-0.05*XC	k(T)=Ae$^{-B/T}$,A=8.50e-16,B=1520

Reactions	Kinetic constants
IPRD+O3→0.4*HO2+0.285*OH+0.048*RCO3+0.048*R2O2 +0.498*CO+0.14*CO2+0.125*HCHO+0.047*CCHO+0.21*MEK +0.1*FACD+0.372*PACD+0.023*GLY+0.742*MGLY+-0.329*XC	k=4.18e-18
C2H4+O3→0.16*HO2+0.16*OH+0.51*CO+0.12*CO2+HCHO +0.37*FACD	k(T)=A$e^{-B/T}$,A=9.14e-15,B=2580
ACYE+O3→1.5*HO2+0.5*OH+1.5*CO+0.5*CO2	k(T)=A$e^{-B/T}$,A=1.00e-14,B=4100
OLE1+O3→0.116*HO2+0.04*RO2R+0.193*OH+0.104*MEO2 +0.004*RO2N+0.023*R2O2+0.368*CO+0.125*CO2+0.5*HCHO +0.154*CCHO+0.384*RCHO+0.002*ACET+0.006*MEK+0.189*PRD2 +0.185*FACD+0.022*AACD+0.112*PACD+0.69*XC	k(T)=A$e^{-B/T}$,A=3.15e-15,B=1701
OLE2+O3→0.093*HO2+0.039*RO2R+0.423*OH+0.29*MEO2 +0.147*MECO3+0.008*RCO3+0.003*RO2N+0.161*R2O2+0.297*CO +0.162*CO2+0.26*HCHO+0.495*CCHO+0.333*RCHO+0.048*ACET +0.032*MEK+0.042*PRD2+0.033*FACD+0.061*AACD +0.222*PACD+0.028*MACR+0.021*MVK+0.125*XC	k(T)=A$e^{-B/T}$,A=8.14e-15,B=1255
MACR+O3→0.108*HO2+0.208*OH+0.1*RCO3+0.1*R2O2 +0.45*CO+0.117*CO2+0.2*HCHO+0.333*FACD+0.9*MGLY+-0.1*XC	k(T)=A$e^{-B/T}$,A=1.40e-15,B=2100
organic radical conversion	
MEO2+NO→NO2+HCHO+HO2	k(T)=A$e^{-B/T}$,A=2.30e-12,B=-360
MECO3+NO→MEO2+CO2+NO2	k(T)=A$e^{-B/T}$,A=7.50e-12,B=-290
RCO3+NO→NO2+CCHO+RO2R+CO2	k(T)=A$e^{-B/T}$,A=6.70e-12,B=-340
BZCO3+NO→NO2+CO2+BZO+R2O2	k(T)=A$e^{-B/T}$,A=6.70e-12,B=-340
MACO3+NO→NO2+CO2+HCHO+MECO3	k(T)=A$e^{-B/T}$,A=6.70e-12,B=-340
R2O2+NO→NO2	k(T)=A$e^{-B/T}$,A=2.6e-12,B=-380
organic radical recombinaison	
MEO2+HO2→COOH	k(T)=A$e^{-B/T}$(300/T)^N,A=3.46e-13,B=-780,N=-0.36
MEO2+HO2→HCHO	k(T)=A$e^{-B/T}$(300/T)^N,A=3.34e-14,B=-780,N=3.53
MEO2+MEO2→MEOH+HCHO	k(T)=A$e^{-B/T}$(300/T)^N,A=6.39e-14,B=-365,N=1.80
MEO2+MEO2→2*HCHO+2*HO2	k(T)=A$e^{-B/T}$,A=7.40e-13,B=520
MECO3+HO2→AACD+0.3*O3	k(T)=A$e^{-B/T}$,A=5.20e-13,B=-980
MECO3+MEO2→0.1*AACD+0.1*HCHO+0.9*HCHO+0.9*HO2 +0.9*MEO2+0.9*CO2	k(T)=A$e^{-B/T}$,A=2.00e-12,B=-500
MECO3+MECO3→2*MEO2+2*CO2	k(T)=A$e^{-B/T}$,A=2.90e-12,B=-500
RCO3+HO2→PACD+0.25*O3	k(T)=A$e^{-B/T}$,A=5.20e-13,B=-980
RCO3+MEO2→CO2+RO2R+CCHO+HCHO+HO2	k(T)=A$e^{-B/T}$,A=2.00e-12,B=-500
RCO3+MECO3→2*CO2+MEO2+CCHO+RO2R	k(T)=A$e^{-B/T}$,A=2.90e-12,B=-500
RCO3+RCO3→2*CCHO+2*RO2R+2*CO2	k(T)=A$e^{-B/T}$,A=2.90e-12,B=-500
BZCO3+HO2→PACD+0.25*O3+4*XC	k(T)=A$e^{-B/T}$,A=5.20e-13,B=-980
BZCO3+MEO2→CO2+BZO+R2O2+HCHO+HO2	k(T)=A$e^{-B/T}$,A=2.00e-12,B=-500
BZCO3+MECO3→2*CO2+MEO2+BZO+R2O2	k(T)=A$e^{-B/T}$,A=2.90e-12,B=-500
BZCO3+RCO3→2*CO2+CCHO+RO2R+BZO+R2O2	k(T)=A$e^{-B/T}$,A=2.90e-12,B=-500
BZCO3+BZCO3→2*BZO+2*R2O2+2*CO2	k(T)=A$e^{-B/T}$,A=2.90e-12,B=-500
MACO3+HO2→PACD+0.25*O3+XC	k(T)=A$e^{-B/T}$,A=5.20e-13,B=-980
MACO3+MEO2→2*HCHO+HO2+CO2+MECO3	k(T)=A$e^{-B/T}$,A=2.00e-12,B=-500
MACO3+MECO3→2*CO2+MEO2+HCHO+MECO3	k(T)=A$e^{-B/T}$,A=2.90e-12,B=-500
MACO3+RCO3→HCHO+MECO3+CCHO+RO2R+2*CO2	k(T)=A$e^{-B/T}$,A=2.90e-12,B=-500
MACO3+BZCO3→HCHO+MECO3+BZO+R2O2+2*CO2	k(T)=A$e^{-B/T}$,A=2.90e-12,B=-500
MACO3+MACO3→2*HCHO+2*MECO3+2*CO2	k(T)=A$e^{-B/T}$,A=2.90e-12,B=-500
BZO+HO2→CRES+-1*XC	k(T)=A$e^{-B/T}$,A=3.80e-13,B=-900
R2O2+HO2→HO2	k(T)=A$e^{-B/T}$,A=3.80e-13,B=-900
R2O2+MEO2→MEO2	k=2e-13
BZO→CRES+RO2R+-1*XC	k=1.e-3
TBUO→ACET+MEO2	k(T)=A$e^{-B/T}$,A=7.5e+14,B=8152
photolytic reactions	
NO2→NO+O3	J(Z)=photorate(NO2)
NO3→NO	J(Z)=photorate(NO3-1)

Reactions	Kinetic constants
NO3→NO2+O3	J(Z)=photorate(NO3-2)
O3→2*OH	J(T,Z,H2O)=photorate(O3-1)
HONO→OH+NO	J(Z)=photorate(HONO)
HNO3→OH+NO2	J(Z)=photorate(HNO3)
HNO4→0.61*HO2+0.61*NO2+0.39*OH+0.39*NO3	J(Z)=photorate(HNO4)
H2O2→2*OH	J(Z)=photorate(H2O2)
PAN→0.6*MECO3+0.6*NO2+0.4*MEO2+0.4*CO2+0.4*NO3	J(Z)=photorate(PAN)
PAN2→0.6*RCO3+0.6*NO2+0.4*CCHO+0.4*RO2R+0.4*CO2+0.4*NO3	J(Z)=photorate(PAN2)
PBZN→0.6*BZCO3+0.6*NO2+0.4*CO2+0.4*BZO+0.4*R2O2+0.4*NO3	J(Z)=photorate(PBZN)
MAPAN→0.6*MACO3+0.6*NO2+0.4*CO2+0.4*HCHO+0.4*MECO3 +0.4*NO3	J(Z)=photorate(MAPAN)
HCHO→2*HO2+CO	J(Z)=photorate(HCHO-1)
HCHO→CO	J(Z)=photorate(HCHO-2)
CCHO→HO2+MEO2+CO	J(Z)=photorate(CCHO)
RCHO→HO2+RO2R+CO+CCHO	J(Z)=photorate(RCHO)
ACET→1.38*MEO2+0.62*MECO3+0.38*CO	J(Z)=photorate(ACET)
MEK→RO2R+MECO3+CCHO	J(Z)=photorate(MEK)
COOH→HO2+OH+HCHO	J(Z)=photorate(COOH)
XOOH→HO2+OH	J(Z)=photorate(XOOH)
GLY→2*HO2+2*CO	J(Z)=photorate(GLY-07R)
GLY→HCHO+CO	J(Z)=photorate(GLY-07M)
MGLY→HO2+MECO3+CO	J(Z)=photorate(MGLY)
BACL→2*MECO3	J(Z)=photorate(BACL)
NPHE→HONO+6*XC	J(Z)=photorate(NPHE)
NPHE→XN+6*XC	J(Z)=photorate(NPHE-2)
BALD→7*XC	J(Z)=photorate(BALD)
AFG1→1.023*HO2+0.173*MEO2+0.305*MECO3+0.5*MACO3 +0.695*CO+0.195*GLY+0.305*MGLY+0.217*XC	J(Z)=photorate(AFG1)
AFG2→PRD2+-1*XC	J(Z)=photorate(AFG2)
MACR→0.67*HO2+0.33*OH+0.67*MECO3+0.33*MACO3 +0.33*R2O2+0.67*CO+0.67*HCHO	J(Z)=photorate(MACR)
MVK→0.4*MEO2+0.4*MACO3+0.6*CO+0.6*PRD2+-2.2*XC	J(Z)=photorate(MVK)
IPRD→1.233*HO2+0.467*MECO3+0.3*RCO3+1.233*CO+0.3*HCHO +0.467*CCHO+0.233*MEK+-0.233*XC	J(Z)=photorate(IPRD)
PRD2→0.913*RO2R+0.4*MECO3+0.6*RCO3+0.087*RO2N +0.677*R2O2+0.303*HCHO+0.163*CCHO+0.78*RCHO+-0.091*XC	J(Z)=photorate(PRD2)
RNO3→0.344*HO2+0.554*RO2R+NO2+0.102*RO2N+0.167*R2O2 +0.135*HCHO+0.444*CCHO+0.137*RCHO+0.008*ACET+0.207*MEK +0.451*PRD2+0.396*XC	J(Z)=photorate(RNO3)
O_3 attack to unsaturated hydrocarbons	
C5H8+O3→0.066*HO2+0.266*OH+0.192*MACO3+0.008*RO2N +0.192*R2O2+0.275*CO+0.122*CO2+0.592*HCHO+0.1*PRD2 +0.204*FACD+0.39*MACR+0.16*MVK+0.15*IPRD+-0.559*XC	k(T)=A$e^{-B/T}$,A=7.86e-15,B=1912
C5H8+NO3→0.749*RO2R+0.187*NO2+0.064*RO2N+0.187*R2O2 +0.936*IPRD+0.813*XN+-0.064*XC	k(T)=A$e^{-B/T}$,A=3.03e-12,B=448
TERPEN+OH→0.759*RO2R+0.042*RCO3+0.2*RO2N+0.388*R2O2 +0.001*CO+0.264*HCHO+0.533*RCHO+0.036*ACET+0.005*MEK +0.255*PRD2+0.009*MGLY+0.014*BACL+0.002*MVK +0.001*IPRD+5.056*XC	k(T)=A$e^{-B/T}$,A=1.87e-11,B=-435
TERPEN+O3→0.052*HO2+0.067*RO2R+0.585*OH+0.126*MECO3 +0.149*RCO3+0.203*RO2N+0.808*R2O2+0.185*CO+0.045*CO2 +0.229*HCHO+0.22*RCHO+0.165*ACET+0.004*MEK+0.409*PRD2 +0.107*FACD+0.043*PACD+0.001*GLY+0.002*MGLY+0.055*BACL +0.001*MACR+0.001*IPRD+3.526*XC	k(T)=A$e^{-B/T}$,A=9.57e-16,B=785
TERPEN+NO3→0.162*RO2R+0.421*NO2+0.019*RCO3+0.397*RO2N +1.347*R2O2+0.01*CO+0.017*HCHO+0.001*CCHO+0.509*RCHO +0.175*ACET+0.001*MGLY+0.003*MACR+0.001*MVK+0.002*IPRD +0.163*RNO3+0.416*XN+4.473*XC	k(T)=A$e^{-B/T}$,A=1.28e-12,B=-490

Reactions	Kinetic constants
APINEN+OH→0.759*RO2R+0.042*RCO3+0.2*RO2N+0.388*R2O2 +0.001*CO+0.264*HCHO+0.533*RCHO+0.036*ACET+0.005*MEK +0.255*PRD2+0.009*MGLY+0.014*BACL+0.002*MVK +0.001*IPRD+5.056*XC	k(T)=A$e^{-B/T}$,A=1.87e-11,B=-435
APINEN+O3→0.052*HO2+0.067*RO2R+0.585*OH+0.126*MECO3 +0.149*RCO3+0.203*RO2N+0.808*R2O2+0.185*CO+0.045*CO2 +0.229*HCHO+0.22*RCHO+0.165*ACET+0.004*MEK+0.409*PRD2 +0.107*FACD+0.043*PACD+0.001*GLY+0.002*MGLY+0.055*BACL +0.001*MACR+0.001*IPRD+3.526*XC	k(T)=A$e^{-B/T}$,A=9.57e-16,B=785
APINEN+NO3→0.162*RO2R+0.421*NO2+0.019*RCO3+0.397*RO2N +1.347*R2O2+0.01*CO+0.017*HCHO+0.001*CCHO+0.509*RCHO +0.175*ACET+0.001*MGLY+0.003*MACR+0.001*MVK+0.002*IPRD +0.163*RNO3+0.416*XN+4.473*XC	k(T)=A$e^{-B/T}$,A=1.28e-12,B=-490
BPINEN+OH→0.759*RO2R+0.042*RCO3+0.2*RO2N+0.388*R2O2 +0.001*CO+0.264*HCHO+0.533*RCHO+0.036*ACET+0.005*MEK +0.255*PRD2+0.009*MGLY+0.014*BACL+0.002*MVK +0.001*IPRD+5.056*XC	k(T)=A$e^{-B/T}$,A=1.87e-11,B=-435
BPINEN+O3→0.052*HO2+0.067*RO2R+0.585*OH+0.126*MECO3 +0.149*RCO3+0.203*RO2N+0.808*R2O2+0.185*CO+0.045*CO2 +0.229*HCHO+0.22*RCHO+0.165*ACET+0.004*MEK+0.409*PRD2 +0.107*FACD+0.043*PACD+0.001*GLY+0.002*MGLY+0.055*BACL +0.001*MACR+0.001*IPRD+3.526*XC	k(T)=A$e^{-B/T}$,A=9.57e-16,B=785
BPINEN+NO3→0.162*RO2R+0.421*NO2+0.019*RCO3+0.397*RO2N +1.347*R2O2+0.01*CO+0.017*HCHO+0.001*CCHO+0.509*RCHO +0.175*ACET+0.001*MGLY+0.003*MACR+0.001*MVK+0.002*IPRD +0.163*RNO3+0.416*XN+4.473*XC	k(T)=A$e^{-B/T}$,A=1.28e-12,B=-490
LIMONE+OH→0.759*RO2R+0.042*RCO3+0.2*RO2N+0.388*R2O2 +0.001*CO+0.264*HCHO+0.533*RCHO+0.036*ACET+0.005*MEK +0.255*PRD2+0.009*MGLY+0.014*BACL+0.002*MVK +0.001*IPRD+5.056*XC	k(T)=A$e^{-B/T}$,A=1.87e-11,B=-435
LIMONE+O3→0.052*HO2+0.067*RO2R+0.585*OH+0.126*MECO3 +0.149*RCO3+0.203*RO2N+0.808*R2O2+0.185*CO+0.045*CO2 +0.229*HCHO+0.22*RCHO+0.165*ACET+0.004*MEK+0.409*PRD2 +0.107*FACD+0.043*PACD+0.001*GLY+0.002*MGLY+0.055*BACL +0.001*MACR+0.001*IPRD+3.526*XC	k(T)=A$e^{-B/T}$,A=9.57e-16,B=785
LIMONE+NO3→0.162*RO2R+0.421*NO2+0.019*RCO3+0.397*RO2N +1.347*R2O2+0.01*CO+0.017*HCHO+0.001*CCHO+0.509*RCHO +0.175*ACET+0.001*MGLY+0.003*MACR+0.001*MVK+0.002*IPRD +0.163*RNO3+0.416*XN+4.473*XC	k(T)=A$e^{-B/T}$,A=1.28e-12,B=-490
OCIMEN+OH→0.759*RO2R+0.042*RCO3+0.2*RO2N+0.388*R2O2 +0.001*CO+0.264*HCHO+0.533*RCHO+0.036*ACET+0.005*MEK +0.255*PRD2+0.009*MGLY+0.014*BACL+0.002*MVK +0.001*IPRD+5.056*XC	k(T)=A$e^{-B/T}$,A=1.87e-11,B=-435
OCIMEN+O3→0.052*HO2+0.067*RO2R+0.585*OH+0.126*MECO3 +0.149*RCO3+0.203*RO2N+0.808*R2O2+0.185*CO+0.045*CO2 +0.229*HCHO+0.22*RCHO+0.165*ACET+0.004*MEK+0.409*PRD2 +0.107*FACD+0.043*PACD+0.001*GLY+0.002*MGLY+0.055*BACL +0.001*MACR+0.001*IPRD+3.526*XC	k(T)=A$e^{-B/T}$,A=9.57e-16,B=785
OCIMEN+NO3→0.162*RO2R+0.421*NO2+0.019*RCO3+0.397*RO2N +1.347*R2O2+0.01*CO+0.017*HCHO+0.001*CCHO+0.509*RCHO +0.175*ACET+0.001*MGLY+0.003*MACR+0.001*MVK+0.002*IPRD +0.163*RNO3+0.416*XN+4.473*XC	k(T)=A$e^{-B/T}$,A=1.28e-12,B=-490
HUMULE+OH→0.759*RO2R+0.042*RCO3+0.2*RO2N+0.388*R2O2 +0.001*CO+0.264*HCHO+0.533*RCHO+0.036*ACET+0.005*MEK +0.255*PRD2+0.009*MGLY+0.014*BACL+0.002*MVK+0.001*IPRD +5.056*XC	k(T)=A$e^{-B/T}$,A=1.87e-11,B=-435

Reactions	Kinetic constants
HUMULE+O3→0.052*HO2+0.067*RO2R+0.585*OH+0.126*MECO3 +0.149*RCO3+0.203*RO2N+0.808*R2O2+0.185*CO+0.045*CO2 +0.229*HCHO+0.22*RCHO+0.165*ACET+0.004*MEK+0.409*PRD2 +0.107*FACD+0.043*PACD+0.001*GLY+0.002*MGLY+0.055*BACL +0.001*MACR+0.001*IPRD+3.526*XC	k(T)=Ae$^{-B/T}$,A=9.57e-16,B=785
HUMULE+NO3→0.162*RO2R+0.421*NO2+0.019*RCO3+0.397*RO2N +1.347*R2O2+0.01*CO+0.017*HCHO+0.001*CCHO+0.509*RCHO +0.175*ACET+0.001*MGLY+0.003*MACR+0.001*MVK+0.002*IPRD +0.163*RNO3+0.416*XN+4.473*XC	k(T)=Ae$^{-B/T}$,A=1.28e-12,B=-490

- The reactions O_3+hν→O(1D), O(1D)+H_2O→2OH, O(1D)+M→O(3P)+M and O(3P)+O_2+M→O_3+M have been combined to reaction O_3+hν→ O(1D) by taking into account H_2O and M concentrations in order to adjust the photolysis frequency.
- The reactions OH+CO→HO2+CO2, HO2+HO2→H2O2 et HO2+HO2+H2O→H2O2 :

$$k\left(T,M\right)=k_1\left(T\right)+k_2\left(T\right)\left[M\right]$$

  The parameters are given in the order A_1, B_1, A_2, B_2
- The reactions OH+HNO3→NO3 :

$$k\left(T,M\right)=k_0\left(T\right)+\frac{k_3\left(T\right)\left[M\right]}{\left(1+\frac{k_3(T)[M]}{k_2(T)}\right)}$$

  The parameters are given in the order $A_0, B_0, A_2, B_2, A_3, B_3$
- Three body Troe reactions :

$$k(T,M)=\frac{k_0(T)[M]}{1+\frac{k_0(T)[M]}{k_\infty(T)}}\times F^Z$$

  with

$$Z=\frac{1}{1+\left(\frac{log_{10}\left(\frac{k_0(T)[M]}{k_\infty(T)}\right)}{N}\right)^2}$$

$$k_0=A_0e^{\left(-\frac{B_0}{T}\right)}\left(\frac{T}{300}\right)^{-n},\ \text{and}\ k_\infty=A_\infty e^{\left(-\frac{B_\infty}{T}\right)}\left(\frac{T}{300}\right)^{-m},$$

  The parameters are given in the order $A_0, n, B_0, A_\infty, m, B_\infty, F, N$

10.3 Aerosol processes

10.3.1 Overview

CHIMERE consists in the baseline gas-phase version with MELCHIOR2 chemistry, together with a sectional aerosol module. This module accounts for 7 species (primary particle material, nitrate, sulfate, ammonium, biogenic secondary organic aerosol (SOA), anthropogenic SOA and water). Potentially, Chloride et Sodium can be included (high computing time). In its initial version the module uses 6 bins from 10 nm to 40 μm. Physical processes into account are described below. See also sections on chemistry (aqueous-phase chemistry, heterogenous chemistry and SOA formation) below. Dry and wet scavenging/deposition are also described in separate sections.

The physical processes accounted for are **coagulation** ([Gelbard and Seinfeld, 1980]), **absorption** ([Nenes et al., 1998]) and **nucleation** ([Kulmala et al., 1998],[Kavouras et al., 1998]). See following subsections for details.

- **Coagulation:** Classical theory already used by [Gelbard and Seinfeld, 1980].
- **Absorption:** Absorption is taken into account for both inorganic and organic species but their processing is different. For inorganic species, equilibrium concentrations are computed with the thermodynamic module ISORROPIA (or a tabulated version) presented in [Nenes et al., 1998]. For secondary organic species, equilibrium concentrations are calculated through a temperature dependent partitioning coefficient ([Pankow, 1994]. Please note that the ISORROPIA code is included in CHIMERE, please check the ISORROPIA web site for downloading the latest version.
- **Nucleation:** The parameterization of [Kulmala et al., 1998] for sulfuric acid nucleation is used. This process, favoured by cold humid atmospheric conditions, affects the number of ultrafine particles. The nucleated flux is added to the smallest bin in the sectional distribution. Although nucleation of condensable organic species has been clearly identified in many experimental studies ([Kavouras et al., 1998], there is no available parameterization. Since the sulfuric acid nucleation process competes with absorption processes, it is expected to occur in weakly particle polluted conditions.

10.3.2 Composition and mathematical representation of aerosols

This section was published in [Bessagnet et al., 2005].

Atmospheric aerosols are represented by their size distributions and compositions. The sectional representation described by [Gelbard and Seinfeld, 1980] has been used for the density distribution function. The sectional approach is quite useful to solve the governing equation for multicomponent aerosols. It discretizes the density distribution in a finite number of bins ([Warren, 1986]). Thus, all particles in section l have the same composition and are characterized by their mean diameter dl. The aerosol module actually uses six bins from 10 nm to 40 μm, following a geometrical progression. For a given x as $x = ln(m)$, with m the particle mass, q(x) is the density distribution as defined in Equation 10.3, Q being the mass concentration function. Q_l^k (μg m-3) is the mass concentration of component k in section l and Q_l (μg m-3) is the total mass concentration in section l (Equation 10.4).

$$q(x) = \frac{dQ}{dx} \tag{10.3}$$

$$Q_l = \int_{x_{l-1}}^{x_l} q(x)dx = \sum_k Q_l^k \tag{10.4}$$

Model species	Species	Type
pPPM	Anthropogenic primary species EC, OCp, and other industrial dusts	primary
pSOA	Anthropogenic and Biogenic secondary organic aerosol (ASOA+BSOA)	secondary
pH2SO4	Equivalent Sulfate(*)	secondary
pHNO3	Equivalent Nitrate(*)	secondary
pNH3	Equivalent Ammonium(*)	primary emitted, secondary transferred
pWATER	Water	

Table 10.4: *List of aerosol species. (*): ions, molecules, crystals*

In the model, particles are composed of species listed in Table 10.4. Sulfate is formed through gaseous and aqueous oxidation of SO_2. Nitric acid is produced in the gas phase by NOx oxidation. N_2O_5 is converted into nitric acid via heterogeneous pathways by oxidation on aqueous aerosols. Ammonia is a primary emitted base converted in the aerosol phase by neutralization with nitric and sulfuric acids. Ammonia, nitrate and sulfate exist in aqueous, gaseous and particulate phases in the model. As an example, in the particulate phase the model species pNH_3 represents an equivalent ammonium as the sum of NH_4^+ ion, NH_3 liquid, NH_4NO_3 solid, etc.

10.3.3 Coagulation

Since Q_l^k is the mass concentration of component k in section l, the mass balance equation for coagulation [Gelbard and Seinfeld, 1980] follows Equation 10.5 :

$$\begin{aligned}\left[\frac{dQ_l^k}{dt}\right]_{coag} &= \frac{1}{2}\sum_{i=1}^{l-1}\sum_{j=1}^{l-1}\left[{}^{1a}\beta_{i,j,l}Q_j^k Q_i + {}^{1b}\beta_{i,j,l}Q_i^k Q_j\right] \\ &- \sum_{i=1}^{l-1}\left[{}^{2a}\beta_{i,l}Q_i Q_l^k - {}^{2b}\beta_{i,l}Q_l Q_i^k\right] \\ &- \frac{1}{2}{}^{3}\beta_{l,l}Q_l Q_l^k - Q_l^k\sum_{i=l+1}^{m}{}^{4}\beta_{i,l}Q_i\end{aligned} \tag{10.5}$$

The sectional coagulation coefficients ${}^{1a}\beta, {}^{1b}\beta, {}^{2a}\beta, {}^{2b}\beta, {}^{3}\beta and {}^{4}\beta$ (Fuch, 1964) depend on particle characteristics and meteorological data such as temperature, pressure and turbulence parameters. For submicronic particles, coagulation is essentially driven by Brownian motions. For coarse particles sedimentation is an efficient process.

10.3.4 Absorption

The absorption flux J ($\mu g m^{-3} s^{-1}$) of a semi-volatile inorganic or organic species onto a monodisperse aerosol is:

$$J = \frac{1}{\tau}(G - G_{eq}) \tag{10.6}$$

with G and G_{eq} ($\mu g m^{-3}$), respectively, are the gas phase and equilibrium concentrations. The characteristic time τ is:

$$\tau = \frac{1 + \frac{8\lambda}{\alpha d}}{2\pi\lambda c d N} \tag{10.7}$$

with λ (m) is the mean free path of air molecules, d (m) the particle diameter, N (particle m^{-3}) the particle number concentration, α the accommodation coefficient of the transferred species and c (m s^{-1}), its mean molecular velocity. For a semi-volatile species k, a mean absorption coefficient H_l^k (s^{-1}) is defined at section l as:

$$\left[\frac{dQ_l^k}{dl}\right]_{abso} = H_l^k Q_l \tag{10.8}$$

$$H_l^k = \frac{12\lambda c_k}{\rho_p d_l^2 (1 + (8\lambda/\alpha_k d_l))}(G^k - G_{l,eq}^k) \tag{10.9}$$

where ρ_p is the particle density (fixed at 1500 kgm^{-3} here). For semi-volatile inorganic species (sulfate, nitrate, ammonium), the equilibrium concentration G_{eq} is calculated using the thermodynamic module ISORROPIA ([Nenes et al., 1998]). This model also determines the water content of particles. Interactions between inorganic and organic species are not taken into account, the thermodynamic of such mixtures still being poorly understood. Equilibrium concentrations for the semivolatile organic species k are related to particle concentrations through a temperature dependent partition coefficient K^p (in $m^3 \mu g^{-1}$) ([Pankow, 1994]):

$$G_{l,eq}^k = \frac{Q_l^k}{OM_l K_k^p} \tag{10.10}$$

with OM ($\mu g m^{-3}$) is the absorbent organic material concentration. Considering the thermodynamic equilibrium between the gas and particulate phases, this coefficient is given by

$$K_k^p = \frac{10^{-6}}{MW_{om}\zeta_k p_k^0} \tag{10.11}$$

with R is the ideal gas constant (8.206 10^{-5}m3 atm mol^{-1}K^{-1}), T the temperature (K), MW$_{om}$ the mean molecular weight (g mol^{-1}), p$_i^0$ the vapor pressure of product i as a pure liquid (atm) and ζ the activity coefficient of species in the bulk aerosol phase. The coefficient ζ, difficult to calculate, is assumed constant and equal to unity. Moreover, an empirical formulae can be used to estimate K$_p$:

$$log(K^p) = -0.61 log(p^0) - 4.74 \tag{10.12}$$

according to [Kaupp and Umlauf, 1992] for organic species.

10.3.5 Nucleation

The parameterization of [Kulmala et al., 1998] for sulfuric acid nucleation is used. This process, favoured by cold humid atmospheric conditions, affects the number of ultrafine particles. The nucleated flux is added to the smallest bin in the sectional distribution. Nucleation of condensable organic species has been clearly identified in many experimental studies ([Kavouras et al., 1998], there is no available parameterization. Since, the sulfuric acid nucleation process competes with absorption processes, it is expected to occur in weakly particle polluted conditions.

10.3.6 ISORROPIA

This section is extracted from the PHD manuscript of Alma Hodzic, 2005.
The inorganic part mainly containing ammonium, sulfates and nitrates is the major part of the particulate matter. This is particularly true in the fine mode (D < 2,5 μm). The thermodynamic equilibrium model ISORROPIA [Nenes et al., 1998], is used to determine the particle/gas partitioning of semi-volatil inorganic species. The model calculate the thermodynamical equilibrium of the system: sulfate-nitrate-ammonium-sodium-chloride-water at a given temperature and relative humidity. The possible species are the following:

Gas phase :	NH_3, HNO_3, HCl, H_2O.
Liquid phase :	NH_4^+, Na^+, H^+, Cl^-, NO_3^-,
	SO_4^{2-}, HSO_4^-, OH^-, H_2O, $HNO_{3(aq)}$, $HCl_{(aq)}$, $NH_{3(aq)}$, $H_2SO_{4(aq)}^2$.
Solid phase :	$(NH_4)_2SO_4$, NH_4HSO_4, $(NH_4)_3H(SO_4)_2$,
	NH_4NO_3, NH_4Cl, NaCl, $NaNO_3$, $NaHSO_4$, Na_2SO_4

Due to its low vapor pressure, sulfuric acid is entirely transfered in the condensed phase. Also, the Sodium is located in the particulate phase. Inorganic aerosols can be a mix of solid and liquid species depending on temperature and humidity. The solid/liquid phase transition is solved by ISORROPIA by computing the deliquescent relative humidities (transition relative humidity between the phases). In the CHIMERE model, the calculation of the thermodynamic equilibrium can be done by interpolating a look-up table (see characteristics in Table 10.5). This look-up table has been pre-calculated and is delivered with the model in the file **AEROMIN.bin**. The partitioning coefficient for the nitrates and ammonium, and the aerosol water content has been calculated for a range of temperature from 260 to 312K, for relative humidity from 0.3 to 0.99 and for concentrations from 10^{-2} to 65 $\mu.g.m^{-3}$. Because of numerical limits, Sodium and Chloride are not accounted for in this table. The active seasalt version needs the to use the on-line coupling.

Variable	Value		Increment
	Min.	Max.	
Temperature (K)	260	312	2.5
Relative Humidity	0.3	0.99	0.05
H_2SO_4, HNO_3, NH_3 ($\mu.g.m^{-3}$)	10^{-2}	65	x 1,5

Table 10.5: *Characteristics of the look-up table used for the calculation of the thermodynamic equilibrium with ISORROPIA.*

The use of the look-up table allows to run the model faster, some errors can occur around each deliquescent point. This approach has been compared to the on-line coupling and tested on an entire year (2001) at the regional scale (0,5^{o}x0,5^o) over Europe.

Species	DRH (298.15K)	Mixing	MDRH (298.15K)
$(NH_4)_2SO_4$	0.799		
NH_4NO_3	0.618	NH_4NO_3, $(NH_4)_2SO_4$	0.600
NH_4HSO_4	0.400	$(NH_4)_3H(SO_4)_2$, NH_4HSO_4	0.360
$(NH_4)_3H(SO_4)_2$	0.690	$(NH_4)_3H(SO_4)_2$, $(NH_4)_2SO_4$	0.675

Table 10.6: *Relative humidity at deliquescent points for the species used by ISORROPIA in the system sulfate-nitrate-ammonium-water.*

The comparison shows the use of an on-line coupling leads to a weak decrease of the mean concentrations (13% for the nitrates, and no more than 2% for the sulfates) on the EMEP site. Ammonium concentrations are slightly increase (1 to 5%). In absolute values, the differences never exceed 0.5 $\mu.g.m^{-3}$ in average for the nitrates and 0.1 $\mu.g.m^{-3}$ for the sulfates and ammonium. The aerosol water content is slightly decreased (3 to 13% ; 0,1 to 2,8 $\mu.g.m^{-3}$.
The sensitivity tests showed very weak differences, less than $\pm$ 20%. The differences are higher in winter compare to summer. The highest differences are observed above 50-60% for the nitrates and ammonium corresponding to the main deliquescent points. Indeed, the look-up table is not enough refined in this zone to account for the strong variations of the concentrations. For the water, the highest differences are observed in the range 95-100% where the absorption of water can increase by a factor of 1000. The differences do not depend on the temperature (not shown here).
The differences obtained when comparing the on-line coupling and the look-up table are small enough compare to the uncertainties in the modelling of the other processes. The look-up table of ISORROPIA is able to determine the partition of NH_4/NH_3 and HNO_3/NO_3.

10.3.7 Multiphase chemistry

10.3.7.1 Sulfur aqueous chemistry

If the aerosol option of the model is selected, Aqueous sulphate chemistry is considered; Sulfate is produced in the following aqueous reactions ([Berge, 1993]; [Hoffmann and Calvert, 1985]; [Lee and Schwartz, 1983]):

- $SO_2^{aq} + O_3^{aq} \rightarrow SO_4^{2-}$
- $HSO_3^- + O_3^{aq} \rightarrow SO_4^{2-}$
- $SO_3^{2-} + O_3^{aq} \rightarrow SO_4^{2-}$
- $SO_2^{aq} + H_2O_2^{aq} \rightarrow SO_4^{2-}$
- $SO_2^{aq} + NO_2^{aq} \rightarrow SO_4^{2-}$
- $SO_3^{2-}(Fe^{3+}) \rightarrow SO_4^{2-}$

- $HSO_3^-(Mn^{2+}) \rightarrow SO_4^{2-}$

SO_2, H_2O_2 and O_3 in the aqueous phase are in equilibrium with the concentrations in the gas phase. Moreover, aqueous SO2 is dissociated into HSO_3^- and SO_3^{2-}. Catalyzed oxidation reactions of sulfur dioxide in aqueous droplets with iron and manganese are considered, following [Hoffmann and Calvert, 1985] among others. Henry's law coefficient and other aqueous equilibrium constants are used ([Seinfeld and Pandis, 1998]). Sulfur chemistry is very pH sensitive. pH is kept bound between 4.5 and 6.0.

10.3.7.2 Heterogeneous chemistry

Again with the aerosol option of the model, a few heterogeneous reactions are also considered. Nitric acid is produced onto existing particles and fog droplets. Although aerosol particles and cloud droplets occupy a very small fraction of the atmosphere, it is now well established that reactions involving gas species onto their surfaces may significantly contribute to atmospheric chemistry cycles. [Jacob, 2000] recommends for ozone model to include a minimal set of reactions with associated uptake coefficients given by [Harrison and Kito, 1990], and other references in [Jacob, 2000]:

- $HO_2 \rightarrow 0.5H_2O_2$ ..... γ = 0.2
- $NO_3 \rightarrow HNO_3$ ..... γ = 0.001
- $NO_2 \rightarrow 0.5HNO_3$ + 0.5HONO ..... γ = 0.0001
- $N_2O_5 \rightarrow 2HNO_3$ ..... γ = 0.01 - 1

The first-order rate constant k for gas heterogeneous loss onto particles is given by:

$$k = \sum_l \left(\frac{d_l}{2D_g} + \frac{4}{V\gamma} \right)^{-1} A_l \tag{10.13}$$

with d_l, the particle diameter (m), D_g, the reacting gas molecular diffusivity (m2 s^{-1}), n, the mean molecular velocity (m s-1), A_l, the total surface area in the particle bin l and gamma the uptake coefficient of reactive species. The uptake coefficient for N_2O_5 is assumed to be temperature-dependent in the range 0.01 - 1 ([De Moore et al., 1994]) with increasing values for decreasing temperatures. A recent study ([Aumont et al., 2003]) suggests that NO2 reactions on wet surfaces could be an important source for HONO production during wintertime smog episodes, so, a new reaction is added (also present in the gas-phase mechanism, see above).

10.3.8 Secondary organic aerosol chemistry

The complete chemical scheme implemented in CHIMERE includes biogenic and anthropogenic precursors (Table 10.7). Biogenic precursors include API (α-pinene and sabinene), BPI (β-pinene and δ^3-carene), LIM (limonene), OCI (myrcene and ocimene) and ISO (isoprene). Anthropogenic precursors include TOL (benzene, toluene and other mono-substituted aromatics), TMB (Trimethylbenzene and other poly-substituted aromatics), and NC4H10 (higher alkanes). SOA formation is represented according to a single-step oxidation of the relevant precursors and gas-particle partitioning of the condensable oxidation products. The gas-particle partitioning formulation has been described in detail by [Pun et al., 2006]. The overall approach consists in differentiating between hydrophilic SOA that are most likely to dissolve into aqueous inorganic particles and hydrophobic SOA that are most likely to absorb into organic particles. The dissolution of hydrophilic SOA is governed by Henry's law whereas the absorption of hydrophobic particles is governed by Raoult's law. The large number of condensable organic compounds is represented by a set of surrogate compounds that cover the range of physico-chemical properties relevant for aerosol formation, i.e., water solubility and acid dissociation for hydrophilic compounds and saturation vapor pressure for hydrophobic compounds. These surrogate compounds were selected by grouping identified particulate-phase molecular products with similar properties. The molecular weight of each surrogate compound is determined based on its structure and functional

groups. The Henry's law constant or the saturation vapor pressure of the surrogate species is derived from the average properties of the group. Other properties are estimated using the structure of each surrogate compound. Enthalpy of vaporization are given in brackets ($kJ.mol^{-1}$) for each SOA coumpounds : AnA0D (88), AnA1D(88), AnA2D(88), BiA0D(88), BiA1D(88), BiA2D(109), AnBmP(88), AnBlP(88), BiBmP(175). The full name of compounds are explicited in Table 10.7 caption. The absorption process in CHIMERE is implemented as in [Bowman et al., 1997]. A dynamical approach is adopted to decribe the gas/particle conversion since the model time-step is about 5 min. and using the approach by [Bowman et al., 1997], the characteristic time for mass transfer can exceed 20 min. for coarse particles.

$$J_i = \frac{1}{\tau_i}(G_i - G_i^{eq}) \tag{10.14}$$

J_i ($\mu g.m^{-3}.s^{-1}$) is the absorption or desorption flux of species i, τ_i (s) is a characteristic time of the mass transfer that depends on particle size and the chemical properties of species i, G_i is the bulk gas-phase concentration of species i and G_i^{eq} is the gas-phase concentration of species i at thermodynamic equilibrium (i.e., at the surface of the particle). The equilibrium gas-phase concentrations are functions of the particle chemical composition, temperature and, for hydrophilic species, relative humidity, as described by [Pun et al., 2006]. The base SOA module was tested against the smog chamber data of [Odum et al., 1997] for anthropogenic compounds and those of [Griffin et al., 1999] for biogenic compounds and was shown to satisfactorily reproduce SOA formation for those compounds [Pun et al., 2006]. Higher alkanes and isoprene were added to the original chemical mechanism of [Pun et al., 2006]. The formation of SOA from higher alkanes follows the formulation of [Zhang et al., 2007] for the stoichiometric SOA yield and it is assumed that the SOA species can be represented by a hydrophobic surrogate compound with a moderate saturation vapor pressure. The formation of SOA from the oxidation of isoprene by hydroxyl radicals is represented with two surrogate products and follows the formulation of [Kroll et al., 2006, Zhang et al., 2007].

10.4 Impact of clouds

10.4.1 Impact on photolysis

In this version clouds are assumed to lie above the model top, so that there is no cloud albedo effect within the model domain depth. For all photolysed species, clear sky photolysis rates $J_c(z)$ are multiplied throughout model columns by an **attenuation coefficient** A(d) depending on the **total cloud optical depth (COD)** d. Using the TUV model, and a large set of CODs for clouds at various altitudes, the attenuation relative to the clear-sky case has been fitted as a function of COD with the formula:

$$A(d) = e^{-0.11d^{2/3}} \tag{10.15}$$

Several options are offered in order to calculate the COD. Total COD, d, is the sum of partial CODs from 3 cloud layers, low clouds d_l, medium clouds d_m and high clouds d_h. The limits between these cloud is user-chosen, but depend on the meteorological model. For MM5, limits of 2000m and 6000m are proposed. For each cloud layer three options are possible for the calculation of the partial cloud optical depth:

- Calculation as a function of Liquid/Ice Water Content in the column; using an assumption of sphericity and equivalent droplet size of 6 microns, an assumption of hexagonal shape for ice particles, the formula for cloud optical depth is $180.C_w + 67.C_i$, where C_w and C_i are respectively the liquid water column (in Kg/m^2) and ice column for this cloud layer.
- Liquid/Ice water are generally unverified and unstable parameters in atmospheric models. Basing a cloud parameterization on such parameters can be risky. A more robust parameterization consists in using relative humidity only. The proposed parameterization consists in parameterizing the COD as a function of the integral **R**, over the cloud depth, of the relative humidity above 75%. It is assumed that small cloud formation (in particular cumulus clouds) starts at 75% relative humidity. Normalization of

Reactions	kinetic rates ($molec.cm^{-3}.s^{-1}$)
TOL+OH → 0.004×AnA0D + 0.001×AnA1D + 0.084×AnBmP + 0.013×AnBlP	1.81×10^{-12}exp(355/T)
TMB+OH → 0.002×AnA0D + 0.002× AnA1D + 0.001×AnA2D + 0.088×AnBmP + 0.006×AnBlP	9.80×10^{-9}/T
NC4H10+OH → 0.07×AnBmP	1.36×10^{-12}exp(190/T)$^{-2}$
API+OH → 0.30×BiA0D + 0.17×BiA1D + 0.10×BiA2D	1.21×10^{-11}exp(444/T)
API+O3 → 0.18×BiA0D + 0.16×BiA1D + 0.05×BiA2D	1.01×10^{-15}exp (-732/T)
API+NO3 → 0.80×BiBmP	1.19×10^{-12}exp(490/T)
BPI+OH → 0.07×BiA0D + 0.08×BiA1D + 0.06×BiA2D	2.38×10^{-11}exp(357/T)
BPI+O3 → 0.09×BiA0D + 0.13×BiA1D + 0.04×BiA2D	1.50×10^{-17}
BPI+NO3 → 0.80×BiBmP	2.51×10^{-12}
LIM+OH → 0.20×BiA0D + 0.25×BiA1D + 0.005×BiA2D	1.71×10^{-10}
LIM+O3 → 0.09×BiA0D + 0.10×BiA1D	2×10^{-16}
OCI+OH → 0.70×BiA0D + 0.075×BiA1D	$5.10\times^{-8}$/T
OCI+O3 → 0.50×BiA0D + 0.055×BiA1D	7.50×10^{-14}/T
OCI+NO3 → 0.70×BiA0D + 0.075×BiA1D	4.30×10^{-9}/T
ISO+OH → 0.232×ISOPA1 + 0.0288×ISOPA2	2.55×10^{-11}exp(410/T)

Table 10.7: *Gas phase chemical scheme for SOA formation in CHIMERE. The surrogate SOA compounds consist of six hydrophilic species that include an anthropogenic nondissociative species (AnA0D), an anthropogenic once-dissociative species (AnA1D), an anthropogenic twice-dissociative species (AnA2D), a biogenic non dissociative species (BiA0D), a biogenic once-dissociative species (BiA1D) and a biogenic twice-dissociative species (BiA2D), three hydrophobic species that include an anthropogenic species with moderate saturation vapor pressure (AnBmP), an anthropogenic species with low saturation vapor pressure (AnBlP) and a biogenic species with moderate saturation vapor pressure (BiBmP), and two surrogate compounds for the isoprene oxidation products.*

R leads to the formulation (for instance for low clouds): d_l = aR/dz, where a=0.02 is chosen such that a 1000m-thick layer has an optical cloud depth of 20.

- An even simpler parameterization can be achieved by making the COD simply proportional to the cloud fraction (if available) for each cloud layer. Coefficient tuning led to proportionality coefficients of: 50 for low-clouds, 10 for medium clouds and 2 for high clouds. This means, for instance, that a sky covered with 100% of high clouds has an optical depth of 2. Tuning was performed with ECMWF cloud fraction data and should change with the meteorological model.

Recommendations The first option using liquid/ice water (whenever available),is based on a variable which can be very model-dependent and which is rarely verified against observations. Moreover it does not take into account fractionary cloudiness. However it may be suited for high/medium clouds which are often stratiform clouds in the midlatitudes. The second option uses cloud fractions (whenever available), which is less meaningful to radiation but could be used when cloud/ice water is not available. The third option uses relative (to liquid water) humidity, and has been tuned using J(NO2) measurements taken over a long period near Paris (manuscript in preparation). The formulation, modifying radiation for RH>0.75 should only be used for low clouds. It has the advantage of being a more robust parameterization since it depends on a highly verified variable. In summary, our preference is: RH formulation for low clouds, and for liquid/ice water formulation (whenever available) for medium and high clouds, and cloud fractions otherwise.
The attenuation coefficient is calculated in the **src/diag/diagmet.f90** diagnostic interface model. It is read in **src/initio/iniphys.f90**, photolysis rates are calculated in routine **src/model/photorates.f90** every coarse time step.

10.4.2 Wet scavenging

10.4.2.1 In cloud scavenging

In cloud, particle scavenging is difficult to model. Particles can be scavenged either by coagulation with cloud droplets or by precipitating drops. Particles also act as cloud condensation nuclei to form new droplets. This latter process of nucleation is the most efficient one in clouds. According to [Tsyro, 2002] and [Guelle et al., 1998], the deposition flux is written as:

$$\left[\frac{dQ_l^k}{dt}_{incl} = \frac{\zeta_1 p_r}{w_1 h} Q_l^k\right] \tag{10.16}$$

with p_r is the precipitation rate released in the grid cell (g cm^{-2} s^{-1}), w$_l$ the liquid water content (g cm^{-3}), h the grid height (cm) and ζ an empirical uptake coefficient (in the range 0-1) depending on particle composition.

10.4.2.2 Sub-cloud scavenging

Particles are scavenged by raining drops, the deposition flux of particles being given by:

$$\left[\frac{dQ_l^k}{dt}_{subcl} = -\frac{apE_1}{u_g} Q_l^k\right] \tag{10.17}$$

with a is an empirical coefficient, p the precipitation rate in the grid cell (g cm^{-2} s^{-1}), E a collision efficiency coefficient between particles and raining drops ([Slinn, 1983] and u$_g$ the falling drop velocity (cm s^{-1}). Assuming a constant drop diameter (2 mm), this parameterization is an approximation of equations described in [Seinfeld and Pandis, 1998] and [Jung et al., 2002]. In the next developments, this equation will be improved.

10.5 Radiative transfers and photochemical reaction rates

10.5.1 Processes taken into account

Up to version 2013b, CHIMERE worked exclusively with tabulated photochemical reaction rates, precalculated using the TUV model, and using a simple parameterization for attenuation by clouds. The photolysis rates were therefore assumed constant on the vertical, and depended only on the zenithal angle and on the presence of clouds, which were assumed to be over model top. These assumptions were justified by the fact that CHIMERE was historically a boundary-layer model.
Since version 2014a, CHIMERE can take into account the following effects on photolysis:

- Effect of ice- and liquid-water clouds on photolysis rates through Mie diffusion
- Effect of aerosols on photolysis rates through absorption and Mie diffusion
- Effect of absorption by ozone on photolysis rates, using real-time ozone concentrations within the model domain instead of climatologies

This has been obtained by including the Fast-JX model for radiative transfer (version 7.0b, see [Wild et al., 2000, Bian et al., 2002]) inside CHIMERE. This model is a model for radiative transfer and photochemical rates that has been designed with the purpose of its inclusions in CTMLs, and is already used in models such as Polair3D, Geos-Chem, UKCA and PHOTOMCAT (e.g. [Voulgarakis et al., 2009, Real and Sartelet, 2011, Telford et al., 2013]). The photolysis rates calculated by fast-JX have been validated in the boundary layer ([Barnars et al., 2004]) as well as in the free troposphere ([Voulgarakis et al., 2009]). Fast-JX is designed to reduce as much as possible the computational cost as much as possible without inducing errors of more than 5% on photochemical reaction rates. Actually, in CHIMERE, the additional computation cost compared to the former formulation with tabulated rates is below 10% of the total computation cost.

From a computaional point of view, the calculation of photochemical reaction rates is performed in three steps (Fig. 10.2):

1. Preprocessing of aerosol optical properties (Mie scattering and absorption) for each aerosol species and bin, generate input files for Fast-JX: necessary only when changing aerosol species or their optical properties
2. Initialisation of Fast-JX model (read input files): at the beginning of each run
3. Online calculation of photochemical reaction rates (every physical time step)

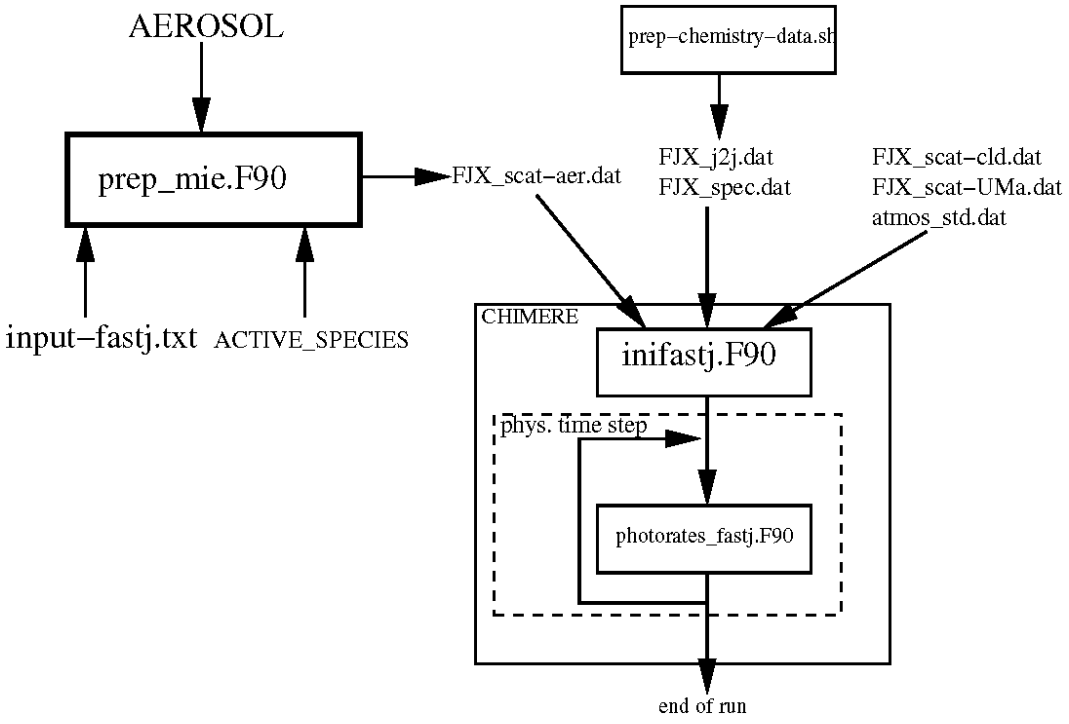


Figure 10.2: *Routines, files and scripts involved in the calculation of radiative transfers*

10.5.2 Optical preprocessing using prep_mie

The Mie calculations for each aerosol species and bins is performed by a short standalone program named prep_mie.F90 (in the src/prep directory). This program is called by chimere-step1.sh and runs in the temporary execution directory. The name of its input and output files is stored in the prep_mie.nml file, in the same directory. prep_mie.F90 needs three input files :

1. AEROSOL : number of bins, their diameters and the list of the AEROSOL species,
2. input-fastj.txt : optical properties of each aerosol species (real and imaginary part of the refraction indices for 5 wavelength - 200 nm, 300 nm, 400 nm, 600 nm and 999 nm), as well as the density and Hanel size growth coefficient. This file needs to include these quantities for ALL aerosol species listed in the AEROSOL file. If the user adds a new aerosol specie, he will need to put its optical and physical properties in the input-fastj.txt file by editing it manually. Species in input-fastj.txt do not need to be in the same order as in the AEROSOL file, but it is requested that all aerosol species listed in the AEROSOL file shall be present in the input-fastj.txt file, with exactly the same name.
3. ACTIVE_SPECIES : list of the active species. This file is used only to check whether prep_mie writes its outputs with all the aerosol species in the right order.

It is worth noting that Fast-JX (as well as CHIMERE) treats distinct bins of a given aerosol species as distinct species. Therefore, prep_mie will perform the Mie calculations for $nbins \times naerospec$ species. The output file of prep_mie is stored in FJX_scat-aer.dat. This file includes, for each of the $nbins \times naerospec$ species, the effective radius, density, the efficiency factor Q, the single-scattering albedo and the first 7 terms of the Taylor expansion of the scattering phase function. These values are written in the exact same order as the order of the aerosol species in the ACTIVE_SPECIES file.
The Mie calculation is based on Michael Mischenko's spher.f code (which is distributed with CHIMERE as well). As it is a relatively long calculation (up to a couple of minutes depending on the computer and on the number of aerosol species and bins), it is performed only if the FJX_scat-aer.dat is absent in the inputdata directory. Therefore, if the user modifies the optical or physical properties of the aerosols in input-fastj.txt, he will need to remove the FJX_scat-aer.dat file from the inputdata directory in order to force recalculation of the scattering phase functions.

10.5.3 Fast-JX initialisation

Fast-JX initialisation is performed by the inifastj.F90 routine. This routine is a wrapper for the INIT_FJX routine of the module fjx_init_mod.f90. INIT_FJX reads the following input files :

1. FJX_spec.dat : cross-sections for photochemical reaction rates.
2. FJX_scat-cld.dat : cloud scattering data
3. FJX_scat-UMa.dat : University of Michigan aerosol scattering data (not used)
4. atmos_std.dat : temperature and ozone climatology - used for radiative transfers above the simulation domain
5. FJX_j2j.dat : file containing the information needed to reorder Fast-JX photochemical reaction rates in the order needed by the CTM - in this case, CHIMERE.

The values read from these input files are stored in arrays that are used for the online calculation of photochemical reaction rates at each physical time step.

10.5.4 Online calculation of photochemical reaction rates

The calculation of the photochemical reaction rates is performed by routinne photorates_fastj.F90, which calls the fast-jx PHOTO_JX routine (in fjx_sub_mod.f90) for each atmospheric column, after filling the input arrays of Fast-JX with the values from the meteorological model (for clouds) and from CHIMERE (for ozone and aerosols). photorates_fastj.F90 finally takes into account the clouds above model top by a simple calculation of the attenuation factor - whereas clouds within the CHIMERE domain are taken into account in details, separating water- and ice-clouds and performing an explicit Mie calculation.

10.5.5 Using the old photorates ?

In CHIMERE versions 2014, it is still possible to use the tabulated photolytic rates from TUV, just as in previous version. To use this option, the switch *ifastj* in chimere.par needs to be set to 0. However, this option will become deprecated in the next distributed version of CHIMERE, and we strongly encourage all users to use the new scheme for radiative transfers.

Bibliography

[Alfaro et al., 1997] Alfaro, S. C., Gaudichet, A., Gomes, L., and Maillé, M. (1997). Modeling the size distribution of a soil aerosol produced by sandblasting. *J. Geophys. Res.*, 102:11,239–11,249.

[Alfaro et al., 1998] Alfaro, S. C., Gaudichet, A., Gomes, L., and Maillé, M. (1998). Mineral aerosol production by wind erosion: aerosol particle sizes and binding energies. *Geophys. Res. Lett*, 25:991–994.

[Alfaro and Gomes, 2001] Alfaro, S. C. and Gomes, L. (2001). Modeling mineral aerosol production by wind erosion: Emission intensities and aerosol size distribution in source areas. *J. Geophys. Res.*, 106:18,075–18,084.

[Anav et al., 2011] Anav, A., Menut, L., Khvorostiyanov, D., and Viovy, N. (2011). Impact of tropospheric ozone on the Euro-Mediterranean vegetation. *Global Change Biology*, 17.

[Andreae and Crutzen, 1997] Andreae, M. and Crutzen, P. (1997). Atmospheric aerosols: biogeochemical sources and role in atmospheric chemistry. *Science*, 276:1052–1058.

[Atkinson et al., 1997] Atkinson, R., Baulsch, D. L., Cox, R. A., Hampton, R. F., Kerr, J. A., Rossi, M. J., and Troe, J. (1997). Evaluated kinetics, photochemical and heterogeneous data. *J. Phys. Chem.*, 26(3):521–1012.

[Aumont et al., 2003] Aumont, B., Chervier, F., and Laval, S. (2003). Contribution of HONO sources to the NOx/HOx/O3 chemistry in the polluted boundary layer. *Atmospheric Environment*, 37(4):487 – 498.

[Baer and Nester, 1992] Baer, M. and Nester, K. (1992). Parameterization of trace gas dry deposition velocities for a regional mesoscale diffusion model. *Ann. Geophys.*, 10:912–923.

[Balkanski et al., 2007] Balkanski, Y., Schulz, M., Claquin, T., and Guibert, S. (2007). Reevaluation of mineral aerosol radiative forcings suggests a better agreement with satellite and aeronet data. *Atmos Chem Phys*, 7:81–95.

[Barnars et al., 2004] Barnars, J. C., Chapman, E. G., Fast, J. D., Schmelzer, J. R., Slusser, J. R., and Shetter, R. E. (2004). An evaluation of the FAST-J photolysis algorithm for predicting nitrogen dioxide photolysis rates under clear and cloudy sky conditions. *Atmos. Environ*, 38:3393–3403.

[Bauer et al., 2004] Bauer, S., Balkanski, Y., Schulz, M., Hauglustaine, D. A., , and Dentener, F. (2004). Heterogeneous chemistry on mineral aerosol surfacesă: a global modelling study on the influence on tropospheric ozone chemistry and comparison to observations. *J Geophys Res*, 109:D02304.

[Berge, 1993] Berge, E. (1993). Coupling of wet scavenging of sulphur to clouds in a numerical weather prediction model. *Tellus*, 45B:1–22.

[Bessagnet et al., 2005] Bessagnet, B., Hodzic, A., Blanchard, O., Lattuati, M., Le Bihan, O., and Marfaing, H. (2005). Origin of particulate matter pollution episodes in wintertime over the Paris Basin. *Atmospheric Environment*, 39(33):6159–6174.

[Bessagnet et al., 2004] Bessagnet, B., Hodzic, A., Vautard, R., Beekmann, M., Cheinet, S., Honoré, C., Liousse, C., and Rouil, L. (2004). Aerosol modeling with CHIMERE: preliminary evaluation at the continental scale. *Atmospheric Environment*, 38:2803–2817.

[Bessagnet et al., 2008] Bessagnet, B., Menut, L., Aymoz, G., Chepfer, H., and Vautard, R. (2008). Modelling dust emissions and transport within Europe: the Ukraine March 2007 event. *Journal of Geophysical Research*, 113:D15202.

[Bian et al., 2002] Bian, H., , and Prather, M. (2002). Fast-J2: accurate simulation of stratospheric photolysis in global chemical models. *J. Atmos. Chem.*, 41:281–296.

[Bicheron et al., 2011] Bicheron, P., Amberg, V., Bourg, L., Petit, D., Huc, M., Miras, B., Brockmann, C., Hagolle, O., Delwart, S., Ranera, F., Leroy, M., and Arino, O. (2011). Geolocation assessment of meris globcover orthorectified products. *IEEE Transactions on geoscience and remote sensing*, 49(8):2972–2982.

[Bowman et al., 1997] Bowman, F. m., Odum, J. R., Seinfeld, J. H., and Pandis, S. N. (1997). Mathematical model for gas-particle parttioning of secondary organic aerosols. *Atmos. Environ.*, 31:3921–3931.

[Cakmur et al., 2004] Cakmur, R. V., Miller, R. L., and Torres, O. (2004). Incorporating the effect of small-scale circulations upon dust emission in an atmospheric general circulation model. *J. Geophys. Res.*, 109:D07201.

[Carter, 1990] Carter, W. P. L. (1990). A detail mechanism for the gas-phase atmospheric reactions of organic compounds. *Atmospheric Environment*, 24:481–518.

[Carter, 2010] Carter, W. P. L. (2010). Development of the SAPRC-07 chemical mechanism. *Atmospheric Environment*, 44(40):5324 – 5335.

[Cheinet and Teixeira, 2003] Cheinet, S. and Teixeira, J. (2003). A simple formulation for the eddy-diffusivity parameterization of cloud-topped boundary layers. *GEOPHYSICAL RESEARCH LETTERS*, 30(18).

[Colella and Woodward, 1984] Colella, P. and Woodward, P. R. (1984). The piecewise parabolic method (PPM) for gas-dynamical simulations. *Journal of Computational Physics*, 11:38–39.

[De Moore et al., 1994] De Moore, W. B., Sandetr, S. P., Golden, D. M., Hampton, R. F., Kurylo, M. J., Howard, C. J., Ravishankara, A. R., Kolb, C. E., and Molina, M. J. (1994). Chemical kinetics and photochimical data for use in stratospheric modelling evaluation. *JPL publication*, 94, 26, JPL, Pasadena, US.

[Derognat et al., 2003] Derognat, C., Beekmann, M., Baeumle, M., Martin, D., and Schmidt, H. (2003). Effect of biogenic volatile organic compound emissions on tropospheric chemistry during the atmospheric pollution over the paris area (esquif) campaign in the ile-de-france region. *JOURNAL OF GEOPHYSICAL RESEARCH-ATMOSPHERES*, 108(D17).

[Ebel et al., 1994] Ebel, A., Friedrich, R., and Rodhe, H. (1994). Tropospheric modelling and emission estimation: Generation of european emission data for episodes (genemis) project, eurotrac annual report 1993, part 5.

[Erisman et al., 1994] Erisman, J. W., van Pul, A., and Wyers, P. (1994). Parameterization of surface resistance for the quantification of atmospheric deposition of acidifying pollutants and ozone. *Atmospheric Environemnt*, 28:2595–2607.

[Fecan et al., 1999] Fecan, F., Marticorena, B., and Bergametti, G. (1999). Parameterization of the increase of aeolian erosion threshold wind friction velocity due to soil moisture for arid and semi-arid areas. *Annals of Geophysics*, 17.

[Folberth et al., 2006] Folberth, G. A., Hauglustaine, D. A., Lathière, J., and Brocheton, F. (2006). Interactive chemistry in the laboratoire de météorologie dynamique general circulation model: model description and impact analysis of biogenic hydrocarbons on tropospheric chemistry. *Atmos. Chem. Phys.*, 6:2273–2319.

[Gelbard and Seinfeld, 1980] Gelbard, F. and Seinfeld, J. H. (1980). Simulation of multicomponent aerosol dynamics. *Journal of colloid and Interface Science*, 78:485–501.

[Gelencser et al., 2002] Gelencser, A., Hoffer, A., Krivacsy, Z., Kiss, G., Molnar, A., and Meszaros, E. (2002). On the possible origin of humic matter in fine continental aerosol. *Journal of Geophysical Research*, 107.

[Ginoux et al., 2001] Ginoux, P., Chin, M., Tegen, I., Prospero, J. M., Holben, B., Dubovik, O., and Lin, S. J. (2001). Sources and distributions of dust aerosols simulated with the GOCART model. *Journal of Geophysical Research*, 106:20255–20273.

[Giorgi, 1986] Giorgi, F. (1986). A particle dry deposition scheme for use in tracer transport models'. *J. Geophys. Res.*, 91:9794–9806.

[Gomes et al., 2003] Gomes, L., Rajot, J. L., Alfaro, S. C., and Gaudichet, A. (2003). Validation of a dust production model from measurements performed in semi-arid agricultural areas of Spain and Niger. *Catena*, 52:257–271.

[Goossens, 2003] Goossens, D. (2003). Effect of soil crustingon the emission and transport of wind-eroded sediment: field measurements on loamy sandy soil. *Geomorphology*, in press.

[Griffin et al., 1999] Griffin, R. J., Cocker, E. R., Flagan, R. C., and Seinfeld, J. H. (1999). Organic aerosol formation from the oxidation of biogenic hydrocarbons. *Journal of Geophysical Research*, 104:3555–3567.

[Guelle et al., 1998] Guelle, W., Balkanski, Y. J., Dibb, J. E., Schulz, M., and Dulac, F. (1998). Wet deposition in a global size-dependent aerosol transport model. 2. Influence of the scavenging scheme on Pb vertical profiles, and deposition. *J. Geophys. Res.*, 103(D22):28875–28891.

[Guenther et al., 2006] Guenther, A., Karl, T., Harley, P., Wiedinmyer, C., Palmer, P., and Geron, C. (2006). Estimates of global terrestrial isoprene emissions using MEGAN (Model of Emissions of Gases and Aerosols from Nature). *Atmos. Chem. Phys.*, 6:3181–3210.

[Hall et al., 1999] Hall, S., Khudaish, E., and Hart, A. (1999). Electrochemical oxidation of hydrogen peroxide at platinum electrodes. part iii: Effect of temperature. electrochim. *Electrochim. Acta*, 44:2455–2462.

[Hansen and Reed, 2000] Hansen, M. C. and Reed, B. (2000). A comparison of the IGBP DISCover and University of Maryland 1 km global land cover products. *International Journal of Remote Sensing*, 21:1365–1373.

[Harrison and Kito, 1990] Harrison, R. and Kito, A. (1990). Field intercomparison of filter pack and denuder sampling methods for reactive gaseous and particulate pollutants. *Atmos. Environ.*, 24:2633–2640.

[Hauglustaine et al., 2014] Hauglustaine, D. A., Balkanski, Y., and Schulz, M. (2014). A global model simulation of present and future nitrate aerosols and their direct radiative forcing of climate. *Atmos Chem Phys*, 14:6863–6949.

[Hauglustaine et al., 2004] Hauglustaine, D. A., Hourdin, F., Jourdain, L., Filiberti, M.-A., Walters, S., Lamarque, J.-F., and Holland, E. A. (2004). Interactive chemistry in the Laboratoire de Meteorologie Dynamique general circulation model: Description and background tropospheric chemistry evaluation. *Journal of Geophysical Research*, 109(D04314). doi:10.1029/2003JD003,957.

[Hicks et al., 1987] Hicks, B. B., Baldocchi, D. D., Meyers, T. P., Hosker Jr., R. P., and Matt, D. R. (1987). A preliminary multiple resistance routine for deriving dry deposition velocities from measured quantities. *Water, Air, Soil Pollut.*, 36.

[Hodzic et al., 2006a] Hodzic, A., Bessagnet, B., and Vautard, R. (2006a). A model evaluation of coarse-mode nitrate heterogeneous formation on dust particles. *Atmos. Environ.*, 40:4158–4171.

[Hodzic et al., 2010a] Hodzic, A., Jimenez, J., Madronich, S., Canagaratna, M., DeCarlo, P., Kleinman, L., and Fast, J. (2010a). Modeling organic aerosols in a megacity: potential contribution of semi-volatile and intermediate volatility primary organic compounds to secondary organic aerosol formation. *Atmos. Chem. Phys.*, 10.

[Hodzic et al., 2010b] Hodzic, A., Jimenez, J., Prevot, A., Szidat, S., Fast, J., and Madronich, S. (2010b). Can 3D Models Explain the Observed Fractions of Fossil and non-Fossil Carbon In and Near Mexico City? *Atmos. Chem. Phys.*, 10.

[Hodzic et al., 2009] Hodzic, A., Jimenez, J. L., Madronich, S., Aiken, A. C., Bessagnet, B., Curci, G., Fast, J., Lamarque, J.-F., Onasch, T. B., Roux, G., Schauer, J. J., Stone, E. A., and Ulbrich, I. M. (2009). Modeling organic aerosols during milagro: importance of biogenic secondary organic aerosols. *Atmospheric Chemistry and Physics*, 9(18):6949–6981.

[Hodzic et al., 2005] Hodzic, A., Vautard, R., Bessagnet, B., Lattuati, M., and Moreto, F. (2005). Long-term urban aerosol simulation versus routine particulate matter observations. *Atmospheric Environemnt*, 39:5851–5864.

[Hodzic et al., 2006b] Hodzic, A., Vautard, R., Chazette, P., Menut, L., and B.Bessagnet (2006b). Aerosol chemical and optical proprties over the Paris area within ESQUIF project. *Atmospheric Chemistry and Physics*, 6:3257–3280.

[Hoffmann and Calvert, 1985] Hoffmann, M. R. and Calvert, J. G. (1985). Chemical transformation modules for eulerian acid deposition models,. EPA/600/3-85/017.

[Honoré et al., 2008] Honoré, C., Rouïl, L., Vautard, R., Beekmann, M., Bessagnet, B., Dufour, A., Elichegaray, C., Flaud, J., Malherbe, L., Meleux, F., Menut, L., Martin, D., Peuch, A., Peuch, V., and Poisson, N. (2008). Predictability of European air quality: The assessment of three years of operational forecasts and analyses by the PREV'AIR system. *Journal of Geophysical Research*, 113:D04301.

[Honoré and Vautard, 2000] Honoré, C. and Vautard, R. (2000). Photochemical regimes in urban atmospheres: The influence of dispersion. *Geophys. Res. Letters*, 27:1895–1898.

[Horowitz, 2003] Horowitz, L. W., e. a. (2003). A global simulation of tropospheric ozone and related tracers: Description and evaluation of mozart, version 2. *J Geophys Res*, 108(D24):4784.

[Iversen and White, 1982] Iversen, J. D. and White, B. R. (1982). Saltation threshold on earth, mars and venus. *Sedimentology*, 29:111–119.

[Jacob, 2000] Jacob, D. J. (2000). Heterogeneous chemistry and tropospheric ozone. *Atmospheric Environment*, 34(34):2131–2159.

[Jung et al., 2002] Jung, C., Kim, Y., and Lee, K. (2002). Analytic solution for polydispersed aerosol dynamics by a wet removal process. *Journal of Aerosol Science*, 33:753–767.

[Kaupp and Umlauf, 1992] Kaupp, H. and Umlauf, G. (1992). Atmospheric gas-particle partitioning of organic compounds: a comparison of sampling methods. *Atmospheric Environment*, 26A:2259–2267.

[Kavouras et al., 1998] Kavouras, I., Mihalopoulos, N., and Stephanou, E. (1998). Formation of atmospheric particles from organic acids produced by forests. *Nature*, 395:683–686.

[Kroll et al., 2006] Kroll, J. H., Ng, N. L., Murphy, S. M., Flagan, R. C., and Seinfeld, J. H. (2006). Secondary organic aerosol formation from isoprene photooxidation. *Environ. Sci. Technol.*, 40:1869–1877.

[Kulmala et al., 1998] Kulmala, M., A., L., and Pirjola, L. (1998). Parameterization for sulfuric acid / water nucleation rates. *J. Geophys. Res.*, 103(No D7):8301–8307.

[Kunit and Puxbaum, 1996] Kunit, M. and Puxbaum, H. (1996). Enzymatic determination of the cellulose content of atmospheric aerosols. *Atmospheric Environment*, 30:1233–1236.

[Lattuati, 1997] Lattuati, M. (1997). *Contribution à l'étude du bilan de l'ozone troposphérique à l'interface de l'Europe et de l'Atlantique Nord: modélisation lagrangienne et mesures en altitude*. Phd thesis, Université P.M.Curie, Paris, France.

[Lee and Schwartz, 1983] Lee, Y. N. and Schwartz, S. E. (1983). *Precipitation scavenging, dry deposition and resuspension, vol. 1.*, chapter Kinetics of oxidation of aqueous sulfur (IV) by nitrogen dioxide. Elsevier, New York.

[Loosmore, 2003] Loosmore, G. (2003). Evaluation and development of models for resuspension of aerosols at short times after deposition. *Atmospheric Environment*, 37:639–647.

[Loosmore and Cederwall, 2004] Loosmore, G. and Cederwall, R. (2004). Precipitation scavenging of atmospheric aerosols for emergency response applications: testing an updated model with new real-time data. *Atmos. Env.*, 38:993–1003.

[Louis et al., 1982] Louis, J., Tiedke, M., and Geleyn, J. (1982). A short history of the pbl parametrization at ecmwf. In *ECMWF Workshop on Planetary Boundary Layer parametrization*, pages 59–80, University of Reading.

[Madronich et al., 1998] Madronich, S., McKenzie, R. E., Bjorn, L. O., and Caldwell, M. M. (1998). Changes in biologically active ultraviolet radiation reaching the earth's surface. *J. Photochem. Photobiol. B:Biology*, 46:5–19.

[Marticorena and Bergametti, 1995] Marticorena, B. and Bergametti, G. (1995). Modeling the atmospheric dust cycle: 1 Design of a soil derived dust production scheme. *J. Geophys. Res.*, 100:16415–16430.

[McRae et al., 1982] McRae, G., Goodin, W., and Seinfeld, J. (1982). Development of a second generation mathematical model for urban air pollution: I. model formulation. *Atmospheric Environment*, 16:679–696.

[Menut, 2008] Menut, L. (2008). Sensitivity of hourly saharan dust emissions to NCEP and ECMWF modelled wind speed. *Journal of Geophysical Research, Atmospheres*, 113:D16201.

[Menut et al., 2007] Menut, L., G.Foret, and G.Bergametti (2007). Sensitivity of mineral dust concentrations to the model size distribution accuracy. *Journal of Geophysical Research, Atmospheres*, 112:D10210.

[Menut et al., 2013] Menut, L., Perez Garcia-Pando, C., Haustein, K., Bessagnet, B., Prigent, C., and Alfaro, S. (2013). Relative impact of roughness and soil texture on mineral dust emission fluxes modeling. *Journal of Geophysical Research*, 118:6505–6520.

[Menut et al., 2005] Menut, L., Schmechtig, C., and Marticorena, B. (2005). Sensitivity of the sandblasting fluxes calculations to the soil size distribution accuracy. *Journal of Atmospheric and Oceanic Technology*, 22, No. 12:1875–1884.

[Menut et al., 2000a] Menut, L., Vautard, R., Beekmann, M., and Honoré, C. (2000a). Sensitivity of Photochemical Pollution using the Adjoint of a Simplified Chemistry-Transport Model. *J. Geophys. Res.*, 105(D12):15379–15402.

[Menut et al., 2000b] Menut, L., Vautard, R., Flamant, C., Abonnel, C., Beekmann, M., Chazette, P., Flamant, P., Gombert, D., Guédalia, D., Lefebvre, M., Lossec, B., D., M., Mégie, G., Perros, P., Sicard, M., and Toupance, G. (2000b). Measurements and modelling of atmospheric pollution over the Paris area: an overview of the ESQUIF Project. *Annales Geophysicae*, 18(11):1467–1481.

[Middleton et al., 1990] Middleton, P., Stockwell, W. R., and Carter, W. P. (1990). Agregation and analysis of volatile organic compound emissions for regional modelling. *Atmospheric Environment*, 24:1107–1133.

[Mircea and Stefan, 1998] Mircea, M. and Stefan, S. (1998). A theoretical study of the microphysical parameterization of the scavenging coefficient as a function of precipitation type and rate. *Atmos. Env.*, 32:2931–2938.

[Monahan, 1986] Monahan, E. C. (1986). *In The Role of Air-Sea Exchange in Geochemical Cycling*, chapter The ocean as a source of atmospheric particles, pages 129–163. Kluwer Academic Publishers, Dordrecht, Holland.

[Nenes et al., 1998] Nenes, A., Pilinis, C., and Pandis, S. (1998). ISORROPIA: A new thermodynamic model for inorganic multicomponent atmospheric aerosols. *Aquatic Geochem.*, 4:123–152.

[Odum et al., 1997] Odum, J. R., Jungkamp, T. P. W., Griffin, R. J., Forster, H. J. L., Flagan, R. C., and Seinfeld, J. H. (1997). Aromatics, reformulated gasoline and atmospheric organic aerosol formation. *Environ. Sci. Technol.*, 31:1890–1897.

[Pankow, 1994] Pankow, J. F. (1994). An absorption model of gas/aerosol partition involved in the formation of secondary organic aerosol. *Atmos. Environ.*, 28:189–193.

[Passant, 2002] Passant, N. (2002). Speciation of uk emissions of nmvoc. (AEAT/ENV/R/0545).

[Pavia and O'Brien, 1986] Pavia, E. and O'Brien, J. (1986). Weibull statistics speed over the ocean. *Journal of Climate and Applied Meteorology*, 25:324–332.

[Peters and Eiden, 1992] Peters, K. and Eiden, R. (1992). Modelling the dry deposition velocity of aerosol particles to a spruce forest. *Atmospheric Environment*, 26A(14):2555–2564.

[Petroff, 2005] Petroff, A. (2005). *Mechanistic study of aerosol dry deposition on vegetated canopies.* PhD thesis, IRPHE, University of Marseille 2.

[Priestley, 1949] Priestley, C. (1949). Heat transport and zonal stress between latitudes. *Quaterly Journal of the Royal Meteorology*, 75:28–40.

[Pryor et al., 2005] Pryor, S., Schoof, J., and Barthelmie, R. (2005). Empirical downscaling of wind speed probability distributions. *J. Geophys. Res.*, 110:D19109.

[Pun et al., 2006] Pun, B. K., Seigneur, C., and Lohman, K. (2006). Modeling secondary organic aerosol formation via multiphase partitioning with molecular data. *Environ. Sci. Technol.*, 40:4722–4731.

[Putaud et al., 2004] Putaud, J.-P., Raes, F., Van Dingenen, R., Bruggemann, E., Facchini, M.-C., Decesari, S., Fuzzi, S., Gehrig, R., Huglin, C., Laj, P., Lorbeer, G., Maenhaut, W., Mihalopoulos, N., Muller, K., Querol, X., Rodriguez, S., Schneider, J., Spindler, G., ten Brink, H., Torseth, K., and Wiedensohler, A. (2004). A european aerosol phenomenology-2: chemical characteristics of particulate matter at kerbside, urban, rural and background sites in europe. *Atmospheric Environment*, 38:2579–2595.

[R. Kurtenbach, 2001] R. Kurtenbach, K.H. Becker, J. G. J. K. J. L. M. S. P. W. R. A. A. G. U. P. (2001). Investigations of emissions and heterogeneous formation of HONO in a road traffic tunnel. *Atmospheric Environment*, 35(20):9506 – 9517. 3385Ð3394.

[Real and Sartelet, 2011] Real, E. and Sartelet, K. (2011). Modeling of photolysis rates over europe: impact on chemical gaseous species and aerosols. *Atmos. Chem. Phys*, 11:1711–1727.

[Reeks and Hall, 2001] Reeks, M. and Hall, D. (2001). Kinetic models for particle resuspension in turbulent flows: theory and measurement. *Journal of Aerosol Science*, 32:1–31.

[Rouïl et al., 2009] Rouïl, L., Honoré, C., Vautard, R., Beekmann, M., Bessagnet, B., Malherbe, L., Meleux, F., Dufour, A., Elichegaray, C., Flaud, J., Menut, L., Martin, D., Peuch, A., Peuch, V., and Poisson, N. (2009). PREV'AIR : an operational forecasting and mapping system for air quality in Europe. *BAMS*, 90:73–83.

[Sander et al., 1999] Sander, G.C. and. Parlange, J.-Y., Smith, R.E.and Haverkamp, R., and Hogarth, W. (1999). Estimation of ponding time for constant surface flux. *Hydrology days Ed. AGU Pub. 19, San Francisco*, pages 402–410.

[Schaap et al., 2007] Schaap, M., Vautard, R., Bergstrom, R., van Loon, M., Bessagnet, B., Brandt, J., Christensen, H., Cuvelier, K., Foltescu, V., Graff, A., E., J. J., Kerschbaumer, A., Krol, M., Langner, J., Roberts, P., Rouil, L., Stern, R., Tarrason, L., Thunis, P., Vignati, E., White, L., Wind, P., and Builtjes, P. H. J. (2007). Evaluation of long-term aerosol simulations from seven air quality models and their ensemble in the eurodelta study. *Atmospheric Environemnt*, 41:2083–2097.

[Schmidt et al., 2001] Schmidt, H., Derognat, C., Vautard, R., and Beekmann, M. (2001). A comparison of simulated and observed ozone mixing ratios for the summer of 1998 in western Europe. *Atmospheric Environment*, 35:6277–6297.

[Schulz et al., 2006] Schulz, M., Textor, C., Kinne, S., Balkanski, Y., Bauer, S., Berntsen, T., Berglen, T., Boucher, O., Dentener, F., Guibert, S., Isaksen, I. S. A., Iversen, T., Koch, D., Kirkevag, A., Liu, X., Montanaro, V., Myhre, G., Penner, J. E., Pitari, G., Reddy, S., Seland, O., Stier, P., and Takemura, T. (2006). Radiative forcing by aerosols as derived from the aerocom present-day and pre-industrial simulations. *Atmos Chem Phys*, 6:5225–5246.

[Seinfeld and Pandis, 1998] Seinfeld, J. H. and Pandis, S. N. (1998). *Atmospheric Chemistry and Physics*. Wiley and sons.

[Shao and Lu, 2000] Shao, Y. and Lu, I. (2000). A simple expression for wind erosion threshold friction velocity. *J. Geophys. Res.*, 105:22,437–22,443.

[Simoneit and Mazurek, 1982] Simoneit, B. and Mazurek, M. (1982). Organic matter of the troposphere, ii natural background of biogenic lipid matter in aerosols over the rural western united states. *Atmospheric Environment*, 16:2139–2159.

[Simpson, 1992] Simpson, D. (1992). Long period modeling of photochemical oxidants in Europe, Calculations for July 1985. *Atmos. Environ.*, 26:1609–1634.

[Slinn, 1983] Slinn, W. (1983). Precipitation scavenging. division of biomedical environmental research, us department of energy, washington, dc. *Atmospheric Sciences and Power Production 1979*.

[Solazzo et al., 2012] Solazzo, E., Bianconi, R., Vautard, R., Appel, K. W., Moran, M. D., Hogrefe, C., Bessagnet, B., Brandt, J., Christensen, J. H., Chemel, C., Coll, I., van der Gon, H. D., Ferreira, J., Forkel, R., Francis, X. V., Grell, G., Grossi, P., Hansen, A. B., Jericevic, A., Kraljevic, L., Miranda, A. I., Nopmongcol, U., Pirovano, G., Prank, M., Riccio, A., Sartelet, K. N., Schaap, M., Silver, J. D., Sokhi, R. S., Vira, J., Werhahn, J., Wolke, R., Yarwood, G., Zhang, J., Rao, S., and Galmarini, S. (2012). Model evaluation and ensemble modelling of surface-level ozone in Europe and North America in the context of AQMEII. *Atmospheric Environment*, 53:60–74.

[Telford et al., 2013] Telford, P. J., Abraham, N. L., Archibald, A. T., Braesicke, P., Dalvi, M., Morgenstern, O., OĆonnor, F. M., Richards, N. A. D., and Pyle, J. A. (2013). Implementation of the Fast-JX photolysis scheme (v6.4) into the UKCA component of the MetUM chemistry-climate model (v7.3). *Geosci. Model Dev.*, 6:161–177.

[Tiedtke, 1989] Tiedtke, M. (1989). A comprehensive mass flux scheme for cumulus parameterization in large-scale models. *Monthly Weather Reviews*, 117:1779–1800.

[Troen and Mahrt, 1986] Troen, I. and Mahrt, L. (1986). A simple model of the atmospheric boundary layer: Sensitivity to surface evaporation. *Boundary-Layer Meteorology*, 37:129–148.

[Tsyro, 2002] Tsyro, S. (2002). First estimates of the effect of aerosol dynamics in the calculation of PM10 and PM2.5. *EMEP report*, 4/02(MSC-W):Norwegian Meteorological Institute, Oslo.

[V. Vestreng, 2005] V. Vestreng, K. Breivik, M. A. A. W. J. G. O. R. J. O. (2005). Inventory Review 2005 - Emission Data reported to CLRTAP and under the NEC Directive - Initial review for HMs and POPs . *EMEP Status report, Norwegian Meteorological Institute, Oslo*.

[Valari and Menut, 2010] Valari, M. and Menut, L. (2010). Transferring the heterogeneity of surface emissions to variability in pollutant concentrations over urban areas through a chemistry transport model. *Atmos Environ*, 44:3229–3238.

[Van Loon et al., 2007] Van Loon, M., Vautard, R., Schaap, M., Bergstrom, R., Bessagnet, B., Brandt, J., Builtjes, P., Christensen, J. H., Cuvelier, K., Graf, A., Jonson, J., Krol, M., Langner, J., Roberts, P., Rouil, L., Stern, R., Tarrason, L., Thunis, P., Vignati, E., White, L., and Wind, P. (2007). Evaluation of long-term ozone simulations from seven regional air quality models and their ensemble average. *Atmospheric Environment*, 41:2083–2097.

[Vautard et al., 2000] Vautard, R., Beekmann, M., and Menut, L. (2000). Applications of adjoint modelling in atmospheric chemistry: sensitivity and inverse modelling. *Environmental Modelling and Software*, 15:703–709.

[Vautard et al., 2001] Vautard, R., Beekmann, M., Roux, J., and Gombert, D. (2001). Validation of a hybrid forecasting system for the ozone concentrations over the Paris area. *Atmos. Environ.*, 35:2449–2461.

[Vautard et al., 2005a] Vautard, R., Bessagnet, B., Chin, M., and Menut, L. (2005a). On the contribution of natural aeolian sources to particulate matter concentrations in europe: testing hypotheses with a modelling approach. *Atm. Environ.*, 39:3291–3303.

[Vautard et al., 2007] Vautard, R., Builtjes, P. H. J., Thunis, P., Cuvelier, K., Bedogni, M., Bessagnet, B., Honoré, C., Moussiopoulos, N., G., P., Schaap, M., Stern, R., Tarrason, L., and Van Loon, M. (2007). Evaluation and intercomparison of Ozone and PM10 simulations by several chemistry-transport models over 4 european cities within the City-Delta project. *Atmospheric Environment*, 41:173–188.

[Vautard et al., 2005b] Vautard, R., Honoré, C., Beekmann, M., and Rouil, L. (2005b). Simulation of ozone during the August 2003 heat wave and emission control scenarios. *Atmospheric Environment*, 39(16):2957–2967.

[Verwer, 1994] Verwer, J. (1994). Gauss-Seidel iteration for stiff odes from chemical kinetics. *Journal on Scientific Computing*, 15:1243–1250.

[Voulgarakis et al., 2009] Voulgarakis, A., Savage, N. H., Wild, O., Carver, G. D., Clemitshaw, K. C., and Pyle, J. A. (2009). Upgrading photolysis in the PHOTOMCAT CTM: model evaluation and assessment of the role of clouds. *Geosci. Model Dev.*, 2:59–72.

[Warren, 1986] Warren, D. R. (1986). *Nucleation and growth of aerosols*. PhD thesis, Dissertation (Ph.D.), California Institute of Technology, Pasadena.

[Wesely, 1989] Wesely, M. (1989). Parameterization of Surface Resistances to Gaseous Dry Deposition in Regional-Scale Numerical Models. *Atmospheric Environment*, 23(23):1293–1304.

[White, 1986] White, B. R. (1986). Encyclopedia of fluid mechanics. *Gulf Publishing, Houston, TX, USA*, pages 239–282.

[Wild et al., 2000] Wild, O., Zhu, X., and Prather, J. (2000). Fast-J: accurate simulation of the in- and below-cloud photolysis in tropospheric chemical models. *J. Atmos. Chem.*, 37:245–282.

[Xuan, 2004] Xuan, J. (2004). Turbulence factors for threshold velocity and emission rate of atmospheric mineral dust. *Atmospheric Environment*, 38:1777–1783.

[Zender et al., 2003] Zender, C., Bian, H., and Newman, D. (2003). Mineral dust entrainment and deposition (dead) model. description and 1990s dust climatology. *Journal of Geophysical Research*, 108:4416.

[Zhang et al., 2001] Zhang, L., Gong, S., Padro, J., and Barrie, L. (2001). A size-segregated particle dry deposition scheme for an atmospheric aerosol module. *Atmospheric Environment*, 35(3):549–560.

[Zhang et al., 2007] Zhang, Y., Huang, J.-P., Henze, D. K., and Seinfeld, J. H. (2007). Role of isoprene in secondary organic aerosol formation on a regional scale. *Journal of Geophysical Research Atmospheres*, 112(D20).

[Zyryanov et al., 2012] Zyryanov, D., Foret, G., Eremenko, M., Beekmann, M., Cammas, J.-P., M.D'Isidoro, Elbern, H., Flemming, J., Friese, E., Kioutsioutkis, I., Maurizi, A., D.Melas, Meleux, F., Menut, L., Moinat, P., Peuch, V.-H., Poupkou, A., Razinger, M., Schultz, M., Stein, O., Suttie, A. M., Valdebenito, A., Zerefos, C., Dufour, G., Bergametti, G., and Flaud, J.-M. (2012). 3D evaluation of tropospheric ozone simulations by an ensemble of regional Chemistry Transport Model. *Atmos Chem Phys*, 12:3219–3240.

Appendix A

References using CHIMERE

A.1 Reference papers

For CHIMERE description overview: see [Menut et al., 2013, GMD]
http://www.geosci-model-dev.net/6/981/2013/gmd-6-981-2013.html

- Menut L, B.Bessagnet, D.Khvorostyanov, M.Beekmann, N.Blond, A.Colette, I.Coll, G.Curci, G.Foret, A.Hodzic, S.Mailler, F.Meleux, J.L.Monge, I.Pison, G.Siour, S.Turquety, M.Valari, R.Vautard and M.G.Vivanco, 2013, CHIMERE 2013: a model for regional atmospheric composition modelling, Geoscientific Model Development, 6, 981-1028, doi:10.5194/gmd-6-981-2013

For CHIMERE used in real-time forecast: see [Rouil et al, 2009] or [Menut and Bessagnet, 2010]

- Rouil L., C.Honore, R.Vautard, M.Beekmann, B.Bessagnet, L.Malherbe, F.Meleux, A.Dufour, C.Elichegaray, J-M.Flaud, L.Menut, D.Martin, A.Peuch, V-H.Peuch, N.Poisson, 2009, PREV'AIR : an operational forecasting and mapping system for air quality in Europe, BAMS, DOI: 10.1175/2008BAMS2390.1
- Menut L. and B.Bessagnet, 2010, Atmospheric composition forecasting in Europe , Annales Geophysicae, 28, 61-74

For CHIMERE used for health impacts: see [Valari et al., 2010]

- Valari M. and L.Menut, 2010, Transferring the heterogeneity of surface emissions to variability in pollutant concentrations over urban areas through a chemistry transport model, Atmospheric Environment, Volume 44, Issue 27, Pages 3229-3238

For CHIMERE used for fires emissions: see [Turquety et al., 2014, GMD]

- Turquety S., L.Menut, B.Bessagnet, A.Anav, N.Viovy, F.Maignan and M.Wooster, 2014, APIFLAME v1.0: High resolution fire emission model and application to the Euro-Mediterranean region, Geosci. Model. Dev., in press

For CHIMERE used for dust: see [Menut et al., 2013, JGR]

- Menut L., C.Perez Garcia-Pando, K.Haustein, B.Bessagnet, C.Prigent and S.Alfaro, 2013, Relative impact of roughness and soil texture on mineral dust emission fluxes modeling, Journal of Geophysical Research Atmospheres, 118, 6505-6520, doi:10.1002/jgrd.50313

A.2 List of papers

1. Cuesta J., M. Eremenko, X. Liu, G. Dufour, Z. Cai, M. Hopfner, T. von Clarmann, P. Sellitto, G. Foret, B. Gaubert, M. Beekmann, J. Orphal, K. Chance, R. Spurr, and J.-M. Flaud, 2013, Satellite observation

of lowermost tropospheric ozone by multispectral synergism of IASI thermal infrared and GOME-2 ultraviolet measurements over Europe, Atmos. Chem. Phys., 13, 9675-9693, 2013

2. Boichu M., L. Menut, D. Khvorostyanov, L. Clarisse, C. Clerbaux, S. Turquety, and P.-F. Coheur, 2013, Inverting for volcanic SO2 flux at high temporal resolution using spaceborne plume imagery and chemistry-transport modelling: the 2010 Eyjafjallajokull eruption case-study, Atmos. Chem. Phys., 13, 6553-6588, 13, 8569-8584, doi:10.5194/acp-13-8569-2013
3. Broquet, G., Chevallier, F., Breon, F.-M., Kadygrov, N., Alemanno, M., Apadula, F., Hammer, S., Haszpra, L., Meinhardt, F., Morgui, J. A., Necki, J., Piacentino, S., Ramonet, M., Schmidt, M., Thompson, R. L., Vermeulen, A. T., Yver, C., and Ciais, P.: Regional inversion of CO2 ecosystem fluxes from atmospheric measurements: reliability of the uncertainty estimates, Atmos. Chem. Phys., 13, 9039-9056, doi:10.5194/acp-13-9039-2013, 2013. on-line paper
4. Colette A., B.Bessagnet, R.Vautard, S.Szopa, S.Rao, S.Schucht, Z.Klimont, L.Menut, G.Clain, F.Meleux, L.Rouil, 2013, European atmosphere in 2050, a regional air quality and climate perspective under CMIP5 scenarios, Atmos. Chem. Phys., 13, 7451-7471
5. Dall'Osto, M., X. Querol, A. Alastuey, M.C. Minguillon, M. Alier, F. Amato, M. Brines, M. Cusack, J.O. Grimalt, A. Karanasiou, T. Moreno, M. Pandolfi, J. Pey, C. Reche, A. Ripoll, R. Tauler, B.L. Van Drooge, M. Viana, R.M. Harrison, J. Giet, D. Beddows, W. Bloss, C. O'Dowd, D. Ceburnis, G. Martucci, N.L. Ng, D. Worsnop, J. Wenger, E. Mc Gillicuddy, J. Sodeau, R. Healy, F. Lucarelli, S. Nava, J.L. Jimenez, F. Gomez-Moreno, B. Artinano, A.S.H. Prevot, L. Pfaffenberger, S. Frey, F. Wilsenack, D. Casabona, P. Jimenez-Guerrero, D. Gross, N. Cots, 2013. Presenting SAPUSS: Solving Aerosol Problem by Using Synergistic Strategies in Barcelona, Spain. Atmos. Chem. Phys. 13, 8991-9019, doi:10.5194/acp-13-8991-2013.
6. Jerez, S., P. Jimenez-Guerrero, J.P. Montavez, R.M. Trigo., 2013. Impact of the North Atlantic Oscillation on the variations of aerosol ground levels through local processes over Europe. Atmos. Chem. Phys. 13, doi:10.5194/acp-13-1-2013.
7. Jimenez-Guerrero, P., S. Jerez, J.P. Montavez, R. M. Trigo, 2013. Uncertainties in future ozone and PM10 projections over Europe from a regional climate multi-physics ensemble. Geophys. Res. Lett. 40, 1-6, , doi:10.1002/2013GL057403.
8. Jimenez-Guerrero, P., J.J. Gomez-Navarro, R. Baro, R. Lorente, N. Ratola, J.P. Montavez, 2013. Is there a common pattern of future gas-phase air pollution in Europe under diverse climate change scenarios? Clim. Change, DOI 10.1007/s10584-013-0944-8.
9. Menut L, B.Bessagnet, D.Khvorostyanov, M.Beekmann, N.Blond, A.Colette, I.Coll, G.Curci, G.Foret, A.Hodzic, S.Mailler, F.Meleux, J.L.Monge, I.Pison, G.Siour, S.Turquety, M.Valari, R.Vautard and M.G.Vivanco, 2013, CHIMERE 2013: a model for regional atmospheric composition modelling, Geoscientific Model Development, 6, 981-1028, doi:10.5194/gmd-6-981-2013, on-line paper
10. Mailler S., D.Khvorostyanov, and L.Menut, 2013, Impact of the vertical emission profiles on background gas-phase pollution simulated from the EMEP emissions over Europe, Atmos. Chem. Phys., 13, 5987-5998, doi:10.5194/acp-13-5987-2013
11. Siour G, A.Colette, L.Menut, B.Bessagnet, I.Coll, F.Meleux, 2013, Bridging the scales in an eulerian air quality model to assess megacity export of pollution, Env. Mod. Software, 46, 271-282
12. Menut L., C.Perez Garcia-Pando, K.Haustein, B.Bessagnet, C.Prigent and S.Alfaro, 2013, Relative impact of roughness and soil texture on mineral dust emission fluxes modeling, Journal of Geophysical Research Atmospheres, 118, 6505-6520, doi:10.1002/jgrd.50313
13. Menut L., B.Bessagnet, A.Colette and D.Khvorostyanov, 2013, On the impact of the vertical resolution on chemistry transport modelling, Atmospheric Environment, 67, 370-384
14. Zhang Q.J., M. Beekmann, F. Drewnick, F. Freutel, J. Schneider, M. Crippa, A. Prevot, U. Baltensperger, L. Poulain, A. Wiedensohler, J. Sciare, V. Gros, A. Borbon, A. Colomb, V. Michoud, J-F. Doussin, H.

A. C. Denier van dr Gon, M. Haeffelin, J.-C. Dupont, G. Siour, H. Petetin, B. Bessagnet, S.N. Pandis, A. Hodzic, O. Sanchez, C. Honore, and O. Perrussel, 2013, Formation of organic aerosol in the Paris region during the MEGAPOLI summer campaign: evaluation of the volatility-basis-set approach within the CHIMERE model, Atmos. Chem. Phys., 13, 5767-5790.

15. Anav A., L. Menut, D. Khvorostyanov, N. Viovy, Comparison of two canopy conductance parameterizations to quantify the interactions between surface ozone and vegetation over Europe, Journal of Geophysical Research - Biogeosciences, 117, G03027, 20 PP., doi:10.1029/2012JG001976
16. Coman, C, G.Foret, M.Beekmann, M.Eremenko, G.Dufour, B.Gaubert, A.Ung, C.Schmechtig, J.-M.Flaud, and G.Bergametti, Assimilation of IASI partial tropospheric columns with an Ensemble Kalman Filter over Europe, Atmos. Chem. Phys.,12,2513-2532,2012.
17. Delcloo A.W., Alex Deckmyn, Rafiq Hamdi, Herman Van Langenhove, Gilles Foret and Hugo De Backer, Coupling of the CTM CHIMERE to the High Resolution LAM ALADIN for Belgium, Air Pollution Modeling and its Application XXI, NATO Science tor Peace and Security Series C: Environmental Security, 2012, Volume 4, Part 2,315-319, DOl: 10.1007/978-94-007 -1359-8 54.
18. Drobinski P., Anav A., Lebeaupin Brossier C., Samson G., Stefanon M., Bastin S., Baklouti M., Beranger K., Beuvier J., Bourdalle-Badief R., Coquart L., D'Andrea F., de Noblet N., Diaze F., Dutay J.C., Ethe C., Foujols M.J., Khvorostiyanov D., Madec G., Maisonnave E., Mancip M., Masson S., Menut L., Palmieri J., Polcher J., Turquety S., Valcke S., Viovy N., Model of the Regional Coupled Earth system (MORCE): application to process and climate studies in vulnerable regions, Env. Mod. Software, 35, 1-18
19. Konovalov, I. B., M. Beekmann, B. D'anna, And C. George, Significant light induced ozone loss on biomass burning aerosol: evidence from chemistry-transport modeling based on new laboratory studies, Geophys. Res. Lett., doi:10.1029/2012GL052432, 2012 in press
20. Jimenez-Guerrero, P., J.P. Montavez, J.J. Gomez-Navarro, S. Jerez, R. Lorente-Plazas, 2012. Impacts of climate change on ground level gas-phase pollutants and aerosols in the Iberian Peninsula for the late XXI century. Atmos. Environ. 55, 483-495, doi:10.1016/j.atmosenv.2012.02.048.
21. Menut L., O.P.Tripathi, A.Colette, R.Vautard, E.Flaounas, B.Bessagnet, 2012, Evaluation of regional climate simulations for air quality modelling purposes, Climate Dynamics, in press, .
22. Menut L., A.Goussebaile, B.Bessagnet, D.Khvorostiyanov, A.Ung, 2012, Impact of realistic hourly emissions profiles on modelled air pollutants concentrations, Atmospheric Environment, pp. 233-244, doi:10.1016/j.atmosenv.2011.11.057
23. Schere, K., J. Flemming, R. Vautard, C. Chemel, A. Colette, C. Hogrefe, B. Bessagnet, F. Meleux, R. Mathur, S. Roselle, R.-M. Hu, R. S. Sokhi, S. T. Rao and S. Galmarini, 2011: Trace gas/aerosol boundary concentrations and their impacts on continental-scale AQMEII modeling domains. Atmospheric Environment, in press.
24. Solazzo, E., R. Bianconi, G. Pirovano, V. Matthias, R. Vautard, M. D. Moran, K. Wyat Appel, B. Bessagnet, J. Brandt, J. H. Christensen, C. Chemel, I. Coll, J. Ferreira, R. Forkel, X. V. Francis and 18 other authors, Operational model evaluation for particulate matter in Europe and North America in the context of AQMEII, Atm. Env., Vol 53, pp 75-92, 2012
25. Solazzo, E., R. Bianconi, R. Vautard, K. Wyat Appel, M. D. Moran, C. Hogrefe, B. Bessagnet, J. Brandt, J.H. Christensen, C. Chemel, I. Coll, H. Denier van der Gon, J. Ferreira, R. Forkel and 22 other authors, Model evaluation and ensemble modelling of surface-level ozone in Europe and North America in the context of AQMEII, Atm. Env., Vol 53, pp 60-74, 2012
26. Tuccella P., G.Curci, G.Visconti, B.Bessagnet, L.Menut and R.Park, 2012, Modelling of gas and aerosol with WRF/Chem over Europe: evaluation against one year of ground-based measurements, Journal of Geophysical Research Atmosphere, vol. 117, D03303, doi:10.1029/2011JD016302

27. Vautard, R., Moran, M. D., Solazzo, E., Gilliam, R. C., Matthias, V., Bianconi, R., Chemel, C., Ferreira, J., Geyer, B., Hansen, A. B., Jericevic, A., Prank, M., Segers, A., Silver, J. D., Werhahn, J., Wolke, R., Rao, S. T., and S. Galmarini, 2012, Evaluation of the meteorological forcing used for the Air Quality Model Evaluation InternationaI Initiative (AQMEII) air quality simulations. Atmos. Environ., doi:10.1016/j.atmosenv.2011.10.065.
28. Wilson R. C., Z. L. Fleming, P. S. Monks, G. Clain, S. Henne, I. B. Konovalov, S. Szopa, and L. Menut, 2012, Have primary emission reduction measures reduced ozone across Europe? An analysis of European rural background ozone trends 1996-2005, , ACP, 12, 437-454
29. Zyryanov D., G. Foret, M. Eremenko, M. Beekmann, J-P Cammas, M.D'Isidoro, H. Elbern, J. Flemming, E. Friese, I. Kioutsioutkis, A. Maurizi, D.Melas, F. Meleux, L. Menut, P. Moinat, V-H Peuch, A. Poupkou, M. Razinger, M. Schultz, O. Stein, A. M. Suttie, A. Valdebenito, C. Zerefos, G. Dufour, G. Bergametti and J-M. Flaud, 2012, 3D evaluation of tropospheric ozone simulations by an ensemble of regional Chemistry Transport Model, Atmospheric Chemistry and Physics, 12, 3219-3240
30. Hodzic, A. and Jimenez, J. L.: Modeling anthropogenically controlled secondary organic aerosols in a megacity: a simplified framework for global and climate models, Geosci. Model Dev., 4, 901-917, doi:10.5194/gmd-4-901-2011, 2011, article
31. Anav A., L.Menut, D.Khvorostiyanov and N.Viovy, Impact of tropospheric ozone on the Euro-Mediterranean vegetation, Global Change Biology, vol. 17, issue 6, DOI: 10.1111/j.1365-2486.2010.02387.x, .
32. Boynard, A., M. Beekmann, G. Foret, A. Ung, S. Szopa, C. Schmechtig, A. Coman, An ensemble assessment of regional ozone model uncertainty with an explicit error representation , Atmos. Env.,Volume 45, Issue 3, January 2011, Pages 784-793.
33. Borrego, C., Monteiro, A., Pay, M.T., Ribeiro, I., Miranda, A.I., Basart, S., Baldasano, J.M.. (2011). How bias-correction can improve air quality forecast over Portugal. Atmospheric Environment, 45, 37, 6629-6641. Broquet, G., F. Chevallier, P. Rayner, C. Aulagnier, I. Pison, M.Ramonet,M. Schmidt, A. T. Vermeulen, and P.
34. Ciais (2011), A European summertime CO2 biogenic flux inversion at mesoscale from continuous in situ mixing ratio measurements, J. Geophys. Res., 116, D23303, doi:10.1029/2011JD016202.
35. Carvalho, A., Monteiro, A., Flannigan, M., Solman, S., Miranda, A.I., Borrego, C. (2011). Forest fires in a changing climate and their impacts on air quality. Atmospheric Environment 45, 5545-5553.
36. Colette A., O.Favez, F.Meleux, L.Chiappini, M.Haeffelin, Y.Morille, L.Malherbe, A.Papin, B.Bessagnet, L.Menut, E.Leoz, L.Rouil, 2010, Assessing in near real time the impact of the April 2010 Eyjafjallajokull ash plume on air quality, Atmospheric Environment, 45, 1217-1221.
37. Jimenez-Guerrero, P., O. Jorba, M.T. Pay, J.P. Montavez, S. Jerez, J.J. Gomez-Navarro, J.M. Baldasano, 2011. Comparison of two different sea-salt aerosol schemes as implemented in air quality models applied to the Mediterranean. Atmos. Chem. Phys. 11, 4833-4850, doi: 10.5194/acp-11-4833-2011.
38. Jimenez-Guerrero, P., J.J. Gomez-Navarro, S. Jerez, R. Lorente-Plazas, J.A. Garcia-Valero, J.P. Montavez, 2011. Isolating the effects of climate change in the variation of secondary inorganic aerosols (SIA) in Europe for the 21st century (1991-2100). Atmos. Environ. 45(4), 1059-1063, doi:10.1016/j.atmosenv.2010.11.022.
39. Kukkonen J., T. Balk, D. M. Schultz, A. Baklanov, T. Klein, A. I. Miranda, A. Monteiro, M. Hirtl, V. Tarvainen, M. Boy, V.-H. Peuch, A. Poupkou, I. Kioutsioukis, S. Finardi, M. Sofiev, R. Sokhi, K. Lehtinen, K. Karatzas, M. Astitha, G. Kallos, M. Schaap, E. Reimer, H. Jakobs, K. Eben. (2011). Operational, regional-scale, chemical weather forecasting models in Europe. Atmos. Chem. Phys. Discuss., 11, 5985-6162.
40. de Fouquet C., L.Malherbe and A.Ung, 2011, Geostatistical analysis of the temporal variability of ozone concentrations. Comparison between CHIMERE model and surface observations, Atmospheric Environment, 45, 3434-3446.

41. Jiménez-Guerrero, P., O. Jorba, M.T. Pay, J.P. Montavez, S. Jerez, J.J. Gomez-Navarro, J.M. Baldasano, 2011. Comparison of two different sea-salt aerosol schemes as implemented in air quality models applied to the Mediterranean. Atmos. Chem. Phys. 11, 4833-4850, doi: 10.5194/acp-11-4833-2011.
42. Jiménez-Guerrero, P., J.J. Gomez-Navarro, S. Jerez, R. Lorente-Plazas, J.A. Garcia-Valero, J.P. Montavez, 2011. Isolating the effects of climate change in the variation of secondary inorganic aerosols (SIA) in Europe for the 21st century (1991-2100). Atmos. Environ. 45(4), 1059-1063, doi:10.1016/j.atmosenv.2010.11.022.
43. Konovalov, I. B., M. Beekmann, I. N. Kuznetsova, A. Yurova, And A. M. Zvyagintsev, Atmospheric impacts of the 2010 Russian wildfires: integrating modelling and measurements of an extreme air pollution episode in the Moscow region, Atmos. Chem. Phys., 11, 10036-10051, 2011.
44. Konovalov I.B., Beekmann, ?., Kuznetsova, I. N., Glazkova, A.?., Vivchar ?.V., ZaripovR.B. (2011) Estimation of an impact of wildfires on air pollution in the Moscow megacity region by the combined use of a chemistry transport model and measurement data, Izvestia, Atmos. Ocean. Phys., 47(4).
45. Kuznetsova, I.N., Konovalov, I.B., Artamonova, A.A., Nakhaev, M.I., Lezina, E.A., Zvyagintsev, A.M., Beekmann, M., The observed and simulated variability of PM10 concentration in Moscow and Zelenograd, Russian Meteorology and Hydrology, 36 (3), 175-184, 2011.
46. Royer,P., Chazette,P., Sartelet,K., Zhang,Q.J., Beekmann,M., And Raut,J.-C., Lidar-derived PM10 and comparison with regional modeling in the frame of the MEGAPOLI Paris summer campaign, Atmos. Chem. Phys., 11, 10705-10726, 2011.
47. Schmechtig, C., B. Marticorene, B. Chatenet, G. Bergametti, J. L. Rajot,and A. Coman, (2011), Simulation of the mineral dust content over Western Africa from the event to the annual scale with the CHIMERE-DUST model, Atmos. Chem. Phys., 11,7185-7207.
48. Valari M., E.Chatignoux and L.Menut, 2011, Using a chemistry transport model to account for the spatial variability of exposure-concentrations in epidemiologic air pollution studies, Journal of the Air and Waste Management Association, 61, 164-179
49. Aulagnier, C., P. Rayner, P. Ciais, R. Vautard, L. Rivier, and M. Ramonet (2010), Is the recent build-up of atmospheric CO2 over Europe reproduced by models, Part 2: An overview with the atmospheric mesoscale transport model CHIMERE, Tellus, Ser. B, 62, 14-25, 2010.
50. Beekmann, M., and R. Vautard, 2010: A modelling study of photochemical regimes over Europe: robustness and variability. Atmos. Chem. Phys. Disc., 10, 10067-10084.
51. Bessagnet B., C.Seigneur, L.Menut, 2010, Impact of dry deposition of semi-volatile organic compounds on secondary organic aerosols, Atmospheric Environment, 10.1016/j.atmosenv.2010.01.027.
52. Borrego C., Monteiro A., Ferreira J., Moraes M.R., Carvalho A., Ribeiro I., Miranda A.I., Moreira M.D. (2010) Modelling the photochemical pollution over the metropolitan area of Porto Alegre, Brazil. Atmospheric Environment 44, 370-380.
53. Coll, I., C. Rousseau, B. Barletta, S. Meinardi and D. R. Blake, Evaluation of an urban NMHC emission inventory by measurements and impact on CTM results, Atm. Env., Vol 44 (31), pp 3843-3855, 2010.
54. Curci, G., Palmer, P. I., Kurosu, T. P., Chance, K., and Visconti, G.: Estimating European volatile organic compound emissions using satellite observations of formaldehyde from the Ozone Monitoring Instrument, Atmos. Chem. Phys., 10, 11501-11517, doi:10.5194/acp-10-11501-2010, 2010
55. Curci, G., Beekmann, M., Vautard, R., Smiatek, G., Steinbrecher, R., Theloke, J., Friedrich, R. (2009), Modelling study of the impact of isoprene and terpene biogenic emissions on European ozone levels, Atmospheric Environment, 43, 1444-1455, doi:10.1016/j.atmosenv.2008.02.070
56. Huijnen, V., H. J. Eskes, A. Poupkou, H. Elbern, K. F. Boersma, G. Foret, M. Sofiev, A. Valdebenito, J. Flemming, O. Stein, A. Gross, L. Robertson, M. D'Isidoro, I. Kioutsioukis, E. Friese, B. Amstrup, R. Bergstrom, A. Strunk, J. Vira, D. Zyryanov, A. Maurizi, D. Melas, V.-H. Peuch, and C. Zerefos,

Comparison of OMI NO2 tropospheric columns with an ensemble of global and European regional air quality models Atmos. Chem. Phys., 10, 3273-3296, 2010.

57. Hodzic A, Jimenez JL, Prevot ASH, et al., 2010, Can 3-D models explain the observed fractions of fossil and non-fossil carbon in and near Mexico City?, Atmospheric chemistry and physics Volume: 10 Issue: 22 Pages: 10997-11016
58. Hodzic A, Jimenez JL, Madronich S, et al., 2010, Modeling organic aerosols in a megacity: potential contribution of semi-volatile and intermediate volatility primary organic compounds to secondary organic aerosol formation, Atmospheric chemistry and physics Volume: 10 Issue: 12 Pages: 5491-5514 Konovalov, I. B., M. Beekmann, A. Richter, J. P. Burrows And A. Hilboll, Multi-annual changes of NOx emissions in megacity regions: nonlinear trend analysis of satellite measurement based estimates, Atmos. Chem. Phys., 10, 8481-8498, 2010.
59. Leitao, J., A. Richter, M. Vrekoussis, A. Kokhanovsky, Q. J. Zhang, M. Beekmann, and J. P. Burrows, On the improvement of NO2 satellite retrievals - aerosol impact on the airmass factors, Atmos. Measurement Technics, 3, 475-493, 2010.
60. Menut L. and B.Bessagnet, 2010, Atmospheric composition forecasting in Europe , Annales Geophysicae, 28, 61-74
61. Rolland M.-N., Gabrielle, B., Laville, P., Cellier, P., Beekmann, M., Gilliot, J.-M., Michelin, J., Hadjar, D., Curci, G., Biophysical modeling of NO emissions from agricultural soils for use in regional chemistry-transport models, Environmental Pollution, 158 (3), 711-722, 2010.
62. Sciare,J., D'argouges,O., Zhang,Q.J., Sarda-Esteve,R., Gaimoz,C., Gros,V., Beekmann,M., And Sanchez,O., Comparison between simulated and observed chemical composition of fine aerosols in Paris (France) during springtime: contribution of regional versus continental emissions, Atmos. Chem. Phys., 10, 11987-12004, 2010. Valari M. and L.Menut, 2010, Transferring the heterogeneity of surface emissions to variability in pollutant concentrations over urban areas through a chemistry transport model, Atmospheric Environment, Volume 44, Issue 27, Pages 3229-3238,
63. Borrego, C., Sa, E., Monteiro, A., Ferreira, J., Miranda, A.I. (2009). Forecasting Human Exposure to Atmospheric Pollutants - a modelling approach. Atmospheric Environment, doi:10.1016/j.atmosenv.2009.07.049.
64. Dufour,G., Wittrock,F., Camredon,M., Beekmann,M., Richter,A., and Burrows,J., SCIAMACHY formaldehyde observations: constraint for isoprene emissions over Europe ? Atmos. Chem. Phys., 9, 1647-1664, 2009.
65. Curci, G., M. Beekmann, R. Vautard, G. Smiatek, R. Steinbrecher, J. Theloke, R. Friedrich, Modelling study of the impact of isoprene and terpene biogenic emissions on European ozone levels, Atmos. Environ. 48, 1444-1455, 2009.
66. Flaounas, E., I. Coll, A. Armengaud and C. Schmechtig, The representation of dust transport and missing urban sources as major issues for the simulation of PM episodes in a Mediterranean area, Atmospheric Chemistry and Physics, Vol 9, pp8091-8101, 2009.
67. Bessagnet B., L.Menut, G.Curci, A.Hodzic, B.Guillaume, C.Liousse, S.Moukhtar, B.Pun, C.Seigneur, M.Schulz, 2009, Regional modeling of carbonaceous aerosols over Europe - Focus on Secondary Organic Aerosols Journal of of Atmospheric Chemistry,
68. Coll, I., Lasry, F., Fayet, S., Armengaud, A., and R. Vautard, 2009, Simulation and evaluation of 2010 emission control scenarios in a Mediterranean area. Atmos. Environ., 43, 4194-4204.
69. de Meij A., Gzella, A., Cuvelier, C., Thunis, P., Bessagnet, B., Vinuesa, J.F., Menut, L., Kelder H., 2009, The impact of MM5 and WRF meteorology over complex terrain on CHIMERE model calculations. ACP ,

70. Foret, G., Hamaoui, L., Schmechtig, C., Eremenko, M., Keim, C., Dufour, G., Boynard, A., Coman, A., Ung, A. and Beekmann, M.: Evaluating the potential of IASI ozone observations to constrain simulated surface ozone concentrations, Atmos. Chem. Phys., 9, 8479-8491, 2009.
71. Hodzic A, Jimenez JL, Madronich S, et al., 2009, Modeling organic aerosols during MILAGRO: importance of biogenic secondary organic aerosols, ATMOSPHERIC CHEMISTRY AND PHYSICS Volume: 9 Issue: 18 Pages: 6949-6981 Konovalov I. B., M. Beekmann, F. Meleux, A. Dutot and G. Foret, Combining deterministic and statistical approaches for PM10 forecasting in Europe, Atm. Env., 43, 2009.
72. Konovalov, I.B., Elanskii, N. F., Zvyagintsev, A. M., Belikov, I. B., and Beekmann, M.: Validation of chemistry transport model of the lower atmosphere in the Central European region of Russia using ground-based and satellite measurement data, Russian Meteorology and Hydrology, 34 (4), 236-242, 2009.
73. Menut L., O.Masson, B.Bessagnet, 2009, Contribution of Saharan dust on radionuclides aerosols activity levels in Europe? The 21-22 February 2004 case study, J. Geophys. Res., 114, D16202, doi:10.1029/2009JD011767.
74. Menut L., I. Chiapello and C. Moulin, 2009, Previsibility of mineral dust concentrations: The CHIMERE-DUST forecast during the first AMMA experiment dry season, Journal of Geophysical Research - Atmospheres, 114, D07202
75. Rouil L., C.Honore, R.Vautard, M.Beekmann, B.Bessagnet, L.Malherbe, F.Meleux, A.Dufour, C.Elichegaray, J-M.Flaud, L.Menut, D.Martin, A.Peuch, V-H.Peuch, N.Poisson, 2009, PREV'AIR : an operational forecasting and mapping system for air quality in Europe, BAMS, DOI: 10.1175/2008BAMS2390.1,
76. Steinbrecher, R., Smiatek, G., Koble, R., Seufert, G., Theloke, J., Hauff, K., Ciciolli, P., Vautard, R., 2009: Intra- and inter-annual variability of VOC emissions from natural and semi-natural vegetation in Europe and neighbouring countries. Atmos. Environ., 43, 1380-1391.
77. Szopa S., G.Foret, L.Menut, A.Cozic, 2009, Impact of large scale circulation on European summer surface ozone: consequences for modeling, Atmospheric Environment, Volume 43, Issue 6, Pages 1189-1195, doi:10.1016/j.atmosenv.2008.10.039,
78. Timmermans, R. M. A., Segers, A. J., Builtjes, P. H. J., Vautard, R., Siddans, R., Elbern, H., Tjemkes, S. A. T., and M. Schaap, 2009, The added value of a proposed satellite imager for ground-level particulate matter analyses and forecasts. IEEE J-STAR, 2, 271-283.
79. Timmermans, R. M. A., Schaap, M., Elbern, H., Siddans, R., Tjemkes, S., Vautard, R., and P. Builtjes, 2009: An observing system simulation experiment (OSSE) for aerosol optical depth from satellites. J. Atmos. Ocean. Technol,26, 2673-2682.
80. Vautard, R., M. Schaap, R Bergstrom, B. Bessagnet, J. Brandt, P.J.H. Builtjes, J.H. Christensen, C. Cuvelier, V. Foltescu, A. Graf, A. Kerschbaumer, M. Krol, P. Roberts, L. Rouil, R. Stern, L. Tarrason, P. Thunis, E. Vignati, P. Wind, 2009, Skill and uncertainty of a regional air quality model ensemble. Atmos. Environ., 43, 4822-4832.
81. Vivanco, M., Palomino, I., Vautard, R., Bessagnet, B., Martin, F., Menut, L., Jimenez, S., 2009: Multi-year assessment of photochemical air quality simulation over Spain, Environmental Modeling and Software, 24, 63-73. Vuolo M.R., H.Chepfer, L.Menut and G.Cesana, 2009, Comparison of mineral dust layers vertical structures modelled with CHIMERE-DUST and observed with the CALIOP lidar, Journal of Geophysical Research - Atmospheres , Vol. 114, D09214, doi:10.1029/2008JD011219,
82. Vuolo M.R., L.Menut and H.Chepfer, 2009, Impact of transport schemes accuracy on modelled dust concentrations variability Journal of Atmospheric and Oceanic Technology, 26, p.1135-1143, doi:10.1175/2008JTECHA1197.1, 2008
83. Bessagnet B., L.Menut, G.Aymoz, H.Chepfer and R.Vautard, 2008, Modelling dust emissions and transport within Europe: the Ukraine March 2007 event, Journal of Geophysical Research - Atmospheres, 113, D15202, doi:10.1029/2007JD009541,

84. Bessagnet, B., L. Menut, G. Curci, A. Hodzic, B. Guillaume, C. Liousse, S. Moukhtar, B. Pun, C. Seigneur and M. Schulz (2008), Regional modeling of carbonaceous aerosols over Europe - Focus on Secondary Organic Aerosols, Journal of Atmospheric Chemistry, 61, 175-202

85. Colette A., Menut L., Haeffelin M., Morille Y., 2008, Impact of the transport of aerosols from the free troposphere towards the boundary layer on the air quality in the Paris area, Atmospheric Environment, Vol 42/2 pp 390-402, DOI: 10.1016/j.atmosenv.2007.09.044,

86. Curci, G., Beekmann, M., Vautard, R., Smiatek, G., Steinbrecher, R., Theloke, J., and R. Friedrich, 2008: Modeling study of the impact of isoprene and terpene emissions on European ozone levels. Atmos. Environ., 43, 1444-14

87. Eremenko, M., Dufour, G., Foret, G., Keim, C., Orphal, J., Beekmann, M., Bergametti, G., and Flaud, J.-M.: Tropospheric ozone distributions over Europe during the heat wave in July 2007 observed from infrared nadir spectra recorded by IASI, Geophys. Res. Lett., 35, doi:10.1029/2008GL034803, 2008.

88. Honoré C., L.Rouil, R.Vautard, M.Beekmann, B.Bessagnet, A.Dufour, C.Elichegaray , J-M.Flaud, L.Malherbe, F.Meleux, L.Menut, D.Martin, A.Peuch, V.-H.Peuch, N.Poisson, 2008 Predictability of European air quality: The assessment of three years of operational forecasts and analyses by the PREV'AIR system, Journal of Geophysical Research, Atmospheres , 113, D04301, `http://dx.doi.org/10.1029/2007JD008761`,

89. Menut L., 2008, Sensitivity of hourly Saharan dust emissions to NCEP and ECMWF modeled wind speed, Journal of Geophysical Research - Atmospheres, 113, D16201, doi:10.1029/2007JD009522,

90. Valari M. and L. Menut, 2008, Does increase in air quality models resolution bring surface ozone concentrations closer to reality?, Journal of Atmospheric and Oceanic Technology, DOI: 10.1175/2008JTECHA1123.1,

91. Vivanco M.G., Palomino I., Vautard R., Bessagnet R., Martin F., Menut L., Jimenez S., 2008, Multi-year assessment of photochemical air quality simulation over Spain, Env. Mod. and Software, doi:10.1016/j.envsoft.2008.05.004

92. Hodzic A., S. Madronich, B. Bohn, S. Massie, L. Menut, and C. Wiedinmyer, 2007, Wildfire particulate matter in Europe during summer 2003: Meso-scale modeling of smoke emissions, transport and radiative effects, Atmospheric Chemistry and Physics, 7

93. Pison I., L.Menut and G.Bergametti, 2007 Inverse modeling of surface NOx anthropogenic emissions fluxes in the Paris area during the ESQUIF campaign, J. Geophys. Res., 112, D24302, doi:10.1029/2007JD008871.

94. Vautard R., M.Maidi, L.Menut, M.Beekmann, A.Colette, 2007 Boundary layer photochemistry simulated with a two-stream convection scheme, Atmospheric Environment, Volume 41, Issue 37, Pages 8275-8287.

95. Pirovano G., I. Coll, M. Bedogni, S. Alessandrini, M. P. Costa, V. Gabusi, F. Lasry, L. Menut, R. Vautard, 2007, On the influence of meteorological input on photochemical modelling of a severe episode over a coastal area, Atmospheric Environment, Volume 41, Issue 30, September 2007, Pages 6445-6464

96. Menut L., G.Forêt and G.Bergametti, 2007, Sensitivity of mineral dust concentrations to the model size distribution accuracy, Journal of Geophysical Research, Atmospheres, 112, D10210, doi:10.1029/2006JD007766.

97. Drobinski P., F. Said, G. Ancellet, J. Arteta, P. Augustin, S. Bastin, A. Brut, J.L. Caccia, B. Campistron, S. Cautenet, A. Colette, B. Cros, U. Corsmeier, I. Coll, A. Dabas, H. Delbarre, A. Dufour, P. Durand, V. Guenard, M. Hasel, N. Kalthoff, C. Kottmeier, A. Lemonsu, F. Lohou, V. Masson, L. Menut, C. Moppert, V.H. Peuch, V. Puygrenier, O. Reitebuch, R. Vautard, 2007, Regional transport and dilution during high pollution episodes in southeastern France: Summary of findings from the ESCOMPTE experiment, Journal of Geophysical Research, Atmospheres, 112, D13105, doi:10.1029/2006JD007494.

98. Deguillaume L., M. Beekmann, L. Menut, Bayesian Monte Carlo analysis applied to regional scale inverse emission modelling for reactive trace gases, Journal of Geophysical Research, Atmospheres, Vol. 112, No. D2, D02307. http://dx.doi.org/10.1029/2006JD007518
99. Konovalov I. B., M. Beekmann, A. Richter, J. P. Burrows, 2005, Inverse modelling of the spatial distributions of NOx emissions on a continental scale using satellite data, Atmposheric Chemistry and Physics , 6, 1747-1770, 2006.
100. Cuvelier, C., Thunis, P., Vautard, R., Amann, M., Bessagnet, B., Bedogni, M., Berkowicz, R., Brandt, J., Brocheton, F., Builtjes, P., Coppalle, A., Denby, B., Douros G., Graf, A., Hellmuth, O., Honoré, C., Hodzic, A., Jonson, J., Kerschbaumer, A., de Leeuw, F., Minguzzi, E., Moussiopoulos, N., Pertot, C., Pirovano, G., Rouil, L., Schaap, M., Stern, R., Tarrason, L., Vignati, E., Volta, M., White, L., Wind, P., Zuber, A., 2006: CityDelta: A model intercomparison to explore the impact of emission reductions in 2010 in European cities in 2010, Atmospheric Environment, in press.
101. Vautard, R., Builtjes, P. H. J., Thunis, P., Cuvelier, K., Bedogni, M., Bessagnet, B., Honoré, C., Moussiopoulos, N., Pirovano G., Schaap, M., Stern, R., Tarrason, L., Van Loon, M., 2006: Evaluation and intercomparison of Ozone and PM10 simulations by several chemistry-transport models over 4 european cities within the City-Delta project, Atmospheric Environment, in press.
102. Hodzic A., B.Bessagnet and R.Vautard, A model evaluation of coarse-mode nitrate heterogeneous formation on dust particles, 1006, Atm.Env, 40, 4158-4171
103. Colette A., Ancellet G., L. Menut and S.R.Arnold, A Lagrangian analysis of the impact of transport and transformation on the ozone stratification observed in the free troposphere during the ESCOMPTE campaign, Atmos. Chem. Phys., 6, 3487-3503, 2006
104. Hodzic A., R. Vautard, P. Chazette, L. Menut and B.Bessagnet, Aerosol chemical and optical properties over the Paris area within ESQUIF project, Atmospheric Chemistry and Physics, 2006, pp.3257-3280. SRef-ID: 1680-7324/acp/2006-6-3257
105. Szopa S., D.Hauglustaine, R.Vautard and L. Menut, Future global tropospheric ozone changes and impact on European air quality, Geophysical Research Letter, 2006, 33, L14805, doi:10.1029/2006GL025860
106. Vautard R., S. Szopa, M. Beekmann, L. Menut, D. A. Hauglustaine, L. Rouil, M. Roemer (2006), Are decadal anthropogenic emission reductions in Europe consistent with surface ozone observations?, Geophys. Res. Lett., 33, L13810, doi:10.1029/2006GL026080
107. Pison I., L. Menut and N.Blond, Inverse modeling of emissions for local photo-oxidant pollution: Testing a new methodology with kriging constraints, Annales Geophysicae, 2006, 24, 1523-1535
108. Hodzic A., R. Vautard, H. Chepfer, P. Goloub, L. Menut, P. Chazette, J.L. Deuze, A. Apituley, P. Couvert, Evolution of aerosol optical thickness over Europe during the August 2003 heat wave as seen from CHIMERE model simulations and POLDER data, Atmospheric Chemistry and Physics, 2006, 1853-1864. SRef-ID: 1680-7324/acp/2006-6-1853
109. Blond, N., Boersma, K. F., Eskes, H. J., van der A, R., Van Rosendael, M., De Smedt, I., Bergametti, G., Vautard, R., 2005. Intercomparison of SCHIAMACHY nitrogen dioxide observations, in-situ measurements and air quality modelling results over Western Europe. J. Geophys. Res., in press.
110. Hodzic, A., Vautard, R., Bessagnet, B., Lattuati, M., and F. Moreto, 2005: On the quality of long-term urban particulate matter simulation with the CHIMERE model. Atmospheric Environment, 39, 5851-5864.
111. Bessagnet B., A.Hodzic, O.Blanchard, M.Lattuati, O.LeBihan, H.Marfaing and L.Rouil, 2005, Origin of particulate matter pollution episodes in wintertime over the Paris basin, Atm.Env., 39, 6159-6174.
112. Menut L., I. Coll and S. Cautenet, 2005, Impact of meteorological data resolution on the forecasted ozone concentrations during the ESCOMPTE IOP 2a and 2b, Atmospheric Research - ESCOMPTE Special Issue, 74, 139-159, 2005

113. Vautard, R., C. Honoré, M. Beekmann, L. Rouil, 2005: Simulation of ozone during the August 2003 heat wave and emission control scenarios, Atmospheric Environment, in press.

114. Vautard R., B.Bessagnet, M.Chin and L. Menut, On the contribution of natural Aeolian sources to particulate matter concentrations in Europe: testing hypotheses with a modelling approach, Atm. Environ., 39, Issue 18, 3291-3303, 2005

115. Monteiro, A., Vautard, R., Borrego, C., and A. I. Miranda, 2005: Long-term simulations of photo oxidant pollution over Portugal using the CHIMERE model, Atmospheric Environment., 39, 3089-3101.

116. Hodzic A., Vautard, R., Bessagnet, B., Lattuati, M., Moreto, F., Long-term urban aerosol simulation versus routine particulate matter observations. Atmospheric Environment, 39, 5851-5864, 2005

117. Vautard R., B.Bessagnet, M.Chin and L.Menut, On the contribution of natural Aeolian sources to particulate matter concentrations in Europe: testing hypotheses with a modelling approach, Atm. Env., 39, Issue 18, 3291-3303, 2005

118. Menut L., I. Coll and S. Cautenet, Impact of meteorological data resolution on the forecasted ozone concentrations during the ESCOMPTE IOP 2a and 2b, Atmospheric Research - ESCOMPTE Special Issue, 74, 139-159, 2005.

119. Bessagnet B., A.Hodzic, R.Vautard, M.Beekmann, S.Cheinet, C.Honoré, C.Liousse and L.Rouil, Aerosol modeling with CHIMERE - preliminary evaluation at the continental scale, Atmospheric Environment, 38, 2803-2817, 2004

120. Blond, N. and R.Vautard, Three-dimensional ozone analyses and their use for short-term ozone forecasts, J. Geophys. Res., 109, D17303, doi:10.1029/2004JD004515, 2004.

121. Wackernagel, H., C. Lajaunie, N. Blond, C. Roth and R. Vautard, Geostatistical risk mapping with chemical transport model output and ozone station data, Ecological Modelling, 179, 177-185, 2004.

122. Hodzic A., Chepfer H., Vautard R., Chazette P., Beekmann M., Bessagnet B., Chatenet B., Cuesta J., Drobinski P., Goloub P., Haeffelin M., Morille Y., 2004: Comparisons of aerosol chemistry-transport model simulations with lidar and sun photometer observations at a site near Paris., J. Geophys. Res., 109, D23201,doi:10.1029/2004JD004735, 2004

123. Konovalov, I., Beekmann, M., Vautard, R., Burrows, J., Richter, A., Nuess, H., and N. Nelansky, 2004: The comparison and evaluation of modelled and GOME measurement derived tropospheric NO2 columns over western and eastern Europe Atmospheric Chemistry and Physics, in press.

124. Labouze, E., C. Honoré, L. Moulay, B. Couffignal, and M. Beekmann, 2004. Photochemical ozone creation potentials: a new set of characterization factors for different gas species at the scale of the Western Europe, Int. Journal of Life Cycle Assessment, Vol.9, Nr.3, 187-195.

125. Monteiro, A., Borrego, C., Vautard, R., and A. I. Miranda, 2004: long-term simulations of photooxidant pollution over Portugal using the CHIMERE model. Atmospheric Environment, submitted.

126. Pison I. and L.Menut, Quantification of the impact of aircraft traffic emissions on tropospheric ozone over Paris area, Atmospheric Env., 38-7, 971-983, 2004

127. Vautard, R., C. Honoré, M. Beekmann, L. Rouil, 2004: Simulation of ozone during the August 2003 heat wave and emission control scenarios, Atmospheric Environment, in press.

128. Zhang, B.-N., R. Vautard and N.-T. Kim Oanh, 2004: Comparison of the UAM-V/SAIMM and CHIMERE/ECMWF Photochemical Modeling System Performance in a Tropical Urban Area, J. Air and Waste Management, in press

129. Beekmann M. and C.Derognat, Monte carlo uncertainty analysis of a regional scale transport chemistry model constrained by measurements from the ESQUIF campaign, Journal of Geophysical Research, ESQUIF special section, 2003

130. Blond, N., Bel, L. and Vautard, R., Three-dimensional ozone data analysis with an air quality model over the Paris area, J. Geophys. Res., 108(D23), 4744, doi:10.1029/2003JD003679, 2003.

131. Derognat C., M.Beekmann, H.Schmidt, R.Vautard, D.Martin, B.Neininger, Effect of biogenic VOC emissions on the tropospheric chemistry during elevated ozone periods in Ile-de-france, Journal of Geophysical Research, ESQUIF special section, 2003
132. Menut L., Adjoint modelling for atmospheric pollution processes sensitivity at regional scale during the ESQUIF IOP2, Journal of Geophysical Research, ESQUIF special section, 2003
133. Sillman S., R. Vautard, L. Menut and D. Kley, O3-NOx-VOC sensitivity and NOx-VOC indicators in Paris: results from models and ESQUIF measurements, Journal of Geophysical Research, ESQUIF special section, 2003
134. Schmidt H. and D.Martin, Continental scale adjoint sensitivity of ozone concentrations in the paris region during the ESQUIF episodes, Journal of Geophysical Research, ESQUIF special section, 2003
135. Vautard R., D. Martin, M. Beekmann, R. Friedrich, A. Jaubertie, D. Kley, M. Lattuati, P. Moral, B. Neininger and J. Theloke, Paris emission inventory diagnostic from the ESQUIF airborne measurements and a chemistry-transport model, Journal of Geophysical Research, ESQUIF special section, 2003
136. Vautard R. et al., A synthesis of the ESQUIF field campaign, Journal of Geophysical Research, ESQUIF special section, 2003
137. Schmidt H., C. Derognat, R.Vautard and M.Beekmann, 'A comparison of simulated and observed ozone mixing ratios for the summer of 1998 in western Europe', Atmospheric Environment, 2001
138. Vautard R., M. Beekmann, J. Roux, D. Gombert, 'Validation of a deterministic forecasting system for the ozone concentrations over the Paris area', Atmospheric Environment, 35 2449-2461, 2001.
139. Honoré, C., Vautard, R., Beekmann, M., Low and High Nox chemical regimes in an urban environment, Environmental Modelling and Software, 15, 559-564, 2000
140. Honoré, C., Vautard, R. and Beekmann, M., Photochemical regimes in urban atmospheres: the influence of dispersion. Geophys. Res. Letters, 27, 1895-1898, 2000.
141. Menut L., R.Vautard, M.Beekmann and C.Honoré, 'Sensitivity of Photochemical Pollution using the Adjoint of a Simplified Chemistry-Transport Model', Journal of Geophysical Research - Atmospheres 105, D12, 15,379-15,402, 2000
142. Menut L., R. Vautard, C. Flamant, C. Abonnel, M. Beekmann, P. Chazette, P. H. Flamant, D. Gombert, D. Guedalia, D. Kley, M.P. Lefebvre, B. Lossec, D. Martin, G. Megie, M. Sicard, P. Perros, G. Toupance, 'Atmospheric pollution over the Paris area: The ESQUIF project', Annales Geophysicae, 18, 1467-1481, 2000
143. Vautard R., M.Beekmann and L. Menut, 'Applications of adjoint modelling in atmospheric chemistry: sensitivity and inverse modelling', Environmental Modeling and Sofware, 15, pp 703-709, 2000
144. Kurtenbach R., K.H Becker, J.A.G. Gomes, J. Kleffmann, J.C. L´orzer, M. Spittler, P. Wiesen, R. Ackermannb, A. Geyer, U. Platt, 'Investigations of emissions and heterogeneous formation of HONO in a road traffic tunnel', Atmospheric Environment, 35 33853394, 2001

Appendix B

History

This section tracks the model evolution over the last versions.

B.1 chimere2008

Version *chimere2008* contained the following improvements and new processes.

- New functionality:
  - ◇ Due to integration of the MEGAN model biogenic emission potentials data and emission rates parameterizations, Chimere can now be used outside Europe if the user provides anthropogenic emissions in the region of interest
  - ◇ Automatic preparation of the file **LANDUSE_<domain>** from the original GLCF global land use database for the desired Chimere domain
  - ◇ Meteorological interface to the WRF model **prepwrf** has been added
  - ◇ Possibility to use aerosol boundary and initial conditions from the LMDz model output
  - ◇ A new mode of **exachim** to display various data slices by a simple mouse click
- Process changes:
  - ◇ Updated Secondary Organic Aerosols (SOA) chemistry: the full MEGAN SOA scheme is now used
- Computational changes:
  - ◇ New format of the emissions interface **emiSURF** and **prepemis**. The emission files are now separated by individual species, which makes the **prepemis** interface simpler and easier to modify. If a simulation spans two consequent months, emissions for each day are now taken from a corresponding month rather than from the first month for all days. One can also choose emission types to use independently: either surface, point, or fire emissions. Hourly changes of fire emissions are now allowed. If emissions are not available for a given species, they are set to zero, and the simulation continues
  - ◇ Reorganized boundary and initial conditions interface for more convenience and code simplicity. User can now choose a global database for each species
  - ◇ Revised vertical interpolations in the boundary and initial conditions interface
  - ◇ Running Open MPI or LAM depending on user system settings. If both realizations are found, preference is given to Open MPI
  - ◇ Simulation parameters are now organized in the form of an array in the top calling script **chimere.sh**. This allows more convenient parameter specification, especially for simulations for several, possibly nested, model domains
  - ◇ The script **chimere-run.sh** has been split into parts corresponding to Chimere components: compilation, meteorological interfaces, emissions, initial and boundary conditions, and Chimere core. It is now possible to run individually one or more of these components.

B.2 V200606

B.2.1 Parallelization

Version V200606 represented a major breakthrough in the model computational speed, since it has been parallelized and can now run on distributed memory clusters and shared memory machines, ranging from the local home-made cluster of PCs, to large supercomputers. However, there are no changes neither in the scientific core of the model, nor in the I/O file formats.
The rationale of the parallelization was :

- the increasing computation time of the aerosol version and of nextcoming, more sophisticated versions,
- the user requirements for higher resolution domains,
- the requirements of air pollution forecast agencies, in terms of forecast computation time.

CHIMERE uses the distributed memory scheme, and an MPI message passing library. It has been tested with Open MPI and LAM/MPI, but should work, with minor changes in the scripts, with MPICH or other MPI compatible parallel environments.
There is one master program, which calls several worker subroutines, each worker been in charge of the processing of a subdomain. Subdomains are the result of a Cartesian division of the main geographical domain by the number of processors.
The master program is in charge of the initializations and file I/O. The workers are in charge of the scientific processing and inter-subdomains boundary conditions updates.
As described above, CHIMERE is basically an MPMD (multiple program, multiple data) application. However, MPMD is only available with MPI-2 compatible environments. To increase CHIMERE portability, its interface has been tweaked to mimic the appearance of an SPMD (single program, multiple data) application, which makes it compatible with widely spread MPI-1 parallel environments.
Despite the tremendous architectural change in the code structure, most scientific subroutines, now called by the worker main subroutine, have remained unchanged.
As far as the user interface is concerned, the only apparent modifications are :

- definition of subdomains in **chimere-mm5** script : **nzdoms** and **nmdoms** parameters.
- use of an MPI library : MPI must be installed for running CHIMERE, even if it runs on only one processor with only one subdomain.

B.2.2 Toolbox

There is a new processing inside **exachim** : the COARDS intermediate file is no longer necessary. Instead, GrADS compliant files are built directly. A new utility, chm2grads.f90, replaces chm2coards.f90. All kinds of CHIMERE grids may be used, not only rectilinear ones. More sophisticated command line options allows for displaying only selected variables and time slots.
The udunits library is no longer used.
A new tool to transform the old CHIMERE binary files into netCDF files, **chmbin2cdf.f90**, has been included in the distribution.
An older tool, **chim2fig**, which used to be distributed with pre-netCDF versions of CHIMERE, has been upgraded to accept netCDF files.

B.2.3 Scripts

New top-level scripts have been added, to run CHIMERE on PC clusters with a PBS-like batch scheduler.
Despite the fact that an interface to ECMWF meteorology is not yet provided in this version, a script to run CHIMERE on ECMWF HPCD computer is provided as an example for running CHIMERE under IBM LoadLeveler and POE environments.

B.2.4 makefiles changes

The directory structure of the src/ tree has been modified, and Makefiles have been rationalized. This allows now for using the parallel compilation capability of the GNU make utility. Also, the meteo interface is run in background, during model compilation. This reduces dramatically the compilation time on multiprocessor machines, allowing for more sophisticated optimizations. Minor bugs have been corrected in Makefile headers.

Appendix C

Some scripts used in the CHIMERE suite

C.1 The *domains/makeCOORDdomains* script for horizontal grid definition

To **create a new COORD file**, you first have to add a new line in the **domainlist.nml** file describing your new domain. After that, run manually the **makeCOORDdomains** script (in the **domains/** directory or here below) with the required domain name:

```
   makeCOORDdomains CONT3
```

with the following *makeCOORDdomains* script:

```
#!/bin/sh

if [ $# -eq 0 ] ; then
  echo "define the domain name"
  exit 0
else
  dom=$1
fi

nzo=`gawk '$1=="'${dom}'" {print $2}' domainlist.nml`
nme=`gawk '$1=="'${dom}'" {print $3}' domainlist.nml`
dx=`gawk '$1=="'${dom}'" {print $4}' domainlist.nml`
dy=`gawk '$1=="'${dom}'" {print $5}' domainlist.nml`
xbotleft=`gawk '$1=="'${dom}'" {print $6}' domainlist.nml`
ybotleft=`gawk '$1=="'${dom}'" {print $7}' domainlist.nml`

touch COORD
\rm COORD
[[ -z ${nzo} || -z ${nme} || -z ${dx} || -z ${dy} || -z ${xbotleft} || -z ${ybotleft} ]] &&\
   { echo "Error reading domainlist.nml. Probably domain ${dom} is not defined. Bye" ; exit 1 ; }

echo "   making horizontal COORD file"
echo "       geometry definition:"
echo "             nodes="${nzo}"x"${nme}
echo "             resol="${dx}"x"${dy}
echo "             south-west point="${xbotleft}"x"${ybotleft}

gawk -v xbotleft=${xbotleft} -v ybotleft=${ybotleft} -v dx=${dx} -v dy=${dy} -v nzo=${nzo} -v nme=$
  for(j=1;j<=nme;j++){
  for(i=1;i<=nzo;i++){
     x=(i-1)*dx
     y=(j-1)*dy
     xlon=xbotleft+x
     xlat=ybotleft+y
```

```
      print  xlon "  " xlat >> "COORD"
   }
   }
}'

mv COORD COORD_${dom}
cp COORD_${dom} HCOORD
```

C.2 The *util/define_geom* script for vertical grid definition

To make your own VCOORD file, go to the directory **util/**, edit the **define_geom** script and adapt the top pressure level to the one you need.
N.B.: It is recommended to have a maximum ptop of 200 hPa since the global model used for boundary conditions delivered data only up to this value.
The define_geom script:

```
#!/bin/sh

#  Defines a geometrical-progression vertical layering
#  For the CHIMERE model. It actually produces sets of
#  Hybrid sigma-p coefficients Ak and Bk such that the
#  pressure at top of layer k is Pk = Ak*1e5 + Bk*Ps in Pa
#  where Ps is Surface pressure

#  Define the parameters below and run the script by just typing "define_geom"

ptop=700    # Pressure at model top
nlay=8      # Number of layers
pre1=995    # Pressure (hPa) of the first layer top when Ps = 1000 hPa
fout=../data/vgrid/VCOORD.8GEOM700

echo ${nlay} ${pre1} ${ptop} | gawk -f geom.awk > ${fout}
```

Recommendations

- When defining manually the hybrid coefficients the user shall verify that under all possible meteorological conditions these layers do not cross one another or get mixed up.
- It is highly recommended that top level be a pressure level ($b_k = 0$), since it has been found to minimize mass loss through top boundary.
- Using the MOZART and LMDz-INCA boundary conditions, one should not use a model top above 200 hPa
- In the present formulation for cloud/radiation/photolysis, it is assumed that the model domain is *below the clouds*, i.e. no cloud albedo is taken into account. This puts constraints on model top to be not too high. This will be changed in future releases.

Appendix D

How To install NetCDF under GNU/Linux

D.1 Background

Since CHIMERE requires a NetCDF package. This note describes how to install NetCDF for the supported compilers.
NetCDF installation has been tested with :

- ifort 32 bits (version 8.1.028)
- ifort 64 bits (version 8.1.027)
- g95 32 bits (version 0.92 20090624)
- g95 64 bits (version 0.91 20080227)
- gfortran 32 bits (version 4.4.2 20091027)
- gfortran 64 bits (version 4.1.2 20080704)
- pgf90 32 bits (version 5.2.4)
- pgf90 64 bits (version pgf90 6.0-5)
- netcdf (version 3.6.3 or 4.1.1 with hdf5-1.8.5)

D.2 Download

- **Download NetCDF** (source package) from the URL :

```
cd /tmp
wget ftp://ftp.unidata.ucar.edu/pub/netcdf/netcdf.tar.gz
```

- **Decompress and detar**

```
tar xvfz netcdf.tar.gz
```

D.3 Configure NetCDF

At the time of writing of this How-To, the current version of NetCDF is 3.6.4. If you downloaded a newer version, replace 3.6.4 by the new version number in the following text.

```
cd netcdf-3.6.3/src
```

The configuration process depends on several environment variables that you shall set according to your compiler. Although it may be possible to link CHIMERE executables compiled with compiler A with the NetCDF library compiled with compiler B, we strongly recommend to use the same compiler. The time you

will spend to install a new NetCDF library is negligible compared to the time you could loose trying to match inconsistent libraries.
We suppose you want to install netcdf somewhere under `/opt` . If you choose to install under `/usr/local`, or under you home directory, replace `/opt` your installation path in the following text.
We also suppose your shell is like `bash` or `ksh` . If you use `csh`, modify the `export` statements according to your shell syntax.

D.3.1 ifort

As root :

```
mkdir /opt/netcdf-3.6.3-ifort
```

As an ordinary user :

```
export FC=ifort
export F90=ifort
export FFLAGS="-fltconsistency"
export CPPFLAGS="-DNDEBUG -DpgiFortran"
./configure --prefix=/opt/netcdf-3.6.3-ifort
make
make test
```

As root :

```
make install
```

D.3.2 g95

As root :

```
mkdir /opt/netcdf-3.6.3-g95
```

As an ordinary user :

```
export CC='gcc'
export CXX='g++'
export CPPFLAGS='-DNDEBUG -DgFortran'
export CFLAGS='-O -g'
export FC='g95'
export F77='g95'
export FFLAGS='-O -g -fno-second-underscore'
export FCFLAGS='-O -g -fno-second-underscore'
./configure --prefix=/opt/netcdf-3.6.3-g95
make
make test
```

As root :

```
make install
```

D.3.3 pgf90

Some versions of pgf90 prior to 5.2 have experienced problems with the F90 interface of NetCDF. Do not try to install a library for which "make test" has failed.
As root :

```
mkdir /opt/netcdf-3.6.3-pgf90
```

As an ordinary user :

```
export CC=/usr/bin/gcc
export CPPFLAGS='-DNDEBUG -DpgiFortran'
export CFLAGS=-O
export FC=pgf90
export FFLAGS="-O -w"
export CXX=g++
./configure --prefix=/opt/netcdf-3.6.3-pgf90
make
make test
```

As root :

```
make install
```

D.3.4 ifort 64 bit on Intel EMT64 or AMD Opteron

As root :

```
mkdir /opt/netcdf-3.6.3-ifort
```

As an ordinary user :

```
export FC=ifort
export F90=ifort
export CFLAGS="-O -m64"
export FFLAGS="-mp"
export CPPFLAGS="-DNDEBUG -DpgiFortran"
./configure --prefix=/opt/netcdf-3.6.3-ifort
make
make test
```

As root :

```
make install
```

D.3.5 g95 64 bit on Intel EMT64 or AMD Opteron

As root :

```
mkdir /opt/netcdf-3.6.3-g95-64
```

As an ordinary user :

```
export CC='gcc'
export CXX='g++'
export CPPFLAGS='-DNDEBUG -DgFortran'
```

```
export CFLAGS='-O -m64'
export FC='g95'
export F77='g95'
export FFLAGS='-O -g -fno-second-underscore'
export FCFLAGS='-O -g -fno-second-underscore'
./configure --prefix=/opt/netcdf-3.6.3-g95-64
make
make test
```

As root :

```
make install
```

D.3.6 pgf90 64 bit on Intel EMT64 or AMD Opteron

Do not try to install a library for which "make test" has failed.
As root :

```
# make install
```

As root :

```
# mkdir /opt/netcdf-3.6.3-pgf90-64
```

As an ordinary user :

```
export CC=/usr/bin/gcc
export CPPFLAGS='-DNDEBUG -DpgiFortran'
export CFLAGS=-O
export FC=pgf90
export F90=pgf90
export FFLAGS="-O -w"
export CXX=g++
./configure --prefix=/opt/netcdf-3.6.3-pgf90-64
make
make test
```

As root :

```
# make install
```

D.4 Manually Configure CHIMERE

Automatic configuration of CHIMERE using config.sh is described in §2.2, p. 17. Here we explain how to configure the model manually.
In the directory `makefiles.hdr/`, you will find 9 files :

```
Makefile.hdr.g95-64-lam
Makefile.hdr.g95-64-ompi
Makefile.hdr.g95-lam
Makefile.hdr.g95-ompi
Makefile.hdr.gfortran-64-lam
Makefile.hdr.gfortran-64-ompi
Makefile.hdr.ifort-64-lam
Makefile.hdr.ifort-64-ompi
Makefile.hdr.ifort-ompi
```

After linking to `Makefile.hdr` the file corresponding to your compiler, MPI library, and system (32 or 64 bit), for instance:

```
ln -sf makefiles.hdr/Makefile.hdr.g95-64-ompi Makefile.hdr
```

modify the lines `my_netcdflib=` and `my_netcdfinc=` in the file mychimere.sh to point to your NetCDF directory. Modify also the PATHs to your HDF5 library given by variables `my_hdflib` and `my_hdfinc`. For instance :

```
export my_netcdfdir=/opt/netcdf-3.6.3-g95
```

If you are using NetCDF4/HDF5:

```
export my_hdfdir=/opt/hdf5-1.8.5-g95
```

Follow the comments in `Makefile.hdr.xxxx` for other options.

Appendix E

How To install MPI under GNU/Linux

E.1 Background

CHIMERE is now parallelized, using the distributed memory scheme, and requires an MPI compatible Message Passing Library to be installed and configured on the host or cluster it will run on.
MPI is required even if CHIMERE is planned to run on a single processor machine !
Several free MPI libraries are available for download. MPICH and LAM/MPI are well known. The newer OpenMPI is claimed to be the continuation of LAM/MPI.
CHIMERE has been tested with LAM/MPI and Open MPI. This HOW-TO describes briefly the installation and basic configuration process for LAM/MPI and Open MPI on a RedHat-like GNU-Linux distribution.
We recommend the precompiled package installation for RedHat-like distributions. However, some 64 bit Linux distributions have a precompiled LAM-MPI binary which is not compatible with other libraries. In that case, you will have to install the LAM-MPI package from source, as described at the end of the document.

Tested with:

- Fedora Core 4
- LAM-7.1.1

E.2 LAM/MPI Installation

RedHat-like distributions include a RPM for LAM/MPI. It is generally called "lam".
Here is the installation process for a Fedora Core 4 system. You must have administrative privileges to perform it.

- If you use YUM as a package tool:

```
yum install lam
```

- If you use RPM:
  - ◇ download lam-7.1.1-7.FC4.i386.rpm from your Fedora repository
  - ◇ you may also want libaio-devel-0.3.104-2.i386.rpm
  - ◇ install :

```
rpm -Uvh libaio-devel-0.3.104-2.i386.rpm lam-7.1.1-7.FC4.i386.rpm
```

- Edit `/etc/lam/lam-bhost.def` to set the list of hosts you will include in your LAM cluster. For instance, for a cluster of 3 bi-processors, `lam-bhost.def` would contain :

```
host1.mycluster.mydomain.edu cpu=2
host2.mycluster.mydomain.edu cpu=2
host3.mycluster.mydomain.edu cpu=2
```

For a uniprocessor machine, `lam-bhost.def` would only contain :

```
localhost
```

- Instead of using the system wide lam-bhost.def, you can create and use your own hosts file, and boot LAM/MPI using this file. A file named "nodelist.example" is provided as a template in this distribution. Edit it according to your environment.

E.3 Testing

- type:

  ```
  lamboot
  ```

  to boot you LAM/MPI environment using system-wide hosts list, or

  ```
  lamboot <my_host_list>
  ```

  to boot your own host list defined in file `<my_host_list>`
- type:

  ```
  lamnodes
  ```

  to verify that all nodes declared in the hosts file are up.

If cas of insuccess, get LAM/MPI documentation from their web site.
Most problems occur because the user is not allowed to perform **rsh** or **ssh** connexions to the hosts listed in hostfile.
Check with your system administrator that you can **ssh** to the target hosts. If the hosts are connected to a private network, ask her/him to allow **rsh** on these hosts. The advantage of using **rsh** is that you can schedule unattended jobs using `cron` or `at` . Otherwise you need to change your ssh passphrase for an empty one, which can be a security issue.

E.4 Uniprocessor users

Parallelism is mainly useful for Air Pollution Forecast Agencies, or for scientists running long periods of reanalysis. For the users who just want to run CHIMERE as they were accustomated to, on a single processor machine, here is a simple summary of what they shall do with LAM/MPI:

- install LAM/MPI as described above

  ```
  yum install lam
  ```

- check that ssh is installed on your machine

  ```
  ssh localhost
  ```

Most modern linux distributions come with ssh installed and configured.

- edit **/etc/lam/lam-bhost.def** to keep only the line

```
localhost
```

- boot LAM/MPI

```
lamboot
```

- Enjoy CHIMERE !

E.5 Installation from source

Thanks to Gabriele Curci at aquila.infn.it

Some 64 bit linux vendors have compiled the lam package with the "second-underscore" option. This leads to an incompatibility between lam and netcdf libraries. If you get error messages like this in your make.log file, you are probably in that case :

```
twostep_mod.f90:(.text+0xbdb6): undefined reference to `mpi_irecv_'
twostep_mod.f90:(.text+0xc2cb): undefined reference to `mpi_issend_'
twostep_mod.f90:(.text+0xc33a): undefined reference to `mpi_irecv_'
twostep_mod.f90:(.text+0xc7f0): undefined reference to `mpi_issend_'
```

To overcome this problem, you have to install LAM-MPI from source. Here is the process, copied from Gabriele's message :

- login as root
- download LAM source, I installed latest version 7.1.2 (wget http://www.lam-mpi.org/download/files/lam-7.1.2.tar.bz2)
- unzip the source (tar jxvf lam-7.1.2.tar.bz2)
- `cd lam-7.1.2`
- `./configure "FC=g77 -fno-second-underscore" --prefix=/usr/local`
- `make`
- `make install`

E.6 Open MPI installation

This section briefly explains how to install Open MPI with g95 and ifort compilers from sources. The sources can be downloaded from the Open MPI home page [http://www.open-mpi.org].

With g95 on a 32 bit system

```
export COMPILO=g95
./configure CC=gcc CXX=g++ F77=$COMPILO  FC=$COMPILO \
            --prefix=/opt/openmpi-1.2.5-$COMPILO \
            --with-mpi-f90-size=medium
make all
make install
edit /etc/profile to set the PATH variable
edit /etc/ld.so.conf.d/openmpi.conf
ldconfig
```

With g95 on a 64 bit system

```
export COMPILO=g95
./configure CC=gcc CXX=g++ F77=$COMPILO FC=$COMPILO \
             CFLAGS=-m64 CXXFLAGS=-m64 FFLAGS=-m64 FCFLAGS=-m64 \
            --prefix=/opt/openmpi-1.2.5-$COMPILO \
            --with-mpi-f90-size=medium
make all
make install
edit /etc/profile to set the PATH variable
edit /etc/ld.so.conf.d/openmpi.conf
ldconfig
```

Build options with ifort for 64 and a 32 bit systems

For a 64 bit system:

```
export CC=gcc
export CXX=g++
export CFLAGS='-O2 -m64'
export CXXFLAGS='-O2 -m64'
export LDFLAGS='-O2'
export FC=ifort
export FCFLAGS='-O2 -m64'
export F77=ifort
export FFLAGS='-O2 -m64'
./configure --prefix=/opt/openmpi-1.2.5-ifort-64 --with-mpi-f90-size=medium
```

For a 32 bit system you need to remove the -m64 flag from the options above.

Appendix F

Notes on using CHIMERE with LAM MPI

You need to make sure that LAM MPI is booted on your system, with the right number of processors. The command to use is:

```
lamnodes
```

The system should respond with a list of active nodes and the number of processors per node. The total number of declared processors should be superior or equal to **nzdoms*nmdoms** (see p.41).
If it does not, boot your MPI environment. With LAM/MPI, to boot the default nodes list, type:

```
lamhalt
lamboot
```

A file named **nodelist.example** is provided here as a template if you want to boot different nodes. To use this file, first edit it according to your environment, taking care to declare at least **nzdoms*nmdoms** processors. Once your **nodelist.example** file is edited, type:

```
lamhalt
lamboot nodelist.example
```

If you want to have an understanding of the impacts of the hostlist file (nodelist.example) read the recommendations in p.41

F.1 Specific case of single node envrionment

In the trivial case of a single node environment, the node list file, either **/etc/lam/lam-bhosts.def** or your own **nodelist.example** should contain only this single line:

```
localhost
```

And you should set **nzdoms=1** and **nmdoms=1** in **chimere.sh**.

In the other trivial case of a single bi-processor node, the node list file, should contain only this single line:

```
localhost cpu=2
```

And you should set **nzdoms=2** and **nmdoms=1** in **chimere.sh**.

Appendix G

Structure of the CHIMERE netCDF files

G.1 EMIS.[domain].[MM].[SPEC].s.nc and EMIS.[domain].[MM].[SPEC].p.nc

```
netcdf EMIS.CONT5.05.NO2.s {
dimensions:
Time = 24 ;
west_east = 79 ;
south_north = 47 ;
bottom_top = 7 ;
type_day = 7 ;
SpStrLen = 23 ;
variables:
float lon(south_north, west_east) ;
lon:units = "degrees_east" ;
lon:long_name = "Longitude" ;
float lat(south_north, west_east) ;
lat:units = "degrees_north" ;
lat:long_name = "Latitude" ;
float EMEP_levels(bottom_top) ;
EMEP_levels:units = "meters" ;
EMEP_levels:long_name = "Cut_off_heights_for_redistribution" ;
float NO2(Time, type_day, bottom_top, south_north, west_east) ;
NO2:units = "molecule/cm2/s" ;
NO2:long_name = "NO2 Emission" ;

// global attributes:
:Title = "CHIMERE emissions" ;
:Sub-title = "Hourly surfacic emission" ;
:Chimere_type = "EMISSIONS" ;
:Generating_process = "Generated by sectoremis" ;
:Conventions = "None" ;
:Domain = "CONT5" ;
:Year = "2003" ;
:Landuse_for_Reggriding = "glcf" ;
:history = "" ;
}

netcdf EMIS.CONT5.01.NO2.p {
dimensions:
Time = 24 ;
west_east = 79 ;
south_north = 47 ;
Sources = 8 ;
type_day = 3 ;

variables:
```

```
float lon(south_north, west_east) ;
lon:units = "degrees_east" ;
lon:long_name = "Longitude" ;
float lat(south_north, west_east) ;
lat:units = "degrees_north" ;
lat:long_name = "Latitude" ;
long Sources_PIG(Sources) ;
Sources_PIG:units = "flag-0-1" ;
Sources_PIG:long_name = "Pig_treatment" ;
float Sources_lat(Sources) ;
Sources_lat:units = "Degrees" ;
Sources_lat:long_name = "Y_coordinate_of_source_point" ;
long Sources_ilat(Sources) ;
Sources_ilat:units = "cell_number" ;
Sources_ilat:long_name = "Y_coordinate_of_source_point" ;
float Sources_lon(Sources) ;
Sources_lon:units = "Degrees" ;
Sources_lon:long_name = "X_coordinate_of_source_point" ;
long Sources_ilon(Sources) ;
Sources_ilon:units = "cell_number" ;
Sources_ilon:long_name = "X_coordinate_of_source_point" ;
float Sources_Temp(Sources) ;
Sources_Temp:units = "Celcius_degree" ;
Sources_Temp:long_name = "Temperature_of_source_point" ;
float Sources_Height(Sources) ;
Sources_Height:units = "Meter" ;
Sources_Height:long_name = "Height_of_source_point" ;
float Sources_Diameter(Sources) ;
Sources_Diameter:units = "Meter" ;
Sources_Diameter:long_name = "Diameter_of_source_point" ;
float Sources_Velocity(Sources) ;
Sources_Velocity:units = "Meter/s" ;
Sources_Velocity:long_name = "Velocity_of_source_point_emission" ;
float NO2(Time, type_day, Sources) ;
NO2:units = "molecule/cm2/s" ;
NO2:long_name = "NO2 Emission" ;

// global attributes:
:Title = "CHIMERE SUITE" ;
:Sub-title = "Hourly point emission" ;
:Chimere_type = "EMISSIONS" ;
:Generating_process = "Generated by distribemis" ;
:Conventions = "None" ;
:Domain = "CONT5" ;
:Emission_version = "2008b" ;
:history = "" ;
}
```

G.2 exdomout.nc

```
netcdf exdomout {
dimensions:
Time = UNLIMITED ; // (13 currently)
DateStrLen = 19 ;
west_east = 67 ;
south_north = 46 ;
bottom_top = 32 ;
variables:
char Times(Time, DateStrLen) ;
float lon(south_north, west_east) ;
```

```
lon:units = "degrees_east" ;
lon:long_name = "Longitude" ;
float lat(south_north, west_east) ;
lat:units = "degrees_north" ;
lat:long_name = "Latitude" ;
float sshf(Time, south_north, west_east) ;
sshf:units = "W/m^2" ;
sshf:long_name = "Surface sensible heat flux" ;
float slhf(Time, south_north, west_east) ;
slhf:units = "W/m^2" ;
slhf:long_name = "Surface latent heat flux" ;
float usta(Time, south_north, west_east) ;
usta:units = "m/s" ;
usta:long_name = "Frictional velocity" ;
float tem2(Time, south_north, west_east) ;
tem2:units = "K" ;
tem2:long_name = "2m air temperature" ;
float soim(Time, south_north, west_east) ;
soim:units = "m^3/m^3" ;
soim:long_name = "Soil Moisture level 1" ;
float hght(Time, south_north, west_east) ;
hght:units = "m" ;
hght:long_name = "PBL height from MM5" ;
float rh2m(Time, south_north, west_east) ;
rh2m:units = "fraction" ;
rh2m:long_name = "Relative Humidity at 2m" ;
float lspc(Time, south_north, west_east) ;
lspc:units = "kg/m^2" ;
lspc:long_name = "Large scale precipitation" ;
float copc(Time, south_north, west_east) ;
copc:units = "kg/m^2" ;
copc:long_name = "convective precipitation" ;
float u10m(Time, south_north, west_east) ;
u10m:units = "m/s" ;
u10m:long_name = "10 m U wind" ;
float v10m(Time, south_north, west_east) ;
v10m:units = "m/s" ;
v10m:long_name = "10 m V wind" ;
float temp(Time, bottom_top, south_north, west_east) ;
temp:units = "K" ;
temp:long_name = "Temperature" ;
float cliq(Time, bottom_top, south_north, west_east) ;
cliq:units = "kg/kg" ;
cliq:long_name = "Cloud liquid water mixing ratio" ;
float rain(Time, bottom_top, south_north, west_east) ;
rain:units = "kg/kg" ;
rain:long_name = "Rain water mixing ratio" ;
float sphu(Time, bottom_top, south_north, west_east) ;
sphu:units = "kg/kg" ;
sphu:long_name = "Specific humidity" ;
float cice(Time, bottom_top, south_north, west_east) ;
cice:units = "kg/kg" ;
cice:long_name = "Ice mixing ratio" ;
float pres(Time, bottom_top, south_north, west_east) ;
pres:units = "Pa" ;
pres:long_name = "Pressure" ;
float alti(Time, bottom_top, south_north, west_east) ;
alti:units = "m" ;
alti:long_name = "Altitude of half-sigma level" ;
float winz(Time, bottom_top, south_north, west_east) ;
winz:units = "m/s" ;
```

```
winz:long_name = "Zonal wind" ;
float winm(Time, bottom_top, south_north, west_east) ;
winm:units = "m/s" ;
winm:long_name = "Meridional wind" ;

// global attributes:
:Title = "CHIMERE SUITE" ;
:Sub-title = "Interpolated Meteo file" ;
:Generating_process = "Generated by prepexmm5" ;
:Conventions = "" ;
:Domain = "CONT3" ;
:history = "File exdomout.nc was generated on",
                   "Tue Nov 15 14:25:27 2005 by <user> on <host>",
                    "from input file EUR1/MMOUT_EUR1_20030730_20030803_S\n" ;
:mm5_nxx = 85 ;
:mm5_nxx_DOT = 86 ;
:mm5_nyy = 75 ;
:mm5_nyy_DOT = 76 ;
:mm5_nlev = 32 ;
}
```

G.3 meteo.nc

```
netcdf meteo.20090312_20090319_test {
dimensions:
Time = UNLIMITED ; // (193 currently)
DateStrLen = 19 ;
west_east = 79 ;
south_north = 47 ;
bottom_top = 8 ;
variables:
float lon(south_north, west_east) ;
lon:units = "degrees_east" ;
lon:long_name = "Longitude" ;
float lat(south_north, west_east) ;
lat:units = "degrees_north" ;
lat:long_name = "Latitude" ;
char Times(Time, DateStrLen) ;
float hght(Time, south_north, west_east) ;
hght:units = "m" ;
hght:long_name = "Boundary layer height" ;
float u10m(Time, south_north, west_east) ;
u10m:units = "m/s" ;
u10m:long_name = "10m zonal wind speed" ;
float v10m(Time, south_north, west_east) ;
v10m:units = "m/s" ;
v10m:long_name = "10m meridional wind speed" ;
float w10m(Time, south_north, west_east) ;
w10m:units = "m/s" ;
w10m:long_name = "10m vertical wind speed" ;
float usta(Time, south_north, west_east) ;
usta:units = "m/s" ;
usta:long_name = "Friction velocity u*" ;
float wsta(Time, south_north, west_east) ;
wsta:units = "m/s" ;
wsta:long_name = "Convection velocity w*" ;
float tem2(Time, south_north, west_east) ;
tem2:units = "K" ;
tem2:long_name = "2m temperature" ;
float soim(Time, south_north, west_east) ;
```

```
soim:units = "m^3/m^3" ;
soim:long_name = "Soil moisture" ;
float sreh(Time, south_north, west_east) ;
sreh:units = "%" ;
sreh:long_name = "Surface relative humidity" ;
float psfc(Time, south_north, west_east) ;
psfc:units = "Pa" ;
psfc:long_name = "Surface pressure" ;
float sshf(Time, south_north, west_east) ;
sshf:units = "W/m2" ;
sshf:long_name = "Surface sensible heat flux" ;
float slhf(Time, south_north, west_east) ;
slhf:units = "W/m2" ;
slhf:long_name = "Surface latent heat flux" ;
float copc(Time, south_north, west_east) ;
copc:units = "mm/h" ;
copc:long_name = "Convective precipitation" ;
float lspc(Time, south_north, west_east) ;
lspc:units = "kg/m^2/h" ;
lspc:long_name = "Large scale precipitation" ;
float topc(Time, south_north, west_east) ;
topc:units = "kg/m^2/h" ;
topc:long_name = "Precipitation" ;
float aerr(Time, south_north, west_east) ;
aerr:units = "s/m" ;
aerr:long_name = "Aerodynamic resistance" ;
float atte(Time, south_north, west_east) ;
atte:units = "[0-1]" ;
atte:long_name = "Radiation attenuation factor" ;
float swrd(Time, south_north, west_east) ;
swrd:units = "W/m2" ;
swrd:long_name = "Shortwave radiation" ;
float winz(Time, bottom_top, south_north, west_east) ;
winz:units = "m/s" ;
winz:long_name = "Zonal wind" ;
float winm(Time, bottom_top, south_north, west_east) ;
winm:units = "m/s" ;
winm:long_name = "Meridional wind" ;
float winw(Time, bottom_top, south_north, west_east) ;
winw:units = "m/s" ;
winw:long_name = "Vertical wind" ;
float temp(Time, bottom_top, south_north, west_east) ;
temp:units = "K" ;
temp:long_name = "Temperature" ;
float sphu(Time, bottom_top, south_north, west_east) ;
sphu:units = "kg/kg" ;
sphu:long_name = "Specific humidity" ;
float airm(Time, bottom_top, south_north, west_east) ;
airm:units = "molecule/m**3" ;
airm:long_name = "Air density" ;
float hlay(Time, bottom_top, south_north, west_east) ;
hlay:units = "m" ;
hlay:long_name = "Layer top altitude" ;
float kzzz(Time, bottom_top, south_north, west_east) ;
kzzz:units = "m2/s2" ;
kzzz:long_name = "Kz diffusion coefficient" ;
float clwc(Time, bottom_top, south_north, west_east) ;
clwc:units = "kg/kg" ;
clwc:long_name = "Liquid (+ice) water content" ;
float cliq(Time, bottom_top, south_north, west_east) ;
cliq:units = "kg/kg" ;
```

```
cliq:long_name = "Cloud liquid water mixing ratio" ;
float rain(Time, bottom_top, south_north, west_east) ;
rain:units = "kg/kg" ;
rain:long_name = "Rain water mixing ratio" ;
float pres(Time, bottom_top, south_north, west_east) ;
pres:units = "Pa" ;
pres:long_name = "Pressure" ;
float cice(Time, bottom_top, south_north, west_east) ;
cice:units = "kg/kg" ;
cice:long_name = "Ice liquid water mixing ratio" ;
float thlay(Time, bottom_top, south_north, west_east) ;
thlay:units = "m" ;
thlay:long_name = "Layer thickness" ;
float dpeu(Time, bottom_top, south_north, west_east) ;
dpeu:units = "kg/m2/s" ;
dpeu:long_name = "Entrainment in updraft" ;
float dped(Time, bottom_top, south_north, west_east) ;
dped:units = "kg/m2/s" ;
dped:long_name = "Entrainment in downdraft" ;
float dpdu(Time, bottom_top, south_north, west_east) ;
dpdu:units = "kg/m2/s" ;
dpdu:long_name = "Detrainment in updraft" ;
float dpdd(Time, bottom_top, south_north, west_east) ;
dpdd:units = "kg/m2/s" ;
dpdd:long_name = "Detrainment in downdraft" ;
float flxu(Time, bottom_top, south_north, west_east) ;
flxu:units = "kg/m2/s" ;
flxu:long_name = "updraft mass flux" ;
float flxd(Time, bottom_top, south_north, west_east) ;
flxd:units = "kg/m2/s" ;
flxd:long_name = "downdraft  mass flux" ;

// global attributes:
:Title = "CHIMERE SUITE" ;
:Sub-title = "Hourly output meteo file" ;
:Chimere_type = "Chimere Meteo" ;
:Generating_process = "Generated by chimere" ;
:Conventions = "None" ;
:Domain = "CONT5" ;
:Chimere_version = "chimere2014b" ;
:history = "unknown" ;
}
```

G.4 AEMISSIONS.nc

```
netcdf AEMISSIONS {
dimensions:
Time = UNLIMITED ; // (24 currently)
west_east = 79 ;
south_north = 47 ;
bottom_top = 8 ;
SpStrLen = 23 ;
DateStrLen = 19 ;
Species = 24 ;

variables:
char Times(Time, DateStrLen) ;
char species(Species, SpStrLen) ;
float lon(south_north, west_east) ;
lon:units = "degrees_east" ;
```

```
lon:long_name = "Longitude" ;
float lat(south_north, west_east) ;
lat:units = "degrees_north" ;
lat:long_name = "Latitude" ;
float APINEN(Time, bottom_top, south_north, west_east) ;
APINEN:units = "molecule/cm2/s" ;
APINEN:long_name = "APINEN Emission" ;
float C2H4(Time, bottom_top, south_north, west_east) ;
C2H4:units = "molecule/cm2/s" ;
C2H4:long_name = "C2H4 Emission" ;
float C2H6(Time, bottom_top, south_north, west_east) ;
C2H6:units = "molecule/cm2/s" ;
C2H6:long_name = "C2H6 Emission" ;
float C3H6(Time, bottom_top, south_north, west_east) ;
C3H6:units = "molecule/cm2/s" ;
C3H6:long_name = "C3H6 Emission" ;
float C5H8(Time, bottom_top, south_north, west_east) ;
C5H8:units = "molecule/cm2/s" ;
C5H8:long_name = "C5H8 Emission" ;
float CH3CHO(Time, bottom_top, south_north, west_east) ;
CH3CHO:units = "molecule/cm2/s" ;
CH3CHO:long_name = "CH3CHO Emission" ;
float CH3COE(Time, bottom_top, south_north, west_east) ;
CH3COE:units = "molecule/cm2/s" ;
CH3COE:long_name = "CH3COE Emission" ;
float CH4(Time, bottom_top, south_north, west_east) ;
CH4:units = "molecule/cm2/s" ;
CH4:long_name = "CH4 Emission" ;
float CO(Time, bottom_top, south_north, west_east) ;
CO:units = "molecule/cm2/s" ;
CO:long_name = "CO Emission" ;
float HCHO(Time, bottom_top, south_north, west_east) ;
HCHO:units = "molecule/cm2/s" ;
HCHO:long_name = "HCHO Emission" ;
float HONO(Time, bottom_top, south_north, west_east) ;
HONO:units = "molecule/cm2/s" ;
HONO:long_name = "HONO Emission" ;
float NC4H10(Time, bottom_top, south_north, west_east) ;
NC4H10:units = "molecule/cm2/s" ;
NC4H10:long_name = "NC4H10 Emission" ;
float NH3(Time, bottom_top, south_north, west_east) ;
NH3:units = "molecule/cm2/s" ;
NH3:long_name = "NH3 Emission" ;
float NO(Time, bottom_top, south_north, west_east) ;
NO:units = "molecule/cm2/s" ;
NO:long_name = "NO Emission" ;
float NO2(Time, bottom_top, south_north, west_east) ;
NO2:units = "molecule/cm2/s" ;
NO2:long_name = "NO2 Emission" ;
float OXYL(Time, bottom_top, south_north, west_east) ;
OXYL:units = "molecule/cm2/s" ;
OXYL:long_name = "OXYL Emission" ;
float SO2(Time, bottom_top, south_north, west_east) ;
SO2:units = "molecule/cm2/s" ;
SO2:long_name = "SO2 Emission" ;
float H2SO4_fin(Time, bottom_top, south_north, west_east) ;
H2SO4_fin:units = "molecule/cm2/s" ;
H2SO4_fin:long_name = "H2SO4_fin Emission" ;
float PPM_big(Time, bottom_top, south_north, west_east) ;
PPM_big:units = "molecule/cm2/s" ;
PPM_big:long_name = "PPM_big Emission" ;
```

```
float PPM_coa(Time, bottom_top, south_north, west_east) ;
PPM_coa:units = "molecule/cm2/s" ;
PPM_coa:long_name = "PPM_coa Emission" ;
float OCAR_fin(Time, bottom_top, south_north, west_east) ;
OCAR_fin:units = "molecule/cm2/s" ;
OCAR_fin:long_name = "OCAR_fin Emission" ;
float BCAR_fin(Time, bottom_top, south_north, west_east) ;
BCAR_fin:units = "molecule/cm2/s" ;
BCAR_fin:long_name = "BCAR_fin Emission" ;
float TOL(Time, bottom_top, south_north, west_east) ;
TOL:units = "molecule/cm2/s" ;
TOL:long_name = "TOL Emission" ;
float TMB(Time, bottom_top, south_north, west_east) ;
TMB:units = "molecule/cm2/s" ;
TMB:long_name = "TMB Emission" ;

// global attributes:
:Title = "CHIMERE SUITE" ;
:Sub-title = "Emissions file - Surfacic + Point sources + Fires" ;
:Generating_process = "Generated by prepemis" ;
:Conventions = "" ;
:Domain = "CONT5" ;
:history = "" ;
}
```

G.5 BEMISSIONS.nc

```
netcdf BEMISSIONS {
dimensions:
Time = UNLIMITED ; // (13 currently)
DateStrLen = 19 ;
west_east = 67 ;
south_north = 46 ;
biospecies = 13 ;
variables:
        char Times(Time, DateStrLen) ;
        float lon(south_north, west_east) ;
        float lat(south_north, west_east) ;
        float C5H8(Time, south_north, west_east) ;
        float APINEN(Time, south_north, west_east) ;
        float BPINEN(Time, south_north, west_east) ;
        float LIMONE(Time, south_north, west_east) ;
        float TERPEN(Time, south_north, west_east) ;
        float OCIMEN(Time, south_north, west_east) ;
        float HUMULE(Time, south_north, west_east) ;
        float NO(Time, south_north, west_east) ;
        float SALT_coa(Time, south_north, west_east) ;
        float NA_coa(Time, south_north, west_east) ;
        float HCL_coa(Time, south_north, west_east) ;
        float H2SO4_coa(Time, south_north, west_east) ;
        float WATER_coa(Time, south_north, west_east) ;

// global attributes:
:Title = "CHIMERE SUITE" ;
:Sub-title = "Bioemissions file" ;
:Generating_process = "Generated by calbio" ;
:Conventions = "" ;
:Domain = "CONT3" ;
:history = "File BEMISSIONS.nc",
                "was generated on Tue Nov 15 14:25:40 2005 ",
```

```
                  "by <user> on <host> from input file",
                  "meteo.nc\n",
}
```

G.6 BOUN_CONCS.nc

```
netcdf BOUN_CONCS {
dimensions:
        Time = UNLIMITED ; // (121 currently)
        DateStrLen = 19 ;
        SpStrLen = 23 ;
        west_east = 101 ;
        south_north = 111 ;
        bottom_top = 20 ;
        h_boundary = 424 ;
        Species = 169 ;

variables:
        char Times(Time, DateStrLen) ;
        char species(Species, SpStrLen) ;
        float lon(south_north, west_east) ;
        float lat(south_north, west_east) ;
        float top_conc(Time, south_north, west_east, Species) ;
        float lat_conc(Time, bottom_top, h_boundary, Species) ;

// global attributes:
                :Title = "CHIMERE SUITE" ;
                :Sub-title = "Fine boundary concentrations file" ;
                :Generating_process = "Generated by prep_CHIMERE" ;
}
```

G.7 end.nc

```
netcdf end.20030730_20030803_heat-wave {
dimensions:
Time = UNLIMITED ; // (1 currently)
DateStrLen = 19 ;
SpecStrLen = 16 ;
Species = 119 ;
west_east = 67 ;
south_north = 46 ;
bottom_top = 8 ;
variables:
float lon(south_north, west_east) ;
lon:units = "degrees_east" ;
lon:long_name = "Longitude" ;
float lat(south_north, west_east) ;
lat:units = "degrees_north" ;
lat:long_name = "Latitude" ;
char species_name(Species, SpecStrLen) ;
char Times(Time, DateStrLen) ;
float APINEN(Time, bottom_top, south_north, west_east) ;
APINEN:units = "molecules/cm3" ;
float C2H4(Time, bottom_top, south_north, west_east) ;
C2H4:units = "molecules/cm3" ;
float C2H6(Time, bottom_top, south_north, west_east) ;
C2H6:units = "molecules/cm3" ;
```

```
float C3H6(Time, bottom_top, south_north, west_east) ;
C3H6:units = "molecules/cm3" ;
float C5H8(Time, bottom_top, south_north, west_east) ;
C5H8:units = "molecules/cm3" ;
float CARNIT(Time, bottom_top, south_north, west_east) ;
CARNIT:units = "molecules/cm3" ;
float CH3CHO(Time, bottom_top, south_north, west_east) ;
CH3CHO:units = "molecules/cm3" ;
float CH3COE(Time, bottom_top, south_north, west_east) ;
CH3COE:units = "molecules/cm3" ;
float CH3COO(Time, bottom_top, south_north, west_east) ;
CH3COO:units = "molecules/cm3" ;
float CH3COY(Time, bottom_top, south_north, west_east) ;
CH3COY:units = "molecules/cm3" ;
float CH3O2(Time, bottom_top, south_north, west_east) ;
CH3O2:units = "molecules/cm3" ;
float CH3O2H(Time, bottom_top, south_north, west_east) ;
CH3O2H:units = "molecules/cm3" ;
float CH4(Time, bottom_top, south_north, west_east) ;
CH4:units = "molecules/cm3" ;
float CO(Time, bottom_top, south_north, west_east) ;
CO:units = "molecules/cm3" ;
float DUSTAQ(Time, bottom_top, south_north, west_east) ;
DUSTAQ:units = "molecules/cm3" ;
float GLYOX(Time, bottom_top, south_north, west_east) ;
GLYOX:units = "molecules/cm3" ;
float H2O2(Time, bottom_top, south_north, west_east) ;
H2O2:units = "molecules/cm3" ;
float H2SO4(Time, bottom_top, south_north, west_east) ;
H2SO4:units = "molecules/cm3" ;
float H2SO4AQ(Time, bottom_top, south_north, west_east) ;
H2SO4AQ:units = "molecules/cm3" ;
float HCHO(Time, bottom_top, south_north, west_east) ;
HCHO:units = "molecules/cm3" ;
float HNO3(Time, bottom_top, south_north, west_east) ;
HNO3:units = "molecules/cm3" ;
float HNO3AQ(Time, bottom_top, south_north, west_east) ;
HNO3AQ:units = "molecules/cm3" ;
float HO2(Time, bottom_top, south_north, west_east) ;
HO2:units = "molecules/cm3" ;
float HONO(Time, bottom_top, south_north, west_east) ;
HONO:units = "molecules/cm3" ;
float ISNI(Time, bottom_top, south_north, west_east) ;
ISNI:units = "molecules/cm3" ;
float MAC(Time, bottom_top, south_north, west_east) ;
MAC:units = "molecules/cm3" ;
float MEMALD(Time, bottom_top, south_north, west_east) ;
MEMALD:units = "molecules/cm3" ;
float MGLYOX(Time, bottom_top, south_north, west_east) ;
MGLYOX:units = "molecules/cm3" ;
float MVK(Time, bottom_top, south_north, west_east) ;
MVK:units = "molecules/cm3" ;
float N2O5(Time, bottom_top, south_north, west_east) ;
N2O5:units = "molecules/cm3" ;
float NC4H10(Time, bottom_top, south_north, west_east) ;
NC4H10:units = "molecules/cm3" ;
float NH3(Time, bottom_top, south_north, west_east) ;
NH3:units = "molecules/cm3" ;
float NH3AQ(Time, bottom_top, south_north, west_east) ;
NH3AQ:units = "molecules/cm3" ;
float NO(Time, bottom_top, south_north, west_east) ;
```

```
NO:units = "molecules/cm3" ;
float NO2(Time, bottom_top, south_north, west_east) ;
NO2:units = "molecules/cm3" ;
float NO3(Time, bottom_top, south_north, west_east) ;
NO3:units = "molecules/cm3" ;
float O3(Time, bottom_top, south_north, west_east) ;
O3:units = "molecules/cm3" ;
float obio(Time, bottom_top, south_north, west_east) ;
obio:units = "molecules/cm3" ;
float obioH(Time, bottom_top, south_north, west_east) ;
obioH:units = "molecules/cm3" ;
float OH(Time, bottom_top, south_north, west_east) ;
OH:units = "molecules/cm3" ;
float oPAN(Time, bottom_top, south_north, west_east) ;
oPAN:units = "molecules/cm3" ;
float oRN1(Time, bottom_top, south_north, west_east) ;
oRN1:units = "molecules/cm3" ;
float oRO2(Time, bottom_top, south_north, west_east) ;
oRO2:units = "molecules/cm3" ;
float oROOH(Time, bottom_top, south_north, west_east) ;
oROOH:units = "molecules/cm3" ;
float OXYL(Time, bottom_top, south_north, west_east) ;
OXYL:units = "molecules/cm3" ;
float PAN(Time, bottom_top, south_north, west_east) ;
PAN:units = "molecules/cm3" ;
float PANH(Time, bottom_top, south_north, west_east) ;
PANH:units = "molecules/cm3" ;
float PPA(Time, bottom_top, south_north, west_east) ;
PPA:units = "molecules/cm3" ;
float PPMAQ(Time, bottom_top, south_north, west_east) ;
PPMAQ:units = "molecules/cm3" ;
float SO2(Time, bottom_top, south_north, west_east) ;
SO2:units = "molecules/cm3" ;
float SOA(Time, bottom_top, south_north, west_east) ;
SOA:units = "molecules/cm3" ;
float SOAAQ(Time, bottom_top, south_north, west_east) ;
SOAAQ:units = "molecules/cm3" ;
float toPAN(Time, bottom_top, south_north, west_east) ;
toPAN:units = "molecules/cm3" ;
float p1PPM(Time, bottom_top, south_north, west_east) ;
p1PPM:units = "molecules/cm3" ;
float p1DUST(Time, bottom_top, south_north, west_east) ;
p1DUST:units = "molecules/cm3" ;
float p1SOA(Time, bottom_top, south_north, west_east) ;
p1SOA:units = "molecules/cm3" ;
float p1H2SO4(Time, bottom_top, south_north, west_east) ;
p1H2SO4:units = "molecules/cm3" ;
float p1HNO3(Time, bottom_top, south_north, west_east) ;
p1HNO3:units = "molecules/cm3" ;
float p1NH3(Time, bottom_top, south_north, west_east) ;
p1NH3:units = "molecules/cm3" ;
float p1WATER(Time, bottom_top, south_north, west_east) ;
p1WATER:units = "molecules/cm3" ;
float p2PPM(Time, bottom_top, south_north, west_east) ;
p2PPM:units = "molecules/cm3" ;
float p2DUST(Time, bottom_top, south_north, west_east) ;
p2DUST:units = "molecules/cm3" ;
float p2SOA(Time, bottom_top, south_north, west_east) ;
p2SOA:units = "molecules/cm3" ;
float p2H2SO4(Time, bottom_top, south_north, west_east) ;
p2H2SO4:units = "molecules/cm3" ;
```

```
float p2HNO3(Time, bottom_top, south_north, west_east) ;
p2HNO3:units = "molecules/cm3" ;
float p2NH3(Time, bottom_top, south_north, west_east) ;
p2NH3:units = "molecules/cm3" ;
float p2WATER(Time, bottom_top, south_north, west_east) ;
p2WATER:units = "molecules/cm3" ;
float p3PPM(Time, bottom_top, south_north, west_east) ;
p3PPM:units = "molecules/cm3" ;
float p3DUST(Time, bottom_top, south_north, west_east) ;
p3DUST:units = "molecules/cm3" ;
float p3SOA(Time, bottom_top, south_north, west_east) ;
p3SOA:units = "molecules/cm3" ;
float p3H2SO4(Time, bottom_top, south_north, west_east) ;
p3H2SO4:units = "molecules/cm3" ;
float p3HNO3(Time, bottom_top, south_north, west_east) ;
p3HNO3:units = "molecules/cm3" ;
float p3NH3(Time, bottom_top, south_north, west_east) ;
p3NH3:units = "molecules/cm3" ;
float p3WATER(Time, bottom_top, south_north, west_east) ;
p3WATER:units = "molecules/cm3" ;
float p4PPM(Time, bottom_top, south_north, west_east) ;
p4PPM:units = "molecules/cm3" ;
float p4DUST(Time, bottom_top, south_north, west_east) ;
p4DUST:units = "molecules/cm3" ;
float p4SOA(Time, bottom_top, south_north, west_east) ;
p4SOA:units = "molecules/cm3" ;
float p4H2SO4(Time, bottom_top, south_north, west_east) ;
p4H2SO4:units = "molecules/cm3" ;
float p4HNO3(Time, bottom_top, south_north, west_east) ;
p4HNO3:units = "molecules/cm3" ;
float p4NH3(Time, bottom_top, south_north, west_east) ;
p4NH3:units = "molecules/cm3" ;
float p4WATER(Time, bottom_top, south_north, west_east) ;
p4WATER:units = "molecules/cm3" ;
float p5PPM(Time, bottom_top, south_north, west_east) ;
p5PPM:units = "molecules/cm3" ;
float p5DUST(Time, bottom_top, south_north, west_east) ;
p5DUST:units = "molecules/cm3" ;
float p5SOA(Time, bottom_top, south_north, west_east) ;
p5SOA:units = "molecules/cm3" ;
float p5H2SO4(Time, bottom_top, south_north, west_east) ;
p5H2SO4:units = "molecules/cm3" ;
float p5HNO3(Time, bottom_top, south_north, west_east) ;
p5HNO3:units = "molecules/cm3" ;
float p5NH3(Time, bottom_top, south_north, west_east) ;
p5NH3:units = "molecules/cm3" ;
float p5WATER(Time, bottom_top, south_north, west_east) ;
p5WATER:units = "molecules/cm3" ;
float p6PPM(Time, bottom_top, south_north, west_east) ;
p6PPM:units = "molecules/cm3" ;
float p6DUST(Time, bottom_top, south_north, west_east) ;
p6DUST:units = "molecules/cm3" ;
float p6SOA(Time, bottom_top, south_north, west_east) ;
p6SOA:units = "molecules/cm3" ;
float p6H2SO4(Time, bottom_top, south_north, west_east) ;
p6H2SO4:units = "molecules/cm3" ;
float p6HNO3(Time, bottom_top, south_north, west_east) ;
p6HNO3:units = "molecules/cm3" ;
float p6NH3(Time, bottom_top, south_north, west_east) ;
p6NH3:units = "molecules/cm3" ;
float p6WATER(Time, bottom_top, south_north, west_east) ;
```

```
p6WATER:units = "molecules/cm3" ;
float M(Time, bottom_top, south_north, west_east) ;
M:units = "molecules/cm3" ;
float O2(Time, bottom_top, south_north, west_east) ;
O2:units = "molecules/cm3" ;
float N2(Time, bottom_top, south_north, west_east) ;
N2:units = "molecules/cm3" ;
float H2O(Time, bottom_top, south_north, west_east) ;
H2O:units = "molecules/cm3" ;
float TOTPAN(Time, bottom_top, south_north, west_east) ;
TOTPAN:units = "molecules/cm3" ;
float NOX(Time, bottom_top, south_north, west_east) ;
NOX:units = "molecules/cm3" ;
float OX(Time, bottom_top, south_north, west_east) ;
OX:units = "molecules/cm3" ;
float HOX(Time, bottom_top, south_north, west_east) ;
HOX:units = "molecules/cm3" ;
float NOY(Time, bottom_top, south_north, west_east) ;
NOY:units = "molecules/cm3" ;
float ROOH(Time, bottom_top, south_north, west_east) ;
ROOH:units = "molecules/cm3" ;
float HCNM(Time, bottom_top, south_north, west_east) ;
HCNM:units = "molecules/cm3" ;
float PM10(Time, bottom_top, south_north, west_east) ;
PM10:units = "molecules/cm3" ;
float PM25(Time, bottom_top, south_north, west_east) ;
PM25:units = "molecules/cm3" ;
float PM10_anth(Time, bottom_top, south_north, west_east) ;
PM10_anth:units = "molecules/cm3" ;
float PM25_anth(Time, bottom_top, south_north, west_east) ;
PM25_anth:units = "molecules/cm3" ;
float PPM10_anth(Time, bottom_top, south_north, west_east) ;
PPM10_anth:units = "molecules/cm3" ;
float PPM25_anth(Time, bottom_top, south_north, west_east) ;
PPM25_anth:units = "molecules/cm3" ;
float pPPM(Time, bottom_top, south_north, west_east) ;
pPPM:units = "molecules/cm3" ;
float pDUST(Time, bottom_top, south_north, west_east) ;
pDUST:units = "molecules/cm3" ;
float pSOA(Time, bottom_top, south_north, west_east) ;
pSOA:units = "molecules/cm3" ;
float pH2SO4(Time, bottom_top, south_north, west_east) ;
pH2SO4:units = "molecules/cm3" ;
float pHNO3(Time, bottom_top, south_north, west_east) ;
pHNO3:units = "molecules/cm3" ;
float pNH3(Time, bottom_top, south_north, west_east) ;
pNH3:units = "molecules/cm3" ;
float pWATER(Time, bottom_top, south_north, west_east) ;
pWATER:units = "molecules/cm3" ;

// global attributes:
:Title = "CHIMERE SUITE" ;
:Sub-title = "Final concentrations file" ;
:Chimere_type = "end" ;
:Generating_process = "Generated by chimere" ;
:Conventions = "None" ;
:Domain = "CONT3" ;
:history = "File end.20030730_20030803_heat-wave.nc",
                  "was generated on Tue Nov  8 12:27:58 2005",
                  "by <user> on <host>\n" ;
}
```

G.8 Fire emissions EMIS.[domain].[MM].[SPEC].f.nc

```
netcdf EMIS.MEDa.06.CO.f {
dimensions:
        west_east = 119 ;
        south_north = 84 ;
        days = 30 ;
        hours = 24 ;
        sources = 315 ;
variables:
        float lon(south_north, west_east) ;
                lon:units = "degrees_east" ;
                lon:long_name = "Longitude" ;
        float lat(south_north, west_east) ;
                lat:units = "degrees_north" ;
                lat:long_name = "Latitude" ;
        float ilatsources(sources) ;
                ilatsources:units = "index" ;
                ilatsources:long_name = "Latitude_of_sources" ;
        float ilonsources(sources) ;
                ilonsources:units = "index" ;
                ilonsources:long_name = "Longitude_of_sources" ;
        float CO(hours, days, sources) ;
                CO:units = "molecule/cm2/s" ;
                CO:long_name = "CO Emission" ;
```